SYNTHESIS, CHARACTERIZATION, AND ANTI-CANCER STRUCTURE-

ACTIVITY RELATIONSHIP STUDIES OF IMIDAZOLIUM SALTS

A Dissertation

Presented to

The Graduate Faculty of The University of Akron

In Partial Fulfillment

of the Requirements for the Degree

Doctor of Philosophy

Michael A. DeBord

May, 2017

SYNTHESIS, CHARACTERIZATION, AND ANTI-CANCER STRUCTURE-

ACTIVITY RELATIONSHIP STUDIES OF IMIDAZOLIUM SALTS

Michael A DeBord

Dissertation

Approved: Accepted

_____   _____
Advisor   Department Chair
Dr. Wiley J. Youngs   Dr. Christopher J. Ziegler

_____   _____
Committee Member   Interim Dean of the College
Dr. Claire A. Tessier   Dr. John Green

_____   _____
Committee Member   Dean of the Graduate School
Dr. Christopher J. Ziegler   Dr. Chad Midha

_____   _____
Committee Member   Date
Dr. Leah P. Shriver

_____
Committee Member
Dr. Hossein Tavana

ii

ABSTRACT

Imidazolium salts have received significant attention for their anti-cancer properties. Human cancer cell lines have been treated with hundreds of imidazolium salts and many have shown promise for clinical potential. The leader of this class is YM155, a survivin suppressor that has gone through clinical trials but is not yet approved by the Food and Drug Administration (FDA) for the treatment of cancer. Numerous studies have been compiled to create structure activity relationships addressing what functional groups can help increase anti-proliferative effects and which functional groups produce imidazolium salts with weak anti-cancer properties. The general trend throughout the literature is that lipophilicity increases anti-cancer potential. Unfortunately, little is known about the mechanism of action, cellular target, and specificity of imidazolium salts which are all limiting factors towards progression into clinical applications.

Chapter II describes the synthesis and characterization of a series of N,N'-bis(naphthylmethyl) imidazolium salts. These compounds were also tested for their in vitro anti-cancer properties against several non-small cell lung cancer cell lines and found to be highly active. Each compound had low aqueous solubility, but could be solubilized by a cyclodextrin that is FDA approved for drug formulations. In vitro mechanism of action studies were also performed on one compound and suggested the compound induced an apoptotic mode of cell death.

Chapter III provides the synthesis and characterization of a related series of compounds with higher aqueous solubility. The major findings included the incorporation of quinolylmethyl moieties, similar to naphthylmethyl substituents, to increase aqueous solubility without drastically lowering anti-cancer activity. It was also determined that the anion plays a significant role in the aqueous solubility of these imidazolium salts.

Chapter IV presents the synthesis, characterization, and in vitro analysis of a series of bis-imidazolium salts. Each of these compounds has two positively charged imidazole rings to increase the hydrophilic nature compared to other lipophilic derivatives. These compounds follow trends found in the literature concerning their structure-activity relationships: enhanced lipophilicity produces compounds with higher in vitro anti-cancer activity. Chapter V provides concluding remarks.

DEDICATION

I would like to dedicate this dissertation to all of my family and friends who have been

there for me while I've been in school, especially my wife Katie, for her all her love and

support.

ACKNOWLEDGEMENTS

I would first like to thank my advisor, Dr. Wiley J. Youngs. You truly have been an inspiration to me throughout my time here at Akron. I have learned a tremendous amount about chemistry and how to become successful in my future endeavors, whatever that may be. I know I will never have a boss like you again the rest of my life because I consider you more of a friend than a boss, and I will cherish that forever. You not only have been somebody to let me learn and grow on my own, but were there to guide me in the right direction and help me when I needed it.

Thanks to my co-advisor, Dr. Claire A. Tessier. I appreciate all of the guidance and suggestions you have given me over the last five years. I know my group meetings and presentations were not always the most interesting to an inorganic chemist like yourself, but you were always curious about my research and gave thoughtful insight to help me look at problems from a different perspective.

I would like to thank Dr. Matthew J. Panzner for everything you have done for me during my time at Akron. Any time something went wrong or I had a problem I could not figure out, you were there to save the day. I have learned so much from you about chemistry, cooking, and life. You are an amazing person and I have been lucky to get to know you and learn to not only be a better chemist but a better person from you.

Thanks to all my committee members as well. I enjoyed all of the classes I have taken from each of you and appreciate the help and guidance you have provided for my research during my time here at Akron.

Finally, I want to thank all of the graduate and undergraduate students of the Youngs and Tessier group while I have been here. All of your help during group meetings and every day in the lab have shaped me to become the chemist I am. A special thanks to Pat for your help teaching me the chemistry when I initially joined the group and how to use the X-ray diffractometer, and a special thanks to Nikki for teaching me how to grow cell cultures and do the MTT assays. I've enjoyed everything from racquetball with Pat, Ben, Jason, and Nick, to our games of Settlers with Marie, Mike, Steven, and Nick. You guys have made this experience incredible enjoyable and I couldn't have done it without you.

TABLE OF CONTENTS

x

LIST OF TABLES

xiv

LIST OF FIGURES

Figure   Page

xx

LIST OF EQUATIONS

CHAPTER I

INTRODUCTION

1.1. Introduction

This chapter will describe imidazolium salts and their applications, the synthesis of imidazolium salts, the toxicity and anti-cancer properties of imidazolium salts. Imidazolium salts are products of the alkylation of both nitrogen atoms of the imidazole ring, a five-membered, aromatic heterocycle with two nitrogen atoms separated by one carbon. Imidazole is ubiquitously found in nature, most notable as part of the essential amino acid histidine[1] and the signaling molecule histamine.[2] An example of a generic imidazolium salt is shown in Figure I-1. Average resonance form of an imidazolium salt with the numbering scheme that is used throughout the dissertation. An imidazolium salt consists of a cation and an anion pair. The cation is of upmost importance when discerning the anti-cancer properties that will be discussed; however, an abundance of research has been performed to understand the role of the anion and to determine what can be used as an anion to affect the activity. The anion also impacts the solubility of the imidazolium salt which will be further discussed. When describing the cation and anion, the cation will always be referred to by a specific number, and the anion will be specified

after the number if the cation is shown with more than one anion throughout the dissertation.
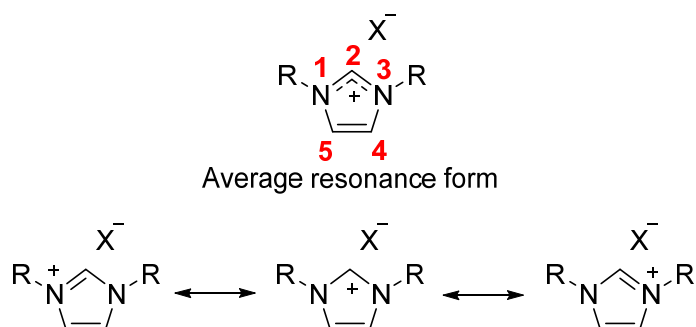
Figure I-1. Average resonance form of an imidazolium salt with the numbering scheme that is used throughout the dissertation.

1.2. Synthesis of imidazolium salts

Imidazolium salts can be easily and readily synthesized to be highly functionalized at all positions of the imidazole ring. However, they are most easily substituted and modified at the N^1 and N^3 positions. Symmetric or asymmetric imidazolium salts, concerning the substituents at the N^1 and N^3 positions, can be synthesized. The most common route is to alkylate both nitrogens on an imidazole core in subsequent steps.[3] One can use this approach for the synthesis of symmetric[4] and asymmetric[5,6] imidazolium salts. Imidazolium salts can also be synthesized by cyclization of diamine intermediates, produced from the reaction of primary amines with glyoxal. However, this synthetic route limits the products to symmetrical imidazolium salts and is less commonly used.[7,8]

1.3. Application of Imidazolium salts

Imidazolium salts can be used for a variety of applications. One such application, and probably the most famous, uses imidazolium salts as precursors to free and metal N-heterocyclic carbenes (NHC).[9] This may be the most well-known application considering Robert Grubb's shared the Nobel Prize in Chemistry in 2005 for his work on olefin metathesis, including his well-known ruthenium, N-heterocyclic carbene, second-generation catalyst.[10] Arduengo also played a major role in carbene chemistry as he was the first to isolate a free N-heterocyclic carbene.[11] The use of ionic liquid imidazolium salts as green solvents is rapidly gaining interest due to properties that many of them possess such as low vapor pressure and melting points, thermal stabilities, non-flammabilities and supposedly limited toxicities to the environment.[12] Originally these were also thought to be eco-friendly, and many are, but the toxicity of these ionic liquid imidazolium salts will be further discussed below. Finally, the medicinal potential of imidazolium salts is increasing drastically. Herein, the anti-cancer properties of imidazolium salts will be thoroughly reviewed and discussed; however, the anti-microbial,[13,14] and anti-oxidant[15] properties of imidazolium salts also have been of interest.

1.4. Toxicity and anti-cancer properties of ionic liquid imidazolium salts

The in vitro toxicity of ionic liquids against the rat cancer cell line IPC-81(leukemia) has been thoroughly reviewed in 2007 by Ranke.[16] The most important feature of these results suggest that the structure influences the cytotoxicity of the ionic

liquid. As seen with respect to other libraries of compounds, those with long chain alkyls have the highest toxicity. Also, the anion can have some effect considering compounds with the same cation and different anions have shown different toxicities.

The toxicity of several imidazolium salts against two human colorectal cancer cell lines, HT-29 and CaCo-2, was evaluated in 2007 by Frade et al. (Table I-2).[17] The effect of the cation and the anion were both evaluated to determine if certain anions would be safer for the environment with the use of ionic liquids. The imidazolium salts consisted of imidazoles with a methyl group at the N^1 position and various alkyl, ethers, and alcohols at the N^3 position (Table I-1). Compounds with the ether or alcohol chains were inactive against both cell lines tested, no matter the identity the anion was. Imidazolium salts with longer alkyl chains had higher toxicity than those with short alkyl chains. Compound **I-6** was the most active with $logEC_{50}$ (EC_{50} = concentration to induce a response in 50% of the population) values of 2.46 and 2.78 μM as the BF_4^- salt. When considering the anion, PF_6^-, acesulfame$^-$, saccharin$^-$, and $N(Tf)_2^-$ were less toxic than BF_4^- and $[DCA]^-$.

Table I-1. Structures of imidazolium salts **I-1**-**I-6** including all possible anions. Table modified from that in reference 17.
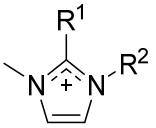
Cation	R^1	R^2	Anion and its abbreviation	
I-1	H	$(CH_2)_2OH$		BF_4^-
I-2	H	$((CH_2)_2O)_2CH_3$		PF_6^-
I-3	H	$(CH_2)_3CH_3$	[DCA]⁻	NC–N⁻–CN
I-4	CH₃	$(CH_2)_3CH_3$	Acesulfame⁻	
I-5	H	$(CH_2)_7CH_3$	Saccharin⁻	
I-6	H	$(CH_2)_9CH_3$	N(Tf)₂⁻	F_3CO_2S–N⁻–SO_2CF_3
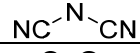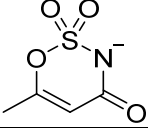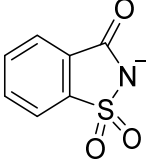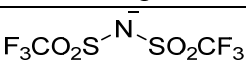
Table I-2. LogEC50 vales of ionic liquid imidazolium salts **I-1-I-6** against the HT-29 and CaCo-2 cell lines. Table modified from that in reference 17.

Compound	LogEC$_{50}$ (μM)	
	HT-29	CaCo-2
I-2-PF$_6$	NT	NT
I-1-PF$_6$	NT	NT
I-3-PF$_6$	NT	NT
I-5-PF$_6$	3.53	3.19
I-1-BF$_4$	NT	NT
I-2-BF$_4$	NT	NT
I-4-BF$_4$	> 3.78	NT
I-3-BF$_4$	> 3.78	> 3.48
I-5-BF$_4$	3.60	3.34
I-6-BF$_4$	2.46	2.78
I-3-NTF2	NT	NT
I-1-acesulfame	NT	NT
I-3-acesulfame	NT	NT
I-1-saccharin	NT	NT
I-3-saccharin	NT	NT
I-3-DCA	> 3.78	NT

*NT stands for non-toxic and represented negligible change in viability

The toxicity of three ionic liquids against the human breast carcinoma cell line, MCF7, was evaluated in 2008 by Kumar et al. (Figure I-2).[18] It was once again found that the compounds with more lipophilicity were more toxic. The three compounds tested had a methyl group at the N^1 position and a propyl, hexyl, or octyl alkyl chain at the N^3 position. The propyl and hexyl derivative used the NTF2 anion described above and can be directly compared considering the anion can have an effect on toxicity as discussed previously.[17] Compound **I-8-N(Tf)$_2$** was more active with an IC$_{50}$ value of 0.643 mM compared to **I-7-N(Tf)$_2$** with an IC$_{50}$ value of 6.297 mM. Compound **I-5-BF$_4$** was also toxic with an IC$_{50}$ value of 0.691 mM.
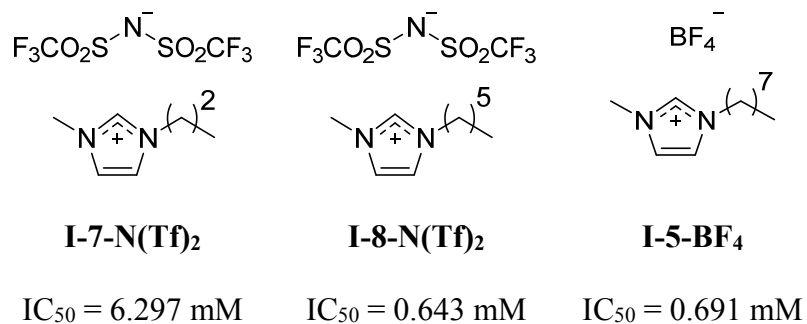
Figure I-2. Structures of ionic liquids evaluated for their toxicity against the MCF7, human breast cancer cell line. Compounds are from reference 18.

In 2009 Frade et al. reported the in vitro toxicity of a panel of ionic liquid imidazolium salts with a methyl group at the N^1 position and alkyl, benzyl, carboxylic acid, or ester group at the N^3 position except for **I-11** which had benzyl groups at both the N^1 and N^3 positions (Table I-3) against the CaCo-2, human colon carcinoma cell line (Table I-4).[19] Several of these cations were discussed above, but with different anions than previously described. The toxicity of each compound was deemed either 'toxic,' meaning it decreased or increased the cell viability by over 30% or 'non-toxic,' meaning there was less than a 30% difference in cell viability when compared to control cells. The general trend is again that as the alkyl chain length increases the toxicity also increases and imidazolium salts with highly hydrophilic carboxylic acid groups were non-toxic; whereas, imidazolium salts with two benzyl groups are generally more toxic than those with one benzyl group. It seems that the substituents at the N^1 and N^3 positions of the imidazolium salts have a larger impact on toxicity than does the anion; however, the only $FeCl_4^-$ anion derivative, **I-3-FeCl₄**, was toxic. This cation was not shown to be toxic when combined with any other anion.

Table I-3. Structures of ionic liquid imidazolium salts with toxicity towards the CaCo-2, human colon carcinoma, cell line. Table modified from that in reference 19.

Compound	R^1	R^2	Abbreviation	Anion
I-3	CH_3	$(CH_2)_3CH_3$		BF_4^-
I-1	CH_3	$(CH_2)_2OH$		PF_6^-
I-4	CH_3	$(CH_2)_3CH_3$	DCA^-	
I-5	CH_3	$(CH_2)_7CH_3$	$N(Tf)2^-$	
I-6	CH_3	$(CH_2)_9CH_3$	ACS^-	
I-9	CH_3	$(CH_2)_{10}COOEt$	SAC^-	
I-10	CH_3	$(CH_2)_{10}COOH$	CMS^-	
I-11	CH_2Ph	CH_2Ph	CBS^-	
I-12	CH_3	CH_2Ph		Cl^-
				$FeCl_4^-$
				Br^-
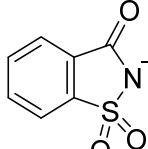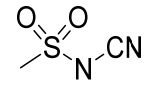
Table I-4. Results of a toxicity study of several ionic liquids against the CaCo-2, human colon carcinoma, cell line. Table modified from that in reference 19.

Cation	Anion				
	BF_4^-/PF_6^-	$DCA^-/N(Tf)_2^-$	ACS^-/SAC^-	CMS^-/CBS^-	$Cl^-/FeCl_4^-/Br^-$
I-3	-/-	-/-	-/-	NT/NT	-/T/-
I-1	-/-	-/-	-/-	NT/NT	-/-/-
I-4	-/-	-/-	-/-	-/-	-/-/-
I-5	-/-	T/NT	-/T	NT/-	-/-/-
I-6	-/-	-/-	-/-	-/-	T/-/-
I-9	T/T	T/-	-/-	-/-	-/-/T
I-10	NT/NT	NT/-	-/-	-/-	-/-/-
I-11	-/-	T/T	-/T	-/-	NT/-/-
I-12	-/-	NT/T	-/NT	-/-	NT/-/-

'T' = toxic

'NT' = non-toxic

'-' = compound not tested

Malhotra and Kumar reported the anti-tumor activity of imidazolium-based ionic liquids by submitting purchased imidazolium salts to the National Cancer Institute's (NCI) Developmental Therapeutic Program's (DTP) NCI-60 human tumor cell line screen to create a structure-activity relationship (SAR) (Table I-5).[20] All ionic liquids contained a methyl group at the N^1 position and differing substituents at the N^3 position, including either an alkyl chain, ranging from n = 3 to 17 carbons, an ethanol chain, an ether chain, or a benzyl group. The anion was also varied for certain cations to elucidate the effect the anion has on anti-cancer properties. It was found that compounds with alkyl chains of n = 7 or less carbons were inactive; whereas, compounds with n = 11-17 carbons were active and those with the alcohol, ether, and aromatic functional groups were inactive. The anion seemed to have no effect on the activity of these imidazolium salts. It was concluded that

longer chain lengths and higher lipophilicity increased the activity of this series of compounds and the activity of these imidazolium salts can be fine-tuned by altering the substituents of the imidazole ring to optimize the properties.

Table I-5. The structure and toxicity of several ionic liquids screened in the NCI-60 human tumor cell line one-dose assay. Table modified from that in reference 20.

Compound	n	X	Activity
I-7	3	$(CF_3SO_2)_2N$	Not active
I-13	5	$(CF_3SO_2)_2N$	Not active
I-13	5	$(C_2F_5)_3F_3P$	Not active
I-14	7	BF_4	Not active
I-14	7	$C_8H_{17}SO_4$	Not active
I-14	7	Cl	Not active
I-14	7	PF_6	Not active
I-15	11	Cl	Active
I-15	11	BF_4	Active
I-16	15	Cl	Active
I-17	17	Cl	Active
I-17	17	PF_6	Active
I-17	17	$(CF_3SO_2)_2N$	Active
I-17	17	$(C_2F_5)_3F_3P$	Active
I-1 =		$(CF_3SO_2)_2N$	Not active
I-18 =		$(CF_3SO_2)_2N$	Not active
I-12 =		PF_6	Not active
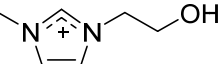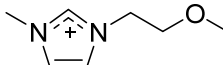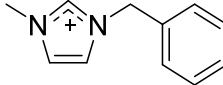
In 2010, Zhang et al. investigated the in vitro anti-cancer properties of three imidazolium salt ionic liquids against the Hela299 cell line (Figure I-3).[21] All compounds had a methyl substituent at the N^1 position, and either a butyl or hexyl substituent at the N^3

position. These compounds did not exhibit anti-proliferative effects on the Hela299 cell

line with IC_{50}values over 10 µg/mL.

I-3-BF₄   **I-3-PF₆**   **I-8-Cl**
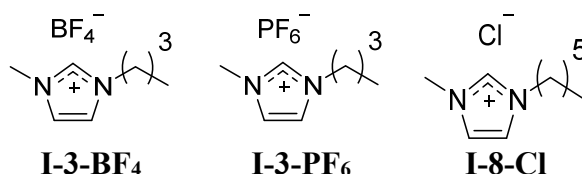
Figure I-3. Structure of imidazolium salts with low toxicity against the Hela299 cell line.

Compounds are from reference 21.

In an attempt to better understand the physical properties of ionic liquids, in 2011

Hossain et al. investigated the toxicity of four imidazolium salt ionic liquids against the

MCF7 human breast cancer cell line (Figure I-4).[22] The compounds evaluated had either a

proton, methyl, ethyl, or butyl chain at the N^1 position and a hydroxyhexyl chain at the N^3

position. The compound with the longest alkyl chain at the N^1 position, **I-22**, had the

highest toxicity with an IC_{50} value of 2.8 mM; whereas the remaining compounds had IC_{50}

(concentration that inhibits the growth of 50% of cell relative to control cells) values of 4.1

mM, 6.2 mM, and 6.9 mM corresponding to the compounds with an ethyl, methyl, and

proton at the N^1 position respectively.

I-19 **I-20** **I-21** **I-22**
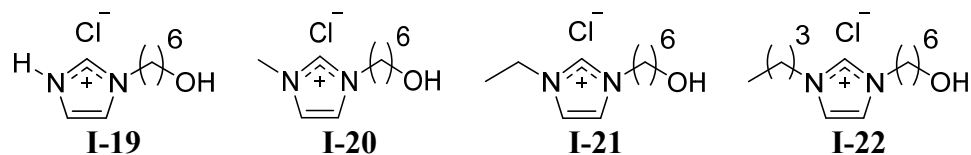
Figure I-4. Structures of hydroxyhexyl substituted imidazolium salt ionic liquids with toxicity towards the MCF7, human breast cancer, cell line. Compounds are from reference 22.

In 2012, Kaushik et al., reported the in vitro anti-cancer properties of two imidazolium salt ionic liquids against the T98G, brain cancer, cell line, and normal cells, the HEK cell line.[23] Compound **I-23** had a methyl chain at the N^1 position and a proton at the N^3 position; whereas, compound **I-3-Cl** had a methyl at the N^1 position and a butyl chain at the N^3 position (Figure I-5). The anti-proliferative effects were evaluated against both cell lines in a dose- and time-dependent manner. **I-3-Cl** was more potent with IC_{50} values less than 0.09 mg/mL at 48 and 72 hours exposure. **I-23** had IC_{50} values between 0.79 mg/mL and 0.30 mg/mL. The ionic liquids were less toxic to the HEK cells at the time exposures assessed.

I-23 **I-3-Cl**
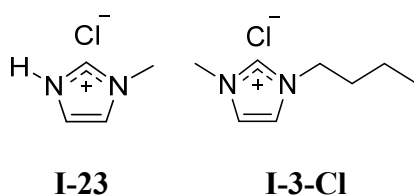
Figure I-5. Structure of imidazolium salt ionic liquids with in vitro anti-proliferative affects against a brain cancer cell line, T98G. Compounds are from reference 23.

In 2013, Wang et al., released a toxicity study of four imidazolium salt ionic liquids using the MCF7 human breast cell line.[24] The imidazolium salts all had a methyl substituent

at the N^1 position and an ethyl, hexyl, octyl, or dodecyl substituent at the N^3 position (Figure I-6). The results were in the form of pEC_{50} or the negative logarithm of the EC_{50} value. Similar to previous results, as the alkyl chain length increased, as did the toxicity to the MCF7 breast cancer cells. The most toxic compound was **I-26** with a pEC_{50} value of 4.484; whereas **I-5-Cl**, **I-14-BF₄**, and **I-24** had pEC_{50} values of 3.007, 2.814, and 2.658, respectively.

I-24	**I-14-BF₄**	**I-5-Cl**	**I-26**
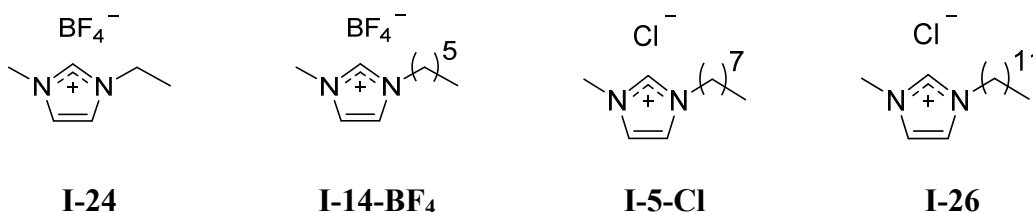
Figure I-6. Structures of imidazolium salt ionic liquids with toxic affects towards the human breast cancer cell line, MCF7. Compounds are from reference 24.

The toxicity of a series of imidazolium salt ionic liquids against a human lung cancer cell line, A549, was evaluated by Chen et al. in 2014 (Table I-7).[25] This series of compounds incorporated imidazolium salts with a methyl or vinyl group at the N^1 position and an alkyl chain of varying lengths at the N^3 position. A bis-imidazolium salt was also evaluated, containing two vinyl groups and a nonyl alkyl chain linker. The results are summarized in Table I-6 and suggest that the substituents at the N^1 and N^3 positions directly affect the toxicity. Compounds with a methyl at the N^1 position have less activity than those with a vinyl group at the N^1 position and the same substituent at the N^3 position. Compounds with longer alkyl chains at the N^3 position have more toxicity than compounds with shorter alkyl chains and the same substituent at the N^1 position. Although the substituents at the N^1 and N^3 positions have a significant effect on the toxicity of these

13

imidazolium salts, the anion does play a role in the toxicity. The BF_4^- derivatives were the least toxic; whereas, the $N(Tf)_2^-$ anion derivatives were the most toxic.

Table I-6. The structures of several cationic and anionic portions of imidazolium salts whose toxicity was evaluated against the A549, human lung carcinoma, cell line. Compounds are from reference 25.

$R^1\text{-}N\overset{+}{\underset{}{\diamondsuit}}N\text{-}R^2$			Abbreviation	Anion
Compound	R^1	R^3		
I-24	CH_3	$(CH_2)CH_3$	Cl	Cl^-
I-3	CH_3	$(CH_2)_3CH_3$	Br	Br^-
I-5	CH_3	$(CH_2)_7CH_3$	I	I^-
I-27	$CHCH_2$	$(CH_2)_3CH_3$	FeCl4	$\left[\begin{array}{c} Cl \\ | \\ Cl-Fe-Cl \\ | \\ Cl \end{array}\right]^-$
I-28	$CHCH_2$	$(CH_2)_5CH_3$	BF4	$\left[\begin{array}{c} F \\ | \\ F-B-F \\ | \\ F \end{array}\right]^-$
I-29	$CHCH_2$	$(CH_2)_7CH_3$	PF6	$\left[\begin{array}{c} F \\ F\diagdown|\diagup F \\ P \\ F\diagup|\diagdown F \\ F \end{array}\right]^-$
I-30	$CHCH_2$	$(CH_2)_8CH_3$	NTf2	$F_3CO_2S\overset{N^-}{\diagup\diagdown}SO_2CF_3$
I-31	$CHCH_2$	$(CH_2)_{11}CH_3$		
I-32	$\diagup\diagdown N\overset{+}{\diamondsuit}N\diagdown(\ )_9 N\overset{+}{\diamondsuit}N\diagdown\diagup$			
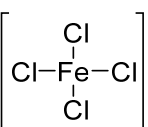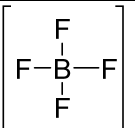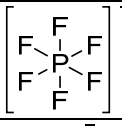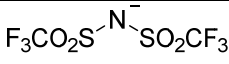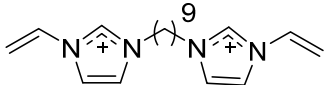
Table I-7. EC$_{50}$ values of several imidazolium salts against the A549, human lung carcinoma, cell line. Table modified from that in reference 25.

Compound	EC$_{50}$ (mM)
I-3-Cl	11.784
I-5-Cl	0.538
I-3-PF$_6$	19.409
I-5-PF$_6$	0.787
I-24-Br	65.707
I-3-FeCl$_4$	7.384
I-3-I	25.599
I-3-NTf$_2$	2.366
I-24-BF$_4$	111.569
I-3-BF$_4$	73.776
I-5-BF$_4$	0.830
I-27-Cl	0.991
I-28-Cl	0.561
I-29-Cl	0.465
I-27-Br	1.987
I-28-Br	1.644
I-29-Br	0.181
I-28-NTf$_2$	0.209
I-30-NTf$_2$	0.091
I-32-NTf$_2$	31.698
I-31-NTf$_2$	0.0056

In 2014, Paterno et al. published a multivariate insight describing the toxicity of a large class of imidazolium salt ionic liquids to establish structure-activity relationships (SAR).[26] Data from the literature was used in a modeling program to evaluate the affect the structure has on the toxicity. The major finding of the article suggested that the toxicity of imidazolium salt ionic liquids was directly proportional to the alkyl chain length, as chain length increases, so does the toxicity. However, there was a limit considering once the alkyl chain length become too long the toxicity again decreased, with the formation of micelle aggregates as a possible explanation for this observation. Also, the inclusion of

oxygen heteroatoms can help reduce the toxicity. Lower toxicity was observed in short and long chain alkyls with heteroatoms incorporated into the chain when compared to alkyl chains of equal lengths. However, medium chain ether substituents were more toxic than long and short chain ether chains. The possibility of micelle formation was once again suggested as a possible explanation for the lower toxicity of longer ether chain substituents.

Ferraz et al. published an anti-tumor study on imidazolium salt ionic liquids with ampicillin as the anion as a possible combination drug (Figure I-7).[27] The cationic portion of both imidazolium salts had a methyl substituent at the N^1 position and either an ethyl or hydroxyethyl substituent at the N^3 position. Both compounds were exposed to a panel of human tumor cells in vitro including the T46D (breast), PC3 (prostate), HepG2 (liver), MG63 (osteosarcoma), and RKO (colon) cell lines. The compounds were also exposed to two primary cell lines, the GF (gingival fibroblasts) and SF (skin) cell lines to determine the toxicity to normal cells. Compound **I-1-AMP** was very toxic to the cancerous cell lines tested with IC_{50} values ranging from 0.146 μM to 0.738 μM and LD_{50} values ranging from 0.297 μM to 1.240 μM. Compound **I-1-AMP** was notably less toxic to the normal cell lines tested with IC_{50} values of 5.084 μM (SF) and 0.462 μM (GF) and LD_{50} (concentration that kills 50% of a test population) values of 22.600 μM (SF) and 30.470 μM (GF). Compound **I-24-AMP** was less active with IC_{50} values ranging from 0.269 μM to above the concentrations tested and LD_{50} values ranging from 1.122 μM to 209.700 μM. Compound **I-24-AMP** also showed toxicity towards the normal cell lines with IC_{50} values of 6.366 μM (SF) and 0.853 μM (GF) and LD_{50}values of 6.366 μM (SF) and 9.357 μM (GF); thereby, showing less specificity towards cancerous tissue than **I-1-AMP**.

16

I-24-AMP   **I-1-AMP**   AMP
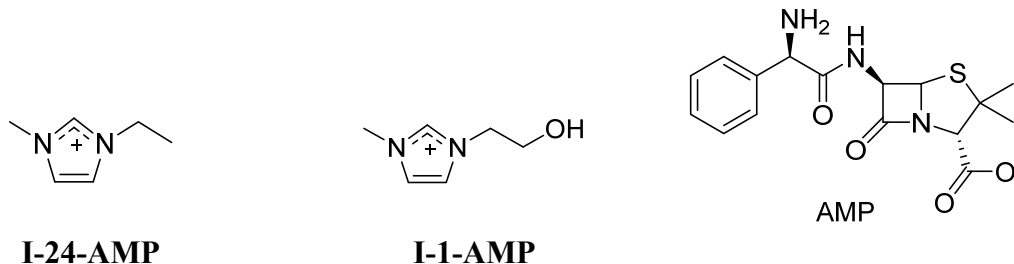
Figure I-7. Structure of ampicillin based imidazolium salt ionic liquids with in vitro anti-cancer activity towards several human tumor cell lines. Compounds are from reference 27.

The toxicity of **I-26-Br** was determined against the HepG2 liver carcinoma cell line in 2015 by Li et al. (Figure I-8).[28] Compound **I-26-Br** had an IC_{50} value of 9.8 μM after 24 hours of compound exposure. The authors also claim that **I-26-Br** caused apoptosis based on the observation of an increase in cell morphology changes in relation to an increase in concentration of compound exposure.

I-26-Br

Figure I-8. Structure of **I-26-Br** which has toxicity towards the liver cancer cell lines HepG2. Compound is from reference 28.

Little is known about the mechanism of action of imidazolium salt ionic liquids. The toxicity and various mechanistic studies of **I-5-Br** were evaluated by Li et al. in 2015 to better understand how these imidazolium salt ionic liquids with long chain alkyls are able to inhibit growth and kill human cells (Figure I-9).[29] Results from the cell viability assay suggest that the toxicity of **I-5-Br** is concentration dependent and the EC_{50} value

after 24 hour compound exposure was 439.46 µM. **I-5-Br** was shown to induce apoptosis in HepG2 cells based on results from a double labelled, Annexin V and propidium iodide (PI), flow cytometry experiment. The number of cells that had gone through apoptosis and necrosis combined was increased from 8.00% in control cells to 30.08% in cells treated with **I-5‑Br**. Compound **I-5-Br** was also shown to increase reactive oxygen species (ROS) concentrations, cause p53 and bax up-regulation, suppress bcl-2 transcription, and promote enzymatic activity of several caspase enzymes including caspase-3, casepage-8, and caspase-9.
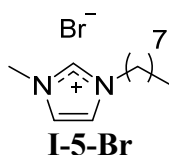
I-5-Br

Figure I-9. Structure of **I-5-Br**, an imidazolium salt ionic liquid that is toxic towards HepG2 cells and can induce an apoptotic mode of cell death. Compound is from reference 29.

The anti-cancer properties of imidazolium salt ionic liquids with a butyl substituent at the N^1 position and various alkyl, ether, and ester groups at the N^3 position were evaluated against the HEPG2 (hepatocellular carcinoma), MCF7 (breast adenocarcinoma), and HCT116 (colon carcinoma) human tumor cell lines (Table I-8).[30] Of the compounds tested, compounds **I-35**, **I-36**, and **I-38** were the most active with IC_{50} values ranging from 2.8 mg/mL to 9.4 mg/mL, 2.8 mg/mL to 6.6 mg/mL, and 5.8 mg/mL to 9.9 mg/mL respectively. This follows the trends seen previously that compounds with the more lipophilic substituents at the N^3 position such as the $(CH_2)_3Ph$, $(CH_2)_4OPh$, and $(CH_2)_2Ph$

in **I-35**, **I-36**, and **I-38,** respectively, were more toxic than the compounds with more hydrophilic side chains such as the ester functional groups in **I-34** and **I-37**.

Table I-8. The structure of several imidazolium salts and their toxicity against multiple human cancer cell lines. Table modified from that in reference 30.
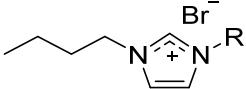
Br^- $N \overset{+}{\frown} N - R$		IC$_{50}$ (mg/mL)		
Compound	R	HEPG2	MCF7	HCT116
I-34	$(CH_2)_3COOCH_2CH_3$	19.1	11.8	22.3
I-35	$(CH_2)_3Ph$	9.4	3.0	2.8
I-36	$(CH_2)_4OPh$	2.8	6.6	2.7
I-37	$(CH_2)_4COOCH_2CH_3$	11.8	7.8	5.5
I-38	$(CH_2)_2Ph$	9.9	5.8	7.5

Ionic liquids have also been considered for their ability to stabilize proteins in their native conformation. In 2016, a study was performed using ionic liquids to stabilize a hemocyanin protein from a marine snail species, *Rapana thomasiani*, and to evaluate the in vitro anti-cancer properties against human breast cancer.[12] The cationic portion of the imidazolium salt had a methyl substituent at the N^1 position and an ethyl substituent at the N^3 position (Figure I-10). The anion consisted of numerous, deprotonated free amino acids (AA), which had an effect on the cytotoxicity of the imidazolium salt pair and the imidazolium salt-protein complex. Compounds **I-24-AA** were exposed to the breast cancer cell line, MCF7, and murine fibroblasts, 3T3, at two concentrations and data was reported as % cell viability and not the typically reported IC$_{50}$ or EC$_{50}$ values. The only **I-24-AA** derivatives with notable cytotoxicity was the isoleucinate derivative at 4.7 mM exposure with 44.8% viability against the MCF7 cell line, and 77.8% viability against the 3T3 cell

line; therefore, showing some specificity towards the human tumor cells. The hemocyanin protein alone was shown to increase the viability of the fibroblast cell lines in a dose-dependent manner compared to control cells, with no effect on the viability of the MCF7 cell line. When the hemocyanin protein is complexed with imidazolium salts, the leucinate, isoleucinate, and thriptophanate complexes were the most cytotoxic with MCF7 cell viabilities of 34.7%, 37.3%, and 47.4% respectively. The 3T3 percent viability for these three derivatives was two-fold greater suggesting these protein-imidazolium salt complexes have some selectivity towards cancer cells.
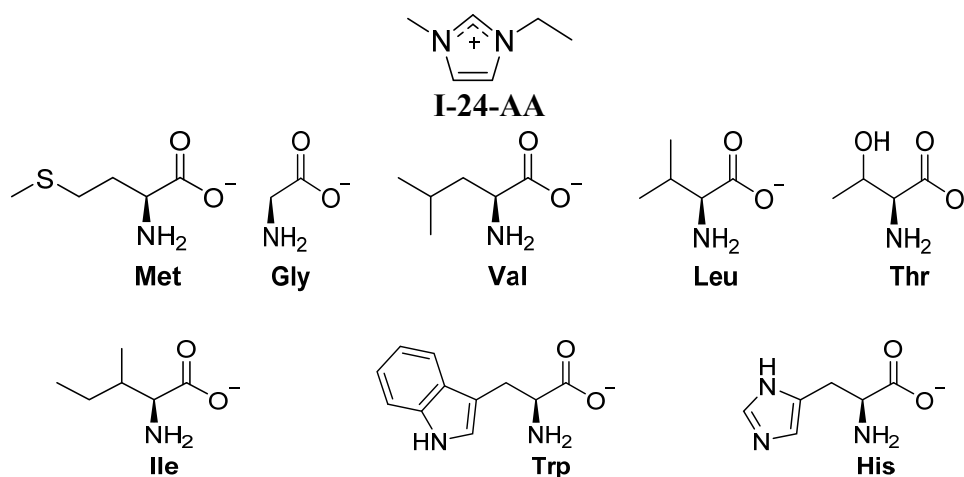
Figure I-10. Strucutre of imidazolium salts, **I-24-AA**, conataining numerous free, deprotonated amino acids as the anion. Compound are from reference 12.

1.5. Anti-cancer properties of imidazolium salts

The first report of imidazolium salts with anti-cancer activity included **I-39** (Lepidiline A) and **I-40** (Lepidiline B) which were extracted from the roots of *Lepidium meyenii* (Figure I-11).[31] These two natural products were tested for their anti-cancer

properties against a panel of human cancer cell lines including the A549 (lung carcinoma), UMUC3 (bladder carcinoma), HT-29 (colon adenocarcinoma), PC-3 (prostate adenocarcinoma), PACA2 (pancreatic adenocarcinoma), A498$_2$LM (kidney carcinoma), MDA231 (breast carcinoma), and FDIGROV (ovarian carcinoma) cell lines. Compound **I‑39** was only active against the FDIGROV ovarian carcinoma cell line with an ED$_{50}$ value of 7.39 µg/mL, whereas **I-40** was effective against the UMUC3 (6.47 µg/mL), PACA2 (1.38 µg/mL), MDA231 (1.66 µg/mL), and FDIGROV (5.26 µg/mL) cell lines. Both compounds were inactive against the A-549, HT-29, PC-3, and A498$_2$LM cell lines. The only difference in structure between **I-39** and **I-40** is a methyl group at the C^2 position for **I-40** versus a proton at the C^2 position for **I-39**. The slight difference in structure seems to make a substantial difference in the anti-proliferative effects of these compounds.

I-39   **I-40**

Figure I-11. Structure of the first imidazolium salts evaluated for anti-cancer properties, Lepidiline A and Lepidiline B. Compounds are from reference 31.

In 2004, Musumarra designed a series of imidazolium salts with heteroaryl substituents at the C^2 position linked to the imidazole ring by an ethylenic bridge and methyl groups at the N^1(N^3) positions and investigated their anti-tumor properties against breast and prostate cancers (Table I-9).[32] These compounds were derivatives of previously reported pyridinium cations that had anti-tumor activity against breast and prostate cancers.[33] Results from studies with the pyridinium cations suggested that compounds with

three heteroaromatic rings and one halogen atom were the most active. Results from this more recent study involving imidazolium salts were consistent with previous results considering compound **I-44** and **I-45** had the highest anti-cancer activity against the breast (MCF7) and prostate (LNCap) cancer cell lines tested.[32] Results were reported as log GI_{50} values (growth inhibition of 50% of cells relative to control cells), similar to how the NCI reports values, meaning the growth inhibition of 50% of cells relative to control cells. Compound **I-44** had log GI_{50} values of -5.86 (MCF7) and -5.38 (LNCap) or 1.38 µM and 4.17 µM respectively; whereas, **I-45** was more active with log GI_{50} values of -6.21 (MCF7) and -5.42 (LNCap) or 0.62 µM and 3.8 µM, respectively.

Table I-9. Structure and log GI_{50} values of imidazolium salts with heteroaryl groups at the C^2 position. Table modified from that in reference 32.
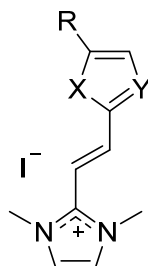
Structural details	Log GI_{50} values	
	MCF7	LNCap
I-41: X = O; Y = C; R = H	> -4	> -4
I-42: X = O; Y = C; R = Me	-4.48	-4.78
I-43: X = O; Y = C; R = Br	-4.40	> -4
I-44: X = O; Y = C; R = 2-ClPh	-5.86	-5.38
I-45: X = O; Y = C; R = 4-BrPh	-6.21	-5.42
I-46: X = S; Y = C; R = Br	-4.84	-4.52
I-47: X = N-Me; Y = C; R = H	> -4	> -4

Masumarra used these results to design a new molecular modelling program called Volsurf which was used to design new anti-tumor agents and predict their in vitro anti-tumor activities.[34] The program suggested new functional groups at the 5-position of the furan ring would result in increased anti-cancer activities. Changes from the above compounds include altering the position of the chloro group on the phenyl ring, adding a second halogen to the phenyl ring, and adding an ether moiety to the halogen-substituted phenyl ring (Table I-10). Again, values were reported as the log GI_{50} value similar to the NCI reported values so comparisons could be made. The anti-cancer properties of these compounds were only determined against the MCF7 breast cancer cell line (Table I-10). Adding a second halogen to the ring yielded the compound with the highest anti-cancer activity, **I-50**, of these next generation derivatives with a log GI_{50} value of -6.72 or 0.19 µM. Compound **I-51**, with a chloride and methoxy ether substituent, had the next highest activity with a log GI_{50} value of $^-$6.65 or 0.22 µM. This was closely followed by **I-49**, with a chloride at the 4-position of the phenyl ring, with a log GI_{50} value of -6.20 or 0.63 µM. Finally, the worst modification was moving the chloride substituent to the 3-position as in **I-48**. Compound **I-48** had a log GI_{50} value of -5.76 or 1.74 µM, which was roughly equivalent to the chloride at the 2-position in the earlier reported derivative.[32] Overall, these values were consistently lower suggesting the new modelling program was effective in predicting more potent derivatives although experimental values were lower than the theoretical values predicted by the program.

23

Table I-10. Structure and $\log_{50}$ values of imidazolium salts with heteroaryl groups at the C^2 position designed by the computer modeling program Volsurf. Table modified from that in reference 34.
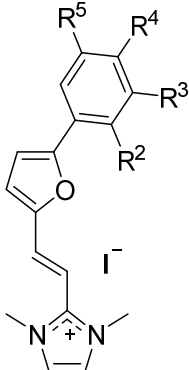
	Log GI_{50} value MCF7
I-48: R^3 = Cl; $R^2 = R^4 = R^5$ = H	-5.76
I-49: R^4 = Cl; $R^2 = R^3 = R^5$ = H	-6.20
I-50: $R^2 = R^5$ = Cl; $R^3 = R^4$ = H	-6.72
I-51: R^3 = Cl; R^4 = OMe; $R^2 = R^5$ = H	-6.65

A third modification made to these ethylene bridged imidazolium salts, by the Fortuna group with the help of Musumarra, was replacing the oxygen in the furan moiety with a sulfur to evaluate the anti-cancer properties of thiofuran derivatives (Figure I-12).[35] The Volsurf+ program was used again to predict ideal candidates for the third generation imidazolium salts. These synthetic derivatives focused on the thiofuran moiety and adding a third aromatic substituent, but they did not include the halogen substituent the authors claimed to be necessary for high activity in the previous manuscripts. These derivatives were less active than the related 1st and 2nd generation furan compounds. Compound **I-52** with a phenyl substituent at the C-4 position of the thiofuran had log GI_{50} values of -6.00 (MCF7) and -4.70 (LNCap) or 1.00 µM and 19.95 µM respectively. Altering the position of the phenyl substituent to the C-5 position of the thiofuran moiety resulted in slightly

worse activity for the MCF7 cell line (log GI_{50} value of -5.84 or 1.45 μM) and slightly better activity for the LNCap cell line (log GI_{50} value of -5.08 or 8.32 μM) for **I-53**. Finally, the third modification was another thiofuran substituent bound to the 5-position of the thiofuran. This chemical modification resulted in GI_{50} values of -5.33 (MCF7) and -5.22 (LNCap) or 4.68 μM and 6.03 μM respectively for **I-54**. These structural differences did not enhance the activity of their previously published derivatives but did add to the SAR they have established with the library of compounds published to further enhance the field.

I-52   **I-53**   **I-54**
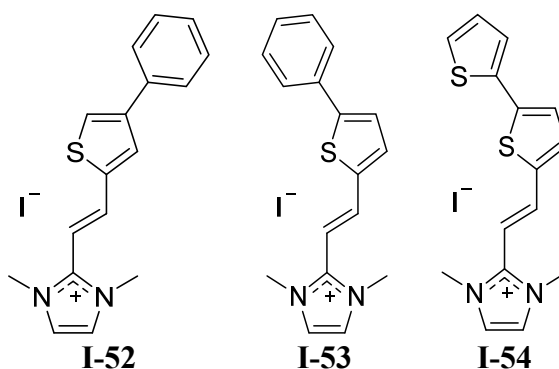
Figure I-12. Strucutre of compounds **I-52-I-54** with poor anti-cancer activity. Compounds are from reference 35.

In 2013, Barresi et al., part of the Fortuna research group, published another series of heteroaryl ethylenes and evaluated their in vitro anti-cancer properties against breast cancer, the MCF7 cell line.[36] Only one compound from this series was an imidazolium salt, Figure I-13. Barresi used the computer modeling program, Volsurf+ to predict the chemotherapeutic potential of these compounds, and correctly predicted **I-55** to be inactive against the MCF7 cell line. Results from the anti-tumor studies were reported as log GI_{50} values, with **I-55** having a value greater than -4.00, meaning the actual value was above the range of concentrations tested in the experiment.

25
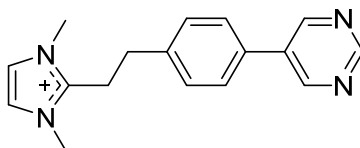
I-55

Figure I-13. Structure of **I-55**, a heteroaryl ethylene imidazolium salt that is inactive against the MCF7, human breast cancer, cell line. Compound is from reference 36.

YM155, **I-56** (Figure I-14), is the only imidazolium salt to enter clinical trials for the treatment of cancer thus far. The anti-tumor properties of this compound was first established when it was discovered to inhibit the protein survivin, which is a member of the family of proteins that inhibit apoptosis.[37] Survivin was found to be highly expressed in cancer cells with limited expression in most non-cancerous tissue.[38] Compound **I-56** was found to inhibit the promoter activity at low nanomolar ranges and induce apoptosis in human hormone-refractory prostate cancer cells in vitro.[37] In an orthotopic xenograft model of hormone-refractory prostate cancer, the PC-3 model, **I-56** was able to inhibit 80% of the growth of tumors when compared to control cells. In a phase I clinical trial, **I-56** could be safely administered without severe toxicities.[39] The results were favorable and suggested further exploration of the **I-56**, including possible future use in combination with other chemotherapeutics. Unfortunately, a phase II study with **I-56** used in combination with carboplatin or paclitaxel resulted in minimal response to the use of **I-56** in patients with non-small cell lung cancer, but the drug was well tolerated. Although **I-56** was not effective in the treatment of non-small cell lung cancer (NSCLC) clinically, it could still have potential for other malignancies such as chondrosarcoma considering **I-56** was able to inhibit growth in vitro and it could safely be administered to patients in clinical trials.[40]

26

I-56
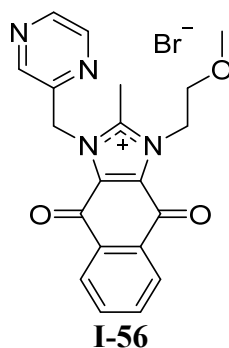
Figure I-14. Structure of YM155, **I-56**. This compound is from reference 37.

Zhang and Yang have been leaders in the field, publishing manuscripts on imidazolium salts with high anti-cancer activity for over a half decade, specializing in hybrid imidazolium salts.[6,41–54] The first report was in 2009 describing the synthesis and anti-cancer activity of phenacylimidazolium bromides,[41] which had previously received attention for use as oral hypoglycemic agents[55] and in the synthetic route to produce 3-substituted L-histidines.[56] A large number of imidazolium salts with a phenylacyl or alkylacyl groups at the N^1 position and various substituents including aromatic and alkyl substituents at the N^3 position were synthesized (Table I-11) and tested for their anti-cancer properties against several human cancer cell lines: HL-60 and K562 (myeloid leukemia), A431 (epidermoid carcinoma), Hep-2 (laryngeal carcinoma), Skov-3 (ovarian carcinoma), MKN-28 (gastric carcinoma), SMMC-7721 (liver carcinoma) and GLC-15 (lung carcinoma) (Table I-12).[41] The anti-cancer activity of each compound was presented as an IC_{50} value. It was found that alkyl groups were the least active of the compounds tested and a mesityl substituent at the N^1 position, and either a $C_6H_4(OCH_3)$-4 substituent or a naphthylacyl substituent at the N^3 position were the most active such as **I-75** with IC_{50}

values less than 5 µM against all the cell lines (except the SMMC-7721) tested and higher

activity than cisplatin against all but the MKN-28 gastric carcinoma cell line.

Table I-11. Structural details of novel phenacylimidazolium bromides with in vitro anti-

cancer activity against a variety of human tumor cell lines. Table modified from that in

reference 41.

Compound	R^1	R^4/R^5	R^3
I-57	t-C_4H_9	H	C_6H_5
I-58	t-C_4H_9	H	$C_6H_4(OCH_3)$-4
I-59	$C_6H_2(CH_3)_3$-2,4,6	H	t-C_4H_9
I-60	adamantyl	H	C_6H_5
I-61	adamantyl	H	$C_6H_4(OCH_3)$-4
I-62	adamantyl	H	2-naphthyl
I-63	$CH_2CH_2C_6H_2(OCH_3)_2$-3,4	H	$C_6H_4(OCH_3)$-4
I-64	$CH_2CH_2C_6H_2(OCH_3)_2$-3,4	H	2-naphthyl
I-65	$C_6H_2(CH_3)_3$-2,4,6	H	C_6H_5
I-66	$C_6H_2(CH_3)_3$-2,4,6	H	$C_6H_4(OCH_3)$-4
I-67	$C_6H_4(CH_2COCH_3)$-4	H	C_6H_5
I-68	$C_6H_4(CH_2COCH_3)$-4	H	$C_6H_4(OCH_3)$-4
I-69	$C_6H_4(NO_2)$-4	H	$C_6H_4(OCH_3)$-4
I-70	$C_6H_2(CH_3)_3$-2,4,6	H	2-naphthyl
I-71	$C_6H_3(i$-$C_3H_7)_2$-2,6	H	$C_6H_4(OCH_3)$-4
I-72	$C_6H_3(i$-$C_3H_7)_2$-2,6	H	2-naphthyl
I-73	$C_6H_2(CH_3)_3$-2,4,6	H	$C_6H_3(3$-CH_2OCH_2-4)
I-74	$C_6H_3(i$-$C_3H_7)_2$-2,6	H	$C_6H_3(3$-CH_2OCH_2-4)
I-75	$C_6H_2(CH_3)_3$-2,4,6	CH_3	2-naphthyl
I-76	$C_6H_2(CH_3)_3$-2,4,6	H	$C_6H_4(Br)$-4
I-77	$C_6H_3(i$-$C_3H_7)_2$-2,6	H	$C_6H_4(Br)$-4

Table I-12. IC$_{50}$ values of phenylacylimidazolium bromides against several human tumor cell lines. Table modified from that in reference 41.

Compound	IC$_{50}$ (μM)							
	HL-60	A431	Skov-3	MKN-28	K562	SMMC-7721	Hep-2	GLC-15
I-57	> 200	> 200	> 200	> 200	> 200	> 200	> 200	> 200
I-58	> 200	66.5	> 200	> 200	> 200	> 200	116.8	178.8
I-59	112.6	> 200	191.8	> 200	> 200	154.4	132.0	> 200
I-60	39.0	13.3	59.3	197.5	> 200	107.9	93.4	108.0
I-61	14.7	6.3	5.6	158.1	1.5	27.9	7.1	59.3
I-62	4.2	6.4	4.0	12.8	3.4	7.7	0.8	0.8
I-63	50.4	187.6	37.4	> 200	> 200	62.3	62.3	33.4
I-64	54.2	75.0	11.0	85.4	168.8	34.4	77.2	50.2
I-65	31.3	15.6	39.9	> 200	> 200	62.3	> 200	> 200
I-66	3.1	1.7	1.6	5.0	2.4	4.7	1.5	2.2
I-67	25.8	7.0	> 200	> 200	> 200	53.4	> 200	53.5
I-68	44.4	14.5	61.1	140.1	16.7	91.6	84.8	26.5
I-69	8.6	75.5	26.6	112.7	112.6	> 200	41.6	97.6
I-70	2.8	4.4	2.1	8.7	2.7	6.8	0.7	0.4
I-71	1.1	4.2	5.0	10.0	2.6	9.9	2.8	5.1
I-72	1.5	14.7	1.9	9.6	0.4	10.5	3.5	6.2
I-73	6.1	18.2	31.5	85.3	70.1	33.5	12.3	23.5
I-74	4.5	5.1	25.5	59.6	12.1	44.3	11.6	36.9
I-75	4.1	3.9	3.7	1.7	0.2	9.8	1.9	4.3
I-76	13.4	5.4	33.1	76.6	21.4	23.8	22.1	36.9
I-77	3.8	4.6	11.3	35.3	2.8	10.9	9.2	18.4
cisplatin	4.7	2.0	1.7	4.3	4.7	9.2	1.5	5.7

Following the results of this study to find potent anti-cancer imidazolium salts, Zhang synthesized a novel phenylacylimidazolium salt, 1-mesityl-3-(2-naphthoylmethano)-1H-imidazolium bromide, (**I-78** or MNIB in the literature) (Figure I-15).[42] This novel compound combined the mesityl group at the N^1 position and a naphthylacyl group at the N^3 position that was found to produce highly active compounds previously.[41] The anti-cancer properties of **I-78** were evaluated against several different types of human tumors including human chronic myelogenous leukemia (K562),

hepatocellular carcinoma (SMMC-7221), bladder tumor (EJ), laryngeal carcinoma (Hep-2), lung tumor (A549), hepatocellular liver carcinoma (HepG2), and Burkitt's lymphoma (Raji) by the MTT assay with results given as IC_{50} values (Table I-13).[42] All IC_{50} values were between 0.3 and 5.0 µg/mL (0.7 – 11.5 µM) with the highest anti-cancer activity against the Hep-2 and Raji cell lines, 0.3 µg/mL (0.7 µM) and 0.7 µg/mL (1.61 µM) respectively. The highest IC_{50} value was against the A549 cell line at 5.0 µg/mL (11.5 µM). However, the low IC_{50} values against a variety of cell lines suggests **I-78** could be used as a broad spectrum chemotherapeutic. Compound **I-78** was shown to cause an increase in the number of apoptotic cells when compared to control cells by labelling cells with Annexin V FITC and PI (measured by cytometry). Compound **I-78** was also shown to increase the length of the G1 phase of the cell cycle in a dose-dependent manner which was a suggested cause for the apoptotic mode of cell death. The ability of **I-** to reduce tumor growth was evaluated using a lung xenograft model of A549 cells subcutaneously injected into mice. The tumors were allowed to grow to an average volume of 100 mm^3 before any treatment. Tumor volume in control mice had an average growth of 7.8-fold; whereas, growth in tumor volume increased by 5.3-fold and 3.1-fold in mice treated with **I-78** at concentrations of 4 mg kg^{-1} dose$^-$1 and 8 4 mg kg^{-1} dose, respectively, every two days for the duration of the study. Tumor growth was stunted in mice treated with **I-78** compared to mice with no treatment and suggest merit for future studies with **I-78** to continue to evaluate the clinical potential of the compound.

I-78
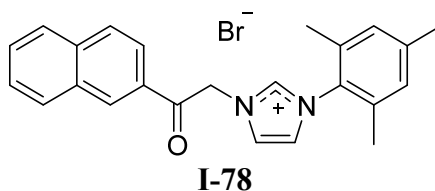
Figure I-15. Structure of **I-78**, known as MNIB in the literature. This compoind is from reference 42.

Table I-13. IC$_{50}$ values for **I-78** against several human tumor cell lines. Table modified from that in reference 42.

Compound	IC$_{50}$ value (µg/mL)						
	K562	SMMC-7721	EJ	Hep-2	A549	HepG2	Raji
I-78	1.7	1.8	1.2	0.3	5.0	2.2	0.7

Following the success of MNIB, a series of dihydrobenzofuran-based imidazolium salts were synthesized and evaluated for their anti-cancer properties against a variety of human cancer cell lines (Table I-14 and Table I-15).[43] The motivation to combine MNIB with benzofuran was based on benzofuran compounds in the literature with anti-cancer properties and the ability to induce apoptosis in cells.[57–59] The benzofuran-imidazole hybrids were exposed to the human cancer cell lines HL-60 (myeloid leukemia), SMMC-7221 (liver carcinoma), A549 (lung carcinoma), MCF-7 (breast carcinoma), and SW480 (colon carcinoma) and compared to each other to create a SAR.[43] Results were given as IC$_{50}$ values in micromolar concentrations. It was found that the most active benzofuran ligands contained methyl or chloro substituents on the benzofuran and the most active substituent at the N^3 position was a naphthylacyl or 4-methoxynaphthylacyl substituent. Compound **I-102** was the most active derivative; whereas, **I-94** was highly active and

31

selective against the MCF-7 breast carcinoma cell line. Due to these properties, these two

derivatives were the lead compounds from this series for future modifications.

Table I-14. Structure of substituted-dihydrobenzofuran imidazolium salt, hybrid

derivatives. Table modified from that in reference 43.
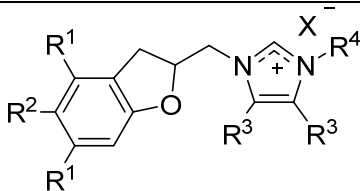
Compound	R^1	R^2	R^3	R^4	X
I-79	H	H	H	Naphthylacyl	Br
I-80	H	H	H	4-Bromophenacyl	Br
I-81	H	H	H	4-Methoxyphenacyl	Br
I-82	H	H	H	2-Bromobenzyl	Br
I-83	H	H	H	Pentyl	I
I-84	H	H	H	Allyl	Br
I-85	H	H	H	2'Phenyl-phenacyl	Br
I-86	H	H	H	Benzyl	Br
I-87	H	OMe	H	Naphthylacyl	Br
I-88	H	OMe	H	Benzyl	Br
I-89	H	OMe	H	4-Bromophenacyl	Br
I-90	H	OMe	H	2'Phenyl-phenacyl	Br
I-91	H	OMe	H	2-Bromobenzyl	Br
I-92	H	OMe	H	Pentyl	I
I-93	H	OMe	H	4-Methoxyphenacyl	Br
I-94	H	Cl	H	Naphthylacyl	Br
I-95	H	Cl	H	4-Bromophenacyl	Br
I-96	H	Cl	H	Allyl	Br
I-97	H	Cl	H	2-Bromobenzyl	Br
I-98	H	Cl	H	Benzyl	Br
I-99	H	Cl	H	4-Methoxyphenacyl	Br
I-100	H	Cl	Me	4-Bromophenacyl	Br
I-101	H	Cl	Me	4-Methoxyphenacyl	Br
I-102	Me	H	H	Naphthylacyl	Br
I-103	Me	H	H	4-Bromophenacyl	Br
I-104	Me	H	H	Pentyl	I
I-105	Me	H	H	2-Bromobenzyl	Br
I-106	Me	H	H	Allyl	Br
I-107	Me	H	H	4-Methoxyphenacyl	Br
I-108	Me	H	H	Benzyl	Br

Table I-15. IC$_{50}$ values (µM) of substituted-dihydrobenzofuran imidazolium salt, hybrid

derivatives. Table modified from that in reference 43.

Compound	IC$_{50}$ values (µM)				
	MCF-7	HL-60	SMMC-7721	A549	SW480
I-79	25.67	18.18	> 40	35.17	> 40
I-80	> 40	> 40	> 40	> 40	> 40
I-81	> 40	> 40	> 40	> 40	> 40
I-82	> 40	> 40	> 40	> 40	> 40
I-83	> 40	> 40	> 40	> 40	> 40
I-84	> 40	> 40	> 40	> 40	> 40
I-85	> 40	> 40	> 40	> 40	> 40
I-86	> 40	> 40	> 40	> 40	> 40
I-87	> 40	> 40	> 40	> 40	> 40
I-88	> 40	> 40	> 40	> 40	> 40
I-89	> 40	> 40	> 40	> 40	> 40
I-90	> 40	> 40	> 40	> 40	> 40
I-91	> 40	> 40	> 40	> 40	> 40
I-92	> 40	> 40	> 40	> 40	> 40
I-93	> 40	> 40	> 40	> 40	> 40
I-94	5.78	10.86	27.18	17.60	16.55
I-95	> 40	> 40	> 40	> 40	> 40
I-96	> 40	> 40	> 40	> 40	> 40
I-97	> 40	> 40	> 40	> 40	> 40
I-98	> 40	> 40	> 40	> 40	> 40
I-99	13.97	23.90	30.92	23.52	> 40
I-100	14.75	12.97	27.62	24.68	23.11
I-101	7.70	8.95	20.02	10.69	> 40
I-102	7.95	6.18	15.23	12.35	14.63
I-103	14.13	11.96	> 40	21.35	17.81
I-104	> 40	> 40	> 40	> 40	> 40
I-105	20.62	35.74	37.51	28.99	> 40
I-106	> 40	> 40	> 40	> 40	> 40
I-107	15.02	8.40	22.41	17.89	33.02
I-108	> 40	> 40	> 40	> 40	> 40

Following the first report of dihydrobenzofuran-imidazolium salt hybrid compounds for anti-cancer activity, a second report was published in 2012 focusing on changing the imidazole core to create a SAR (Table I-16).[44] The anti-cancer properties of

several imidazolium salts were evaluated against a panel of human cancer cell lines including Skov-3 (ovarian carcinoma), HL-60 (myeloid leukemia), and MCF-7 (breast carcinoma) by their IC_{50} values. The group of imidazoles evaluated included imidazole, 2-methylimidazole, 2-ethylimidazole, and benzimidazole. Compound **I-114**, a benzimidazolium salt with a benzofuran substituent at the N^1 position and a benzyl substituent at the N^3 position, was the most active (9.1 µg mL^{-1} or 21.6 µM) with over three‑fold higher activity against the Skov-3 ovarian carcinoma cell line when compared to the other imidazolium salts (20.8 µg mL^{-1} or 65.6 µM for **I-109** (2Me)). The imidazolium, 2-methylimidazolium, and 2-ethylimidazolium salts had similar IC_{50} values against the Skov-3 cell line. Compound **I-114** was also the only active salt against the HL-60 and MCF-7 cell lines; whereas, the other imidazole derivatives were completely inactive at the highest concentration tested (40 µg mL^{-1}). The conclusion from this series of compounds was benzimidazolium salts have the highest activity and benzyl substituents at the N^3 position were more active than 2-bromobenzyl and butyl substituents.

Table I-16. IC$_{50}$ values of benzofuran substituted imidazolium salts comparing the affect the imidazole core has on the anti-cancer properties. Table modified from that in reference 44.
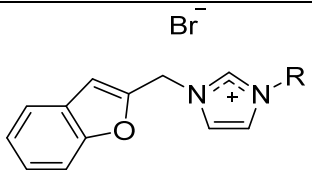
Compound	R^4	Imidazole Ring	IC$_{50}$ (μM)		
			Skov-3	HL-60	MCF-7
I-109	Benzyl	Imidazole	20.8	> 40	> 40
I-110	Benzyl	2-Methylimidazole	25.4	> 40	> 40
I-111	Benzyl	2-Ethylimidazole	23.2	> 40	> 40
I-112	2-Bromobenzyl	2-Ethylimidazole	35.1	> 40	> 40
I-113	Butyl	2-Ethylimidazole	39.5	> 40	> 40
I-114	Benzyl	Benzimidazole	9.1	7.4	12.5

These benzofuran-substituted imidazolium salts were active imidazolium salts and served as a starting point for the synthesis of novel compounds including 2-phenylbenzofuran imidazolium salts.[45] 2-Phenylbenzofuran based compounds (Figure I-16) found in the literature served as examples of natural product inhibitors of the hypoxia-inducible factor-1 protein, which can help promote tumor growth under hypoxic conditions,[60] and breast carcinoma tumor growth inhibitors.[61] A second report in 2012 by Yang and Zhang reported the synthesis and in vitro anti-cancer properties of a series of 2-phenylbenzofuran-imidazolium salts (Table I-17).[45] This series of 2-phenylbenzofuran derivatives was exposed to a panel of human tumor cell lines in vitro including SMMC-7721 (myeloid liver carcinoma), SW480 (colon carcinoma), MCF-7 (breast carcinoma), A549 (lung carcinoma), and HL-60 (leukemia) cells to determine their IC$_{50}$ values and create a SAR. It was interesting to note that the neutral imidazole, **I-115** , with a 2-

phenylbenzofuran substituent at the N^1 position and no substituent at the N^3 position was completely inactive, suggesting the positive charge of imidazolium salts is necessary for activity. As seen previously, the phenacyl groups were more active than the benzyl or alkyl groups. Finally, of the phenacyl groups, the naphthylacyl, 4-bromophenylacyl, and 2'-phenyl-phenacyl groups had similar activities and were the most potent of the phenacyl groups at the N^3 position.
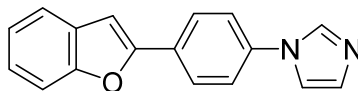
I-115

Figure I-16. Structure of 2-phenybenzofuran substituted imidazole. This compoind is from

reference 45.

Table I-17. Structures and IC_{50} values of 2-phenylbenzofuran substituted imidazolium

salts. Table modified from that in reference 45.

	R	X	SMMC-7721	SW480	MCF-7	A549	HL-60
I-115	-	-	> 40	> 40	> 40	> 40	> 40
I-116	Benzyl	Br	15.10	19.92	26.94	25.35	5.37
I-117	2-Bromobenzyl	Br	4.38	12.71	14.29	9.77	1.97
I-118	Allyl	Br	27.04	> 40	13.65	33.49	14.49
I-119	Butyl	I	12.73	> 40	31.39	21.71	11.76
I-120	Phenacyl	Br	3.71	10.34	11.90	12.94	2.61
I-121	4-Hydroxyphenacyl	Br	> 40	> 40	> 40	> 40	> 40
I-122	4-Methoxyphenacyl	Br	3.71	6.93	11.28	9.79	2.26
I-123	4-fluorophenacyl	Br	13.54	16.77	16.69	19.65	12.33
I-124	4-Bromophenacyl	Br	3.39	2.85	2.84	8.46	3.15
I-125	Naphthylacyl	Br	1.65	3.38	5.87	10.93	2.49
I-126	2'-Phenyl-phenacyl	Br	3.31	6.93	6.90	6.79	2.70

A second report considering a series of imidazolium salt hybrid compounds with 2-

phenylbenzofuran ligands was presented in 2013.[48] However, the ligands were more

specifically described as 2-phenyl-3-alkylbenzofurans and connected to the N^1 position of

the imidazole ring by the benzofuran moiety versus attachment to the phenyl ring.

Motivation for this series of compounds came from the above mentioned 2-phenybenzofuran derivatives and from the natural product ebenfuran III isolated from *Onobrychis ebenoides* which has in vitro anti-cancer activity against human breast cancer.[62] The 2-phenyl-3-alkylbenzofuran imidazolium salt hybrid compounds were exposed to a panel of human cancer cell lines in vitro including the HL-60 (leukemia), SMMC-7221 (myeloid liver carcinoma), A549 (lung carcinoma), MCF-7 (breast carcinoma), and SW480 (colon carcinoma) cell lines to determine their anti-cancer properties, which were reported as IC_{50} values, and determine a SAR (Table I-18). Several SARs were established from this large series of compounds. Several imidazole rings were compared with equivalent substituents at the N^1 and N^3 position and compounds with the 2-ethylimidazole had the lowest IC_{50} values. However, those with benzimidazole cores were also very highly active and comparable to the 2-ethylimidazole compounds. A new substituent was introduced at the N^3 position, 2-bromobenzyl, which had the highest activity compared to all other substituents at the N^3 position. Compounds with naphthylacyl substituents at the N^3 position also had high activity similar to previous reports. In conclusion, compound **I-148** had the highest anti-cancer activity with IC_{50} values ranging from 0.08 to 0.55 μM suggesting that the 2-bromobenzyl at the N^3 position and 2-ethylimidazole are essential to the high activity seen in combination with the 2-phenyl-3alkylbenzofuran substituent. The ability of **I-148** to inhibit mTOR, the mammalian target of rapamycin which is involved in cell growth and proliferation,[63] signaling was evaluated using molecular docking studies. Compound 31 was able to dock with an upstream regulator of the mTOR signaling pathway namely P13Kλ.

Table I-18. Structure and anti-cancer properties (IC$_{50}$) of 2-phenylbenzofuran imidazolium salts. Table modified from that in reference 48.
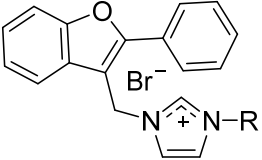
Compound	Imidazole	R	HL-60	SMMC-7721	A549	MCF-7	SW480
I-127	Imidazole	Phenacyl	2.49	9.83	> 40	15.45	15.49
I-128	Imidazole	4-Hydroxyphenacyl	> 40	> 40	> 40	> 40	> 40
I-129	Imidazole	4-Methoxyphenacyl	2.28	16.49	16.27	10.27	11.92
I-130	Imidazole	4-Fluorophenacyl	2.98	13.44	> 40	14.62	15.54
I-131	Imidazole	4-Bromophenacyl	1.57	17.77	13.76	3.65	3.36
I-132	Imidazole	Naphthylacyl	2.06	9.42	13.97	3.68	3.48
I-133	Imidazole	2-Bromobenzyl	1.86	6.61	11.23	5.58	10.35
I-134	Benzimidazole	Phenacyl	1.97	8.46	12.21	3.92	3.44
I-135	Benzimidazole	4-Hydroxyphenacyl	13.04	20.66	33.99	16.22	18.16
I-136	Benzimidazole	4-Methoxyphenacyl	0.61	16.60	9.12	23.78	> 40
I-137	Benzimidazole	4-Fluorophenacyl	2.03	9.41	11.79	3.13	3.29
I-138	Benzimidazole	4-Bromophenacyl	2.11	2.94	5.25	4.08	4.37
I-139	Benzimidazole	Naphthylacyl	2.34	2.63	4.50	3.24	3.61
I-140	Benzimidazole	Benzyl	1.96	4.81	7.09	3.49	3.26
I-141	Benzimidazole	2-Bromobenzyl	0.64	2.10	3.34	4.78	5.56
I-142	2-Ethylimidazole	Phenacyl	2.09	5.01	12.50	7.53	11.89
I-143	2-Ethylimidazole	4-Hydroxyphenacyl	13.15	13.13	27.08	17.39	> 40
I-144	2-Ethylimidazole	4-Methoxyphenacyl	0.58	11.81	12.90	3.17	5.69
I-145	2-Ethylimidazole	4-Fluorophenacyl	0.99	8.13	14.56	5.03	11.33
I-146	2-Ethylimidazole	4-Bromophenacyl	0.72	6.07	12.76	2.89	3.58
I-147	2-Ethylimidazole	Naphthylacyl	0.61	2.30	5.35	3.03	3.14
I-148	2-Ethylimidazole	2-Bromobenzyl	0.08	0.52	0.55	0.51	0.47

A modified report on the synthesis and cytotoxic activities of a series of compounds with modification made to the benzofuran ligand was published in 2013. The report focused on the use of a 2-benzylbenzofuran substituent (Table I-19).[47] Motivation for this series of hybrid compounds came from a report of modified 2-benzylbenzofuran compounds with cytotoxic activity.[64] The series of N^1-substituted 2-benzylbenzofuran hybrid imidazolium salts includes different imidazole cores and different N^3-substituted phenacyl ligands.[47] The cytotoxic activities of this series was evaluated against a panel of

human cancer cell lines in vitro including the HL-60 (leukemia), A540 (lung carcinoma), SW480 (colon carcinoma), MCF-7 (breast carcinoma), and SMMC-7721 (myeloid liver carcinoma) cell lines. Several derivatives were found to have high anti-cancer activity comparable to cisplatin. The results from the SAR study with this series of compounds suggested that the benzimidazole ring contributed to the most active compounds and, as described above, naphthylacyl and 4-methoxyphenacyl ligands at the N^3 position produced the most active derivatives.

Table I-19. Structure and anti-cancer properties of 2-phenylbenzofuran imidazolium salts.

Modified from that in reference 47.
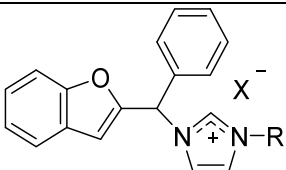
				IC$_{50}$ value (μM)				
Com-pound	Imidazole	R	X	HL-60	A549	SW 480	MCF-7	SMMC-7721
I-149	Imidazole	Allyl	Br	> 40	> 40	> 40	> 40	> 40
I-150	Imidazole	Butyl	I	> 40	> 40	> 40	> 40	> 40
I-151	Imidazole	Benzyl	Br	> 40	> 40	> 40	> 40	> 40
I-152	Imidazole	4-Nitrobenzyl	Br	> 40	> 40	> 40	> 40	> 40
I-153	Imidazole	Phenacyl	Br	> 40	> 40	> 40	> 40	> 40
I-154	Imidazole	4-Fluorophenacyl	Br	> 40	> 40	> 40	> 40	> 40
I-155	Imidazole	4-Bromophenacyl	Br	2.64	15.50	15.53	11.99	5.50
I-156	Imidazole	4-Hydroxyphenacyl	Br	> 40	> 40	> 40	> 40	> 40
I-157	Imidazole	4-Methoxyphenacyl	Br	2.99	14.60	15.43	16.13	8.47
I-158	Imidazole	Napthylacyl	Br	1.93	7.77	14.23	3.12	3.47
I-159	2-MeImidazole	Allyl	Br	> 40	> 40	> 40	> 40	> 40
I-160	2-MeImidazole	Butyl	I	> 40	> 40	> 40	> 40	> 40
I-161	2-MeImidazole	Benzyl	Br	> 40	> 40	> 40	> 40	> 40
I-162	2-MeImidazole	Phenacyl	Br	3.17	18.77	> 40	10.24	14.76
I-163	2-MeImidazole	4-Fluorophenacyl	Br	4.70	21.71	12.68	10.70	14.51
I-164	2-MeImidazole	4-Bromophenacyl	Br	3.30	26.10	14.50	15.19	11.05
I-165	2-MeImidazole	4-Hydroxyphenacyl	Br	> 40	> 40	> 40	> 40	> 40
I-166	2-MeImidazole	4-Methoxyphenacyl	Br	1.65	8.00	14.41	9.84	5.29
I-167	2-MeImidazole	Napthylacyl	Br	1.85	8.57	4.48	2.24	4.29
I-168	2-Ethylimidazole	Allyl	Br	> 40	> 40	> 40	> 40	> 40
I-169	2-Ethylimidazole	Butyl	I	> 40	> 40	> 40	> 40	> 40
I-170	2-Ethylimidazole	Benzyl	Br	2.06	6.52	3.75	5.24	7.14
I-171	2-Ethylimidazole	Phenacyl	Br	2.64	13.72	19.14	13.96	10.59
I-172	2-Ethylimidazole	4-Fluorophenacyl	Br	2.38	7.36	> 40	13.77	10.88
I-173	2-Ethylimidazole	4-Bromophenacyl	Br	2.94	14.05	15.48	9.50	6.14
I-174	2-Ethylimidazole	4-Hydroxyphenacyl	Br	> 40	> 40	> 40	> 40	> 40
I-175	2-Ethylimidazole	4-Methoxyphenacyl	Br	2.17	5.43	17.11	9.50	7.07
I-176	2-Ethylimidazole	Napthylacyl	Br	1.86	3.23	16.38	4.20	4.48
I-177	Benzimidazole	Allyl	Br	> 40	> 40	> 40	> 40	> 40
I-178	Benzimidazole	Butyl	I	2.87	12.30	29.33	15.43	7.03
I-179	Benzimidazole	Benzyl	Br	1.05	6.92	6.31	9.16	3.63
I-180	Benzimidazole	4-Nitrobenzyl	Br	10.99	> 40	14.00	16.40	11.51
I-181	Benzimidazole	Phenacyl	Br	2.69	14.38	15.45	9.59	5.34
I-182	Benzimidazole	4-Fluorophenacyl	Br	2.10	9.15	13.62	12.01	3.98
I-183	Benzimidazole	4-Bromophenacyl	Br	2.68	4.76	3.75	3.35	3.99
I-184	Benzimidazole	4-Hydroxyphenacyl	Br	> 40	> 40	> 40	> 40	> 40
I-185	Benzimidazole	4-Methoxyphenacyl	Br	1.02	3.57	3.55	2.29	3.09
I-186	Benzimidazole	Napthylacyl	Br	1.12	3.43	3.18	3.13	2.35

A study of a series of hybrid 2-alkylbenzofuran imidazolium salts derivatives was published in 2014.[51] This series of hybrid compounds was modelled after the naturally occurring benzofuran compound denthyrsin, which had anticancer activity against leukemia, breast and cervical cancers.[65] This library of compounds included the 2-alkylbenzofuran attached to the N^1 position of various imidazole cores with acyl and alkyl substituents attached to the N^3 position (Table I-20).[51] The in vitro anti-cancer properties of these 2-alkylbenzofuran derivatives were determined against the HL-60 (leukemia), SW480 (colon carcinoma), A549 (lung carcinoma), MCF-7 (breast carcinoma), and SMMC-7721 (myeloid liver carcinoma) cell lines and reported as IC_{50} values in micromolar concentration (Table I-20). Although previous results had suggested the benzimidazole core yields the best anti-cancer properties, the 2-methylimidazole and 2-ethylimidazole derivatives with naphthylacyl and methoxyphenacyl groups were the most active, such as compound **I-204** and **I-207** with IC_{50} values of 0.78 (HL-60), 0.28 (SW480), 0.37 (A549), 1.44 (MCF-7), and 11.59 (SMMC-7721) and 1.04 (HL-60), 1.03 (SW480), 4.97 (A549), 1.09 (MCF-7), and 3.50 (SMMC-7721), respectively. The authors reported that collectively, the 2-alkylbenzofuran hybrids, when compared to the 2-phenylbenzofuran hybrids, had better anti-cancer properties against the SW480, A549, and MCF-7 cells lines and worse anti-cancer properties against the HL-60 and SMMC-7721 cell lines. The authors attributed the differences in activity to steric effects and charge distribution. It was suggested that these compounds would also be able to inhibit the mTOR pathway considering **I-204** and **I-207** were able to dock with the PI3K$_\lambda$ protein using a molecular modeling approach, which is involved in the mTOR pathway.

Table I-20. The structure and anti-cancer properties of 2-alkylbenzofuran imidazolium salts. Table modified from that in reference 51.
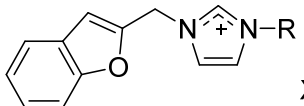
			IC$_{50}$ values (μM)				
Com-pound	Imidazole	R	HL-60	SW480	A549	MCF-7	SMMC-7721
I-187	Imidazole	Phenacyl	> 40	> 40	> 40	> 40	> 40
I-188	Imidazole	4-Methoxyphenacyl	> 40	> 40	> 40	> 40	> 40
I-189	Imidazole	4-Hydroxyphenacyl	> 40	> 40	> 40	> 40	> 40
I-190	Imidazole	4-Bromophenacyl	10.35	> 40	12.17	18.02	13.41
I-191	Imidazole	Naphthylacyl	6.27	17.06	9.95	12.70	8.08
I-192	Imidazole	2-Bromobenzyl	> 40	> 40	> 40	> 40	> 40
I-193	Imidazole	Allyl	> 40	> 40	> 40	> 40	> 40
I-194	Imidazole	Butyl	> 40	> 40	> 40	> 40	> 40
I-195	Benzimidazole	Phenacyl	> 40	> 40	> 40	> 40	> 40
I-196	Benzimidazole	4-Methoxyphenacyl	3.91	23.13	7.18	14.56	13.55
I-197	Benzimidazole	4-Hydroxyphenacyl	> 40	> 40	> 40	> 40	> 40
I-198	Benzimidazole	4-Bromophenacyl	1.69	4.20	2.54	2.46	3.58
I-199	Benzimidazole	Naphthylacyl	3.62	17.13	6.73	3.72	6.44
I-200	Benzimidazole	2'Phenyl-phenacyl	6.77	9.75	12.64	9.83	14.82
I-201	Benzimidazole	2-Bromobenzyl	2.48	14.69	2.63	7.48	6.83
I-202	Benzimidazole	Butyl	> 40	> 40	> 40	> 40	> 40
I-203	2-Methylimidazole	Phenacyl	> 40	> 40	> 40	> 40	> 40
I-204	2-Methylimidazole	4-Methoxyphenacyl	0.78	0.28	0.37	1.44	11.59
I-205	2-Methylimidazole	4-Hydroxyphenacyl	> 40	> 40	> 40	> 40	> 40
I-206	2-Methylimidazole	4-Bromophenacyl	> 40	> 40	> 40	> 40	> 40
I-207	2-Methylimidazole	Naphthylacyl	1.04	1.03	4.97	1.09	3.50
I-208	2-Methylimidazole	2'Phenyl-phenacyl	4.44	9.96	14.82	6.79	11.31
I-209	2-Methylimidazole	2-Bromobenzyl	1.28	3.89	2.96	2.24	10.22
I-210	2-Methylimidazole	Allyl	> 40	> 40	> 40	> 40	> 40
I-211	2-Ethylimidazole	Phenacyl	> 40	> 40	> 40	> 40	> 40
I-212	2-Ethylimidazole	4-Methoxyphenacyl	0.40	1.02	1.13	3.05	8.43
I-213	2-Ethylimidazole	4-Hydroxyphenacyl	> 40	> 40	> 40	> 40	> 40
I-214	2-Ethylimidazole	4-Bromophenacyl	1.87	1.34	25.65	4.47	7.51
I-215	2-Ethylimidazole	Naphthylacyl	1.45	1.69	7.44	2.59	4.26
I-216	2-Ethylimidazole	2'Phenyl-phenacyl	2.25	7.15	10.28	3.30	6.16

A paper on a series of hybrid dibenzo[b,d]furan imidazolium salts was published in 2013.[46] Motivation to substitute imidazolium salts at the N^1 position with the dibenzo[b,d]furan ligands originated from the high anticancer activity of similar natural

product compounds isolated from *Aspergillus taichungensis*.[66] This series of imidazolium salts included different imidazoles (imidazole, 2-methylimidazole, and benzimidazole), either a phenyl or methyl substituent on the methylene group bridging the N^1 position of the imidazole to the dibenzo[b,d]furan ligand, and various phenacyl substituents at the N^3 position (Table I-21 and Table I-22).[46] The in vitro anti-cancer properties of this series of compounds was evaluated against the human cancer cell lines HL-60 (leukemia), MCF-7 (breast carcinoma), A549 (lung carcinoma), SW480 (colon carcinoma), and SMMC-7221 (myeloid liver carcinoma) (Table I-23 and Table I-24). Compounds **I-265**, **I-232**, and **I-249** were found to be the most active with IC_{50} values in the nanomolar range for the HL-60 cell line and less than 4 μM for all other cell lines. The SAR study from this series of compounds also suggested that the benzimidazole ring and naphthylacyl substituent at the N^3 position were essential for the best anti-cancer properties. Also, the phenyl group versus a methyl group bound to the bridging methylene of the dibenzo[b,d]furan ligand resulted in higher activity. Compound **I-265** was also shown to induce apoptosis in SMMC-7221 cells by the Annexin V-FITC/PI double-labeled cell cytometry experiment which may have been due to **I-265** causing cell cycle arrest at the G1 phase in the cell cycle.

Table I-21. Structures of dibenzo[b,d]furan imidazolium salts with in vitro anti-cancer activity towards multiple human cancer cell lines. Table modified from that in reference 46.
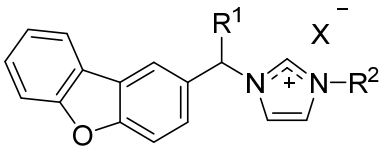
Compound	Imidazole	R^1	R^2	X
	Imidazole	Me	Butyl	I
I-217	Imidazole	Me	Butyl	I
I-218	Imidazole	Me	Benzyl	Br
I-219	Imidazole	Me	Phenacyl	Br
I-220	Imidazole	Me	4-Hydroxyphenacyl	Br
I-221	Imidazole	Me	4-Methoxyphenacyl	Br
I-222	Imidazole	Me	4-Bromophenacyl	Br
I-223	Imidazole	Me	4-Fluorophenacyl	Br
I-224	Imidazole	Me	Naphthylacyl	Br
I-225	2-Methylimidazole	Me	Butyl	I
I-226	2-Methylimidazole	Me	4-Nitrobenzyl	Br
I-227	2-Methylimidazole	Me	Phenacyl	Br
I-228	2-Methylimidazole	Me	4-Hydroxyphenacyl	Br
I-229	2-Methylimidazole	Me	4-Methoxyphenacyl	Br
I-230	2-Methylimidazole	Me	4-Bromophenacyl	Br
I-231	2-Methylimidazole	Me	4-Fluorophenacyl	Br
I-232	2-Methylimidazole	Me	Naphthylacyl	Br
I-233	Benzimidazole	Me	Butyl	I
I-234	Benzimidazole	Me	4-Nitrobenzyl	Br
I-235	Benzimidazole	Me	Phenacyl	Br
I-236	Benzimidazole	Me	4-Hydroxyphenacyl	Br
I-237	Benzimidazole	Me	4-Methoxyphenacyl	Br
I-238	Benzimidazole	Me	4-Bromophenacyl	Br
I-239	Benzimidazole	Me	4-Fluorophenacyl	Br
I-240	Benzimidazole	Me	2'phenyl-phenacyl	Br
I-241	Benzimidazole	Me	Naphthylacyl	Br
I-242	Imidazole	Ph	Butyl	I
I-243	Imidazole	Ph	4-Nitrobenzyl	Br
I-244	Imidazole	Ph	Phenacyl	Br
I-245	Imidazole	Ph	4-Hydroxyphenacyl	Br
I-246	Imidazole	Ph	4-Methoxyphenacyl	Br
I-247	Imidazole	Ph	4-Bromophenacyl	Br
I-248	Imidazole	Ph	4-Fluorophenacyl	Br
I-249	Imidazole	Ph	2'phenyl-phenacyl	Br
I-250	Imidazole	Ph	Naphthylacyl	Br
I-251	2-Methylimidazole	Ph	Butyl	I
I-252	2-Methylimidazole	Ph	4-Nitrobenzyl	Br
I-253	2-Methylimidazole	Ph	4-Hydroxyphenacyl	Br

Table I-22. Continuation of Table I-21. Structures of dibenzo[b,d]furan imidazolium salts with in vitro anti-cancer activity towards multiple human cancer cell lines. Table modified from that in reference 46.
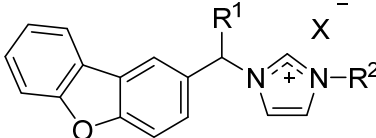
Compound	Imidazole	R^1	R^2	X
I-254	Imidazole	R^1	R^2	X
I-255	2-Methylimidazole	Ph	4-Bromophenacyl	Br
I-256	2-Methylimidazole	Ph	4-Fluorophenacyl	Br
I-257	2-Methylimidazole	Ph	Naphthylacyl	Br
I-258	Benzimidazole	Ph	Butyl	I
I-259	Benzimidazole	Ph	4-Nitrobenzyl	Br
I-260	Benzimidazole	Ph	Phenacyl	Br
I-261	Benzimidazole	Ph	4-hydroxyphenacyl	Br
I-262	Benzimidazole	Ph	4-Methoxyphenacyl	Br
I-263	Benzimidazole	Ph	4-Bromophenacyl	Br
I-264	Benzimidazole	Ph	4-Fluorophenacyl	Br
I-265	Benzimidazole	Ph	Naphthylacyl	Br

Table I-23. In vitro anti-cancer study results of dibenzo[b,d]furan imidazolium salts against

multiple human cancer cell lines. Table modified from that in reference 46.

Compound	IC$_{50}$ values (μM)				
	HL-60	MCF-7	A-549	SW480	SMMC-7721
I-217	5.63	9.11	12.81	24.11	14.17
I-218	11.35	13.80	> 40	> 40	22.48
I-219	2.55	14.09	27.01	14.43	12.05
I-220	> 40	> 40	> 40	> 40	> 40
I-221	3.45	9.02	12.21	12.68	9.98
I-222	2.95	4.08	13.74	6.85	11.02
I-223	2.64	16.74	22.64	16.41	17.51
I-224	2.46	3.50	8.46	3.69	6.43
I-225	3.08	6.60	12.96	10.04	7.98
I-226	14.55	> 40	> 40	> 40	> 40
I-227	2.85	4.49	17.89	10.07	3.02
I-228	12.19	26.42	28.58	37.45	13.33
I-229	0.70	1.29	3.02	5.78	1.43
I-230	2.67	6.77	12.85	11.80	6.40
I-231	2.96	16.24	15.41	12.28	4.70
I-232	0.60	1.655	3.86	3.09	2.15
I-233	1.67	9.41	8.55	11.06	3.78
I-234	5.93	13.75	32.30	13.42	18.41
I-235	2.46	12.51	18.10	14.55	8.51
I-236	2.35	14.15	20.06	16.27	24.07
I-237	2.05	3.42	5.95	3.18	2.95
I-238	0.66	3.08	3.54	3.18	2.62
I-239	1.67	3.85	13.65	9.77	6.31
I-240	2.79	9.35	12.71	10.52	5.40
I-241	1.65	3.14	3.46	2.95	2.24
I-242	1.10	6.03	11.44	13.05	8.13
I-243	10.82	10.32	28.55	19.07	15.32
I-244	2.14	6.29	17.66	9.05	11.41
I-245	2.61	7.05	6.80	15.16	6.28
I-246	2.09	4.12	7.27	3.76	5.59
I-247	2.13	3.32	7.70	2.11	10.83
I-248	3.00	4.00	10.15	5.16	14.49
I-249	0.52	1.46	3.75	2.36	2.38
I-250	1.91	2.78	5.86	2.57	3.61
I-251	3.81	11.89	21.37	28.43	13.05
I-252	8.74	15.30	> 40	18.22	18.50
I-253	3.92	11.76	26.21	14.33	8.84
I-254	0.59	2.42	1.90	3.73	2.08
I-255	2.25	3.45	9.46	1.98	3.93
I-256	2.13	3.23	4.88	1.89	4.22
I-257	0.98	2.31	3.78	2.62	2.57
I-258	1.12	3.37	4.61	8.00	2.93
I-259	4.60	9.26	21.68	16.70	13.18

Table I-24. Continuation of Table I-23. In vitro anti-cancer study results of dibenzo[b,d]furan imidazolium salts against multiple human cancer cell lines. Table modified from that in reference 46.

Compound	IC$_{50}$ values (μM)				
	HL-60	MCF-7	A-549	SW480	SMMC-7721
I-260	2.30	2.50	13.58	3.54	4.61
I-261	2.89	9.15	17.71	15.61	10.84
I-262	0.64	4.78	3.34	5.56	2.10
I-263	2.10	2.91	3.80	3.83	3.36
I-264	2.18	1.87	12.11	3.60	3.57
I-265	0.93	1.04	3.54	3.59	2.86

A slight modification to the dibenzo[b,d]furan hybrid imidazolium salts was reported in 2014. The report focused on a library of 2,3,5,6-tetrahydrobenzo[1,2-b:4,5-b']difuran imidazolium salt hybrids.[49] A novel tetrahydrobenzodifuran compound derived from *Cyperus rhizomes* with in vitro anti-cancer activity against human T-cell leukemia Jurkat cells[67] inspired this series of imidazolium salt hybrid compounds. This hybrid series consisted of the novel 2,3,5,6-tetrahydrobenzo[1,2-b:4,5-b']difuran ligand at the N^1 position; a variety of imidazoles including imidazole, 2-methylimidazole, benzimidazole, and 5,6-dimethylbenzimidazole; and substituted benzyl substitutents, substituted phenacyl substitutents, and a new substituent, 2-naphthylmethyl, at the N^3 position (Table I-25).[49] The in vitro anti-cancer properties of these hybrid imidazolium salts were evaluated against the HL-60 (myeloid leukemia), MCF-7 (breast carcinoma), SW480 (colon carcinoma), A549 (lung carcinoma), and SMMC-7221 (liver carcinoma) human cancer cell lines (Table I-25). Results from the in vitro studies against this panel of human cancer cell lines suggested the 5,6-dimethylbenzimidazole and the 2-naphthylmethyl substituent at the N^3 position contributed to form the most active compound, **I-297**, of the series with IC$_{50}$ values

of 0.26 μM (HL-60), 0.20 μM (MCF-7), 0.26 μM (SW480), 0.83 μM (A549), and 1.81 μM (SMMC-7721). It was thought that **I-297** may also be able to inhibit the mTOR pathway considering it was shown to dock with the PI3K protein using a molecular modeling approach.

Table I-25. Structures and IC$_{50}$ values of 2,3,5,6-tetrahydrobenzo[1,2-b:4,5-b']difuran imidazolium salt hybrid compounds. Table modified from that in reference 49.
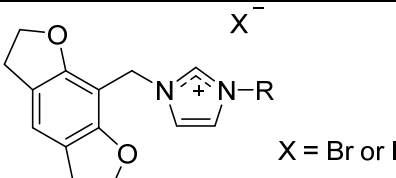
| Com-pound | Imidazole | R | IC$_{50}$ (μM) | | | | |
			HL-60	MCF-7	SW 480	A549	SMMC-7721
I-266	Imidazole	Benzyl	12.27	16.70	25.07	32.92	> 40
I-267	Imidazole	4-Methylbenzyl	1.84	3.49	4.72	6.64	10.28
I-268	Imidazole	4-Bromobenzyl	2.22	12.16	15.67	34.29	28.60
I-269	Imidazole	4-Nitrobenzyl	> 40	> 40	> 40	> 40	> 40
I-270	Imidazole	2-Naphthylmethyl	1.13	2.90	3.62	7.22	10.49
I-271	Imidazole	Phenacyl	> 40	> 40	> 40	> 40	> 40
I-272	Imidazole	4-Bromophenacyl	3.66	14.65	17.46	39.93	> 40
I-273	Imidazole	4-Methoxyphenacyl	> 40	> 40	> 40	> 40	> 40
I-274	Imidazole	Naphthylacyl	1.09	3.43	4.63	9.08	9.02
I-275	2-Methylimidazole	Benzyl	3.96	15.79	9.65	11.48	17.17
I-276	2-Methylimidazole	4-Methylbenzyl	0.63	6.98	3.50	3.39	2.59
I-277	2-Methylimidazole	4-Bromobenzyl	0.77	3.46	10.08	7.81	13.08
I-278	2-Methylimidazole	4-Nitrobenzyl	> 40	> 40	> 40	> 40	> 40
I-279	2-Methylimidazole	2-Naphthylmethyl	0.51	0.65	3.89	1.86	3.36
I-280	2-Methylimidazole	Phenacyl	3.61	18.80	32.26	32.80	> 40
I-281	2-Methylimidazole	4-Bromophenacyl	1.99	4.26	13.85	10.22	15.03
I-282	2-Methylimidazole	4-Methoxyphenacyl	0.82	4.66	15.11	5.82	6.45
I-283	2-Methylimidazole	Naphthylacyl	1.04	1.21	4.61	3.61	7.64
I-284	Benzimidazole	Butyl	1.65	1.58	4.06	9.60	8.56
I-285	Benzimidazole	Benzyl	1.21	0.80	2.45	3.83	5.48
I-286	Benzimidazole	4-Methylbenzyl	0.42	0.27	0.92	0.96	2.13
I-287	Benzimidazole	4-Bromobenzyl	0.58	2.36	1.84	3.58	7.45
I-288	Benzimidazole	2-Naphthylmethyl	0.31	1.13	0.57	0.55	1.35
I-289	Benzimidazole	Phenacyl	2.03	5.16	3.77	3.16	8.22
I-290	Benzimidazole	4-Bromophenacyl	1.17	1.60	3.20	5.44	6.41
I-291	Benzimidazole	4-Methoxyphenacyl	0.87	2.96	2.75	5.63	5.13
I-292	Benzimidazole	Naphthylacyl	0.83	1.19	2.93	3.30	5.17
I-293	5,6-DiMe Benz	Butyl	0.57	0.94	0.89	1.48	1.25
I-294	5,6-DiMe Benz	Benzyl	0.50	0.69	1.01	1.62	0.73
I-295	5,6-DiMe Benz	4-Methylbenzyl	0.40	0.65	0.64	1.06	2.21
I-296	5,6-DiMe Benz	4-Bromobenzyl	0.79	0.97	0.96	1.45	1.81
I-297	5,6-DiMe Benz	2-Naphthylmethyl	0.26	0.20	0.26	0.83	1.81
I-298	5,6-DiMe Benz	Phenacyl	1.23	1.04	1.21	4.39	3.97
I-299	5,6-DiMe Benz	4-Bromophenacyl	1.18	1.02	1.63	4.13	3.07
I-300	5,6-DiMe Benz	4-Methoxyphenacyl	0.95	0.61	1.41	2.55	4.89
I-301	5,6-DiMe Benz	Naphthylacyl	0.98	0.83	1.36	3.28	3.92

Another study in 2014 revealed a series of 1-(indol-3-yl)methyl hybrid imidazolium salts with anti-cancer properties.[50] The 1-(indol-3-yl)methyl ligand was incorporated into the hybrid imidazolium salts because of indole-based compounds in the literature with high anti-cancer activity against lung cancer.[68] The series of hybrid imidazolium salts has the 1-(indol-3-yl)methyl ligand at the N^1 position; imidazole, 2-methylimidazole, benzimidazole, or a 5,6-dimethylbenzimidazole imidazole core; and various phenacyl groups at the N^3 position (Table I-26). The in vitro anti-cancer properties of these indole-based imidazolium salts were evaluated against the HL-60 (leukemia), SMMC-7721 (myeloid liver carcinoma), A549 (lung carcinoma), MCF-7 (breast carcinoma), and SW480 (colon carcinoma) human cancer cell lines (Table I-27). These indole compounds were not as active as the previously described benzodifuran derivatives; however, the most active compounds used the 5,6-dimethylbenzimidazole and naphthylacyl substituent at the N^3 position similar to previously described compounds. There was no difference in the observed activities between compounds only differing in structure by either the 'Ts' or 'Boc' substituent bound to the indole nitrogen. The most active compound was compound **I-328** with a naphthylacyl-substituent and the 5,6-dimethylbenzimidazole core. Compound **I-328** was also able to induce apoptosis as determined by an Annexin V-FITC/PI double-labelled cell cytometry experiment with 48% apoptotic cells at 24 hours from 16 μM compound exposure. With a slight increase in the percentage of cells in the S phase of the cell cycle in a cell cycle analysis assay, authors suggest that **I-328** may induce S phase arrest. [50]

Table I-26. Structures of 1-(indol-3-yl)methyl hybrid imidazolium salt hybrid compounds with anti-cancer properties. Table modified from that in reference 50.
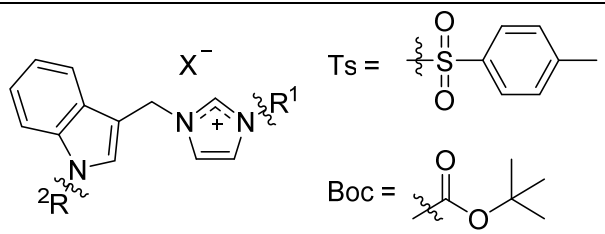
Compound	Imidazole	R	R^2
I-302	2-Methylimidazole	Phenacyl	Ts
I-303	2-Methylimidazole	4-Hydroxyphenacyl	Ts
I-304	2-Methylimidazole	4-Methoxyphenacyl	Ts
I-305	2-Methylimidazole	4-Bromophenacyl	Ts
I-306	2-Methylimidazole	Naphthylacyl	Ts
I-307	Benzimidazole	Phenacyl	Ts
I-308	Benzimidazole	4-Hydroxyphenacyl	Ts
I-309	Benzimidazole	4-Methoxyphenacyl	Ts
I-310	Benzimidazole	4-Bromophenacyl	Ts
I-311	Benzimidazole	Naphthylacyl	Ts
I-312	2-Methylimidazole	Phenacyl	Ts
I-313	2-Methylimidazole	4-Hydroxyphenacyl	Ts
I-314	2-Methylimidazole	4-Methoxyphenacyl	Ts
I-315	2-Methylimidazole	4-Bromophenacyl	Ts
I-316	2-Methylimidazole	Naphthylacyl	Ts
I-317	5,6-Dimethylbenzimidazole	Phenacyl	Ts
I-318	5,6-Dimethylbenzimidazole	4-Hydroxyphenacyl	Ts
I-319	5,6-Dimethylbenzimidazole	4-Methoxyphenacyl	Ts
I-320	5,6-Dimethylbenzimidazole	4-Bromophenacyl	Ts
I-321	5,6-Dimethylbenzimidazole	Naphthylacyl	Ts
I-322	Benzimidazole	Phenacyl	Boc
I-323	Benzimidazole	4-Hydroxyphenacyl	Boc
I-324	Benzimidazole	4-Methoxyphenacyl	Boc
I-325	Benzimidazole	4-Bromophenacyl	Boc
I-326	Benzimidazole	Naphthylacyl	Boc
I-327	5,6-Dimethylbenzimidazole	4-Hydroxyphenacyl	Boc
I-328	5,6-Dimethylbenzimidazole	Naphthylacyl	Boc

Table I-27. Results from an anti-cancer study of 1-(indol-3-yl)methyl hybrid imidazolium salts. Table modified from that in reference 50.

Compound	IC$_{50}$ values (µM)				
	HL-60	SMMC-7721	A549	MCF-7	SW480
I-302	3.80	15.88	18.35	14.11	17.79
I-303	11.03	22.04	18.76	> 40	> 40
I-304	2.15	10.40	11.38	4.35	15.11
I-305	2.92	34.68	19.08	16.71	> 40
I-306	3.63	17.56	8.85	19.66	> 40
I-307	9.55	13.99	12.77	16.33	16.01
I-308	17.96	> 40	> 40	> 40	> 40
I-309	2.65	12.84	13.60	10.50	16.38
I-310	2.85	12.24	7.78	3.70	12.55
I-311	3.24	13.76	16.31	5.44	16.01
I-312	4.53	13.75	12.29	11.52	15.35
I-313	12.72	> 40	> 40	> 40	> 40
I-314	1.89	7.43	9.83	7.06	15.52
I-315	4.03	11.61	13.06	16.37	17.23
I-316	2.32	10.49	10.81	3.23	13.23
I-317	7.11	14.92	14.22	13.54	17.25
I-318	17.59	> 40	> 40	> 40	> 40
I-319	3.00	10.11	10.70	5.01	14.43
I-320	3.03	9.30	11.45	3.16	5.51
I-321	2.74	9.03	8.25	3.17	10.12
I-322	11.82	14.45	17.38	15.44	17.02
I-323	> 40	> 40	> 40	> 40	> 40
I-324	4.57	13.59	10.72	15.11	16.76
I-325	10.55	13.34	10.67	15.88	17.92
I-326	3.09	11.18	4.81	6.81	16.06
I-327	15.24	19.10	25.01	22.29	> 40
I-328	2.48	3.60	3.51	3.19	11.57

A report on a series of 2-substituted indoline hybrid imidazolium salts, related to the indole hybrid imidazolium salts discussed above, was published in 2015.[52] Compounds bearing a 2-substituted indoline moiety had anti-cancer activity against multiple cancer cell types in vitro including breast, colon, lung, and renal cancers.[69,70] These compounds served

as inspiration to incorporate indoline moieties into hybrid imidazolium salts as potential chemotherapeutics. The series of indoline substituted imidazolium salts including the 2-substituted indoline at the N^1 position of the imidazole also included numerous imidazole rings (imidazole, benzimidazole, 2-methylbenzimidazole, and 5,6-dimethylbenzimidazole) and phenacyl or alkyl substituents at the N^3 position of the imidazole (Table I-28). The in vitro anti-cancer properties of this series of hybrids was evaluated against a panel of human cancer cell lines including the HL-60 (myeloid leukemia), A549 (lung carcinoma), SMMC-7721 (liver carcinoma), MCF-7 (breast carcinoma), and SW480 (colon carcinoma) cell lines (Table I-28). The cytotoxic activities of numerous derivatives were very high and comparable to other hybrid imidazolium salts. The most active compounds contained a substituted benzimidazole ring (2-methylbenzimidazole or 4,5-dimethylbenzimidazole) and a naphthylacyl or 2-naphthylmethyl substituent at the N^3 position. Compound **I-346** comprising a 2-methylbenzimidazole and naphthylacyl group at the N^3 position had the best cytotoxic activity with IC_{50} values of 0.24 μM (HL-60), 0.98 μM (A549), 1.09 μM (SMMC-7721), 1.13 μM (MCF-7), and 1.18 μM (SW480). Compound **I-346** was shown to induce apoptosis in a higher percentage of cells than negative control cells in a dose-dependent manner after 48 hours using the Annexin V-FITC/PI double-labelled cell cytometry experiment.

Table I-28. Structures and results from an anti-cancer study of 2-substituted indoline hybrid imidazolium salts. Table modified from that in reference 52.
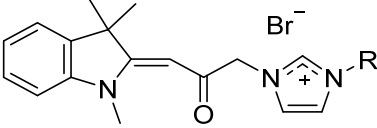
Com-pound	Imidazole	R	HL-60	SMMC-7721	A549	MCF-7	SW480
							IC$_{50}$ values (µM)
I-329	Imidazole	2-Bromobenzyl	0.69	5.45	3.00	6.33	11.71
I-330	Imidazole	Phenacyl	3.54	22.13	> 40	22.39	> 40
I-331	Imidazole	4-Bromophenacyl	2.20	8.42	15.48	10.45	18.48
I-332	Imidazole	4-Methoxyphenacyl	1.84	5.70	10.77	23.90	15.59
I-333	Imidazole	Naphthylacyl	0.73	2.45	8.37	3.37	9.29
I-334	Benzimidazole	4-Methylbenzyl	0.70	1.98	2.93	2.96	4.54
I-335	Benzimidazole	2-Bromobenzyl	0.39	1.10	1.21	3.96	2.54
I-336	Benzimidazole	2-Naphthylmethyl	0.47	1.10	1.40	1.91	2.23
I-337	Benzimidazole	Phenacyl	2.03	10.26	16.95	23.76	15.64
I-338	Benzimidazole	4-Bromophenacyl	1.48	5.80	8.41	3.76	4.47
I-339	Benzimidazole	Naphthylacyl	0.67	2.13	2.85	4.47	2.85
I-340	2-Methylbenzimidazole	4-Methylbenzyl	0.24	1.09	0.77	2.03	4.95
I-341	2-Methylbenzimidazole	2-Bromobenzyl	0.29	1.29	0.96	1.68	1.86
I-342	2-Methylbenzimidazole	2-Naphthylmethyl	0.40	0.87	1.02	1.92	2.04
I-343	2-Methylbenzimidazole	Phenacyl	1.86	4.46	10.64	8.04	5.49
I-344	2-Methylbenzimidazole	4-Bromophenacyl	0.69	3.01	8.25	1.95	4.19
I-345	2-Methylbenzimidazole	4-Methoxyphenacyl	0.43	1.03	2.78	2.17	1.71
I-346	2-Methylbenzimidazole	Naphthylacyl	0.24	1.09	0.98	1.13	1.18
I-347	5,6-dimethylbenzimidazole	4-Methylbenzyl	0.41	0.75	0.64	2.06	2.02
I-348	5,6-dimethylbenzimidazole	2-Bromobenzyl	0.60	1.27	0.89	1.38	2.04
I-349	5,6-dimethylbenzimidazole	2-Naphthylmethyl	0.69	1.21	1.21	1.20	2.34
I-350	5,6-dimethylbenzimidazole	Phenacyl	0.64	2.45	3.74	2.36	3.84
I-351	5,6-dimethylbenzimidazole	4-Bromophenacyl	0.94	2.44	4.28	2.42	2.74
I-352	5,6-dimethylbenzimidazole	4-Methoxyphenacyl	0.38	1.88	1.67	2.50	3.46
I-353	5,6-dimethylbenzimidazole	Naphthylacyl	0.47	1.11	1.82	1.83	2.33

A modification to the dibenzo[b,d]furan ligand discussed above came in the form of a fluorene ligand in a series of hybrid imidazolium salts with a 3-substituted fluorene

ligand incorporated at the N^1 position of the imidazolium salts.[54] Several compounds with the fluorene ligand, such as the natural peptide Ixorapeptide, isolated from *Ixora cocinea*,[71] have in vitro anti-cancer activity against liver, breast, and colon cancer cells.[72] These compounds encouraged the synthesis of this new hybrid series of imidazolium salts that utilize various imidazoles (imidazole, 2-methylimidazole, benzimidazole, 2-methylbenzimidazole, and 5,6-dimethylbenzimidazole) and various phenacyl or alkyl groups at the N^3 position in addition to the fluorene substituent at the N^1 position (Table I-29).[54] The in vitro anti-proliferative effects of this hybrid series of compounds was evaluated against several human tumor cell lines including the HL-60 (myeloid leukemia), SMCC7721 (liver carcinoma), A549 (lung carcinoma), MCF-7 (breast carcinoma), and SW480 (colon carcinoma) cell lines (Table I-29). Results suggested that the substituted benzimidazoles (2-methylbenzimidazole and 4,5-dimethylbenzimidazole) and the naphthylacyl and 4-methoxyphenacyl ligands at the N^3 position contributed to form the most potent derivatives of the compounds tested. Compounds **I-368**, **I-375**, and **I-380** were also exposed to normal lung epithelial cells, the BEAS-2B cell line, to determine their toxicity to healthy tissue. Only compound **I-368** had an appreciable difference in the IC_{50} value when compared to the cancerous cell line A549 (16.26 μM for BEAS-2B and 2.58 μM for A549).

Table I-29. Structures and evaluation of the anti-cancer properties of hybrid imidazolium salts with a 3-substitueted fluorene ligand. Table modified from that in reference 54.
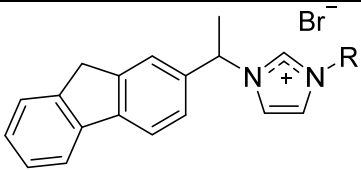
Com-pound	Imidazole	R	HL-60	SMMC-7721	A549	MCF-7	SW480
			IC$_{50}$ value (µM)				
I-354	Imidazole	4-Bromophenyl	2.17	6.76	10.45	4.42	11.94
I-355	Imidazole	Phenacyl	3.49	18.08	23.41	17.68	13.74
I-356	Imidazole	4-Bromophenacyl	1.75	5.34	4.02	3.03	3.85
I-357	Imidazole	4-Fluorphenacyl	2.92	16.49	15.29	15.70	12.56
I-358	Imidazole	4-Methoxyphenacyl	1.10	7.56	9.38	4.52	9.00
I-359	Imidazole	Naphthylacyl	1.01	4.13	3.40	3.17	3.44
I-360	2-Methylimidazole	4-Bromobenzyl	1.09	4.47	6.75	6.64	11.03
I-361	2-Methylimidazole	Phenacyl	1.47	8.25	11.01	12.35	13.11
I-362	2-Methylimidazole	4-Bromophenacyl	1.90	8.80	9.06	7.92	12.68
I-363	2-Methylimidazole	4-Methoxyphenacyl	0.52	2.70	2.86	3.01	10.84
I-364	2-Methylimidazole	Naphthylacyl	0.79	2.65	2.15	2.92	8.89
I-365	Benzimidazole	4-Bromobenzyl	0.74	3.42	4.05	2.61	3.14
I-366	Benzimidazole	Phenacyl	0.76	4.54	8.84	3.17	2.89
I-367	Benzimidazole	4-Bromophenacyl	1.38	3.40	3.01	2.30	3.25
I-368	Benzimidazole	4-Methoxyphenacyl	0.56	2.22	2.58	1.80	2.54
I-369	Benzimidazole	Naphthylacyl	1.23	3.23	4.04	2.44	3.11
I-370	2-Methylbenzimidazole	4-Bromobenzyl	0.60	2.38	3.64	2.78	2.15
I-371	2-Methylbenzimidazole	Phenacyl	0.63	1.97	4.49	2.58	2.43
I-372	2-Methylbenzimidazole	4-Bromophnacyl	0.81	2.43	4.63	3.43	2.82
I-373	2-Methylbenzimidazole	4-Fluorophenacyl	0.68	5.47	9.08	3.12	2.72
I-374	2-Methylbenzimidazole	4-Methoxyphenacyl	0.59	2.04	2.47	2.79	2.28
I-375	2-Methylbenzimidazole	Naphthylacyl	0.57	1.38	1.82	2.51	2.36
I-376	5,6-Dimethylbenzimidazole	4-Bromobenzyl	0.45	2.17	2.62	2.99	3.04
I-377	5,6-Dimethylbenzimidazole	Phenacyl	0.68	2.44	3.43	3.14	3.28
I-378	5,6-Dimethylbenzimidazole	4-Bromophenacyl	0.58	2.30	3.25	2.79	2.70
I-379	5,6-Dimethylbenzimidazole	4-Fluorophenacyl	1.78	2.82	6.74	3.71	4.43
I-380	5,6-Dimethylbenzimidazole	4-Methoxyphenacyl	0.50	1.69	1.61	2.41	2.41
I-381	5,6-Dimethylbenzimidazole	Naphthylacyl	0.87	2.31	2.59	3.02	3.04

A study of a series of hybrid imidazolium salts with carbazole ligands, a similar structure to the dibenzo[b,d]furan and fluorene moiety, at the N^1 position of the imidazole ring was published in 2015.[53] Motivation for this series of compounds came from natural product compounds containing the carbazole ligand isolated from the roots of *Clausena harmandiana*.[73] Each compound in this hybrid series contained a carbazole moiety linked to the N^1 position of the imidazole ring by a three, four, or five carbon chain; an imidazole, benzimidazole, or 5,6-dimethylbenzimidazole; and a phenacyl or alkyl substituent at the N^3 position (Table I-30 and Table I-31).[53] The in vitro cytotoxic activities of each carbazole-imidazolium salt was evaluated against several human cancer cell lines including the HL-60 (myeloid leukemia), SMMC-7721 (liver carcinoma), A549 (lung cancer), MCF-7 (breast cancer), and the SW480 (colon cancer) cell lines to create a SAR (Table I-32 and Table I-33). Compounds with the 5,6-dimethylbenzimidazole and either a 2-bromobenzyl or naphthylacyl substituent at the N^3 position were the most active. Compound **I-429** was the most active with IC$_{50}$ values of 0.51 μM (HL-60), 1.40 μM (MCF-7), 2.38 μM (SMMC-7721), 2.48 μM (SW480), and 3.12 μM (A549). Compound **I-429** was also shown to induce apoptosis at a significantly higher rate than negative control in a dose-dependent manner and cause G2/M phase cell cycle arrest.

Table I-30. Structures of carbazole-substituted imidazolium salts with anti-cancer properties. Table modified from that in reference 53.
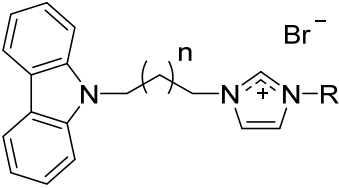
Compound	Imidazole	n	R
I-382	Imidazole	1	Phenacyl
I-383	Imidazole	1	4-Methoxyphenacyl
I-384	Imidazole	1	Naphthylacyl
I-385	Imidazole	1	4-Bromophenacyl
I-386	Imidazole	1	4-Bromobenzyl
I-387	Imidazole	1	4-Methylbenzyl
I-388	Benzimidazole	1	Phenacyl
I-389	Benzimidazole	1	4-Methoxyphenacyl
I-390	Benzimidazole	1	Naphthylacyl
I-391	Benzimidazole	1	4-Bromobenzyl
I-392	Benzimidazole	1	4-Methylbenzyl
I-393	Benzimidazole	1	2-Bromobenzyl
I-394	5,6-Dimethylbenzimidazole	1	Naphthylacyl
I-395	5,6-Dimethylbenzimidazole	1	4-Methoxyphenacyl
I-396	5,6-Dimethylbenzimidazole	1	4-Methylbenzyl
I-397	Imidazole	2	Naphthylacyl
I-398	Imidazole	2	4-Methoxyphenacyl
I-399	Imidazole	2	4-Bromophenacyl
I-400	Imidazole	2	Phenacyl
I-401	Imidazole	2	4-Methylbenzyl
I-402	Imidazole	2	2-Bromobenzyl
I-403	Benzimidazole	2	Naphthylacyl
I-404	Benzimidazole	2	4-Methoxyphenacyl
I-405	Benzimidazole	2	4-Bromophenacyl
I-406	Benzimidazole	2	Phenacyl
I-407	Benzimidazole	2	4-Methylbenzyl
I-408	Benzimidazole	2	2-Bromobenzyl
I-409	5,6-Dimethylbenzimidazole	2	Naphthylacyl
I-410	5,6-Dimethylbenzimidazole	2	4-Methoxyphenacyl
I-411	5,6-Dimethylbenzimidazole	3	4-Bromophenacyl
I-412	5,6-Dimethylbenzimidazole	3	Phenacyl
I-413	5,6-Dimethylbenzimidazole	3	2-Bromobenzyl
I-414	5,6-Dimethylbenzimidazole	3	4-Methylbenzyl
I-415	Imidazole	3	4-Methoxyphenacyl
I-416	Imidazole	3	Naphthylacyl
I-417	Imidazole	3	4-Methylbenzyl
I-418	Benzimidazole	3	Phenacyl
I-419	Benzimidazole	3	4-Methoxyphenacyl

Table I-31. Continuation of Table I-30. Structures of carbazole-substituted imidazolium salts with anti-cancer properties. Table modified from that in reference 53.
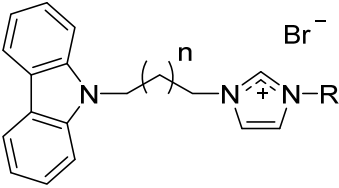
Compound	Imidazole	n	R
I-420	Benzimidazole	3	Naphthylacyl
I-421	Benzimidazole	3	4-Bromophenacyl
I-422	Benzimidazole	3	4-Methylbenzyl
I-423	Benzimidazole	3	2-Bromobenzyl
I-424	5,6-Dimethylbenzimidazole	3	Phenacyl
I-425	5,6-Dimethylbenzimidazole	3	4-Methoxyphenacyl
I-426	5,6-Dimethylbenzimidazole	3	Naphthylacyl
I-427	5,6-Dimethylbenzimidazole	3	4-Bromophenacyl
I-428	5,6-Dimethylbenzimidazole	3	4-Methylbenzyl
I-429	5,6-Dimethylbenzimidazole	3	2-Bromobenzyl

Table I-32. Results from the anti-cancer study of carbazole-substituted imidazolium salts against several human cancer cell lines. Table modified from that in reference 53.

Compound	HL-60	SMMC-7721	A549	MCF-7	SW480
I-382	6.23	24.62	> 40	12.39	> 40
I-383	2.44	13.83	25.11	8.78	19.61
I-384	2.79	6.99	15.4	4.60	9.53
I-385	3.38	11.89	19.62	8.74	12.49
I-386	3.09	13.48	24.78	8.25	12.20
I-387	2.15	13.65	19.82	6.90	14.98
I-388	3.22	15.79	25.87	13.99	15.00
I-389	2.28	11.58	15.57	5.92	12.26
I-390	2.80	3.27	5.65	2.69	3.28
I-391	2.95	15.67	18.19	3.88	9.57
I-392	1.17	10.24	12.66	3.85	5.22
I-393	1.94	8.54	12.24	3.78	7.41
I-394	1.74	3.19	3.89	2.66	3.32
I-395	1.99	6.59	11.11	2.46	3.38
I-396	9.93	4.89	9.14	10.10	13.67
I-397	ND	ND	ND	ND	ND
I-398	1.34	8.41	11.07	2.54	11.74
I-399	2.42	10.22	15.70	3.95	14.16
I-400	2.98	11.69	19.04	19.98	16.39
I-401	0.84	5.74	3.92	2.24	9.56
I-402	0.49	3.04	2.92	1.95	4.33
I-403	2.37	3.53	2.80	2.41	3.33
I-404	0.56	2.78	5.16	2.39	3.37
I-405	2.30	3.56	3.74	2.54	2.80
I-406	0.98	6.32	12.94	2.98	3.84
I-407	2.60	3.57	3.15	2.32	3.59
I-408	0.71	3.66	3.58	2.14	3.08
I-409	3.34	2.41	3.16	1.65	2.50
I-410	3.71	2.34	3.60	1.78	2.31
I-411	1.80	3.71	4.40	3.35	3.38
I-412	0.56	3.74	6.32	2.88	2.97
I-413	0.54	2.78	2.83	4.49	5.62
I-414	0.70	3.30	3.10	4.10	6.58
I-415	0.68	6.34	4.83	3.04	8.69
I-416	0.87	2.93	2.99	2.59	4.50
I-417	0.55	3.05	2.29	1.91	4.45
I-418	2.67	5.41	14.03	3.13	3.83
I-419	0.66	2.16	2.80	1.60	2.43
I-420	1.36	2.58	3.02	2.25	3.40
I-421	2.19	2.88	3.89	3.88	3.39
I-422	0.57	2.55	2.65	2.82	3.19
I-423	0.64	2.16	3.00	2.39	2.54
I-424	1.25	3.31	4.19	3.21	3.48
I-425	0.94	2.83	3.39	2.50	3.58

Table I-33. Continuation of Table I-32. Results from the anti-cancer study of carbazole-substituted imidazolium salts against several human cancer cell lines. Table modified from that in reference 53.

Compound	HL-60	SMMC-7721	A549	MCF-7	SW480
I-426	0.76	2.21	2.98	1.94	3.23
I-427	2.60	2.71	3.74	3.32	3.64
I-428	0.56	2.00	2.84	2.10	2.88
I-429	0.51	2.38	3.12	1.40	2.48

A paper on a series of hybrid tetrahydro-β-carboline-imiazolium salts was published in 2016.[6] These compounds were modelled from compounds that contain the tetrahydro-β-carboline moiety and have medicinal, specifically anti-cancer, applications in the literature.[74] The structures of compounds in this hybrid series entails the tetrahydro-β-carboline moiety linked to the N^1 position of the imidazole ring by a ethylacyl group; an imidazole, benzimidazole, 2-ethylimidazole, or 5,6-dimethylbenzimidazole; and alkyl or phenacyl groups at the N^3 position (Table I-34). The in vitro anti-cancer properties were evaluated against a panel of human cancer cell lines including the HL-60 (myeloid leukemia), SMMC-7721 (liver carcinoma), A549 (lung carcinoma), MCF-7 (breast carcinoma), and SW480 (colon carcinoma) cell lines (Table I-35). The most active compounds of this series were those with the 5,6-dimethylbenzimidazole ring and either a 2-naphthylmethyl or naphthyacyl substituent at the N^3 position as with compound **I-459** whose IC_{50} values were 2.61 μM (HL-60), 14.15 μM (A549), 17.13 μM (SMMC-7721), 2.79 μM (MCF-7), and 9.46 μM (SW480). These values are higher, suggesting the compound is less active, than the previous published hybrid imidazolium salts with different substituents at the N^1 position; however, **I-459** had an IC_{50} of > 40 μM against

62

the normal lung epithelial cell line BEAS-2B, compared to 17.13 μM for the cancerous A549 cell line, suggesting the compound may exhibit selective cytotoxicity towards cancerous tissue. Compound **I-459** induced apoptosis at a significantly higher rate in a dose-dependent manner than cells treated with no drug and caused cell cycle arrest at the G1 phase.

Table I-34. Structures of tetrahydro-β-carboline hybrid imidazolium salts. Table modified from that in reference 6.
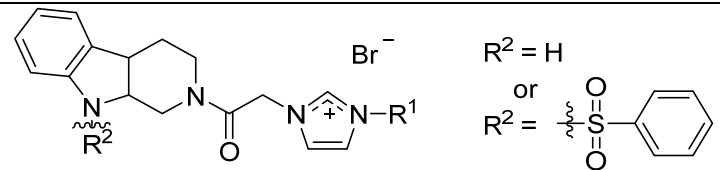
Compound	R^1	Imidazole	R^2
I-430	Phenacyl	Imidazole	H
I-431	Naphthylacyl	Imidazole	H
I-432	Phenacyl	Benzimidazole	H
I-433	4-Methoxyphenacyl	Benzimidazole	H
I-434	4-Bromophenacyl	Benzimidazole	H
I-435	Naphthylacyl	Benzimidazole	H
I-436	4-Bromobenzyl	Benzimidazole	H
I-437	4-Nitrobenzyl	Benzimidazole	H
I-438	2-Naphthylmethyl	Benzimidazole	H
I-439	Phenacyl	Imidazole	PhSO$_2$
I-440	Naphthylacyl	Imidazole	PhSO$_2$
I-441	Phenacyl	2-Ethylimidazole	PhSO$_2$
I-442	4-Bromophenacyl	2-Ethylimidazole	PhSO$_2$
I-443	Naphthylacyl	2-Ethylimidazole	PhSO$_2$
I-444	4-Methylbenzyl	2-Ethylimidazole	PhSO$_2$
I-445	2-Naphthylmethyl	2-Ethylimidazole	PhSO$_2$
I-446	Phenacyl	Benzimidazole	PhSO$_2$
I-447	4-Bromophenacyl	Benzimidazole	PhSO$_2$
I-448	4-Methoxyphenacyl	Benzimidazole	PhSO$_2$
I-449	Naphthylacyl	Benzimidazole	PhSO$_2$
I-450	4-Methylbenzyl	Benzimidazole	PhSO$_2$
I-451	4-Nitrobenzyl	Benzimidazole	PhSO$_2$
I-452	2-Napthylmethyl	Benzimidazole	PhSO$_2$
I-453	Phenacyl	5,6-Dimethylbenzimidazole	PhSO$_2$
I-454	4-Bromophenacyl	5,6-Dimethylbenzimidazole	PhSO$_2$
I-455	4-Methoxyphenacyl	5,6-Dimethylbenzimidazole	PhSO$_2$
I-456	Naphthylacyl	5,6-Dimethylbenzimidazole	PhSO$_2$
I-457	4-Methylbenzyl	5,6-Dimethylbenzimidazole	PhSO$_2$
I-458	4-Nitrobenzyl	5,6-Dimethylbenzimidazole	PhSO$_2$
I-459	2-Naphthylmethyl	5,6-Dimethylbenzimidazole	PhSO$_2$

Table I-35. IC$_{50}$ values of tetrahydro-β-carboline hybrid imidazolium salts. Table modified from that in reference 6.

Compound	IC$_{50}$ values (μM)				
	HL-60	SMMC-7721	A549	MCF-7	SW480
I-430	> 40	> 40	> 40	> 40	> 40
I-431	> 40	> 40	> 40	> 40	> 40
I-432	> 40	> 40	> 40	> 40	> 40
I-433	> 40	> 40	> 40	> 40	> 40
I-434	21.81	27.59	> 40	20.47	32.35
I-435	11.09	19.80	> 40	17.56	16.69
I-436	10.68	30.39	> 40	19.51	> 40
I-437	> 40	> 40	> 40	> 40	> 40
I-438	3.54	13.23	18.02	12.24	17.46
I-439	> 40	> 40	> 40	> 40	> 40
I-440	3.32	12.11	14.21	3.74	11.80
I-441	> 40	> 40	> 40	> 40	> 40
I-442	11.87	16.77	> 40	8.28	35.62
I-443	2.47	10.67	13.39	10.44	10.14
I-444	2.56	12.48	22.13	3.37	11.84
I-445	2.77	12.81	14.16	2.61	12.81
I-446	14.39	24.60	21.41	16.44	13.60
I-447	10.61	17.28	31.23	16.59	11.81
I-448	3.97	14.95	18.27	11.34	13.58
I-449	3.24	15.03	8.78	8.05	11.01
I-450	3.04	14.78	17.01	7.68	11.70
I-451	13.58	23.35	35.36	17.42	12.44
I-452	4.34	14.74	17.28	10.33	11.76
I-453	10.18	14.50	22.75	11.26	13.19
I-454	3.75	15.30	> 40	4.97	10.47
I-455	3.39	13.18	23.70	8.23	16.37
I-456	3.08	14.77	> 40	3.90	16.17
I-457	4.30	15.13	29.52	10.17	14.20
I-458	12.81	33.19	> 40	10.81	> 40
I-459	2.61	14.15	17.13	2.79	9.46

In 2011, Gopalan et al. published a study of three imidazolium salts which presented their in vitro anti-cancer properties against hepatocellular carcinoma, mechanism of action evaluation, and an in vivo hepatocellular carcinoma study in mice.[75] The three

imidazolium salts were either symmetrically substituted with a benzyl or isopropyl substituent at both the N^1 and N^3 positions, **I-460** and **I-461**, respectively, or asymmetrically substituted with a mesityl substituent at the N^1 position and a 4-acetate-benzyl substituent at the N^3 position, **I-462** (Figure I-17). Compound **I-461** was not found to be active against the HLE cell line, hepatocellular carcinoma; however, **I-460** and **I-462** were found to be active with IC_{50} values of 100 µM and 120 µM, respectively. These two compounds were inactive against three non-cancerous cell lines, including breast, lung, and liver cell lines. Both compounds were shown to induce cell cycle arrest in the G1 phase with approximately a 14% increase in cells in the G1 phase when compared to control cells. Along with inducing cell cycle arrest at the G1 phase, both compounds were able to reduce expression levels of the survivin proteins, which are involved with anti-apoptotic events, and found in a number of liver carcinoma cell lines. Both compounds were administered to nude mice inoculated with the Huh7 cell line, hepatocellular carcinoma, found to aggressively produce tumor masses in mice. Compound **I-460** was able to reduce tumor mass by 31% compared to control mice, but also caused a reduction in body weight by 9%; whereas, **I-462** was able to reduce tumor volume by 60% with no reduction in body weight for the mice.
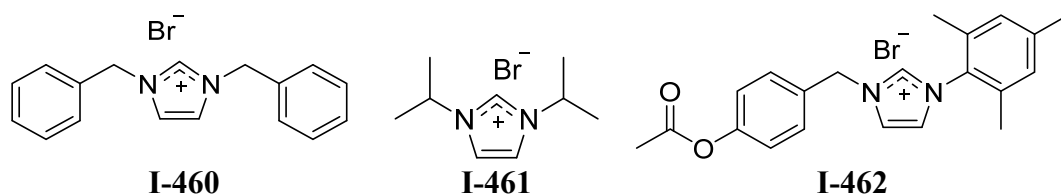
I-460   **I-461**   **I-462**

Figure I-17. Strucutres of imidazolium salts evaluated for anti-cancer properties against hepatocellular carcinoma. Compounds are from reference 75.

Although the Youngs group began investigating imidazolium salts as precursors to metal N-heterocyclic carbene complexes to study their antimicrobial and anti-tumor properties,[76–81] it was quickly discovered that the anti-tumor properties were largely due to the imidazolium salt precursors.[3] It was suggested that the in vitro anti-cancer properties of imidazolium salts against several NSCLCs were highly dependent on the substituents at the N^1 and N^3 positions of the imidazole ring and chemical modifications could be made to the C^4 and/or C^5 positions without altering the anti-proliferative effects.[4] N,N'-bis(naphthylmethyl)imidazolium salts were found to be the most active of the derivatives published (Figure I-18 and Table I-36). Imidazolium salts with one naphthylmethyl and one alkyl chain at the N^1 and N^3 positions, respectively, had varying activities. Compounds with alkyl chains of n = 5 or less carbons had moderate to poor activity; whereas, those with alkyl chains of n = 6 or more carbon atoms had high anti-cancer activity in the low micro-molar range. This information supports the data previously published by Malhotra's NCI-60 human tumor cell line screen on the effects lipophilicity plays on the anti-cancer properties of ionic liquids.[20] Exchanging one naphthylmethyl group for a benzyl group reduced the activity significantly whereas exchanging both naphthylmethyl groups for benzyl groups resulted in an inactive compound. Changing the linking moiety joining the imidazole ring to the naphthalene substituent from a methyl to ethyl group seemed to have little effect on the anti-cancer properties of the compound, just as altering the connectivity from the 2-position to the 1-position of the naphthalene ring had little effect on the activity. Although these naphthylmethyl substituted imidazolium salts had potent anti-cancer activity against NSCLC, unfortunately, there were limited in their clinical potential by poor

aqueous solubility. The final modification to the N^1 position was adding a nitrogen heteroatom to the naphthalene ring in the form of a quinoline substituent to increase aqueous solubility which also had minimal effects on the anti-cancer properties, but again insufficient solubility for systemic administration. Direct comparisons were made to N,N'-bis(naphthylmethyl)imidazolium salts with differing groups at the $C^4(C^5)$ positions including protons, chlorides, and a benzimidazolium salt. These three derivatives had comparable anti-cancer properties suggesting this could be a position for chemical modification to add solubilizing and/or targeting groups.

I-463

I-464

I-465

I-466

I-467

I-468

I-469

I-470: n = 1
I-471: n = 2
I-472: n = 3
I-473: n = 4
I-474: n = 5
I-475: n = 6
I-476: n = 8
I-477: n = 11

I-478

I-479

I-480

I-481

I-482

I-483
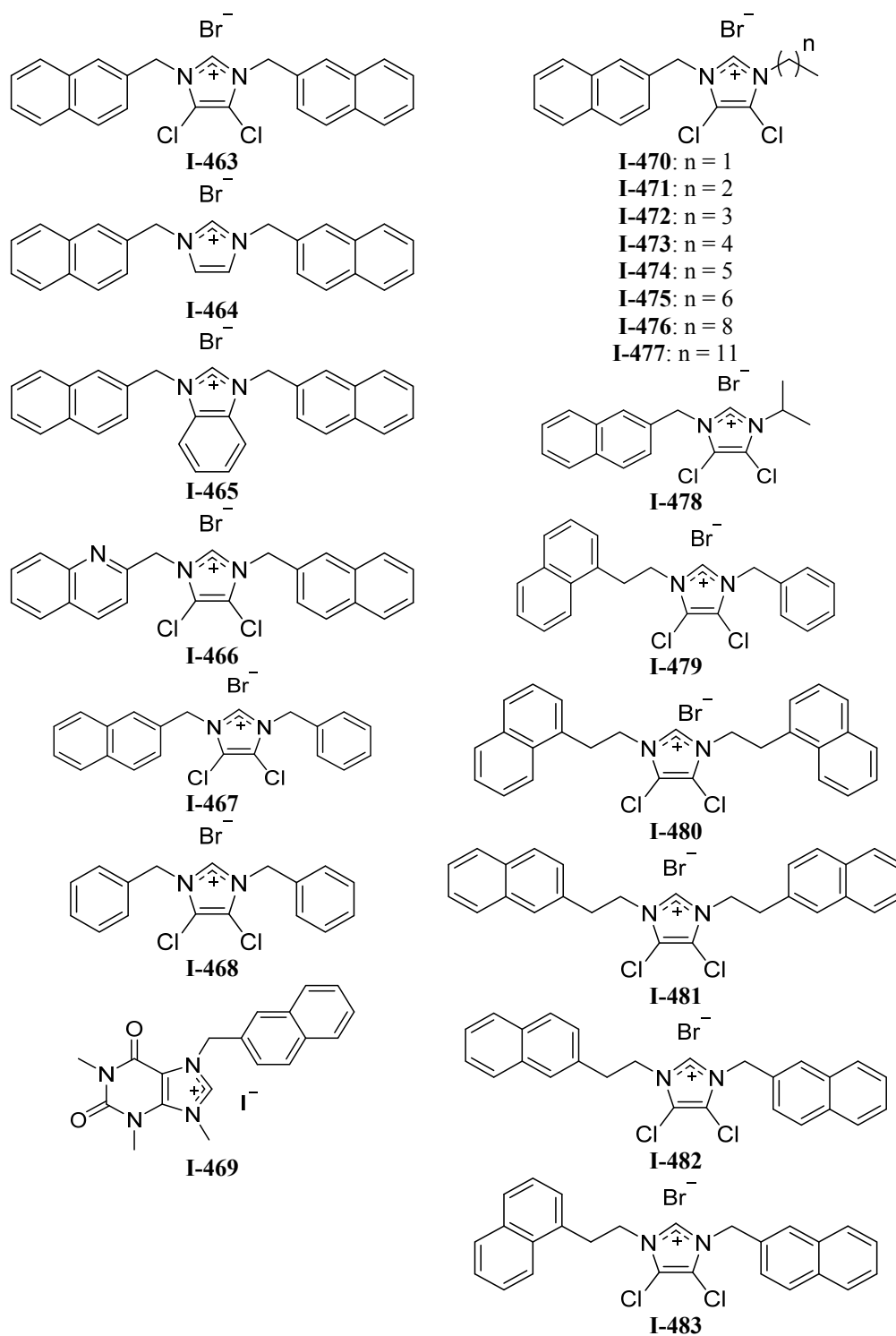
Figure I-18. Strucutres of naphthylmethyl substituted imidazolium salts. Compounds are from reference 4.

69

Table I-36. IC$_{50}$ values of naphthylmethyl-substituted imidazolium salts against several NSCLC cell lines. Results taken from reference 4.

Compound	IC$_{50}$ (µM)		
	NCI-H460	NCI-H1975	HCC827
I-463	5	6	8
I-464	4	6	9
I-465	3	4	5
I-466	10	5	9
I-467	15	12	15
I-468	> 30	> 30	> 30
I-469	> 30	> 30	> 30
I-470	26	> 30	> 30
I-471	19	22	> 30
I-472	13	10	12
I-473	10	12	12
I-474	5	5	8
I-475	6	4	6
I-476	10	3	3
I-477	5	4	N.D.
I-478	> 30	20	> 30
I-479	12	14	> 30
I-480	8	8	11
I-481	8	8	8
I-482	4	7	9
I-483	5	6	7

N.D. = not determined

The Youngs groups further explored chemical modifications at the $N^1(N^3)$ and $C^4(C^5)$ positions to create a SAR with various hydrophilic and lipophilic substituents at each of these positions (Figure I-19).[82] The anticancer properties of eight imidazolium salts with naphthylmethyl substituents at the $N^1(N^3)$ positions and a variety of lipophilic and hydrophilic substituents at the $C^4(C^5)$ positions were evaluated. These modifications included methyl, hydroxymethyl, carbamate, carboxylic acid, ester, and phenyl

substituents. The $C^4(C^5)$-phenyl substituted derivative, **I-484**, was the most active (IC_{50}: NCI-H460 - 3, NCI-H1975 - < 1, HCC827 - 2) closely followed in activity by the lipophilic derivative **I-487** with a methyl substituent at the C^4 position (IC_{50}: NCI-H460 - 3, NCI-H1975 - 3, HCC827 – 4). The more hydrophilic carboxylic acid and hydroxymethyl derived compounds, **I-485** and **I-488** respectively, had the worst anti-cancer properties of the group (IC_{50}: NCI-H460 - > 30, NCI-H1975 - > 30, HCC827 - > 30; and NCI-H460 - > 30, NCI-H1975 - 11, HCC827 - > 30 respectively). The histamine derived imidazolium salts (**I-489**, **I-490**, **I-491**) and ester moiety, **I-486**, had moderate activities suggesting that certain groups could be used to increase solubility without hindering the anti-cancer properties whereas other functional groups were too detrimental to the activity. Compound **I‑484** and **I-487** were also tested by the NCI's DTP in the NCI-60 human tumor cell line screen revealing both compounds had high anti-cancer activity in the one- and five-dose assay against the nine NSCLC cell line tested.
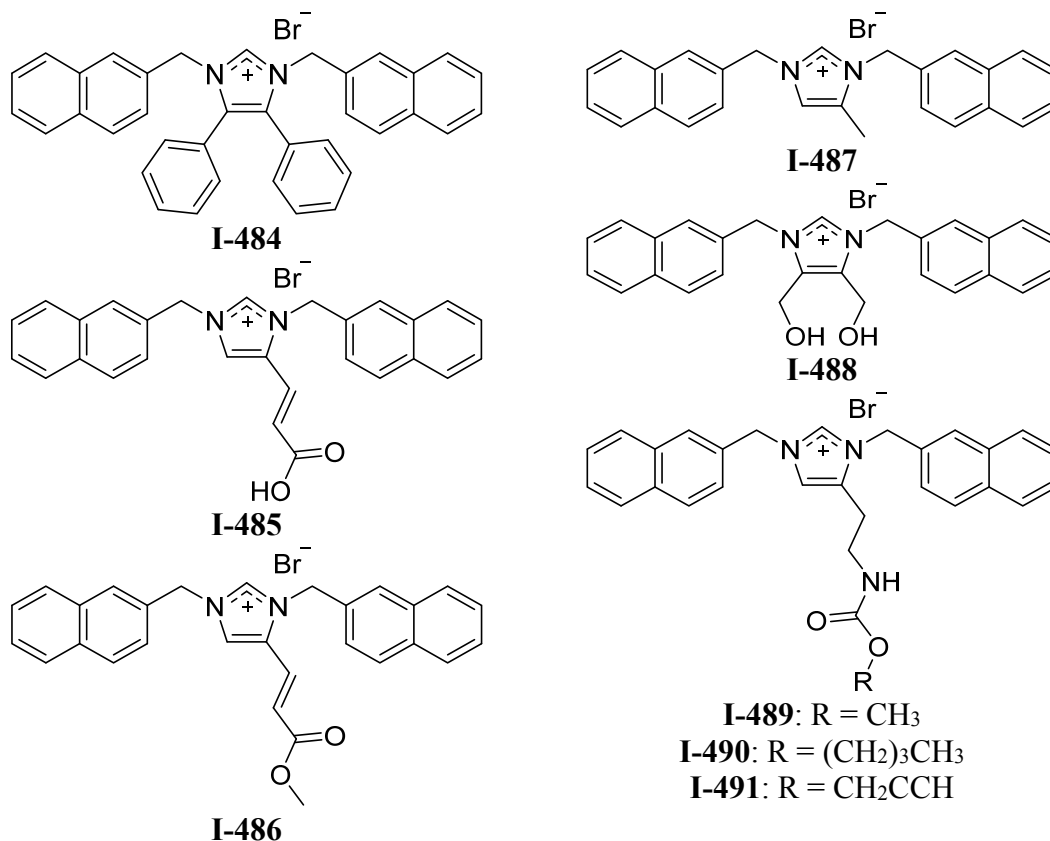
Figure I-19. Strucutres of $C^4(C^5)$-substituted imidazolium salts with the highly active naphthylmethyl substituent at the N^1 and N^3 positions. Compounds are from reference 82.

Considering **I-484** was highly active against the NSCLC cell lines tested, this was further modified at the $N^1(N^3)$ positions in an attempt to increase aqueous solubility and maintain the high anti-cancer activity (Figure I-20).[82] Compounds **I-492-I-496** were strategically synthesized with planar aromatic groups similar to the naphthalene moiety, such as quinoline and 6-methoxy-naphthalene substituents, that included heteroatoms to increase the aqueous solubility. These five derivatives, with various combinations of these three planar, bicyclic ring systems were synthesized and tested for their anti-cancer properties against NSCLC. All of these derivatives had IC$_{50}$ values of 3 μM or less against

the three NSCLC cell lines tested (NCI-H460, NCI-H1975, and HCC927). Unfortunately, noticeable differences in solubility were not observed for any of these derivatives because the solubilities were still extremely poor (< 0.5 mg/mL).

I-492: $R^1 = R^3$ = NapOMe, X = Cl
I-493: R^1 = NapOMe, R^3 = Nap X =Br
I-494: R^1 = Quin, R^3 = NapOMe, X = Cl
I-495: R^1 = Quin, R^3 = Nap, X = Br
I-496: $R^1 = R^3$ = Quin, X = Br
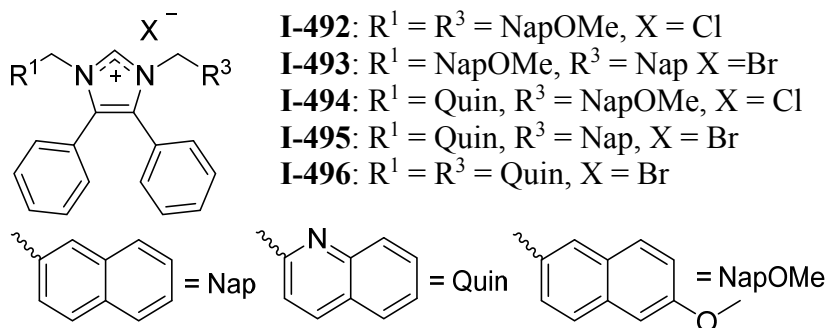
Figure I-20. Structures of $C^4(C^5)$-phenyl substituted imidazolium salts with multiple planar, aromatic substituents at the N^1 and N^3 positions. Compounds are from reference 82.

Considering the high anti-cancer activity of the lipophilic 4,5-diphenylimidazolium salt derivatives, the Youngs group published a report on a series of benzimidazolium salts in 2016 (Table I-37).[83] The in vitro anti-cancer properties of these benzimidazolium salts were evaluated against a panel of non-small cell lung cancer cells lines (Table I-38). This series of benzimidazolium salts had a variety of lipophilic and hydrophilic functional groups at the N^1 and N^3 positions as well as the C^2, C^5, and C^6 positions. A SAR was established from combining the anti-cancer properties and structures of each benzimidazolium salt. Results from this study suggested that the most lipophilic compounds possessed the highest anti-cancer activity. However, as with other derivatives, these lipophilic derivatives have poor aqueous solubility. Certain hydrophilic functional groups inactivate the compounds, such as carboxylic acids; whereas, mildly hydrophilic substituents such as quinolylmethyl groups at the N^1 and/or N^3 positions and ethers at the

C^2, C^5, and/or C^6 positions increased the aqueous solubility without having a drastic impact on the anti-proliferative properties. Two N^1/N^3-naphthylmethyl substituted neutral benzimidazoles, **I-523** and **I-524** were also tested for their anti-cancer properties and found to be inactive against the lung cancer cells lines tested. This suggested that the positive charge of the benzimidazolium salt is necessary for the benzimidazolium salt to possess high anti-cancer activity, in addition to the details provided above. The NCI's DTP also found **I-465**, **I-499**, **I-506**, **I-509**, **I-510**, and **I-520** to be active in the 60-human tumor cell line one-dose assay screen. Compound **I-520** was administered to C57/BL6 mice in a preliminary in vivo toxicity study. Although the compound was toxic at the tested dose, the toxicity study provided information for future toxicity trials and lung xenograft models.

Table I-37. Structures of benzimidazolium salts with lipophilic and hydrophilic substituents at the N^1, C^2, N^3, C^4, and C^5 positions. Compounds are from reference 83.

Compound	R^1	R^2	R^3	R^5	R^6	X
I-465	Nap	H	Nap	H	H	Br
I-497	Nap	H	Nap	OCH_3	H	Br
I-498	Nap	H	Nap	CO_2CH_3	H	Br
I-499	Nap	H	Nap	CH_3	CH_3	Br
I-500	Nap	H	Nap	CO_2CH_3	CO_2CH_3	Br
I-501	Nap	H	Nap	CO_2CH_2Nap	H	Br
I-502	Nap	H	Nap	CO_2H	CO_2H	Cl
I-503	Nap	H	Nap	CO_2H	H	Br
I-504	Nap	$CH_2CO_2CH_3$	Nap	H	H	Br
I-505	Nap	$(CH_2)_2CO_2CH_3$	Nap	H	H	Br
I-506	Nap	CH_3	Nap	H	H	Br
I-507	Nap	$(CH_2)_2CO_2H$	Nap	H	H	Cl
I-508	Nap	CH_2CH_3	Nap	H	H	Br
I-509	Nap	$(CH_2)_2CH_3$	Nap	H	H	Br
I-510	Nap	$(CH_2)_3CH_3$	Nap	H	H	Br
I-511	Nap	$(CH_2)_6CH_3$	Nap	H	H	Br
I-512	Nap	$(CH_2)_2OCH_3$	Nap	H	H	Br
I-513	Nap	$(CH_2)_3OH$	Nap	H	H	Br
I-514	Quin	$(CH_2)_3OH$	Nap	H	H	Br
I-515	Quin	$(CH_2)_3OH$	Quin	H	H	Cl
I-516	Quin	H	Quin	H	H	Cl
I-517	Quin	CH_3	Quin	H	H	Cl
I-518	Quin	H	Quin	CH_3	CH_3	Cl
I-519	Nap	$O(CH_2CH_2O)_2CH_3$	Nap	H	H	Br
I-520	Quin	$O(CH_2CH_2O)_2CH_3$	Nap	H	H	Br
I-521	Quin	$O(CH_2CH_2O)_2CH_3$	Quin	H	H	Cl
I-522	Nap	$O(CH_2CH_2O)_2CH_3$	Nap	CH_3	CH_3	Br
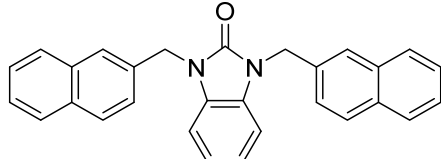
I-523
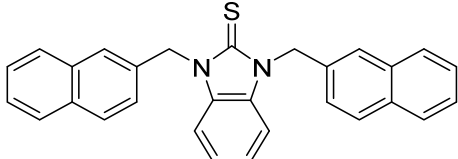
I-524

Table I-38. IC$_{50}$ values of benzimidazolium salts against a panel of NSCLC call lines. Table modified from that reference 83.

Compound	IC$_{50}$ values(μM)			
	NCI-H460	NCI-H1975	HCC827	A549
cisplatin	3	11	6	8
I-465	3	4	5	n/a
I-497	4	2	4	6
I-498	9	7	12	16
I-499	2	2	2	3
I-500	26	15	20	23
I-501	4	4	7	7
I-502	> 30	> 30	> 30	> 30
I-503	16	23	> 30	12
I-504	7	6	8	8
I-505	4	2	4	8
I-506	3	2	4	4
I-507	> 30	> 30	> 30	> 30
I-508	3	< 1	4	3
I-509	2	< 1	< 1	2
I-510	2	< 1	2	2
I-511	< 1	< 1	< 1	< 1
I-512	3	2	3	3
I-513	4	4	6	10
I-514	4	3	11	12
I-515	11	7	17	25
I-516	4	3	6	10
I-517	3	2	7	9
I-518	2	< 1	3	4
I-519	3	3	5	5
I-520	3	< 1	6	3
I-521	4	< 1	4	9
I-522	< 1	< 1	2	2
I-523	> 30	19	> 30	> 30
I-524	> 30	> 30	> 30	> 30

1.6. Conclusion and future outlook

Imidazolium salts are a class of compounds that have received substantial attention for their medicinal applications, particularly their anti-cancer properties. Hundreds of imidazolium salts have been tested for their anti-cancer properties against a variety of cancers and several trends and SARs have emerged. The first suggests that lipophilic imidazolium salts are the most active of all derivatives. The most lipophilic compounds had the highest anti-cancer activities; whereas, adding highly hydrophilic functional groups can diminish the anti-cancer properties possessed by related derivatives. However, addition of certain functional groups and inclusion of particular heteroatoms can help to increase the hydrogen bonding capabilities without severely hindering the high anti-cancer activity. One imidazolium salt, YM-155 or **I-56**, has gone through clinical trials for the potential treatment of cancer but is not yet FDA approved for the treatment of any cancers. One limitation for these imidazolium salts is the limited knowledge of their mechanism of action. The absence of this information may be hindering the future of these compounds considering a limited understanding of how these compounds kill human cells can be quite dangerous by potentially causing severe side effects. In vivo studies have been performed on murine models, with some imidazolium salts proving to be quite toxic; whereas, others were able to reduce the volume of a tumor without drastically affecting the heath of the animals, meaning limited weight loss and death. Imidazolium salts have a promising future considering the properties they possess for the treatment of malignancies in vitro, but knowledge concerning the mechanism of action is vital to their development.

CHAPTER II

SYNTHESIS, CHARACTERIZATION, AND IN VITRO ANTI-TUMOR STUDIES OF

N,N'-BISNAPHTHYLMETHYL 2-ALKYL SUBSTITUTED IMIDAZOLIUM SALTS

2.1. Introduction

Lung cancer causes more deaths than any other type of cancer, and it is estimated that there will be over 155,000 deaths in the United States due to lung cancer in 2017.[84] Lung cancer is classified into two types, small cell and non-small cell lung carcinomas (NSCLC), the latter of which makes up 83% of lung cancers. The current treatments for NSCLC include surgery, radiation, and chemotherapy.[85] Many chemotherapeutic strategies include the use of a combination of organic-based drugs and metal-based platinum drugs. Among the platinum-based therapeutics, cisplatin is the most commonly prescribed as a first line treatment for NSCLC.[86] However, treatment with platinum-based drugs commonly elicits severe adverse side effects, including nephrotoxicity (*e.g.*, 20% of patients treated with high doses of cisplatin undergo severe renal dysfunction).[87] Patient relapse may also occur as malignant cells become resistant to treatment with

cisplatin.[88] The five-year survival rate for patients with NSCLC is only 21%; the average for all other cancers is 68%.[89] Therefore, there is a clear need for new chemotherapeutic agents that can effectively target this form of cancer while offering a more favorable side effect profile.

During our group's investigation of the anti-tumor activity of silver carbene complexes, it was discovered that certain imidazolium salt precursors had very high anti-tumor activity against certain NSCLC cell lines.[3] Imidazolium salts with naphthylmethyl substituents in the N^1 and N^3 positions yielded the highest activity.[4] The first imidazolium salt of this class with high anti-cancer activity against several NSCLC lines was 4,5-dichloro-1,3-bis(naphthalen-2-ylmethyl)imidazolium bromide (**IS23** or **I-463**; Figure II-1). Although **I-463** displayed high anticancer activity, comparable to the chemotherapeutic agent cisplatin, it had extremely poor water solubility, which would impair its distribution upon systemic administration.[4] The balance between water solubility and high anti-cancer activity has represented a major obstacle for the potential clinical use of lipophilic imidazolium salts.
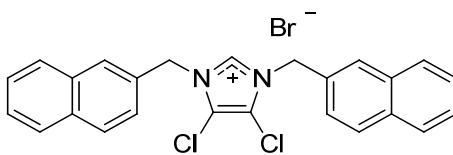
Figure II-1. Structure of 4,5-dichloro-1,3-bis(naphthalen-2-ylmethyl)imidazolium bromide (**IS23/I-463**).

Several other imidazolium salts have been reported with high anti-cancer activity and poor water solubility. However, molecular excipients, such as cyclodextrins (CD),

have been used to improve drug solubility and the bioavailability of such compounds.[90] Cyclodextrins have a hydrophobic internal cavity that can interact with hydrophobic drugs of certain size and polarity.[91] Also, cyclodextrins have two types of alcoholic functional groups that make up a hydrophilic outer shell. Together, these two properties allow a host-guest interaction to form between the cyclodextrin and the hydrophobic drug that can be solubilized in aqueous media.[92] Cyclodextrins are generally regarded as safe (GRAS) by the Food and Drug Administration (FDA) for use as food additives and are a part of several major drug formulations.[93]

Imidazolium salts have been reported in conjunction with cyclodextrins previously.[94,95] Herein, we report the use of cyclodextrins to solubilize imidazolium salts for their potential use as anticancer agents, which, to our knowledge, would be the first report of this kind. A series of imidazolium salts bearing 2-naphthylmethyl substituents at the N^1 and N^3 positions and varying alkyl substituents in the C^2 position have been synthesized. All compounds have been tested for in vitro efficacy with and without the use of cyclodextrin. These compounds display anticancer activity comparable to that of **I-463** and cisplatin, with significantly increased solubility when combined with cyclodextrin.

2.2. Results and Discussion

2.2.1. Synthesis and Characterization

Compounds **II‑1‑II‑5** were synthesized by the general synthetic route outlined in Equation II-1 based upon previously published procedures.[4,96] The starting imidazole was

80

deprotonated with a slight excess of potassium hydroxide followed by addition of 2-(bromomethyl)naphthalene. The mixture was refluxed overnight, which resulted in formation of a white precipitate (presumed to be potassium bromide) that was removed by filtration. 2-(Bromomethyl)naphthalene was added to the filtrate and the mixture was refluxed overnight. Compounds **II‑1** and **II‑3** precipitated from hot acetonitrile. Compounds **II‑2**, **II‑4**, and **II‑5** precipitated after the addition of diethyl ether to the reaction mixture. All compounds were washed with diethyl ether to remove any excess 2-(bromomethyl)naphthalene. Compound **II‑2** was recrystallized from ethanol. Compounds **II‑3**, **II‑4**, and **II‑5** were recrystallized from acetonitrile.
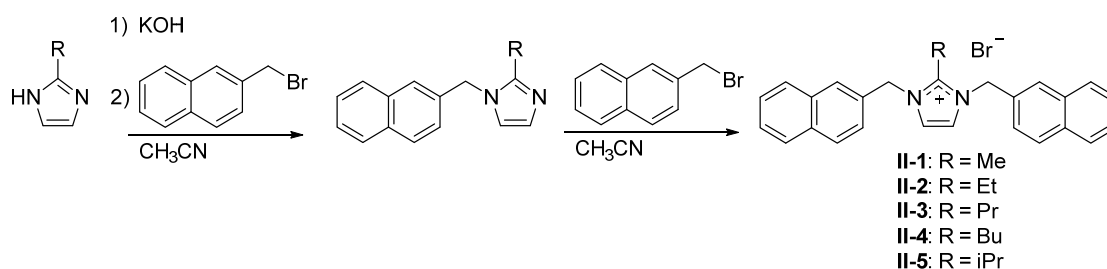
Equation II-1. Synthesis of compounds **II‑1‑II‑5**.

All compounds were characterized by ^{1}H and ^{13}C NMR spectroscopy, mass spectrometry, elemental analysis, and melting point determination. Additionally, compounds **II‑1**, **II‑2**, **II‑4**, **II‑5**, and the cationic portion of **II‑3**, as the perchlorate salt, were characterized by single-crystal X-ray crystallography. In the ^{1}H NMR spectra, the chemical shifts of the methylene linkers bridging the imidazole ring and the naphthalene rings were used as evidence for the formation of the imidazolium salts (Figure II-2). The chemical shift of the methylene linker in the mono-naphthylated intermediates ranged from

81

5.32 ppm to 5.35 ppm. The second naphthylation and resulting formation of the desired imidazolium salt was indicated by an increase in the integration of this methylene resonance and a downfield shift due to the deshielding effect of the cationic imidazolium ring. Compounds **II‑1‑II‑5** had chemical shifts in the range from 5.62 ppm to 5.81 ppm for this methylene linker, which was consistent with related compounds.[4,78,79] The ^{13}C NMR spectra for compounds **II‑1‑II‑5** were consistent with the proposed structures. Every resonance from compounds **II‑1‑II‑5** can be accounted for in each of the spectra. The methyl and methylene resonances are easily distinguished in each of the spectra, but due to the complex nature of the aromatic carbons, the aromatic resonances were not assigned.
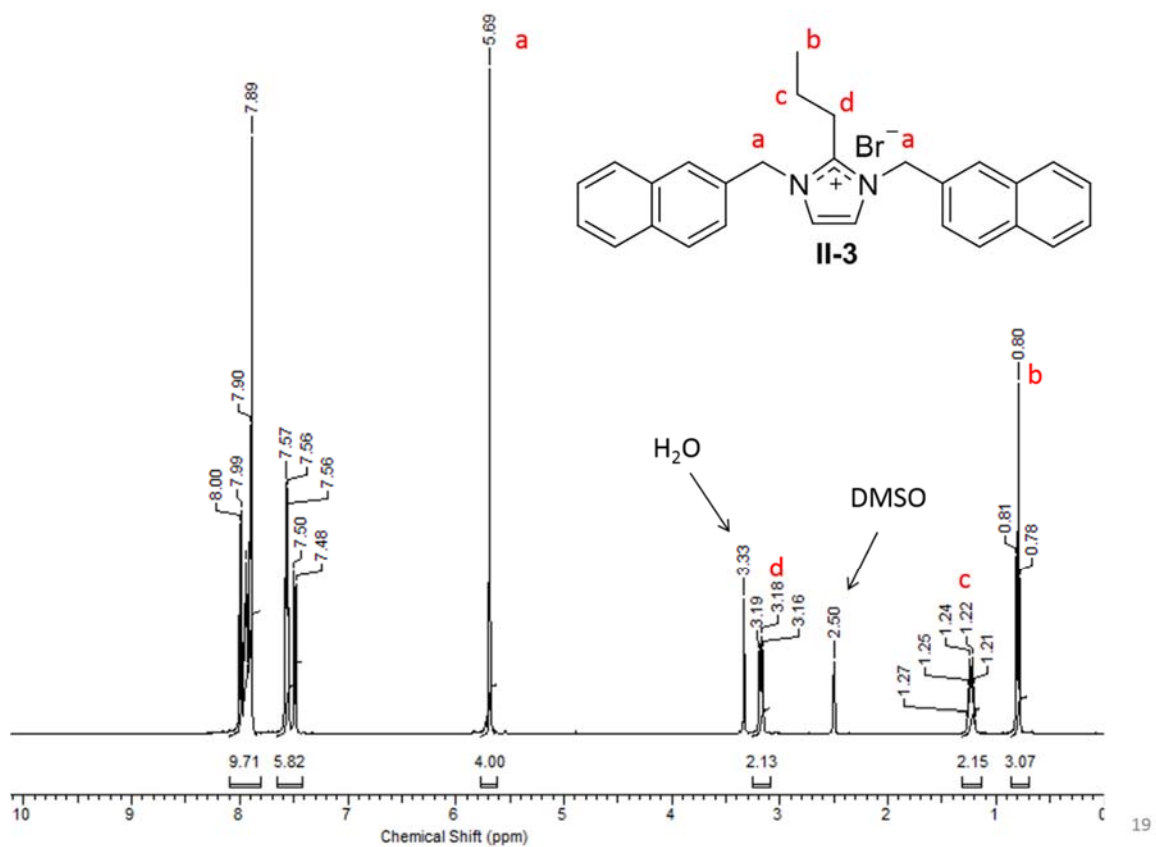
Figure II-2. ^{1}H NMR spectrum of **II-3**. Resonances are labelled with red letters with the corresponding protons on the strucutre. Aromatic protons were not labelled.

Compounds **II‑1**, **II‑2**, **II‑4**, **II‑5**, and the perchlorate salt derivative of **II‑3** were characterized by single-crystal X-ray crystallography. A single crystal of **II‑1** (Figure II‑3) was grown from a combination of methanol and ethyl acetate. A single crystal of **II-5** was grown from acetonitrile (Figure II-4). Single crystals of **II‑2** and **II‑4** suitable for single crystal X-ray analysis were obtained by slow evaporation of an ethanol solution (Figure II-5 and Figure II-6). Two molecules of compound **II‑4** co-crystallized with one molecule of ethanol. Single crystals of **II-3** could not be obtained. Anion exchange of bromide for perchlorate was performed by dissolving compound **II‑3** in methanol and adding silver perchlorate. A precipitate formed, presumed to be silver bromide, and was removed by filtration. A single crystal of the perchlorate derivative of **II‑3, II‑3‑ClO₄**, was obtained from methanol/diethyl ether at -5 °C (Figure II-7).
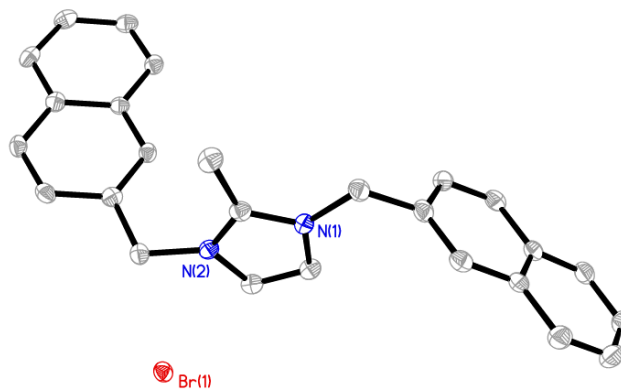
Figure II-3. Thermal ellipsoid plot of **II‑1** with thermal ellipsoids drawn at 50% probability. Hydrogen atoms and carbon labels have been removed for clarity.
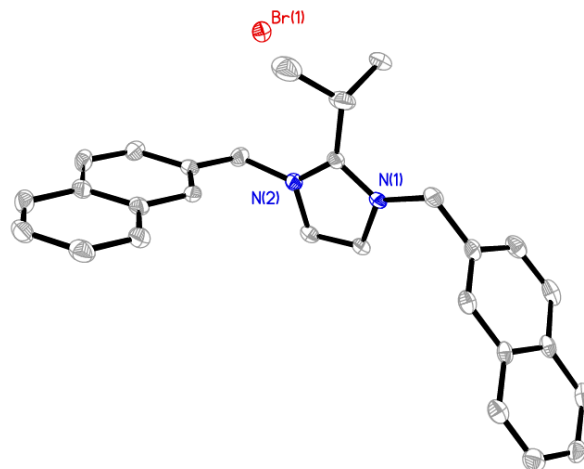
Figure II-4. Thermal ellipsoid plot of **II‑5** with thermal ellipsoids drawn at 50% probability. Hydrogen atoms and carbon labels have been removed for clarity.
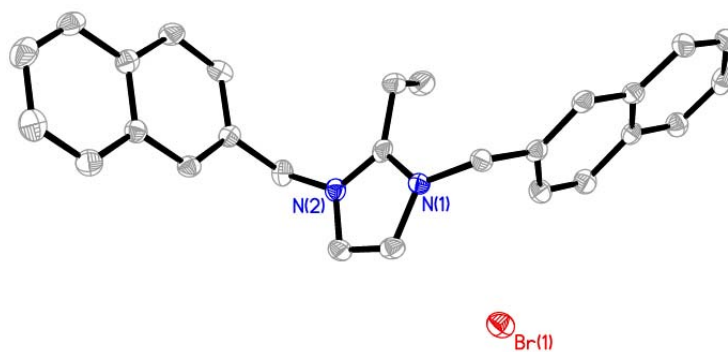
Figure II-5. Thermal ellipsoid plot of **II‑2** with thermal ellipsoids drawn at 50% probability. Hydrogen atoms and carbon labels have been removed for clarity.
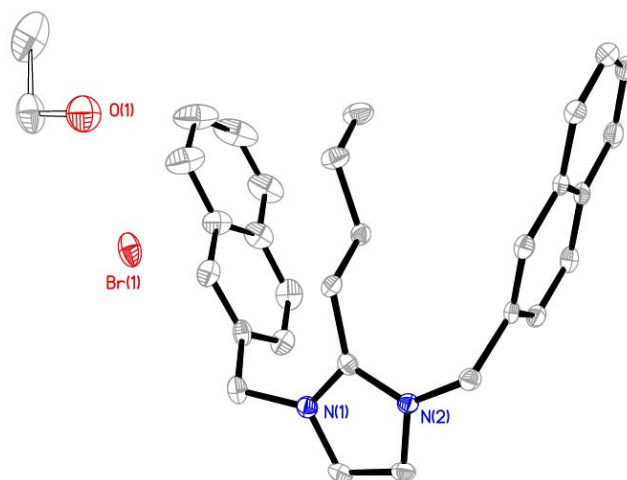
Figure II-6. Thermal ellipsoid plot of **II-4-C₂H₆O** with thermal ellipsoids drawn at 50% probability. Hydrogen atoms and carbon labels have been removed for clarity.
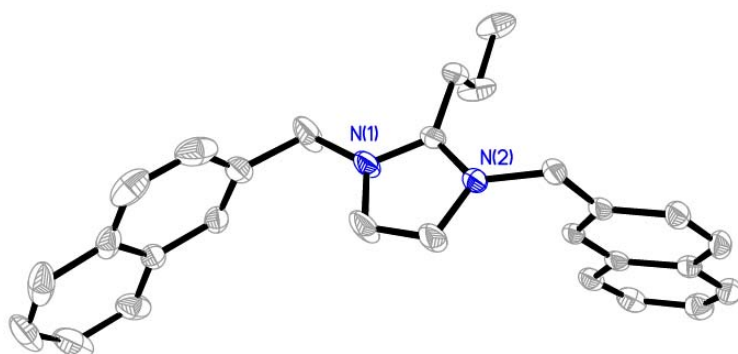
Figure II-7. Thermal ellipsoid plot of **II-3-ClO₄**, the cationic portion of **II-3** with a perchlorate anion. Thermal ellipsoids are drawn at 50% probability. Hydrogen atoms, the disordered perchlorate anion, and carbon labels have been removed for clarity.

2.2.2. In vitro studies

2.2.2.1. MTT assay

The anti-cancer activity of compounds **II‑1** and **II‑4** (Figure II-8 and Table II-1) and compounds **II‑2**, **II‑3**, and **II‑5** (Figure II-8, Figure II-9, and Table II-1) were evaluated against several NSCLC cell lines (NCI-H460, NCI-H1975, A549, and HCC827) to create a SAR. Cells were exposed to compounds **II‑1‑II‑5** or cisplatin for 72 hours, at which time the MTT assay was utilized to determine cell viability. The anti-proliferative effects of compounds **II‑1‑II‑5** were evaluated by their IC_{50} values, where the IC_{50} value denotes the drug concentration at which there was 50% inhibition in cell viability relative to control cells. The major disadvantage of imidazolium salts with naphthylmethyl substituents on both nitrogen atoms is their low water solubility.[4] Compounds **II‑1‑II‑5** continued to manifest suboptimal water solubility. Therefore, solutions of each compound were prepared by first dissolving the compound in DMSO and then diluting with water to a final concentration of 1% DMSO in water. Compounds were further diluted into growth medium with a maximum DMSO concentration of 0.032% that was added to the cells. A solution of cisplatin was prepared by adding the compound to pure water and stirring at room temperature for several hours.
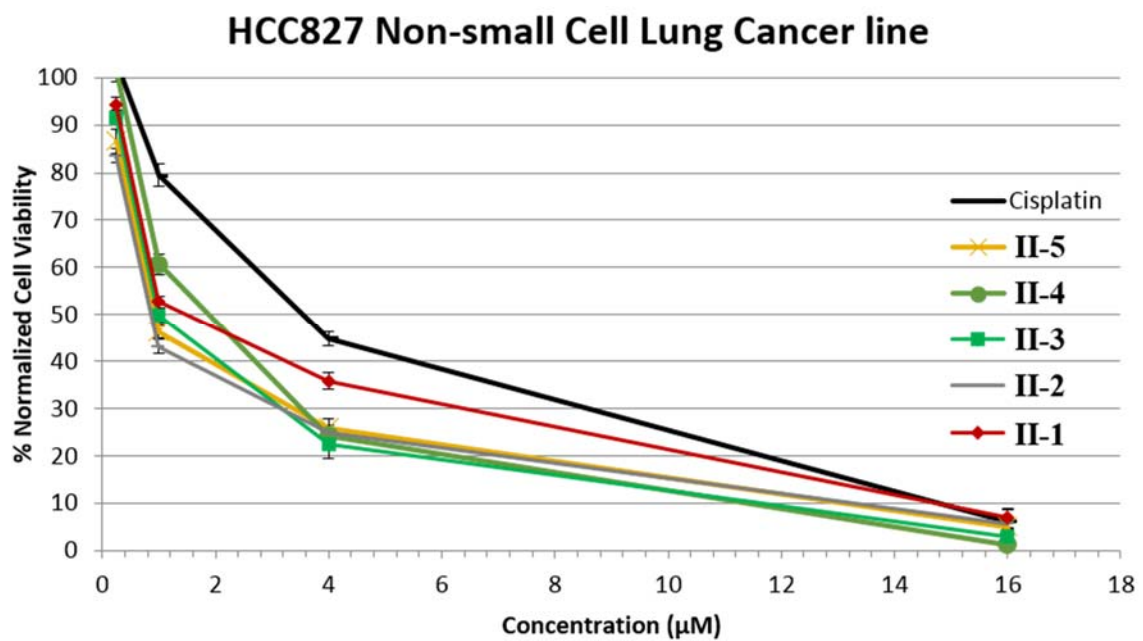
Figure II-8. Plot of MTT results from MTT assay of compounds **II‑1‑II‑5** and cisplatin against the HCC827 NSCLC line.
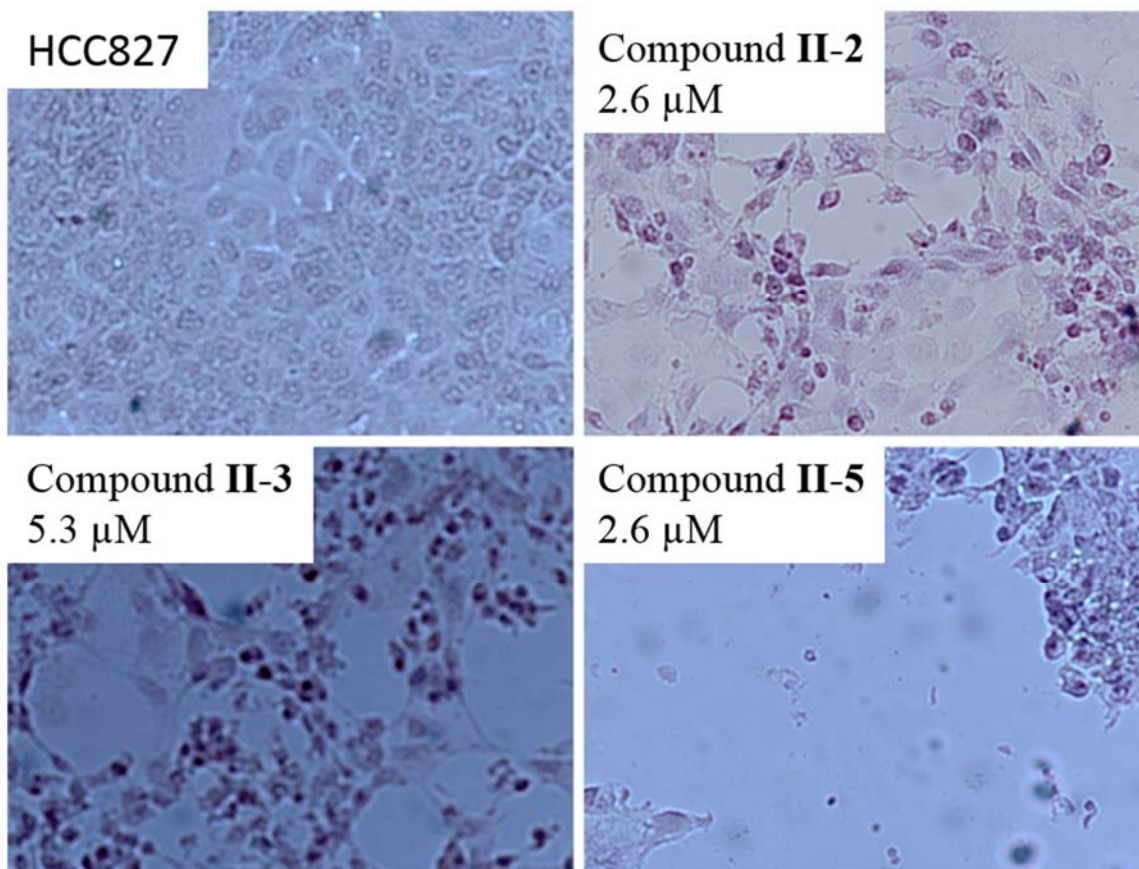
Figure II-9. Microscopic appearance of HCC827 cells after 72 hours of exposure to medium alone (upper left panel) or to compounds **II‑2**, **II‑3**, or **II‑5** at the indicated concentrations.

Compounds **II‑2**, **II‑3**, and **II‑5** exhibited higher solubility in the water/DMSO solution than compounds **II‑1** and **II‑4**. Compounds **II‑2**, **II‑3**, and **II‑5** remained soluble once water was added to the DMSO solution. However, slight precipitation was observed upon addition of water to the DMSO solutions of compounds **II‑1** and **II‑4**. Although the structure of **II-1** would suggest it was the least lipophilic, the compound crystallizes readily from a variety of organic solvents suggesting the compound is tightly packed in its

crystalline form and difficult to solubilize. Compounds **II-2**, **II-3**, and **II-5** likely have higher solubility in water due to the higher number of degrees of freedom in the alkyl chain linkers; **II-4** has become too lipophilic to be solubilized even with the further increase in degrees of freedom in the butyl chain. Although the solubility of compounds **II‑1**‑**II‑5** in pure water is low (< 0.5 mg/mL), the anti-proliferative activity of these compounds was measured in order to evaluate the addition of functional groups at the C^2 position, with the goal of adding water-solubilizing groups in the future.

All of the synthesized compounds demonstrated high activity against all four NSCLC lines, comparable to the well-known chemotherapeutic agent cisplatin and to **I‑463** (Table II-1).[4] Although the solubilities of compounds **II‑1**‑**II‑5** varied in the water/DMSO solution, the anti-tumor properties were similar with alkyl chains ranging from a methyl group to a butyl group in length, along with the more sterically hindering isopropyl group. These results suggest that steric bulk in the C^2 position does not reduce the high anti-cancer activity seen with previous derivatives.

Table II-1. IC50 values of compounds **II‑1‑II‑5**, cisplatin, and **IC23** dissolved in 1% DMSO/water solution and a 10% by weight solution of 2-HPβCD.

IC$_{50}$ value after 72 hours (µM)				
	Cancer Cell Line			
Compound	NCI-H460	NCI-H1975	NCI-A549	HCC827
II‑1 (Me w/DMSO)	2.53 ± 0.09	0.83 ± 0.02	3.42 ± 0.10	2.34 ± 0.48
II‑1 (Me w/2-HPβCD)	2.70 ± 0.11	0.75 ± 0.02	3.43 ± 0.19	1.98 ± 0.39
II‑2 (Et w/DMSO)	0.92 ± 0.01	0.66 ± 0.01	2.63 ± 0.07	1.15 ± 0.18
II‑2 (Et w/2-HPβCD)	0.99 ± 0.08	0.56 ± 0.04	2.34 ± 0.19	0.97 ± 0.17
II‑3 (Pr w/DMSO)	1.91 ± 0.24	0.85 ± 0.07	2.93 ± 0.03	1.45 ± 0.27
II‑3 (Pr w/2-HPβCD)	2.13 ± 0.06	0.63 ± 0.12	2.81 ± 0.11	1.25 ± 0.27
II‑4 (Bu w/DMSO)	2.62 ±0.04	1.74 ± 0.13	3.50 ± 0.06	2.64 ± 0.10
II‑4 (Bu w/2-HPβCD)	2.43 ± 0.06	1.02 ± 0.07	3.25 ± 0.14	2.18 ± 0.31
II‑5 (iPr w/DMSO)	0.92 ± 0.03	0.69 ± 0.01	2.54 ± 0.05	1.29 ± 0.22
II‑5 (iPr w/2-HPβCD)	0.86 ± 0.03	0.62 ± 0.03	2.13 ± 0.26	1.14 ± 0.32
cisplatin	2.92 ± 0.34	9.77 ± 0.41	5.63 ± 0.49	4.76 ± 0.87
I-463 (DMSO)*	5	5	9	6

* Results taken from reference Wright et al. 2015

To our knowledge, there are no approved drugs on the market that are co-formulated with DMSO and used for the treatment of cancer. Therefore, a different vehicle would be necessary to aid in increasing the water solubility of these potent anti-cancer agents allowing them to be systemically administered. We chose to use the compound 2-hydroxypropyl-β-cyclodextrin (2-HPβCD) synthesized from a chemical modification of β-cyclodextrin isolated from the digestion of starch by bacteria.[93,97] The solubilities of compounds **II‑1‑II‑5** were determined with differing amounts of 2-HPβCD in water. All compounds were soluble at amounts greater than 4.4 mg/mL (~ 5.0 mM) in a 20% by weight solution (w/v) of 2-HPβCD in water. However, some toxicity was observed in the MTT assay in control cells with high concentrations of 2-HPβCD added to growth medium.

Toxicity is not a concern of using 2-HPβCD to solubilize lipophilic compounds, considering that marketed formulations of lipophilic drugs can be co-administered with up to 16 g/day of 2-HPβCD by intravenous injection.[93] Due to some toxicity observed at high concentrations of 2-HPβCD, solutions were idealized by minimizing the amount of 2-HPβCD used to solubilize compounds **II‑1‑II‑5,** aiming to reduce or eliminate any toxicity from the excipient. Compounds **II‑1‑II‑4** were able to be solubilized at concentration of greater than 4.4 mg/mL in a 10% 2-HPβCD by weight solution in water. This was the initial concentration of 2-HPβCD the compounds were dissolved in prior to further dilution and exposure to cells. Compound **II‑5** was mostly soluble at this concentration, yielding a clear solution with minor insoluble material. By using 2-HPβCD to solubilize compounds **II‑1‑II‑4**, the water solubilities increased from less than 0.5 mg/mL to over 4.4 mg/mL making them viable candidates for novel chemotherapeutics for the treatment of NSCLC.

The in vitro MTT assay was conducted with compounds **II‑1‑II‑5** dissolved in the 2-HPβCD aqueous solution to confirm there was no reduction in the anti-proliferative effects of compounds **II‑1‑II‑5**. Cells treated with compounds **II‑1‑II‑5** were compared to control cells treated with 2-HPβCD to account for any effect the vehicle had on the cells. The maximum concentration of 2-HPβCD in treated wells was 0.008% by weight. The concentration of 2-HPβCD in all control wells was 0.008% by weight. Cells treated with fresh medium were also compared to cells treated with 2-HPβCD and virtually no toxicity was observed (when considering the four different cell lines tested, cells treated with 2-HPβCD grew at rates of 96‑106% when compared to cells treated with pure medium).

Compounds **II‑1**‑**II‑5** all displayed high anti-cancer activity when dissolved in 2-HPβCD against all four NSCLC lines tested (Table II-1). All IC_{50} values were comparable to values recorded when dissolving the compounds in DMSO suggesting the vehicle has no effect on the overall in vitro efficacy of these compounds. Although 2-HPβCD is FDA approved and GRAS, we wanted to confirm that it had no effects on the anti-cancer properties of our compounds considering an interaction was necessary for the compounds to be solubilized in water.

The anti-tumor properties were similar for the methyl, ethyl, propyl, butyl, and the more sterically hindering isopropyl group with IC_{50} values ranging from 0.66 μM to 3.50 μM. When closely evaluating the IC_{50} values, **II-1** and **II-4** had the highest IC_{50} values against each of the four NCSLC cell lines. This suggests that the poor solubility may have played a role in the anti-cancer properties. In previous studies evaluating imidazolium salts with increasing alkyl chain length, the compounds with the longest alkyl chain had the highest anti-cancer activity.[4,20] A clear distinction is not made with this small group of compounds and cannot be used to further confirm results seen previously. However, these compounds may be too similar to observe results seen previously with alkyl chains ranging from three to 17 carbons. All five compounds were most effective against the NCI-H1975 cell line with IC_{50} values ranging from 0.66 μM to 1.74 μM with **II-2** having 15-fold better activity than cisplatin. These compounds were more active than previously published derivatives with either one or two quinolylmethyl substituents at the N^1 and/or N^3 positions.[98] This information greatly contributes to the SAR we have established with this class of imidazolium salts.

93

As discussed previously in the case of **I-463**, naphthylmethyl-substituted imidazolium salts have high anticancer activity towards certain NSCLC cell lines. Compounds **II‑1**‑**II‑5** collectively have the lowest IC_{50} values of imidazolium salts with two 2-(naphthylmethyl) substituents when compared to those tested previously.[4] Compounds **II‑1**‑**II‑5** also have similar IC_{50} values against the A549 cell line compared to imidazolium salts with one naphthylmethyl substituent and one dibenzofuran derivative.[49] However, there is no discussion of the water solubility of these compounds and only a reference to a review of ionic liquids (Ranke, et al. 2007) whose toxicity increased with decreased water solubility.[99] Also, compounds **II‑1**‑**II‑3** and **II‑5** all had sub-micromolar IC_{50} values against the NCI-H1975 cell line, making them an order of magnitude more potent than cisplatin against this cell line. These results suggest that added lipophilicity at the 2-position of these imidazolium salts was beneficial for the compound's anti-proliferative properties. The reason for lower IC_{50} values for compounds **II‑1**‑**II‑5** compared to previously reported analogous compounds is unknown at this time. It is possible that these alkyl substituents at the C^2 position enhance lipophilicity enough to allow uptake into the cell by passive diffusion across the membrane at a faster rate, but we have no evidence to confirm this. The high anti-cancer activity of **II‑1**‑**II‑5** suggests that chemical modifications can be made to the C^2 position of naphthylmethyl substituted imidazolium salts in attempt to either enhance water solubility further, thus depleting the need for cyclodextrin, or add targeting moieties.

94

2.2.2.2. NCI-60 human tumor cell line study

The National Cancer Institute's (NCI) Developmental Therapeutics Program (DTP) tested **II‑1‑II‑4** in their 60 human tumor cell line one-dose and five-dose assays. The 60 human tumor cell line panel consists of nine non-small cell lung cancer lines, two of which we also tested in our laboratory, the NCI-H460 and A549 lines. In the one-dose assay, each cell line is exposed to the tested compound at a single dose (10 μM). Results are given as a growth percentage relative to the initial number of cells at the beginning of the study. Briefly, cells are plated at a density relative to their doubling rate and incubated overnight. Compounds are exposed to the cells at 10 μM for 24 hours. Growth percentage is calculated by comparing the protein density at the end of the experiment to the protein density at the beginning of the experiment. Full experimental details can be found on the NCI's DTP webpage (https://dtp.cancer.gov/discovery_development/nci-60/methodology.htm).

Results for compounds **II‑1‑II‑4** can be found in Table II-2. As described above, each compound has high anti-cancer activity against all NSCLC cell lines tested. When averaging the growth percentages for each compound against the nine NSCLC lines tested, a clear pattern can be observed with the anti-cancer properties. As the alkyl chain lengthens, the cells exhibit a lower growth percentage. This suggests that lipophilicity of these compounds is correlated with anticancer activity. These results are consistent with previously described naphthylmethyl-substituted imidazolium salts with a variety of substituents at the C^4 and C^5 positions.[82]

Table II-2. Growth % values for NSCLC cell lines treated with **II‑1** ‑ **II‑4** in the NCI-60 human tumor cell line one-dose assay.

Compound	Cell Line									Average
	A549/ATCC	EKVX	HOP-62	HOP-92	NCI-H226	NCI-H23	NCI-H322M	NCI-H460	NCI-H522	
II‑1	42.30	46.99	18.00	-20.33	18.99	5.53	48.92	9.12	n/a	21.19
II‑2	28.54	11.92	11.94	-31.42	6.75	-14.57	44.31	5.54	-25.40	4.18
II‑3	31.63	21.10	5.82	-38.34	0.23	-28.22	23.19	3.26	n/a	2.33
II‑4	29.75	14.36	-2.71	-38.22	-0.47	-23.78	23.26	-13.07	n/a	-1.36

Compounds **II‑1‑II‑4** were also tested in the five-dose assay by the NCI's DTP. In this assay, cells are exposed to compounds at concentrations of 10 nM, 100 nM, 1 µM, 10 µM, and 100 µM. Results for this assay are given as GI50, growth inhibition of 50% of cell relative to control cells; TGI, total growth inhibition relation to control cells; and LC50, lethal concentration for 50% of cells relative to control cells. Results are summarized in Table II-3 and full plots for the NSCLC cell lines exposed to each compound can be found in Figure II-10, Figure II-11, Figure II-12, and Figure II-13. All GI50 values in are in the mid nanomolar range to low micromolar range. TGI values range from 1.44 µM to 21.3 µM. Finally, LC50 values range from the low micromolar concentration to greater than 100 µM. Only two LC50 values were given for **II‑4** with results from the NCI-H23 and NCI-H322M cell lines. These results are not surprising with all GI50 values in the mid nanomolar to low micromolar range considering these results were similar to the IC_{50} values found by our MTT experiments. These results also suggest that these imidazolium salts are capable of completely inhibiting the growth of NSCLC lung cancer cells and killing NSCLC cells at higher concentrations. The results are promising from the five-dose assay and confirm that these are potent anti-cancer agents against NSCLC.

Table II-3. Results from the NCI-60 human tumor cell line five-dose assay for compounds **II-1** -

II-4. GI50, TGI, and LC50 values are given in µM concentrations.

Cell Line	II-1			II-2			II-3			II-4		
	GI50	TGI	LC50	GI50	TGI	LC50	GI50	TGI	LC50	GI50	TGI	LC50
A549/ATCC	3.81	21.3	66.1	2.59	13.9	57.9	2.67	12.1	60.3	1.67	3.24	n/a
EKVZ	2.32	17.1	52.4	0.766	5.55	35.8	1.71	11.4	60.5	1.35	3.47	n/a
HOP-62	1.60	8.35	45.3	1.42	3.65	9.36	1.26	2.80	6.19	1.29	2.75	n/a
HOP-92	0.673	3.64	26.4	0.338	1.77	1.77	0.863	2.66	7.58	0.844	2.35	n/a
NCI-H226	1.85	10.4	64.1	1.08	3.82	3.82	1.31	3.92	> 100	1.35	2.93	n/a
NCI-H23	0.717	2.93	10.4	0.396	2.02	2.02	0.521	2.51	9.77	0.793	2.31	5.85
NCI-H322M	2.46	10.4	32.9	2.12	6.71	6.71	1.96	6.00	23.8	1.38	2.75	5.48
NCI-H460	1.59	10.7	44.0	0.724	2.15	2.15	1.22	3.01	7.44	1.25	2.82	n/a
NCI-H522	0.256	1.81	6.72	0.303	1.44	1.44	0.378	1.68	4.92	0.491	1.89	n/a

98
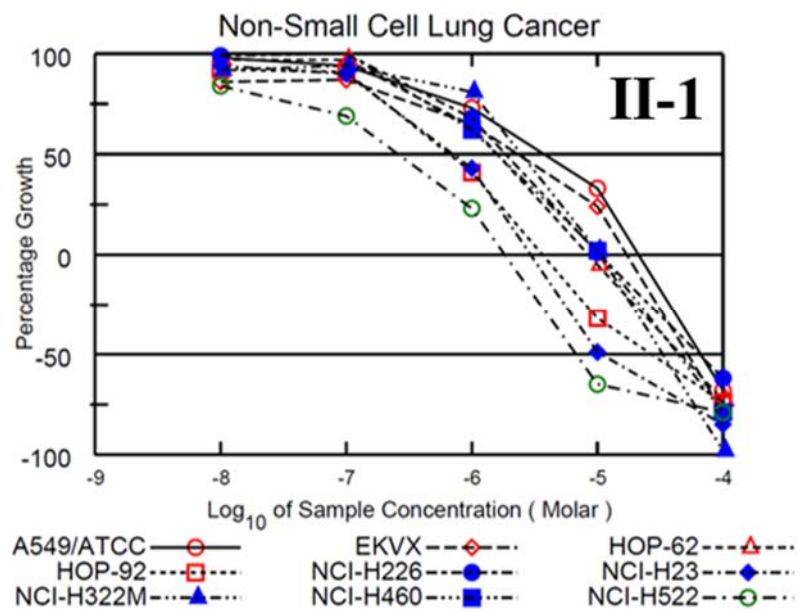
Figure II-10. Growth percentage plot of NSCLC cell lines exposed to **II‑1** in the NCI-60

cell line screen 5-dose assay.
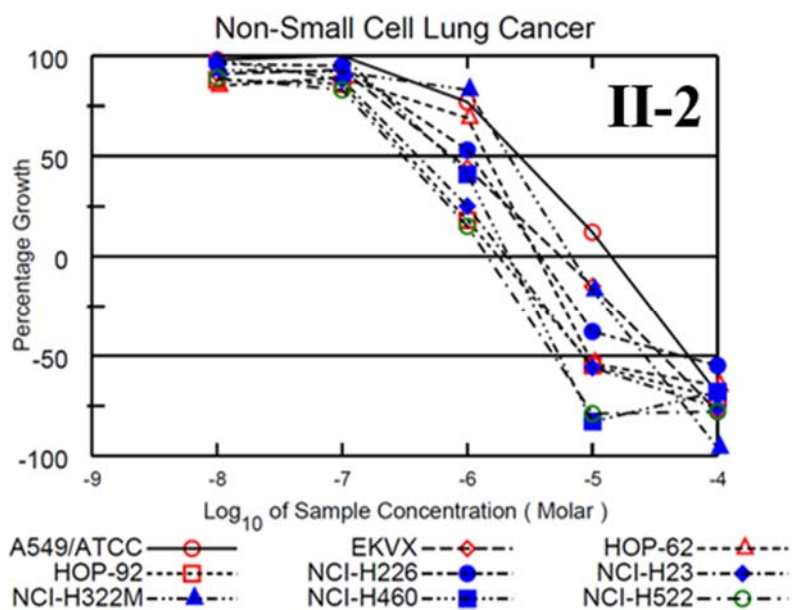
Figure II-11. Growth percentage plot of NSCLC cell lines exposed to **II‑2** in the NCI-60

cell line screen 5-dose assay.
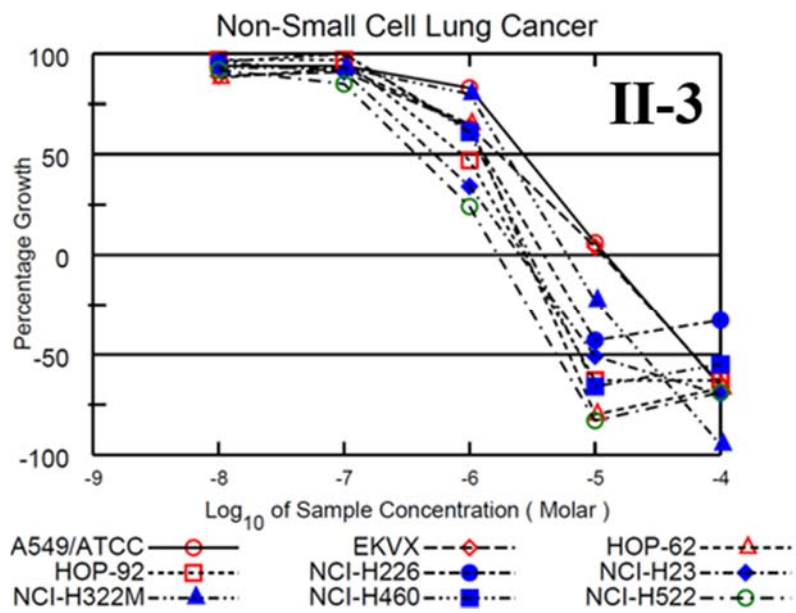
Figure II-12. Growth percentage plot of NSCLC cell lines exposed to **II‑3** in the NCI-60

cell line screen 5-dose assay.
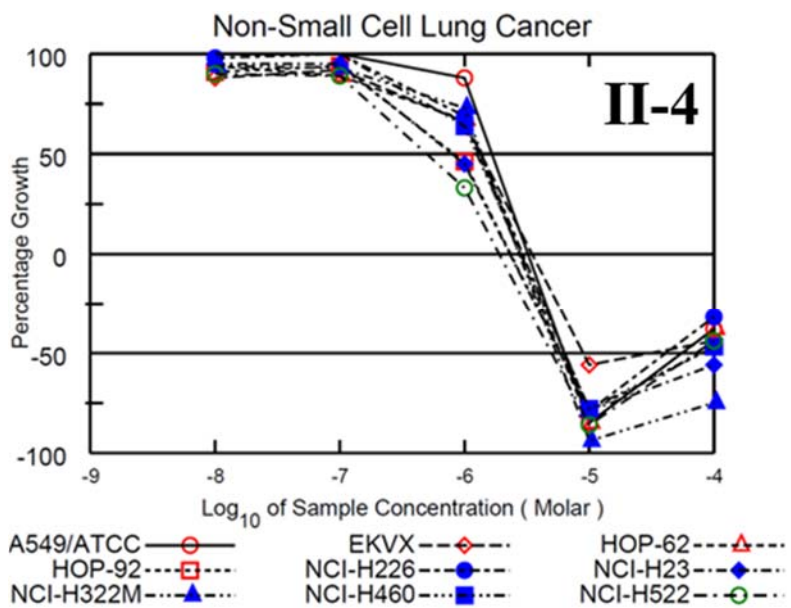
Figure II-13. Growth percentage plot of NSCLC cell lines exposed to **II‑4** in the NCI-60

cell line screen 5-dose assay.

2.2.2.3. Annexin V assay

Little is known about the mechanism of cell death upon treatment with the various imidazolium salts with naphthylmethyl substituents that have been reported thus far. It was reported previously that **I-463** and a C^4 and C^5 hydrogen-substituted derivative (**I-487**) were able to induce apoptosis in the NCI-H460 cell line.[4,82] An Annexin V apoptosis detection kit was utilized to determine if **II-2** caused apoptosis or if cellular death resulted from necrosis. In cells that undergo apoptosis, phosphatidylserine (PS) is detected on the outside of the cellular membrane.[100] This occurs during the early stages of apoptosis because cell membrane asymmetry and integrity is lost allowing PS to translocate to the outer leaflet of the cell membrane where it can interact with Annexin V, which is conjugated to FITC (fluorescein isothiocyanate) to give fluorescence detectable by microscopy. In order to fully distinguish apoptosis from necrosis, a secondary stain is necessary. Propidium iodide (PI), which interacts with DNA, is a cell membrane impermeable compound. It only has the ability to enter cells that have compromised membranes, which occurs later in the process of apoptosis.[100] The progression in time of cells from having strictly green fluorescence to green and red fluorescence is indicative of apoptosis. On the other hand, necrotic cells would be visualized with both green and red fluorescence even at early time points.

The Annexin V assay was performed with compound **II-2** to determine if adding an alkyl group to the C^2 position would influence the initiation of cellular death. For example, morphological changes such as cell shrinkage, rounding, and detachment occurred in H460 cells within the first hour when treated with **I-463**, but morphological

changes and strong green fluorescence suggesting apoptosis were not apparent with the I‑487 until 3 hours. These results indicate that subtle changes to the imidazole scaffold can have drastic effects on anti-proliferative efficacy. Strong green fluorescence was observed for II‑2 when dissolved in a water/DMSO solution (the stock solution was prepared the same as in the MTT assay), at time points similar to that of IC23 (*i.e.*, 1 hour). However, when II‑2 was dissolved in the 10% by weight 2-HPβCD aqueous solution, strong green fluorescence was not observed until the 12-hour time point (Figure II-14 and Figure II-15).

The presence of blebbing, is another indicator of the apoptotic mode of cell death. Compound II‑2 was shown to cause blebbing when administered with either DMSO or 2-HPβCD as the solubilizing vehicle. However, a stark contrast can be seen in the time frames of when this occurs. When in DMSO, blebbing occurs at 6 hours of treatment whereas with 2-HPβCD, blebbing is not seen until 14 hours of treatment at the earliest (Figure II-16 and Figure II-17). This shows us that not only does compound II‑2 cause apoptosis in two independent Annexin V trials, but that the vehicle used to administer it has an effect on compound availability and timely progression of cell fate.

For potential chemotherapeutics, the apoptotic cell death pathway is desirable considering there are increased levels of inflammation and other issues when cells undergo death by a necrotic pathway. It is known that when compounds are dissolved in cyclodextrin solutions there is equilibrium between the freely dissolved compound and the compound in complex with the cyclodextrin. Therefore, the delay in detecting the early stages of apoptosis visualized in cells treated with II‑2 dissolved in 2-HPβCD compared to II‑2 dissolved with DMSO was not surprising.

102
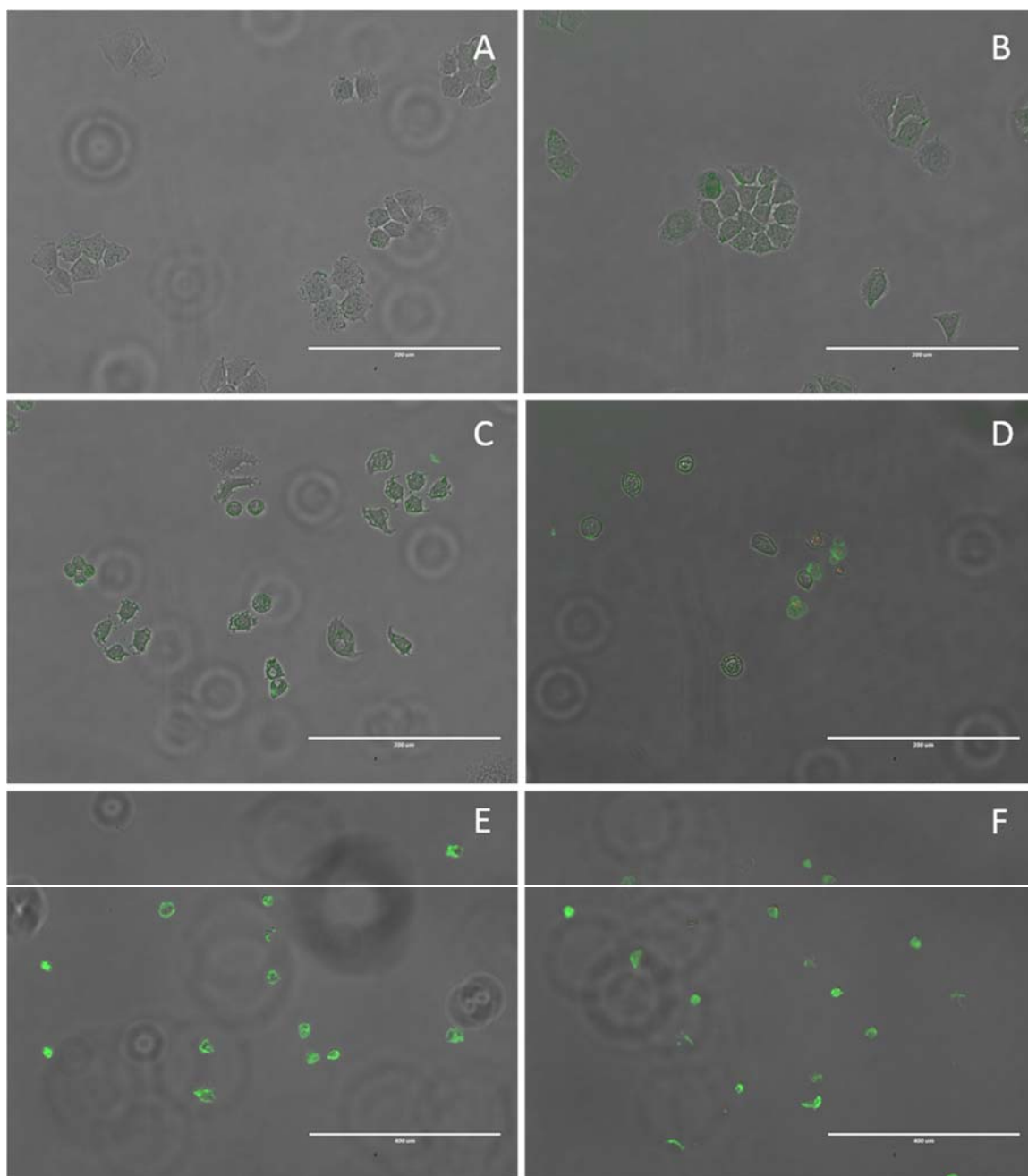
Figure II-14. Images of the Annexin V assay on H460 cells grown in 6-well plates using compound **II‑2** in 1% DMSO aqueous solution as the compound treatment. All images taken using a 20x objective unless otherwise stated. Images are presented as a merged image of the normal transmitted light, green fluorescence and red fluorescence figures. (A) DMSO control, 12 hours. (B) Cisplatin control, 12 hours. (C) Compound **II‑2**, 1 hour. (D) Compound **II‑2**, 3 hours. (E) Compound II-2, 6 hours, 10x objective. (F) Compound II-2, 12 hours, 10x objective. (A-D) Scale bars equal 200 µm; (E and F) Scale bars equal 400 µm.
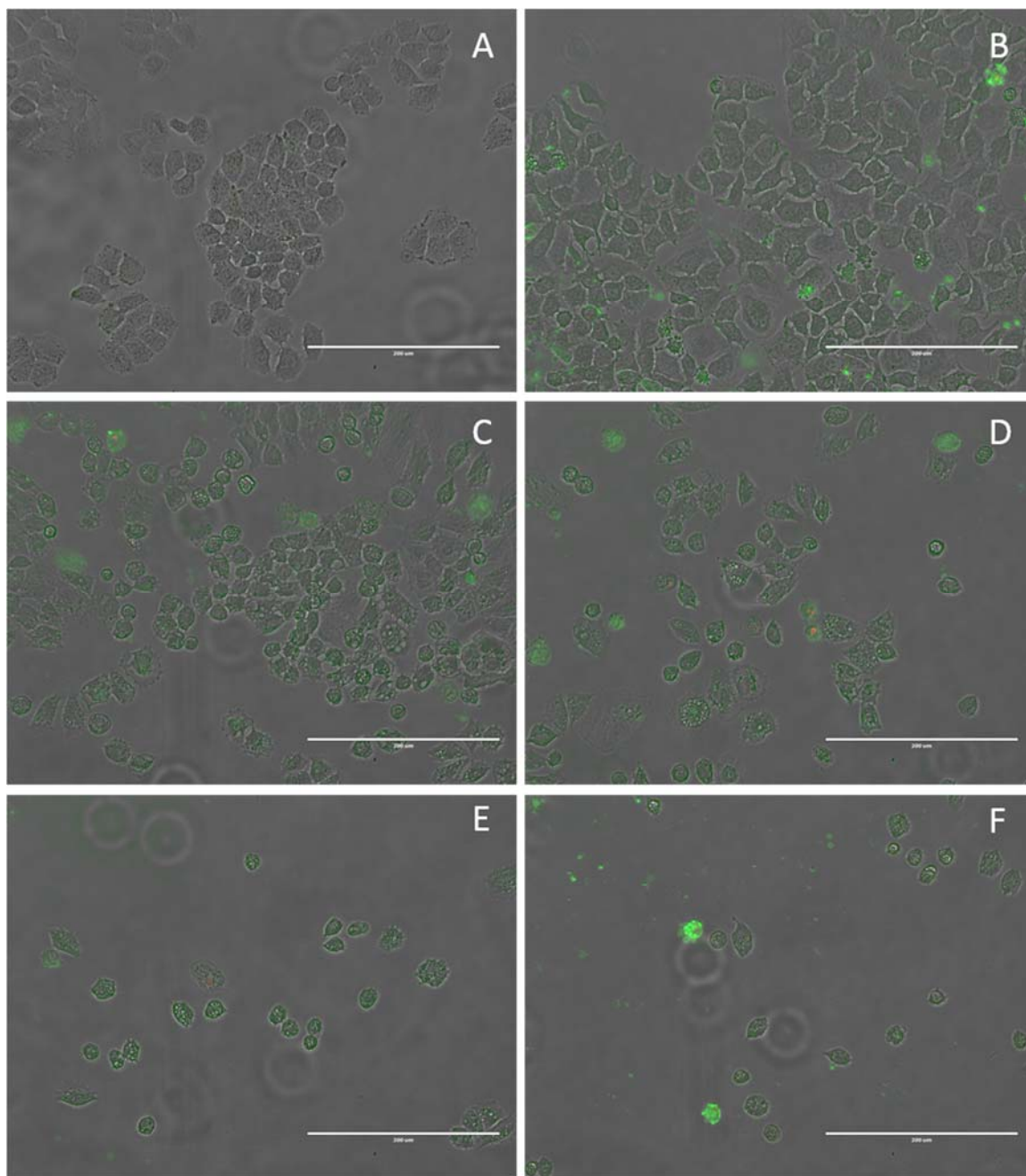
Figure II-15. Images of the Annexin V assay on H460 cells grown in 6-well plates using compound **II‑2** in 10% by weight 2-HPβCD aqueous solution as the compound treatment. All images taken using a 20x objective. Images are presented as a merged image of the normal transmitted light, green fluorescence and red fluorescence figures. (A) 2-HPβCD control, 20 hours. (B) Cisplatin control, 20 hours. (C) Compound **II‑2**, 12 hour. (D) Compound II-2, 14 hours. (E) Compound II-2, 17 hours. (F) Compound II-2, 20 hours. Scale bars equal 200 μm.
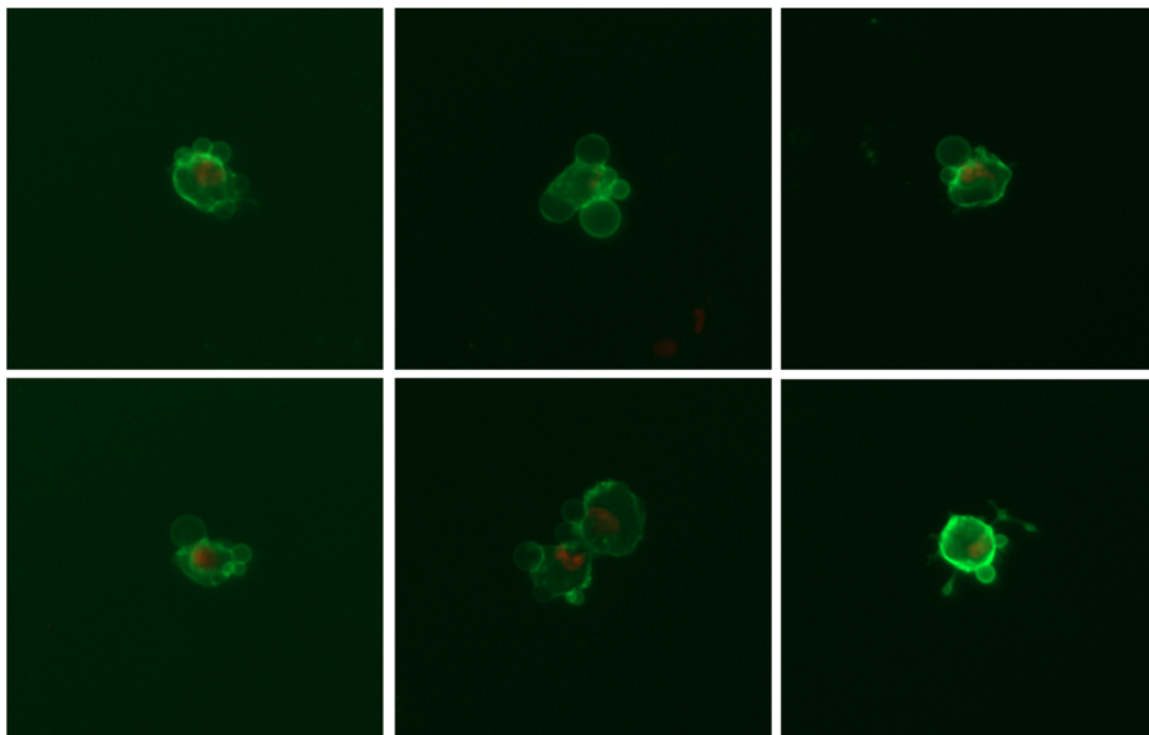
Figure II-16. Images of the Annexin V assay on H460 cells grown in 6-well plates using compound **II‑2** in 1% DMSO aqueous solution as the compound treatment. All images taken using a 20x objective. Images are presented as a merged image of the green fluorescence and red fluorescence figures, omitting the normal transmitted light image for blebbing clarity. All images taken at the 3-hour time point.
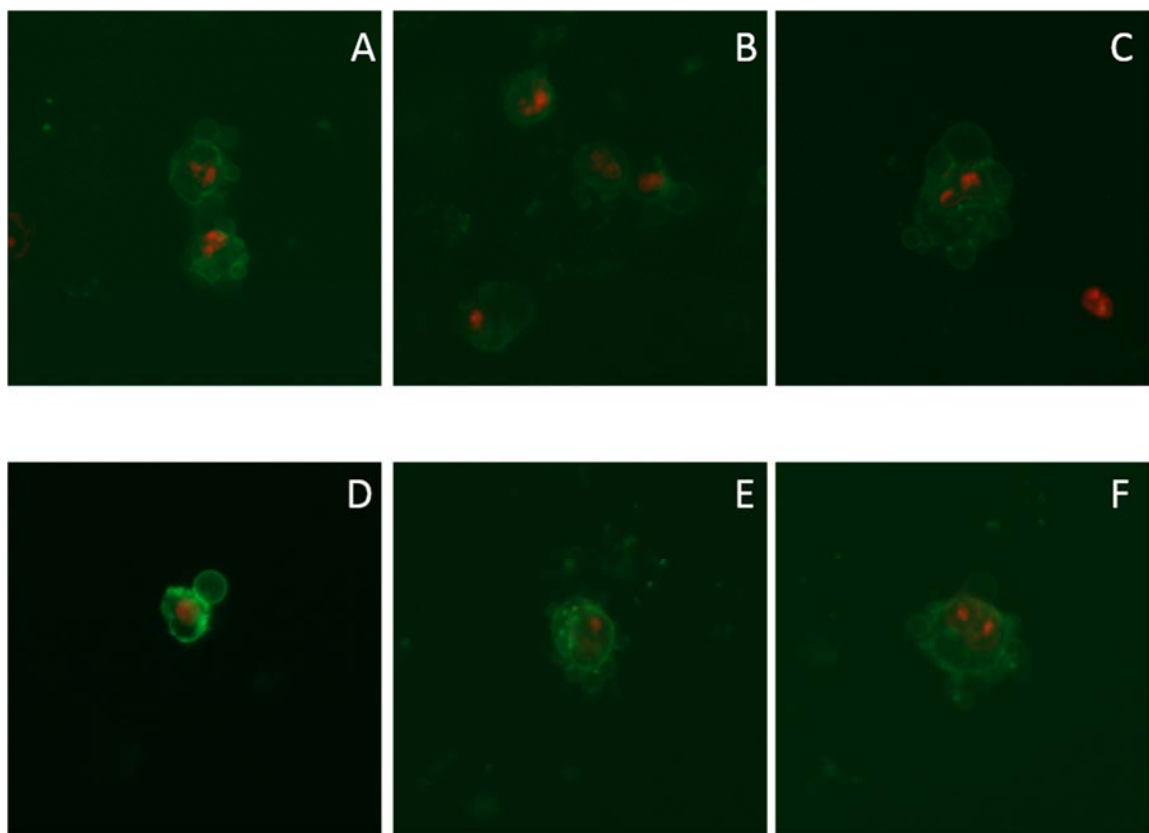
Figure II-17. Images of the Annexin V assay on H460 cells grown in 6-well plates using compound **II‑2** in 10% by weight 2-HPβCD aqueous solution as the compound treatment. All images taken using a 20x objective. Images are presented as a merged image of the green fluorescence and red fluorescence figures, omitting the normal transmitted light image for blebbing clarity. Images A-C were taken at the 14-hour time point and D-F were taken at the 17-hour time point.

2.2.2.4. DNA Interaction Assays

In order to better understand how this class of compounds causes the process of apoptosis to occur, the study of interactions with DNA was investigated. This potential mechanism was chosen due to the planar aromatic nature of these compounds, which is

similar to other known DNA intercalators.[101] In order to determine the level of interaction of **II‑2** with DNA, viscosity measurements and fluorescent intercalator displacement (FID) assays were completed using calf thymus DNA (CT-DNA). The viscosity measurement can suggest if the compound being tested is capable of intercalating into the base pairs of DNA. Intercalators cause strain to the normal helical structure of DNA which is accounted for with a subtle unwinding of the DNA. This unwinding causes the DNA to lengthen and thus increases viscosity. If a compound interacts as a groove binder or does not interact with DNA, the viscosity will remain unchanged.[102] The FID assay also looks at interaction with DNA but through fluorimetry. A solution of ethidium bromide and CT-DNA is known to have strong fluorescence and if ethidium bromide is displaced by the compound being tested the fluorescence intensity will decrease. Displacement can either come from an intercalator or a strong groove binder such as netropsin, which is a common positive control used in this assay.[103]

Results of the viscosity and FID studies showed that compound **II‑2** did not have an apparent interaction with CT-DNA when compared to controls (Figure II-18 and Figure II-19). Solutions made in 2-HPβCD were completely soluble. However, a small amount of insoluble material remained after attempting to dissolve 3 mg of compound **II‑2** in 1 mL of the 10% DMSO solution. The insolubles remained in the sample vial and therefore did not disrupt viscosity measurements. For the FID, a 2 mg/mL solution was prepared instead which remained completely soluble. For viscosity, ethidium bromide was used as a positive control and netropsin was used as a negative control. Vehicle controls were also run on the 10% DMSO aqueous solution used as well as the 10% by weight 2-HPβCD aqueous

solution. In regards to the FID assay, netropsin was used as a positive control with vehicle controls included as well. The data show that compound **II‑2** does not change the results relative to vehicle controls in either study. While DNA is therefore an unlikely target for these compounds, there are many other intracellular mechanisms that can be investigated.
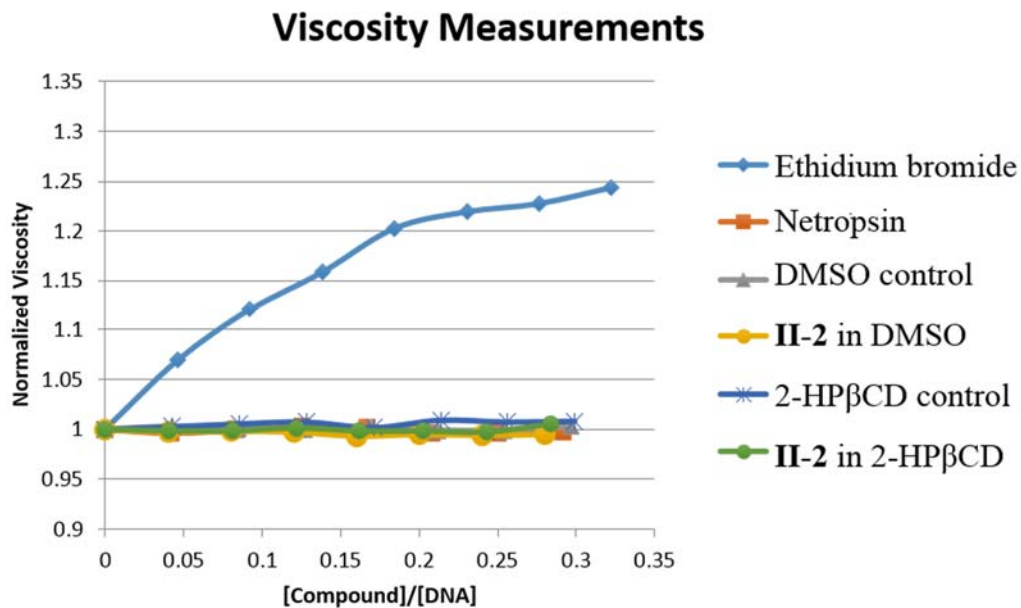
Figure II-18.Plot of viscosity of compound **II‑2** using CT-DNA relative to controls.
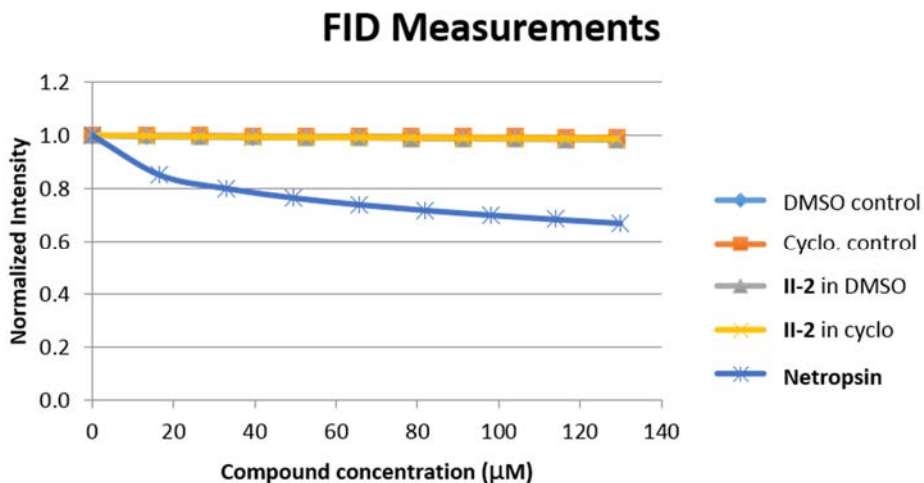
Figure II-19. Plot of FID results of compound **II‑2** using CT-DNA relative to controls.

2.2.2.5. Mitochondrial JC-1 assay

After determining that DNA was not a viable cellular target for compound **II‑2**, the mitochondria was considered as an intracellular target considering it has been previously reported that delocalized lipophilic cations (DLCs) can target the mitochondria of cells.[104,105] Imidazolium salts containing naphthylmethyl substituents at the N^1 and N^3 positions can be classified as DLCs, and thus mitochondria were studied for their potential role in the mechanism of action. One assay that can be utilized to study mitochondrial function is the JC-1 assay. JC-1 is a cationic dye that can accumulate in the mitochondria with intact membrane potentials (Figure II-20). This mitochondrial membrane potential, or MMP, is caused by a proton gradient across the inner membrane and is important for the production of ATP by the enzyme ATP synthase.[106] The formation of J-aggregates by a high concentration of JC-1 in the matrix of mitochondria produces red fluorescence. However, when MMP is disrupted, J-aggregates do not congregate in the matrix and

109

fluorescence is shifted from red to green as the monomer disperses in the cell. Interestingly, the structure of JC-1 shows some similarities to the imidazolium salts presented here.[107] Healthy cells with intact MMP will display red fluorescence in the mitochondria with green fluorescence in the cytosol, and cells with disrupted MMP will show green fluorescence with a decrease in the amount of red fluorescence or no red fluorescence at all.
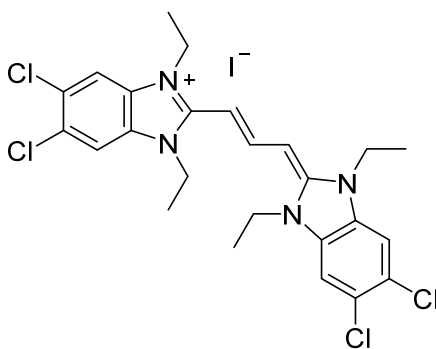
Figure II-20. Structure of JC-1.

The H460 cell line was treated with **II‑2** at a concentration of 40 μM (the same as for the Annexin V assay) for 1 hour and 2.5 hours (Annexin V showed blebbing at 3 hours when using DMSO for solubilization). The stock solution of **II-2** was prepared by dissolving the compound in DMSO and diluting with water similar to the MTT and Annexin V assays. However, there was minimal red fluorescence seen at either time point; whereas, cells exposed to the media and vehicle control solutions had intact MMP. This suggested that at a concentration of 40 μM, **II‑2** had disrupted the MMP of the majority of mitochondria by 1 hour. It was presumed that a shorter time frame was necessary to observe the progression of fluorescence from normal MMP to disrupted MMP. In an attempt to observe the progression of fluorescence from normal MMP to disrupted MMP, the H460

cells were treated with **II‑2** at 40 μM for 30 minutes and 1 hour prior to adding JC-1.

Unfortunately, the 30-minute time point also showed minimal red fluorescence; whereas, media control cells had red fluorescence suggesting the mitochondria were still intact. Figure II-21 shows a comparison of the 30-minute and 1-hour treatment of cells with **II‑2** demonstrating the lack of red fluorescence at both time points.
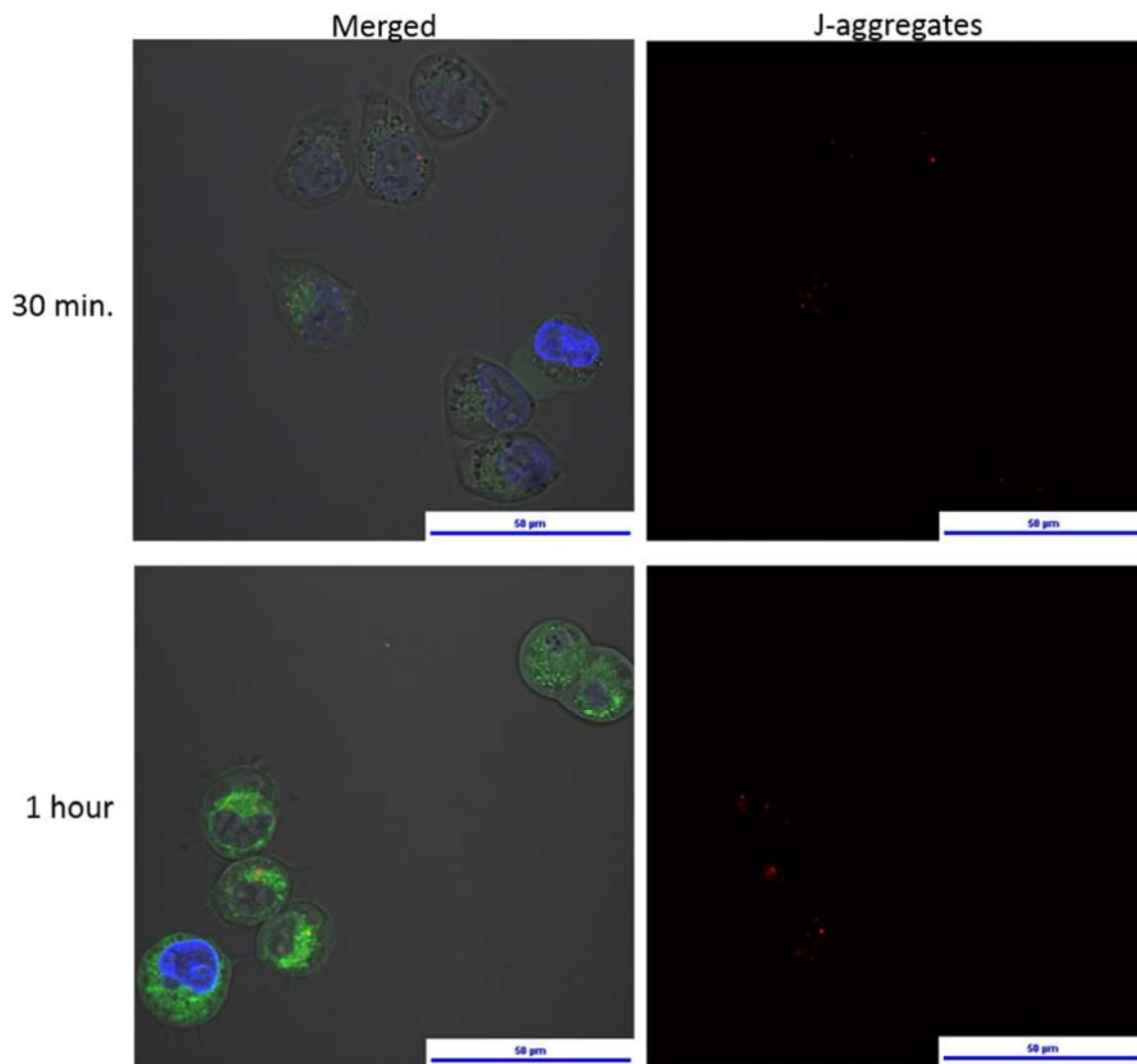
Figure II-21. Images of the JC-1 assay on H460 cells grown in 35 mm glass bottom dishes using compound **II‑2** at 40 μM in a 1% DMSO aqueous solution as the compound treatment. All images were taken using a 100x objective. Images are presented as a merged image of the normal transmitted light, green fluorescence, blue fluorescence, and red fluorescence figures (merged column) or the red fluorescence alone (J-aggregates column) at the specified time frames. Scale bars equal 50 μm.

In order to visualize the progression of red fluorescence to the lack of red fluorescence at time points feasible for cellular treatment and imaging, the concentration of **II‑2** was decreased from 40 μM to 20 μM. Compound **II-2** was exposed to cells for 15 minutes and 1 hour at this concentration. Red fluorescence was observed at 15 minutes and the 1 hour time point with an apparent decrease in intensity for cells treated with **II‑2** for 1 hour; unfortunately, we do not have quantitative data to support this claim. A positive control, carbonylcyanide m-chlorophenylhydrazone (CCCP), was used to verify the assay. Similarly to the cells treated with **II‑2**, mitochondria potential was decreased compared to the media control cells, as shown by an apparent decrease in red fluorescence signal, as with **II-2**, we do not yet have quantitative data to support this claim. Results of this assay suggest that **II‑2** may have disrupted the MMP, visualized by the decrease in observed red fluorescence of cells (Figure II-22). To our knowledge, this is the first report to indicate that N,N'-bisnaphthylmethyl imidazolium salts may target the mitochondria of H460 lung cancer cells as part of their mechanism of action. These results, in accordance with the Annexin V assay, give important information regarding the cellular target and mechanism of action for **II‑2** against the NCI-H460 NSCLC cell line. In the JC-1 assay, cells treated with **II‑2** at a concentration of 40 μM were visualized to have completely disrupted MMP by the 30-minute time point. Images from the Annexin V assay, at the same concentration of **II‑2**, show green fluorescence of cells with normal morphology at 1 hour and cellular blebbing at 3 hours indicating that MMP disruption occurs early during the process of apoptosis, possibly prior to the translocation of PS to the outer leaflet. Although this MMP disruption does not prove that mitochondria are the cellular target of **II-2**, it does further

113

suggest that **II-2** causes apoptosis considering the MMP is disrupted early during the apoptotic pathway.[108] Further studies to confirm these results include quantification of fluorescence from the JC-1 assay and utilizing other cellular assays to determine mitochondrial reactive oxygen species (ROS) production.
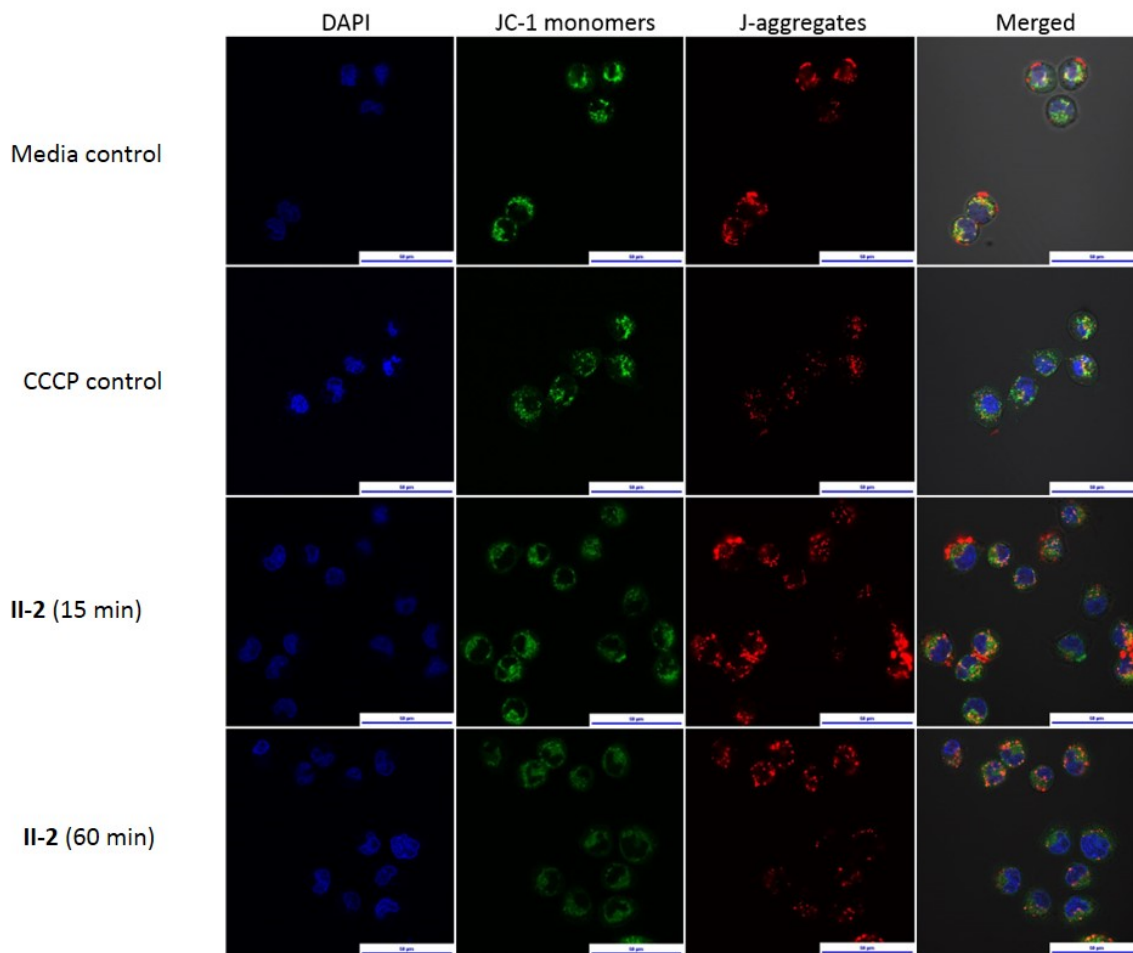
Figure II-22. Images of the JC-1 assay on H460 cells grown in 35 mm glass bottom dishes using compound **II‑2** at 20 μM in 1% DMSO aqueous solution as the compound treatment. All images were taken using a 100x objective. Images are presented as the individual fluorescence images followed by the merged image of the normal transmitted light, green fluorescence, blue fluorescence, and red fluorescence figures. Scale bars equal 50 μm.

2.2.2.6. NSCLC cell characteristics

Understanding the characteristics of the cells these compounds have been exposed to, may give information towards the mechanism of action (most information obtained in

115

this section was found on the ATCC website where cells were purchased from, https://www.atcc.org/). Only the four NSCLC cell lines used in our lab will be evaluated (NCI-H460, NCI-H1975, HCC827, and A549). All four cell lines are NSCLC. The NCH0H460 cell line is a large cell lung carcinoma cancer type. The other three cell lines, NCI-H1975, HCC827, and A549, have the adenocarcinoma cancer type. Both the NCI-H460 and A549 cell lines are hypotriploid, meaning there is an abnormal chromosome count. The HCC827 cell line has a mutation of the epidermal growth factor receptor that results in proliferation.[109] The NCI-H1975 cell lines has several mutant genes including the epidermal growth factor receptor, the cyclin dependent kinase inhibitor 2A (which under normal function encodes proteins that suppress tumors)[110], the Phosphatidylinositol-4,5-bisphosphate 3-kinase catalytic subunit alpha gene (which is also important for proliferation)[111,112], and the tumor protein p53 (which is responsible for producing the tumor suppressing protein p53)[113]. Compounds II-1-II-5 all seem to inhibit the growth of the NCI-H1975 cell line at the lowest concentration of compound exposure. This could suggest that one of the mechanisms by which these compounds induce apoptosis is by binding to one of the proteins responsible for uncontrollable proliferation of this particular cell line. However, if this were the case, the compound most likely has multiple mechanisms by which it induces apoptosis considering they were able to prevent proliferation in a variety of different cell lines with different mutations.

2.2.3. Preliminary in vivo toxicity study

Considering the high anti-cancer activity of **II‑2** and the Annexin V and JC-1 results obtained, **II‑2** was chosen for a preliminary in vivo toxicity study using C57BL/6 mice. A 20% 2-HPβCD solution was used to fully solubilize **II‑2** and was used as the vehicle control solution. On day zero, vehicle control animals were injected with 100 μL of 2-HPβCD (20% w/v) solution by intraperitoneal (IP) injection; whereas, the experimental group was injected with 100 μL of a 20 mg/kg dose (assuming an average mass of 20 g for each mouse) of **II‑2** dissolved in the 2-HPβCD (20% w/v) solution by IP injection. Vehicle control mice were also injected on days seven, fourteen, twenty‑one, twenty‑five, and twenty‑nine. Experimental mice were only injected again on day fourteen with a 15 mg/kg dose of **II‑2**. Each animal's behavior and weight were closely monitored for the duration of the study (Figure II-23). All mice in the vehicle control group gained weight at a steady pace and survived over the entire course of the study (Figure II-24).

A sharp decrease in weight was observed for all mice treated with **II‑2** after the first injection. On day two, one mouse from the experimental group was found deceased. Both surviving mice treated with **II‑2** began to regain weight on day four and continued this trend until injected with a 15 mg/kg dose on day fourteen. Although average weight loss was around 6%, both animals were sacrificed due to lethargic movement the day after the second injection. Compound **II‑2** proved to be quite toxic at the doses administered. However, this preliminary study results in a starting point for future in vivo studies with **II‑2** involving either a more intensive toxicity study or a lung xenograft model to

117

determine the ability of **II‑2** to inhibit the growth of a tumor and reduce the size of a tumor

mass.

Average weight gain % for mice treated with vehicle control and **II-2**
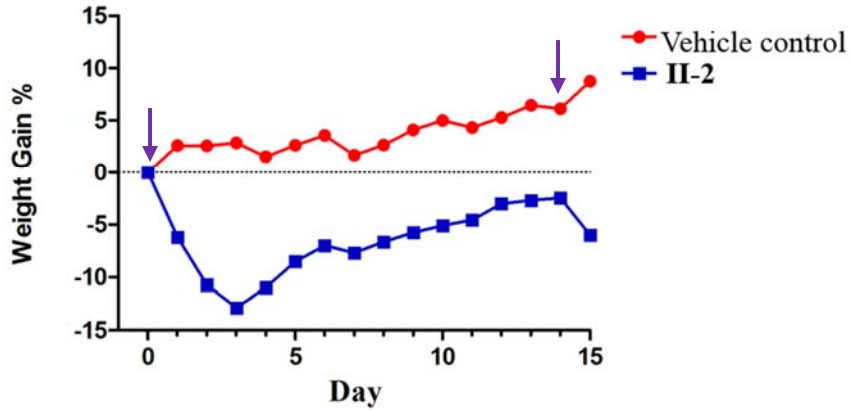
Figure II-23. Weight chart for C57BL/6 mice injected with the vehicle control and **II‑2**.

The purple arrows signify the days mice were injected with **II‑2**.

Kaplan-Meier curve
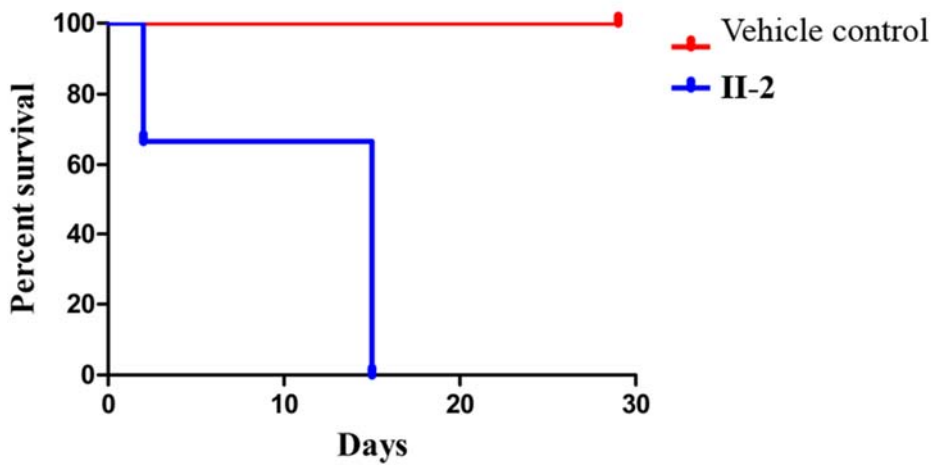
Figure II-24. Kaplan-Meier curve describing survival of C57BL/6 mice treated with the

vehicle control and **II‑2**.

2.3. Conclusions and future outlook

Compounds **II‑1**‑**II‑5** all displayed high anti-cancer activity towards several NSCLC cell lines, as determined by the MTT assay, comparable to cisplatin and previously published imidazolium salts with naphthylmethyl substituents. Compounds **II‑1**‑**II‑4** also displayed high anti-proliferative effects in the NCI-60 human tumor cell line screen one-dose assay. Considering the compounds were active in the one dose assay the NCI's DTP also tested **II‑1**‑**II‑4** in their five-dose assay. All compounds were again highly active in the five-dose assay.

Compound **II‑2** was further tested in an Annexin V assay to determine the mode of cell death. Images from the Annexin V assay suggest an apoptotic mode of cell death similar to related N,N'-bisnapthylmethyl imidazolium salts.[4,82] Mechanism of action studies using **II‑2** included in vitro DNA interaction studies and a JC-1 assay. Compound **II‑2** did not show any interaction with DNA by a viscosity or fluorescent intercalator displacement assay. However, a lack of red fluorescence in cells treated with **II‑2** in the JC-1 assay suggested a disruption of the MMP. This is the first positive information concerning the mechanism of action of N,N'-bisnaphthylmethyl imidazolium salts against NSCLC. Understanding the mechanism of action is essential to the progression into clinical settings and suggesting the mitochondria may be the cellular target is vital for the progression and use of **II‑2** in future studies.

Unfortunately, these lipophilic imidazolium salts have limited aqueous solubility that would prevent the ability to systemically administer them. However, a chemical

excipient, 2-HPβCD, was used to solubilize **II‑1**‑**II‑4** at concentrations of 4.4 mg/mL making them clinically relevant. 2-HPβCD is FDA approved and used in drug formulations. The MTT assay for **II‑1**‑**II‑5** and the Annexin V assay for **II‑2** were also performed with stock solutions of each compound dissolved in a 2-HPβCD solution versus using DMSO since, to our knowledge, DMSO is not used in drug formulations for the treatment of cancer. Results from the MTT assay were strikingly similar when using DMSO or 2-HPβCD to solubilize each compound suggesting the excipient does not cause any difference in the anti-cancer activity of the compound. The Annexin V assay using **II‑2** dissolved in 2-HPβCD also suggested an apoptotic mode of cell death, although the time frame was extended when compared to results taken from the compound initially dissolved with DMSO.

A preliminary in vitro toxicity study using **II-2** suggested the compound was quite toxic at the dose tested causing mortality in one animal days after the first injection. However, this toxicity study provides a starting point for future studies considering this compound is highly cytotoxic towards NSCLC, it could inhibit the growth of a tumor at lower doses without causing severe side effects. Therefore, since **II‑2** could be dissolved at a high concentration with 2-HPβCD and considering we now have some in vitro mechanistic data for **II‑2**, it is a prime candidate for future studies including further in vivo toxicity and lung xenograft experiments.

2.4. Acknowledgements

2.5. Experimental Section

2.5.1. General Procedures

All reactions were carried out under aerobic conditions. 2-Methylimidazole and carbonyl cyanide *m*-chlorophenylhydrazone were purchased from Alpha Aesar. 2-Ethyl imidazole and DAPI were purchased from Acros Organics. 2-Propylimidazole was purchased from Ark Pharm, Inc. 2-Butylimidazole and 2-isopropylimidazole were purchased from TCI. 2-(Bromomethyl)naphthalene was purchased from Waterstone Technologies. 2-Hydroxypropyl-β-cyclodextrin (batch average molecular weight: 1400) was purchased from Tocris Bioscience. JC-1 was purchased from AdipoGen. Glass bottom dishes coated with poly-D-lysine used in the JC-1 assay (P35GC-1.5-14-C) were purchased from MatTek Corporation. FITC Annexin V Apoptosis Detection Kit was purchased from

BD Biosciences. UltraPure™ Calf Thymus DNA Solution, UltraPure™ ethidium bromide, and UltraPure™ DNase/RNase-Free Distilled Water were purchased from Thermos Fisher Scientific. All solvents were purchased from Fisher Scientific. All reagents were used as received without further purification. Melting points were obtained using a MelTemp apparatus with a calibrated thermometer. ^{1}H and ^{13}C NMR spectra were obtained on a Varian 500 MHz instrument with all spectra referenced to residual deuterated solvent (DMSO-d_6: ^{1}H NMR: 2.50 ppm, ^{13}C NMR: 39.5 ppm). Mass spectrometry was performed in the University of Akron mass spectrometry laboratory. Elemental analysis was performed by Atlantic Microlab in Norcross, Georgia.

The human NSCLC cell lines NCI-H1975 and HCC827 were generously provided by Dr. Lindner from the Cleveland Clinic. The human NSCLC cell lines NCI-H460 and A549 were purchased from ATCC (Manassas, VA, USA). All cell lines were grown at 37 °C with 5% CO_2 in RPMI 1640 medium supplemented with 10% fetal bovine serum and passed every 2-3 days.

2.5.2. X-ray analysis

Crystals of the compounds were coated in paratone oil, mounted on a CryoLoop and placed on a goniometer under a stream of nitrogen. Crystal structure data sets were collected on either a Bruker SMART APEX I CCD diffractometer with graphite-monochromated Mo Kα radiation (λ = 0.71073 Å) or a Bruker Kappa APEX II Duo CCD system equipped with a Mo ImuS source and a Cu ImuS micro-focus source equipped with QUAZAR optics (λ = 1.54178 Å). The unit cells were determined by using reflections from

122

three different orientations. Data sets were collected using SMART or APEX II software packages. All data sets were processed using the APEX II software suite.[114,115] The data sets were integrated using SAINT.[116] An empirical absorption correction and other corrections were applied to the data sets using multi-scan SADABS.[117] Structure solution, refinement, and modelling were accomplished by using the Bruker SHELXTL package.[118] The structures were determined by full-matrix least-squares refinement of F^2 and the selection of the appropriate atoms from the generated difference map. Hydrogen atom positions were calculated and $U_{iso}(H)$ values were fixed according to a riding model.

2.5.3. MTT assay

Cells were grown to confluence and plated in 96-well plates at 5,000-7,000 cells per well, depending on the cell line. Cells were incubated for 24 h prior to adding the compounds. Compounds **II‑1**‑**II‑5** were dissolved in either a DMSO/water solution or a 2-HPβCD solution and diluted in fresh medium to the desired concentrations of 16, 4, 1, and 0.25 μM. Cisplatin was dissolved in pure water by stirring for several hours at room temperature and then diluted to the appropriate concentrations. Compounds were added (6 replicates each) and cells were incubated for 72 h, at which time the MTT assay protocol was followed. MTT reagent (10 μL) was added to each well and cells were incubated for 3-4 h, again depending on the cell line. Growth medium was removed by aspiration and DMSO (100 μL) was added to each well. Plates were incubated for 15 min. The optical density was read at 540 nm on a Fisher Scientific Multiskan FC plate reader. Each

experiment was done in triplicate and reported results were averages from each independent experiment.

2.5.4. Annexin V assay

The Annexin V assay was conducted using the components of a FITC Annexin V Apoptosis Detection Kit I. The NCI-H460 cell line was grown in 6-well plates at a density of $1x10^5$ cells per well. After allowing cells to adhere overnight, they were treated with controls or compound **II‑2** at a concentration of 40 μM for the indicated time points. To prepare medium for treatments, cisplatin was first solubilized in DMSO and diluted to give a 1% DMSO/water solution and was further diluted to a 40 μM concentration in culture medium. For compound **II‑2** treatments, the compound was first solubilized in either a 1% DMSO/water solution (solubilizing in the DMSO first before diluting with water) or a 10% by weight aqueous 2-HPβCD solution and further diluted to the aforementioned concentration in culture medium. Treatments consisted of aspirating medium from the respective wells and replacing with either DMSO, 2-HPβCD, cisplatin, or compound **II‑2** supplemented medium (2 wells per treatment type) at time points that allow the treatment times to have the same end point. After treatment, the medium was aspirated, and cells were washed twice with cold PBS. The provided 10X binding buffer was diluted to 1X, and 400 μL was added to each well. Subsequently, 20 μL each of the provided FITC Annexin V and PI was also added to each well. The plates were incubated for 15 min on a platform shaker while covered with aluminum foil at room temperature. After this time, the binding buffer was aspirated from the wells, and 1 mL of the 1X binding buffer was

added to each well for imaging. The fluorescence microscope used was an EVOS fl Digital Inverted Microscope with 10X and 20X objectives.

2.5.5. DNA interaction studies

Buffer used for both viscosity and FID studies consisted of a concentration of 5mM Tris and 50mM NaCl regulated to a pH of 7.2 with hydrochloric acid and was made with UltraPure™ DNase/RNase-Free Distilled Water. DNA solutions for the experiments were made with UltraPure™ Calf Thymus DNA Solution. Concentration of CT-DNA in solution was determined using a Varian Cary 100 Bio UV-Visible Spectrophotometer at 260nm using a molar extinction coefficient of 6600 M^{-1} cm^{-1} to give mononucleotide concentration.[119] Average CT-DNA concentration for viscosity studies was 235 μM and average CT-DNA concentration for FID studies was 150 μM. UltraPure™ ethidium bromide, 10 mg/mL was used as received.

2.5.5.1. Viscosity

An Ostwald viscometer was used for the viscosity measurements. The viscometer was submerged in a water bath held at 30°C so that the entire contained sample was temperature regulated. The time it took for the sample to run between the calibrated lines was recorded three times and the average was used for calculation purposes. The flow time of the buffer alone as well as the CT-DNA solution was tested before each new experiment. The compound was titrated in so that each addition made a final solution with a concentration increase of 10 μM, with the first addition being 10 μM and ending with 70

μM. Compound **II‑2** solutions were made by solubilizing the compound in either a 10% DMSO/water solution (solubilizing in the DMSO first before diluting with water) or a 10% by weight 2-HPβCD aqueous solution. Calculations to plot data were obtained by following procedures outlined by Fu *et al.*[102]

2.5.5.2. Fluorescent intercalator displacement

Fluorescence measurements were taken on a Horiba Jobin Yvon FluoroMax-4 spectrofluorometer. The excitation wavelength was set at 510 nm and emission data were obtained at 601 nm. After adding the CT-DNA solution to the cuvette, ethidium bromide was added to give a final concentration of 25 μM. Additions of compound **II‑2** were added to give a final concentration of roughly 13.3 μM per addition. Compound **II‑2** was either solubilized in a 10% DMSO/water (solubilizing in the DMSO first before diluting with water) or a 10% 2-HPβCD aqueous solution. Normalized intensities were calculated by dividing the intensity of the CT-DNA solution with ethidium bromide by the intensity of the CT-DNA solution with ethidium bromide plus compound **II‑2** and plotted against compound concentration.

2.5.6. JC-1 assay

The JC-1 assay was completed using JC-1 as the MMP fluorescent dye, carbonyl cyanide *m*-chlorophenylhydrazone as the positive control, and DAPI as the nuclear stain. A 5 mg/mL stock solution of JC-1 was prepared by solubilizing 5 mg of JC-1 in 1 mL of DMSO. The JC-1 stock solution was diluted in medium to a final concentration of 10

μg/mL to use as the working concentration. A 1 mg/mL stock solution of DAPI nuclear stain was prepared by solubilizing 10 mg of DAPI in 10 mL of deionized water. The DAPI stock solution was diluted in PBS to a final concentration of 1 μg/mL to use as the working solution. A 20 mg/mL stock solution of CCCP was prepared by solubilizing 100 mg of CCCP in 5 mL of DMSO. The CCCP stock solution was diluted in medium to a final concentration of 20 μg/mL to use as the working solution.

The NCI-H460 cell line was grown in 35-mm glass bottom dishes coated with poly-D-lysine at a cell density of 15,000 cells per well. The cell suspension was added to the glass cover of each well (500 μL) and allowed to adhere for 1 hour before additional medium (2 mL) was added to the plate. Cells were placed in the incubator overnight. Cells were treated with supplemented medium at a concentration of 20-40 μM for compound **II‑2** and at 20 μg/mL (98 μM) of CCCP. Media control cells were treated with growth medium, and vehicle control cells were treated with medium supplemented with an equal volume of the 1% DMSO aqueous solution as used for the compound **II‑2** treatments. Treatments consisted of aspirating medium from respective plates and replacing with 3 mL of the above specified medium. Treatments were completed so that they all ended at the same time and were thus prepared for imaging together. Imaging preparation began with aspirating the treatment medium and replacing with 1 mL of JC-1 supplemented medium (10 μg/mL). Plates were then placed in the incubator for 15 minutes. The JC-1 supplemented medium was then aspirated and cells were washed with PBS. DAPI-supplemented PBS was then added to each plate (1 mL; 5 μg/mL) and plates were placed in the incubator for 15 minutes. DAPI-supplemented PBS was aspirated and cells were

washed twice with PBS. Finally, 1 mL of PBS was placed in each plate for imaging. Cells were imaged using a Nikon A1+ laser scanning confocal microscope using a 100x Plan Apo λ (1.45 NA) objective lens. Excitation was done by 405 nm (DAPI), 488 nm (JC-1), and 561 nm (JC-1) solid state lasers.

2.5.7. In vivo toxicity study

All animal procedures were reviewed and approved by the Institutional Animal Care and Use Committee at the University of Akron. Eight-week-old male C57BL/6 mice were obtained from Charles River laboratories. Animals were housed in a 12h light/dark cycle, and food and water were provided *ad libitum* (n = 3 animals per cage). Prior to the toxicity testing, animals were allowed to acclimate for 5 days. Vehicle control mice received IP injections on days 0, 7, 14, 21,25, and 29 of 100 µL of a 20% 2-HPβCD sterile PBS solution. Experimental mice received 100 µL of a 4 mg/mL 20% 2-HPβCD sterile PBS solution (0.4 mg/100 µL, or ~ 20 mg/kg assuming an average mouse weight of 20 g) of **II‑2** by IP injection on day 0 and a 3 mg/mL or ~ 15 mg/kg IP injection on day 14. Animals were closely monitored and weighed on a daily basis. On day 15, surviving experimental mice were sacrificed. On day 29, the vehicle control animals were sacrificed.

2.5.8. General procedure for the synthesis of compounds **II‑1‑II‑5**

Potassium hydroxide was added to a stirred solution of the 2-alkylimidazole in hot acetonitrile (~ 80 °C), and the reaction was stirred for one hour. 2-(Bromomethyl)naphthalene was added to the mixture, which was refluxed overnight. An

insoluble material formed and was removed by filtration. 2-(Bromomethyl)naphthalene was added to the filtrate and the mixture was refluxed overnight. The product precipitated from hot acetonitrile, or precipitation was induced by addition of diethyl ether. The solid was collected by filtration, washed with diethyl ether, air dried, and recrystallized from the appropriate solvent to yield the product.

2.5.8.1. Synthesis of 2-methyl-1,3-bis(naphthalen-2-ylmethyl)imidazolium bromide (II‑1)

2-Methylimidazole (1.01 g, 12.3 mmol) dissolved in acetonitrile (20 mL) was combined with KOH (0.78 g, 13.9 mmol) and 2-(bromomethyl)naphthalene (2.74 g, 12.4 mmol, first addition; 3.41 g, 15.4 mmol, second addition). Compound II‑1 precipitated from hot acetonitrile (3.54 g, 65% yield). Mp: 242-245 °C. Found C, 70.3; H, 5.4; N, 6.4%. Calculated for $C_{26}H_{23}N_2Br_1$: C, 70.4; H, 5.2; N, 6.3%. ^{1}H NMR (500 MHz, DMSO-d_6) δ = 7.99 (1H, s, Ar), 7.97 (1H, s, Ar), 7.93 (4H, m, Ar), 7.90 (2H, s, Ar), 7.88 (2H, s, Ar), 7.56 (4H, m, Ar), 7.51 (1H, d, Ar), 7.49 (1H, d, Ar), 5.65 (4H, s, CH_2), 2.74 (3H, s, CH_3). ^{13}C NMR (125 MHz, DMSO-d_6) δ = 144.7 (NCN), 132.7 (Ar), 132.5 (Ar), 131.8 (Ar), 128.7 (Ar), 127.8 (Ar), 127.6 (Ar), 126.8 (Ar), 126.6 (Ar), 126.6 (Ar), 125.5 (Ar), 122.1 (Ar), 51.0 (CH_2), 10.0 (CH_3). MS: m/z = 362.9 (theor for M^+ $C_{26}H_{23}N_2^+$ = 363.2).

Crystal data for II‑1: $C_{26}H_{23}N_2Br_1$, M = 443.38, orthorhombic, a = 13.7345(13) Å, b = 13.8204(4) Å, c = 10.9763(10) Å, V = 2051.0(3) Å^3, T = 100(2) K, space group Pca2(1), Z = 4, 15450 reflections measured, 4129 independent reflections (R_{int} = 0.0332). The final R_1 values were 0.0262 ($I > 2\sigma(I)$). The final $wR(F^2)$ values were 0.0586 ($I > 2\sigma(I)$). The

final R_1 values were 0.0308 (all data). The final $wR(F^2)$ values were 0.0610 (all data). A single crystal of **II-1** was obtained by slow evaporation of a concentrated solution of **II-1** dissolved in methanol and ethyl acetate. Crystallographic information file (CIF) can be found on the Cambridge Crystallographic Data Center website (CCDC # 1044144)

2.5.8.2. Synthesis of 2-ethyl-1,3-bis(naphthalen-2-ylmethyl)imidazolium bromide (**II‑2**)

2-Ethylimidazole (1.01 g, 10.4 mmol) dissolved in acetonitrile (20 mL) was combined with KOH (0.71 g, 12.6 mmol) and 2-(bromomethyl)naphthalene (2.56 g, 11.6 mmol, first addition; 3.01 g, 13.6 mmol, second addition). Compound **II‑2** precipitated from addition of diethyl ether and was recrystallized from ethanol (3.00 g, 62% yield). Mp: 220-221 °C. Found C, 70.6; H, 5.7; N, 6.1%. Calculated for $C_{27}H_{25}N_2Br_1$: C, 70.9; H, 5.5; N, 6.1%. ^{1}H NMR (500 MHz, DMSO-d_6) δ = 8.00 (1H, s, Ar), 7.99 (1H, s, Ar), 7.91-7.96 (8H, m, Ar), 7.55-7.57 (4H, m, Ar), 7.51 (1H, s, Ar), 7.49 (1H, s, Ar), 5.70 (4H, s, CH_2), 3.23 (2H, q, CH_2, J = 7.4 Hz), 0.86 (3H, t, CH_3, J = 7.5 Hz). ^{13}C NMR (125 MHz, DMSO-d_6) δ = 148.3 (NCN), 132.7 (Ar), 132.5 (Ar), 132.1 (Ar), 128.7 (Ar), 127.8 (Ar), 127.6 (Ar), 126.7 (Ar), 126.7(Ar), 126.6 (Ar), 125.2 (Ar), 122.4 (Ar), 50.9 (CH_2), 16.6 (CH_2), 11.1 (CH_3). MS: m/z = 377.3 (theor for M^+ $C_{27}H_{25}N_2^+$ = 377.2).

Crystal data for **II‑2**: $C_{27}H_{25}N_2Br_1$, M = 457.40, monoclinic, a = 13.3523(17) Å, b = 9.8237(11) Å, c = 16.542(2) Å, β = 97.385(4)°, V = 2151.8(4) Å^3, T = 100(2) K, space group P2(1)/n, Z = 4, 15661 reflections measured, 4353 independent reflections (R_{int} = 0.0650). The final R_1 values were 0.0408 ($I > 2\sigma(I)$). The final $wR(F^2)$ values were 0.1057 ($I > 2\sigma(I)$). The final R_1 values were 0.0763 (all data). The final $wR(F^2)$ values were 0.1282

(all data). A single crystal of **II-2** was obtained by slow evaporation of a concentrated solution of **II-2** dissolved in ethanol. Crystallographic information file (CIF) can be found on the Cambridge Crystallographic Data Center website (CCDC # 1044145)

2.5.8.3. Synthesis of 2-propyl-1,3-bis(naphthalen-2-ylmethyl)imidazolium bromide

(II‑3)

2-Propylimidazole (1.23 g, 11.7 mmol) dissolved in acetonitrile (20 mL) was combined with KOH (0.97 g, 17.3 mmol) and 2-(bromomethyl)naphthalene (2.78 g, 12.6 mmol, first addition; 2.77 g, 12.5 mmol, second addition). Compound **II‑3** precipitated from hot acetonitrile and was recrystallized from acetonitrile (2.48 g, 46% yield). Mp: 209-211 °C. Found C, 71.0; H, 5.9; N, 5.9%. Calculated for $C_{28}H_{27}N_2Br_1$: C, 71.3; H, 5.8; N, 5.9%. ^{1}H NMR (500 MHz, DMSO-d_6) δ = 8.00 (1H, s, Ar), 7.99 (1H, s, Ar), 7.94 (4H, m, Ar), 7.90 (2H, s, Ar), 7.89 (2H, s, Ar), 7.56 (4H, m, Ar) 7.50 (1H, d, Ar) 7.48 (1H, d, Ar) 5.62 (4H, s, CH$_2$), 3.18 (2H, t, CH$_2$, J = 8.2 Hz), 1.23 (2H, m, CH$_2$), 0.80 (3H, t, CH$_3$, J = 7.4 Hz). ^{13}C NMR (125 MHz, DMSO-d_6) δ = 147.3 (NCN), 132.7 (Ar), 132.5 (Ar), 132.1 (Ar), 128.7 (Ar), 127.7 (Ar), 127.6 (Ar), 126.8 (Ar), 126.7 (Ar), 126.6 (Ar), 125.2(Ar), 122.4 (Ar), 51.0 (CH$_2$), 24.4 (CH$_2$), 20.1 (CH$_2$), 13.2 (CH$_3$). MS: m/z = 391.3 (theor for M^+ $C_{28}H_{27}N_2^+$ = 391.2).

Crystal data for **2-propyl-1,3-bis(naphthalen-2-ylmethyl)imidazolium perchlorate (II‑3-ClO₄)**: $C_{28}H_{27}ClN_2O_4$, M = 490.94, monoclinic, a = 13.5183(9) Å, b = 22.2921(15) Å, c = 7.9695(6) Å, β = 90.528(3)°, V = 2401.5(3) Å^3, T = 100(2) K, space group P2(1)/c, Z = 4, 62780 reflections measured, 4858 independent reflections (R_{int} =

0.0302). The final R_1 values were 0.0445 ($I > 2\sigma(I)$). The final $wR(F^2)$ values were 0.0943

($I > 2\sigma(I)$). The final R_1 values were 0.0538 (all data). The final $wR(F^2)$ values were 0.1011

(all data). A single crystal of **II-3-ClO₄** was obtained by slow evaporation of a concentrated

solution of **II-3-ClO₄** dissolved in methanol and diethylether. Crystallographic information

file (CIF) can be found on the Cambridge Crystallographic Data Center website (CCDC #

1044146)

2.5.8.4. Synthesis of 2-butyl-1,3-bis(naphthalen-2-ylmethyl)imidazolium bromide (**II‑4**)

2-Butylimidazole (1.03 g, 8.3 mmol) dissolved in acetonitrile (15 mL) was

combined with KOH (0.56 g, 10.0 mmol) and 2-(bromomethyl)naphthalene (2.04 g, 9.9

mmol, first addition; 2.21 g, 10.0 mmol, second addition). Compound **II‑4** precipitated

from addition of diethyl ether and was recrystallized from acetonitrile (3.29 g, 81% yield).

Mp: 195-196 °C. Found C, 71.6; H, 6.2; N, 5.6%. Calculated for $C_{29}H_{29}N_2Br_1$: C, 71.8; H,

6.0; N, 5.8%. ^{1}H NMR (500 MHz, DMSO-d_6) δ = 8.00 (1H, s, Ar), 7.98 (1H, s, Ar), 7.92-

7.96 (3H, m, Ar), 7.90 (4H, m, Ar), 7.55-7.59 (4H, m, Ar), 7.48 (1H, d, Ar), 7.46 (1H, d,

Ar), 5.67 (4H, s, CH₂), 3.14 (2H, t, CH₂, J = 8.3 Hz), 1.18 (2H, m, CH₂), 1.01 (2H, m,

CH₂), 0.51 (3H, t, CH₃, J = 7.2 Hz). ^{13}C NMR (125 MHz, DMSO-d_6) δ = 147.4 (NCN),

132.6 (Ar), 132.6 (Ar), 132.1 (Ar), 128.8 (Ar), 127.7 (Ar), 127.6 (Ar), 126.9 (Ar), 126.7

(Ar), 126.7 (Ar), 125.2(Ar), 122.4 (Ar), 51.0 (CH₂), 28.2 (CH₂), 22.8 (CH₂), 21.6 (CH₂),

13.0 (CH₃). MS: m/z = 405.2 (theor for M^+ $C_{28}H_{27}N_2^+$ = 405.4).

Crystal data for **II‑4**: $C_{58}H_{58}N_4Br_2 \cdot C_2H_6O$, M = 1016.97, monoclinic, a = 7.6778(3)

Å, b = 28.1359(8) Å, c = 12.4286(4) Å, β = 106.6230(10)°, V = 2572.64(15) Å^3, T = 100(2)

K, space group P2(1)/c, $Z = 2$, 21381 reflections measured, 5220 independent reflections ($R_{int} = 0.0464$). The final R_1 values were 0.0387 ($I > 2\sigma(I)$). The final $wR(F^2)$ values were 0.0763 ($I > 2\sigma(I)$). The final R_1 values were 0.0524 (all data). The final $wR(F^2)$ values were 0.0808 (all data). A single crystal of **II-4** was obtained by slow evaporation of a concentrated solution of **II-4** dissolved in ethanol. Crystallographic information file (CIF) can be found on the Cambridge Crystallographic Data Center website (CCDC # 1044147)

2.5.8.5. Synthesis of 2-isopropyl-1,3-bis(naphthalen-2-ylmethyl)imidazolium bromide

(II‑5)

2-Isopropylimidazole (1.00 g, 9.1 mmol) dissolved in acetonitrile (15 mL) was combined with KOH (0.61 g, 10.9 mmol) and 2-(bromomethyl)naphthalene (2.21 g, 10.0 mmol, first addition; 2.22 g, 10.0 mmol, second addition). Compound **II‑5** precipitated from addition of diethyl ether and was recrystallized from acetonitrile (3.17 g, 74% yield). Mp: 202-204 °C. Found C, 71.2; H, 5.9; N, 6.3%. Calculated for $C_{28}H_{27}N_2Br_1$: C, 71.3; H, 5.8; N, 5.9%. ^1H NMR (500 MHz, DMSO-d_6) $\delta = 8.02$ (1H, s, Ar), 8.00 (1H, s, Ar), 7.94-7.96 (6H, m, Ar), 7.83 (2H, s, Ar), 7.55-7.56 (4H, m, Ar), 7.47 (1H, s, Ar), 7.45 (1H, s, Ar), 5.81 (4H, s, CH_2), 3.84 (1H, m, CH, J = 7.2 Hz), 1.19 (6H, d, CH_3, J = 7.3 Hz). ^{13}C NMR (125 MHz, DMSO-d_6) $\delta = 149.9$ (NCN), 132.7 (Ar), 132.5 (Ar), 132.4 (Ar), 128.7 (Ar), 127.7 (Ar), 127.6 (Ar), 126.7 (Ar), 126.5 (Ar), 126.1 (Ar), 124.8(Ar), 123.1 (Ar), 51.5 (CH_2), 24.5 (CH), 18.5 (CH_3). MS: m/z = 391.2 (theor for M^+ $C_{28}H_{27}N_2^+ = 391.3$).

Crystal data for **II‑5**: $C_{28}H_{27}N_2Br_1$, $M = 471.43$, monoclinic, $a = 8.05500(10)$ Å, $b = 21.7876(4)$ Å, $c = 12.8572(2)$ Å, $\beta = 100.5490(10)°$, $V = 2218.29(6)$ Å^3, $T = 100(2)$ K,

space group P2(1)/c, $Z = 4$, 18480 reflections measured, 4478 independent reflections (R_{int} = 0.0452). The final R_1 values were 0.0383 ($I > 2\sigma(I)$). The final $wR(F^2)$ values were 0.0849 ($I > 2\sigma(I)$). The final R_1 values were 0.0536 (all data). The final $wR(F^2)$ values were 0.0917 (all data). A single crystal of **II-5** was obtained by slow evaporation of a concentrated solution of **II-5** dissolved in acetonitrile. Crystallographic information file (CIF) can be found on the Cambridge Crystallographic Data Center website (CCDC # 1044148)

CHAPTER III

SYNTHESIS, CHARACTERIZATION, AND IN VITRO SAR EVALUATION OF

N,N'-BIS(ARYLMETHYL)-C^2-ALKYL SUBSTITUTED IMIDAZOLIUM SALTS

3.1. Introduction

Cancer is a disease that kills millions of people each year. Lung cancer is the leading cause of cancer related deaths, accounting for one in every four cancer deaths.[120] Treatments are based upon the type of lung cancer and physical characteristics of the cancer cells. These treatments include surgery, radiation, targeted therapies, and chemotherapy. However, the 5-year survival rate for lung cancer is only 17% suggesting that existing treatments are inadequate for the proper treatment of this disease.

Quinoline motifs have been researched for decades as potential chemotherapeutics (Figure III-1).[121] The first with a quinoline motif and antitumor properties was discovered in 1966 and named camptothecin.[122] Camptothecin prevents the replication of cancerous cells and can induce apoptosis by inhibiting topoisomerase I, a DNA-replicating enzyme.[123] This pentacyclic alkaloid has shown potent activity against

several human tumor cell lines, but is limited by poor aqueous solubility and severe side effects.[124] However, other camptothecin derivatives are Food and Drug Administration (FDA) approved for the treatment of cancer malignancies. This includes irinotecan, which is approved for the treatment of pancreatic cancers,[125] and topotecan, which is FDA approved as a second line treatment for relapsed small-cell lung cancer.[126]
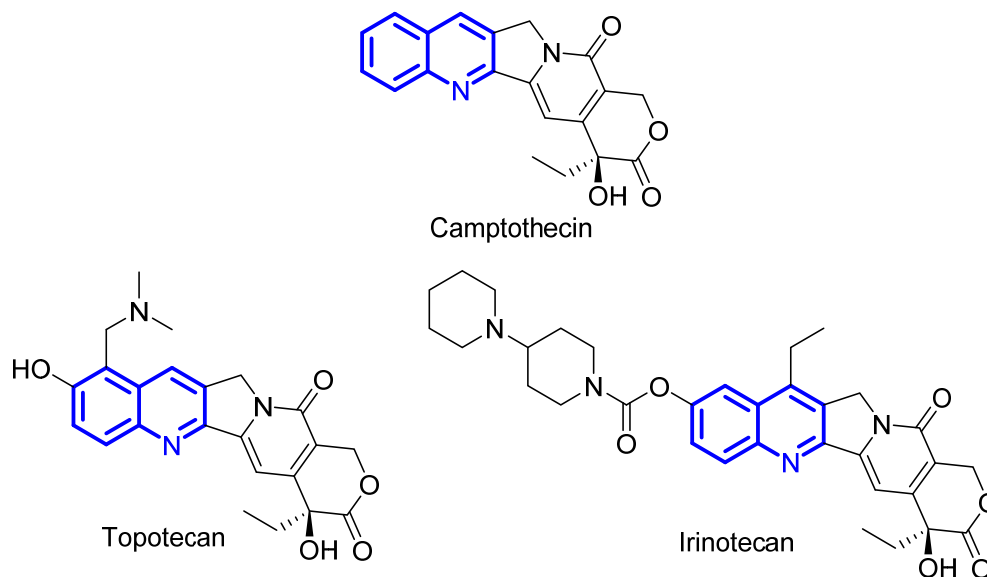
Figure III-1. Structure of the quinoline-based antineoplastic compounds camptothecin, topotecan, and irinotecan.

Imidazolium salts are another class of compounds that have received substantial attention for their anti-tumor properties against a variety of human tumor cell lines.[127] In particular, naphthylmethyl-substituted imidazolium salts, such as **IS29** (**I-464**) with a proton at the C^2 position, were shown to have high anti-proliferative effects against non-small cell lung cancer (NSCLC) (Figure III-2).[4,49] However, the clinical use of **IS29** (**I-464**) was limited by poor water solubility. The quinoline motif is structurally similar to a

136

naphthalene substituent but has a nitrogen heteroatom to increase the hydrogen bonding capabilities and increase aqueous solubility. Also, the nitrogen atom could potentially be protonated to further increase the solubility if necessary.[128] Therefore, the historical quinoline motif and the novel, highly-active naphthylmethyl-based imidazolium salt could be combined to produce potent chemotherapeutics with high aqueous solubility.
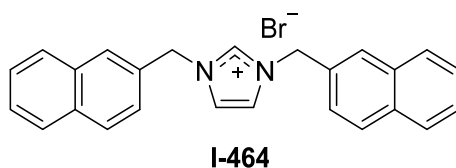
I-464

Figure III-2. Structure of the naphthylmethyl substituted imidazolium salt **I-464.**

Presented herein is the synthesis, characterization, and in vitro structure-activity relationship (SAR) study of a series of C^2-alkyl and $N^1(N^3)$-naphthylmethyl and/or quinolylmethyl substituted imidazolium salts. Various alkyl substituents at the C^2 position were used to fine tune the lipophilic nature of compounds to optimize activity. Quinolylmethyl groups at the N^1 and/or N^3 positions replaced naphthylmethyl groups of previous derivatives to increase aqueous solubility making these novel derivatives clinically relevant for future studies.

137

3.2. Results and discussion

3.3. Synthesis and characterization

Compound **III‑1** was synthesized to evaluate the effect on the anti-cancer properties of the steric bulk and lipophilicity of a phenyl group at the C^2 (Equation III-1). Commercially available 2-phenyl imidazole was deprotonated with sodium hydride and reacted with 2-(bromomethyl)naphthalene. The resulting naphthalene-substituted imidazole was reacted with a second molar equivalent of 2-(bromomethyl)naphthalene to synthesize **III‑1** in moderate yield, 58%, after recrystallization from acetone. The formation of **III‑1** was suggested by the resonance at 5.48 ppm in the ^1H NMR corresponding to the methylene linker bridging the naphthalene rings to the imidazole ring. The structure of the cationic portion of **III‑1**, as the hexafluorophosphate salt, was confirmed by single crystal X-ray crystallography. To obtain a single crystal of **III‑1‑PF$_6$**, **III‑1** was dissolved in a water/methanol mixture. Ammonium hexafluorophosphate was added to the mixture to form a white precipitate which was collected by filtration. The white solid was dissolved in acetonitrile and a single crystal of **III‑1‑PF$_6$** grew from slow evaporation of this concentrated solution (Figure III-3).
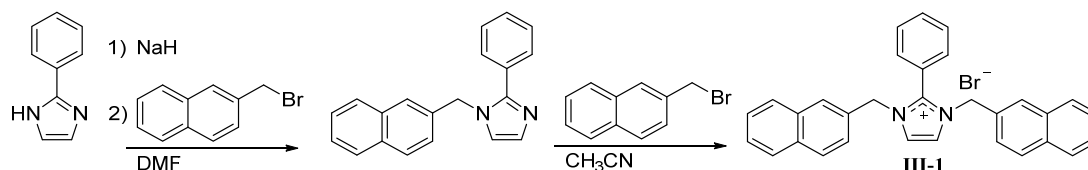
Equation III-1. Synthesis of **III-1** from commercially available 2-phenylimidazole

138
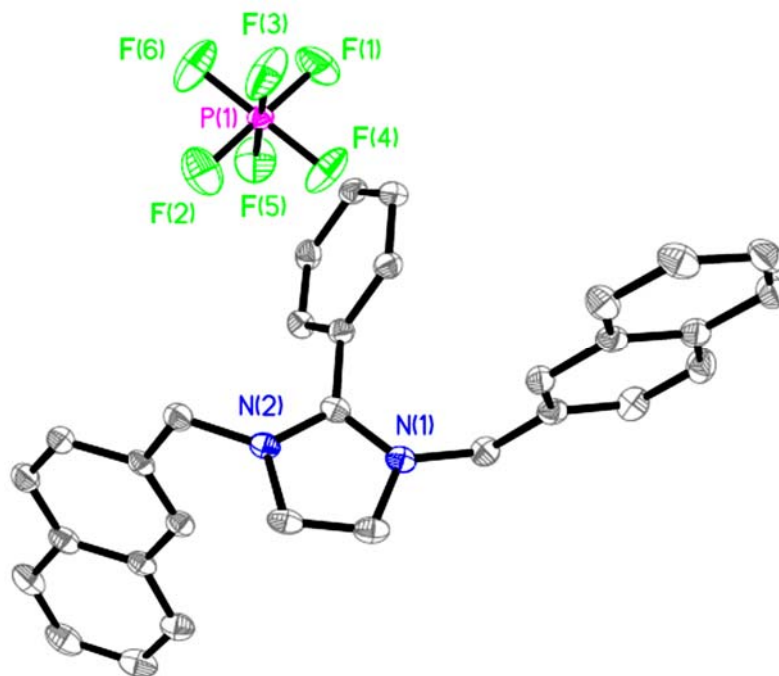
Figure III‑3. X ray crystal structure of **III‑1‑PF₆** with thermal ellipsoids drawn to the 50%

probability level. Carbon labels and hydrogen atoms have been removed for clarity.

Compound **III‑2** was synthesized to evaluate the anti-cancer properties of a N^1, N^3-napthylmethyl substituted imidazolium salt with a hydroxyl group at the C^2 position in attempt to increase the aqueous solubility when compared to other N,N'-bisnaphthylmethyl imidazolium salts, such as **III‑1**. A modified literature procedure was used to synthesize **III-2** (Equation III-2).[129] Previously published **I-464** was reacted with 37% formalin and N,N'-diisopropylethylamine to form **III‑2** in moderate yield, 69%, after recrystallization from acetonitrile. The formation of **III‑2** was suggested by the disappearance of the C^2 proton of **I-464** at 9.50 ppm in the ^{1}H NMR spectrum and appearance of a triplet resonance at 6.27 ppm and doublet resonance at 5.03 ppm in the ^{1}H NMR spectrum of **III‑2**. There was also a downfield shift of the methylene resonance bridging the naphthalene rings and imidazole in the ^{1}H NMR spectrum of **I-464** to **III‑2** from 5.62 ppm to 5.71 ppm, respectively. The structure of **III‑2** was confirmed by single crystal X-ray crystallography (Figure III-4). A single crystal of **III-2** was grown from slow evaporation of a concentrated solution of **III‑2** in acetonitrile.
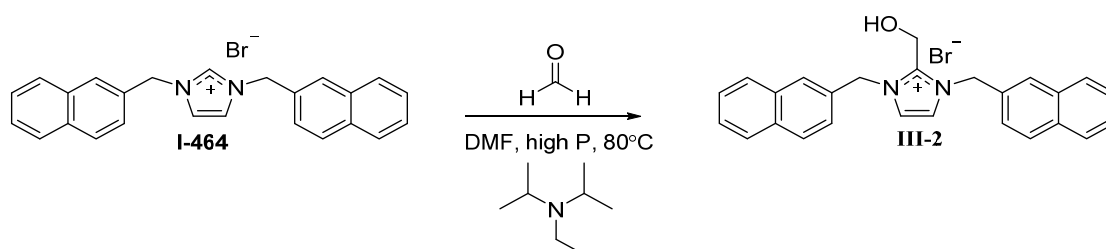
Equation III-2. Synthesis of **III‑2** from the highly active derivative **I-464**.
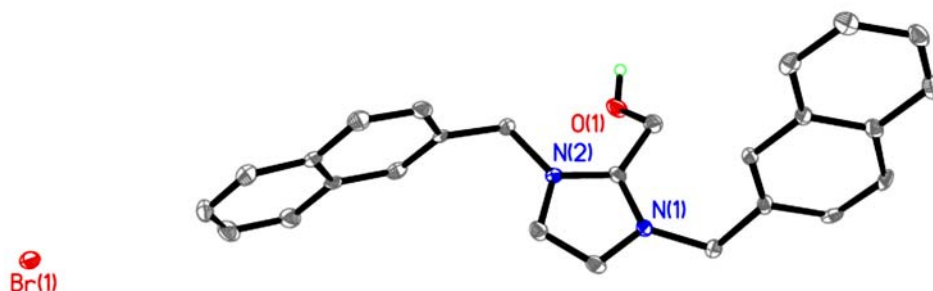
Figure III‑4. Thermal ellipsoid plot of **III‑2** with thermal ellipsoids drawn to the 50% probability level. Carbon labels and hydrogen atoms, except for the hydroxyl proton, have been removed for clarity.

In a separate attempt to increase aqueous solubility, compounds **III‑3**, **III‑4‑Br**, **III‑4‑Cl**, and **III‑5‑III‑7**, with a quinolylmethyl substituent at the N^1 position and a naphthylmethyl substituent at the N^3 position, were synthesized by procedures developed in the Youngs lab[3,4,79,82,96] and evaluated for their anti-cancer properties. The nitrogen heteroatom of the quinoline moiety increases the hydrophilicity of the compound; whereas the naphthalene ring helps to maintain the high anti-cancer activity. Compounds **III‑3** and **III‑4−Br** were synthesized by deprotonating the appropriate imidazole with KOH and the addition of approximately 0.5 and 0.85 molar equivalents of 2-(chloromethyl)quinoline (Equation III-3). Excess imidazole was used to ensure substitution at both nitrogens did not occur. The excess imidazole and generated inorganic salts were washed away with a basic aqueous solution. Once it was confirmed that only the mono-substituted imidazole was present by ^{1}H NMR spectroscopy, the intermediate was reacted with

141

2-(bromomethyl)naphthalene to yield **III‑3** and **III‑4‑Br** in moderate to poor yield, 50% and 23% respectively.
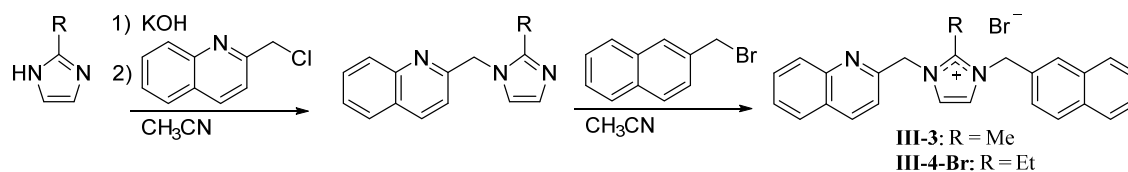
Equation III-3. Synthesis of **III‑3** and **III‑4‑Br**.

Compounds **III‑3** and **III‑4‑Br** were characterized by ^{1}H (Figure III-5) and ^{13}C NMR spectroscopies, high resolution mass spectrometry, and melting point analysis. The most notable resonances in the ^{1}H NMR for **III‑3** and **III‑4‑Br** were two singlet resonances in each spectrum corresponding to the methylene protons bridging the imidazole ring to the quinoline or naphthalene substituent. The chemical shift of these singlet resonances ranged from 5.88 ppm to 5.72 ppm. The appearance of two singlets in this region was indicative of the asymmetrically substituted imidazolium salts differing from the observance of only one singlet resonance in the ^{1}H NMR spectrum of a symmetrically substituted imidazolium salt, such as **III‑1** or **III‑2**.
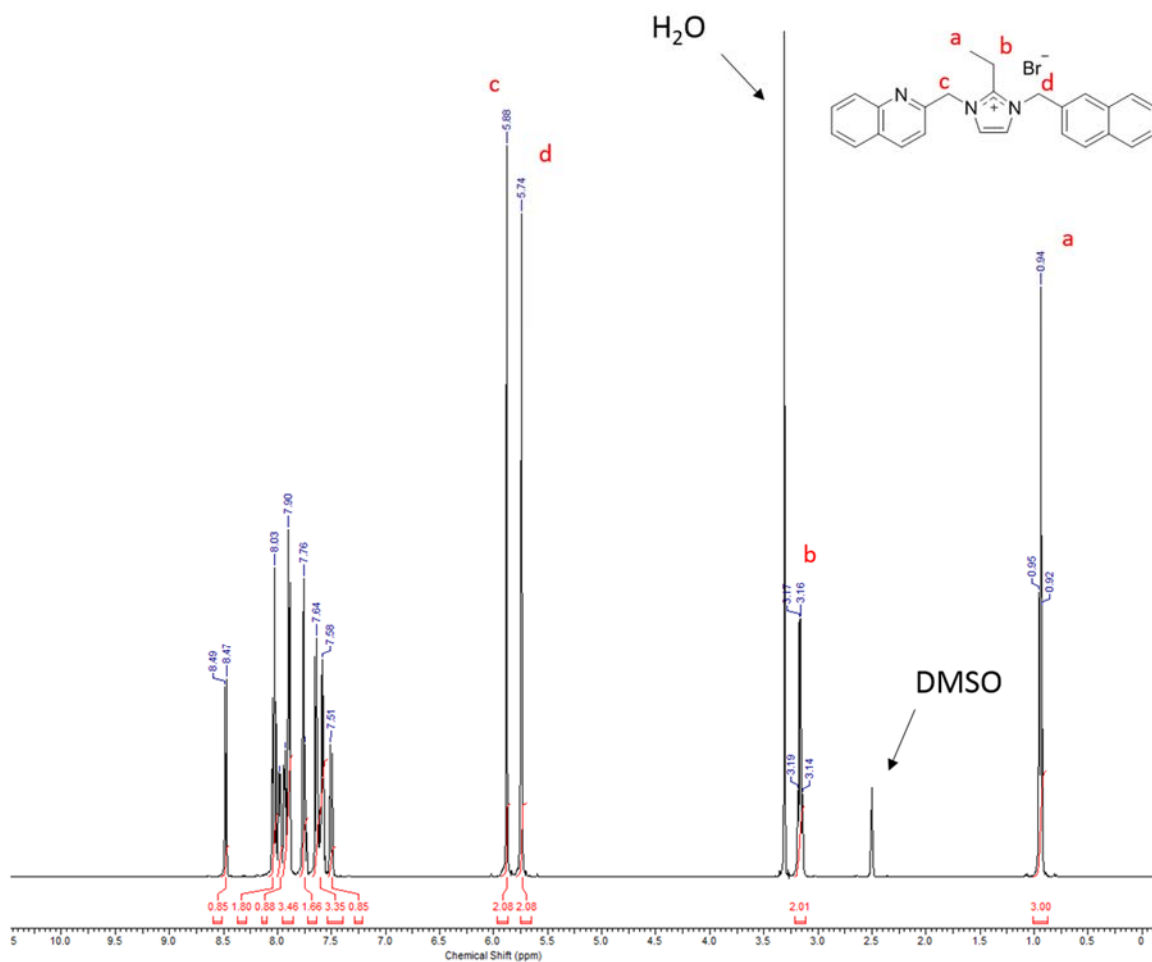
Figure III-5. ^{1}H NMR spectrum of **III-4-Br**.

Compound **III‑4‑Cl** was synthesized for multiple reasons: (1) to crystallize the cationic portion of 'III‑4‑Br' to confirm the structure of the cation and (2) to determine the differences in solubility and anti-cancer activity of the bromide salt versus the chloride salt. 2-Ethylimidzole was deprotonated with potassium hydroxide and reacted with 2-(bromomethyl)naphthalene. Following filtration and removal of a white solid, the mono-alkylated species was reacted with 2-(chloromethyl)quinoline to afford a white solid, **III‑4‑Cl**, in poor yield (Equation III-4).

143
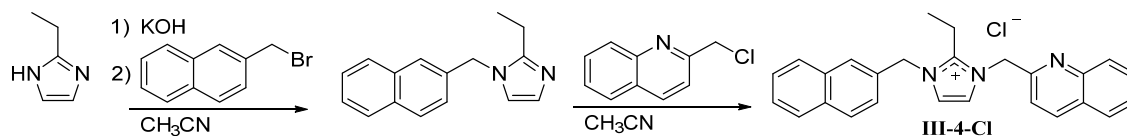
Equation III-4. Synthesis of **III‑4‑Cl**.

Compound **III‑4‑Cl** was characterized by ^{1}H NMR, ^{13}C NMR, and single crystal X-ray crystallography. The two resonances corresponding to the methylenes bridging the aryl group to the nitrogens of the imidazole ring were in the appropriate region of the ^{1}H NMR spectrum, 5.76 ppm and 5.90 ppm, and the ^{13}C NMR, 50.8 ppm and 52.2 ppm. A single crystal suitable for X-ray analysis was obtained by slow evaporation of **III‑4‑Cl** in a concentrated solution of acetonitrile (Figure III-6).
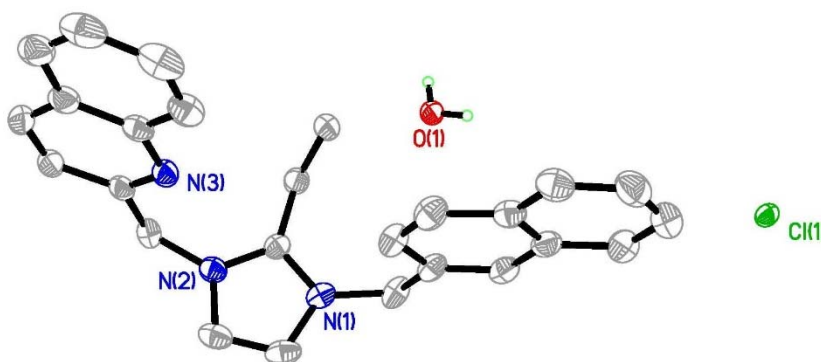
Figure III-6. Thermal ellipsoid plot of **III‑4‑Cl•H$_2$O** with thermal ellipsoids drawn to the 50% probability level. Carbon labels and protons, except for those bound to the water, were removed for clarity.

The asymmetrically substituted derivatives **III‑5** and **III‑6** were more difficult to isolate due to solubility issues of the deprotonated imidazoles (Equation III-5). After

deprotonation of the imidazole and addition of the first aryl halide, a mixture of the starting imidazole, mono-alkylated intermediate, and the imidazolium salt were present. Therefore, a phase transfer catalyst, tetrabutylammonium bromide, was used to help solubilize all reagents and produce the mono-alkylated intermediate without any starting material present. In the first alkylation leading to **III‑6**, excess 2-(bromomethyl)naphthalene was used to ensure the starting imidazole would be completely consumed. However, this produced imidazolium salt impurities to form. Acetone was used to solubilize the mono-alkylated intermediate leaving the imidazolium salt insoluble which was removed by filtration. After confirming the mono-substituted intermediate was the only species present by ^{1}H NMR spectroscopy, 2-(chloromethyl)quinoline was added to synthesize **III‑5** and **III‑6** in moderate to poor yield, 46% and 17% respectively.
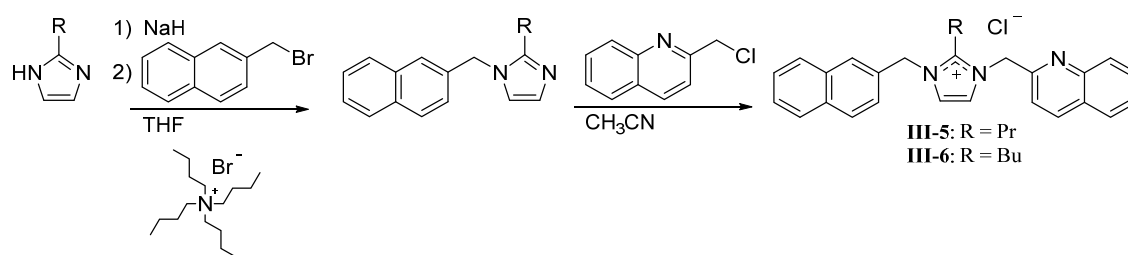
Equation III-5. Synthesis of **III‑5** and **III‑6** using the phase transfer catalyst tetrabutylammonium bromide.

Compounds **III‑5** and **III‑6** were characterized by ^{1}H NMR and ^{13}C NMR spectroscopies, high resolution mass spectrometry, and melting point analysis. Resonances in the ^{1}H NMR spectra used to suggest the products were the two singlets in each spectrum ranging from 5.78 ppm to 5.94 ppm corresponding to the protons bridging the imidazole

145

ring to the quinoline and naphthalene rings. This is consistent with the spectra of **III‑3**, **III‑4‑Br**, and **III‑4‑Cl** discussed above. Compound **III‑5** was also characterized by single crystal X-ray crystallography (Figure III-7). A single crystal of **III‑5**, with a co-crystallized acetonitrile molecule, was grown from slow evaporation of a concentrated solution of **III‑5** dissolved in acetonitrile.
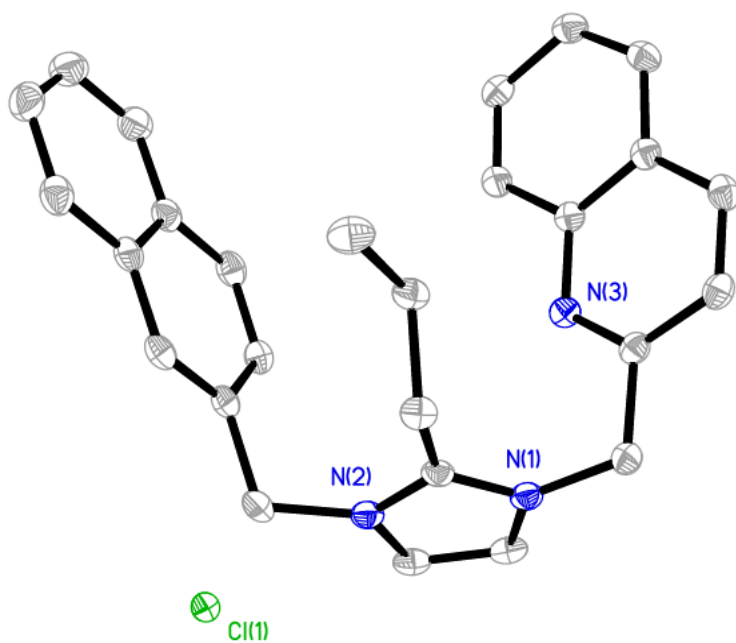
Figure III-7. Thermal ellipsoid plot of **III‑5•CH₃CN** with thermal ellipsoids drawn to the 50% probability level. Carbon labels, hydrogen atoms, and the co-crystallized acetonitrile molecule have been removed for clarity.

Compound **III‑7** was synthesized by reacting 1-(naphthalene-2-ylmethyl)-2-phenylimidazole with excess 2-(chloromethyl)quinoline in refluxing acetonitrile overnight (Equation III-6). The product precipitated after addition of ether and acetone to the reaction

mixture to produce **III‑7** in moderate yield, 58%. ^{1}H NMR and ^{13}C NMR spectroscopies, meting point analysis, and high resolution mass spectrometry were used to characterize **III‑7**. Two singlet resonances with a chemical shift of 5.70 ppm and5.57 ppm in the ^{1}H NMR spectrum suggested the formation of **III‑7**.
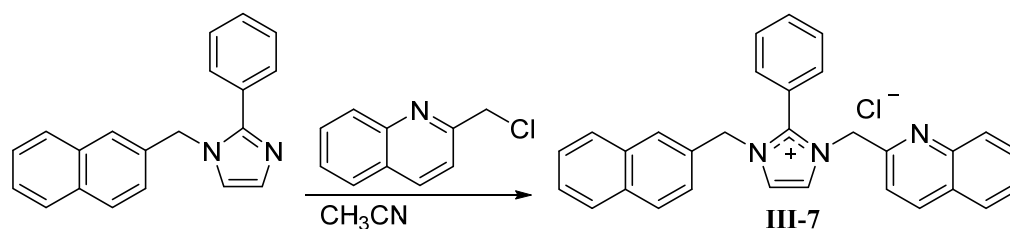
Equation III-6. Synthesis of **III‑7.**

In attempt to synthesize highly hydrophilic compounds, **III‑8‑III‑12** were synthesized with quinolylmethyl substituents at both the N^1 and N^3 positions (Equation III-7). Compounds **III‑8‑III‑12** were synthesized by deprotonation of the appropriate imidazole with potassium hydroxide and addition of one molar equivalent of 2-(chloromethyl)quinoline to form the mono-substituted intermediate. After filtration to remove a white precipitate, a second molar equivalent was added to yield **III‑8‑III‑12** in poor yields, 9−37%.

147
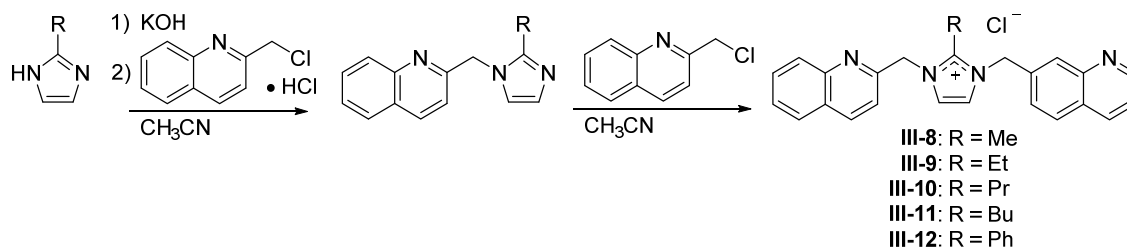
Equation III‑7. Synthesis of the quinolylmethyl derivatives **III‑8**‑**III‑12**.

Compounds **III‑8**‑**III‑12** were characterized by high resolution mass spectrometry, ^{1}H NMR and ^{13}C NMR spectroscopies, and melting point analysis. The most notable resonance in the ^{1}H NMR spectra of **III‑8**‑**III‑12** was the resonance corresponding to the methylene bridging the quinoline groups to the imidazole ring ranging from 5.76 to 5.99 ppm. These values are slightly downfield when compared to resonances corresponding to the bridging methylenes of **III‑1** at 5.48 ppm. This downfield shift is most likely due to the more electronegative nitrogen atom in the quinoline moiety when compared to the naphthalene ring.

Compounds **III‑8**, **III‑10** (as the hydrate **III‑10•1.5(H₂O)**) and the cationic portion of **III‑9** and **III‑11** as the hexafluorophosphate salts (**III‑9‑PF₆** and **III‑11‑ PF₆•1.5(H₂O)**) were analyzed by single crystal X-ray crystallography to confirm their structures (Figure III-8, Figure III-9, Figure III-10, and

Figure III-11 respectively). A single crystal of **III‑8** was grown from slow evaporation of a concentrated solution of deuterated dimethyl sulfoxide. A single crystal of **III‑10•1.5(H₂O)** was grown from a concentrated solution of water. Compounds **III‑9** ‑**PF₆** and **III‑11‑PF₆** were obtained similar to **III‑1‑PF₆** as described above by anion

exchange of **III-9** and **III-11** from a chloride anion to a hexafluorophosphate anion. A single crystal of **III‑9‑PF₆**, was obtained by slow evaporation of a concentrated solution of **III‑9‑PF₆** in acetonitrile and ethanol (1:1). Whereas a single crystal of **III‑11‑PF₆•1.5(H₂O)** was obtained by slow evaporation of a concentrated solution of **III‑11‑PF₆** in acetone and ethanol (1:1).
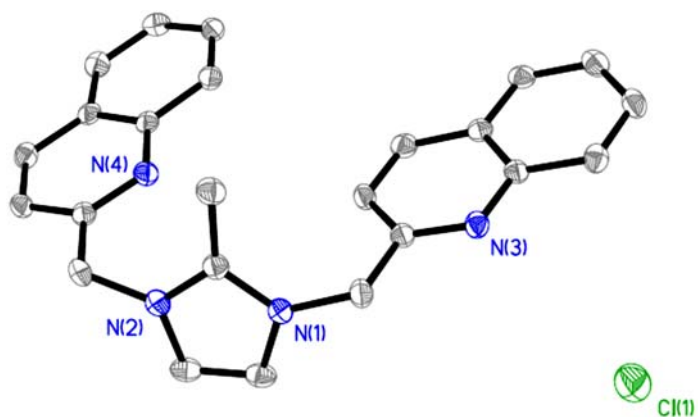
Figure III‑8. Thermal ellipsoid plot of **III‑8** with thermal ellipsoids drawn to the 50% probability level. Carbon labels and hydrogen atoms have been removed for clarity.
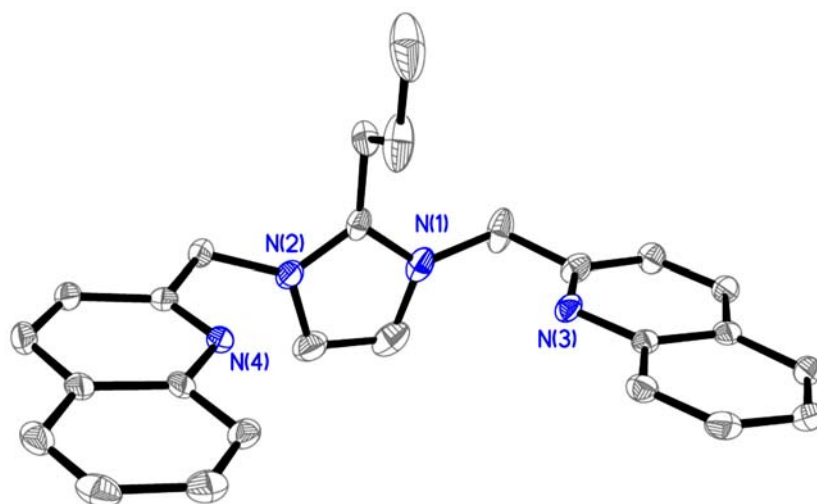
Figure III‑9. Thermal ellipsoid plot of **III‑10•1.5(H₂O)** with thermal ellipsoids drawn to the 50% probability level. Carbon labels, hydrogen atoms, water molecules, and the chloride anion have been removed for clarity.
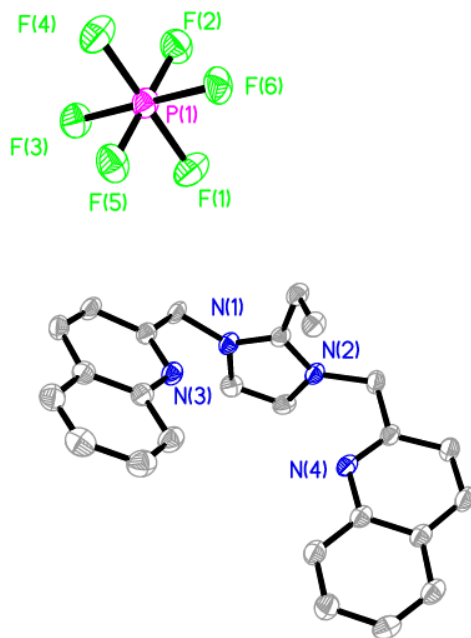
Figure III-10. Thermal ellipsoid plot of **III‑9‑PF₆** with thermal ellipsoids drawn to the 50% probability level. Carbon labels and hydrogen atoms have been removed for clarity.
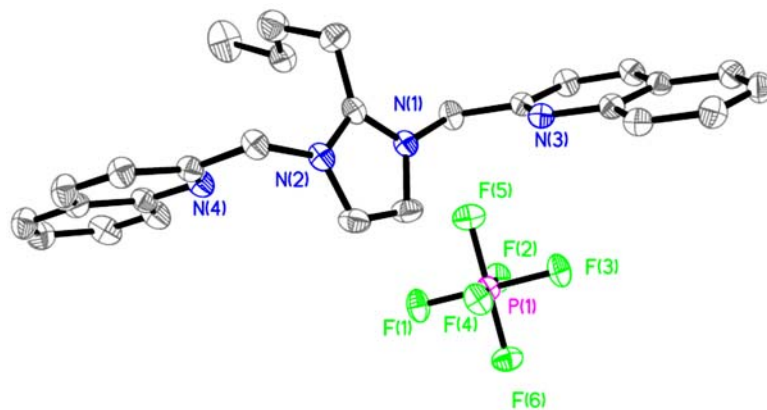
Figure III-11. Thermal ellipsoid plot of **III‑11‑PF₆•1.5(H₂O)** with thermal ellipsoids drawn to the 50% probability level. Carbon labels, hydrogen atoms, and co-crystallized water molecules have been removed for clarity.

3.3.1. Biological evaluation

3.3.1.1. MTT assay

Prior to determining each compounds anti-cancer properties, the aqueous solubility of each compound was studied in detail. Compounds **III‑1‑III‑3**, **III‑4-Br**, **III‑4-Cl**, and **III‑5‑III‑12** had varying degrees of solubility in aqueous solution (Table III-1). Compounds were dissolved in water to a concentration of 1 mM prior to diluting in growth medium to the testing concentrations. However, due to their low solubility in pure water (< 0.5 mg/mL), compounds **III‑1** and **III‑2** were dissolved in DMSO before diluting with water to a final concentration of 1 mM and 1% (v/v) DMSO. The highest final concentration of DMSO in growth medium was 0.032% (v/v) after diluting the stock concentration to the desired testing concentrations. Compounds **III‑3**, **III‑4‑Br**, **III‑4‑Cl**, and **III‑5‑III‑7** had varying solubilities in water. All compounds were soluble at a concentration of 1 mM. However, the more lipophilic derivatives **III‑5‑III‑7** had an aqueous solubility greater than 10 mM, whereas **III‑4‑Br** had a solubility of 5 mM and **III-3** had a solubility < 5 mM. It is interesting to note that the solubility of the **III‑5‑III‑7** is higher than the solubility of **III‑3** and **III‑4‑Br** in water considering **III-5-III-7** has more lipophilicity at the C^2 position. However, the solubility of **III‑4‑Cl** is also greater than 10 mM and therefore at least 2-fold higher than the bromide derivative **III‑4‑Br**. This suggests the anion significantly affects the solubility properties of these imidazolium salts. Compounds **III‑3** and **III‑4‑Br** could be solubilized by 2-hydroxypropyl-β-cyclodextrin

(2-HPβCD), a chemical excipient that is considered 'generally regarded as safe' (GRAS) by the FDA and approved in several drug formulations,[93] at a concentration above 10 mM. Compounds **III‑8‑III‑12** had aqueous solubilities of greater than 80 mM. Therefore, there was no need to use DMSO for the testing of **III‑3**, **III‑4‑Br**, **III‑4‑Cl**, and **III‑5‑12**. These compounds were dissolved in pure water to a concentration of 1 mM and then diluted in growth medium to the desired concentrations. Cisplatin was dissolved in water without the use of DMSO by stirring a 1 mM solution for several hours at room temperature prior to diluting with growth medium.

Table III-1. Aqueous solubilities of compounds **III‑1‑III‑3**, **III‑4‑Br**, **4‑Cl**, and **III‑5‑III‑12** in mM.

Compound	Aqueous solubility (mM)
III‑1	< 0.5 mM
III‑2	< 0.5 mM
III‑3	< 5 mM
III‑4‑Br	~ 5 mM
III‑4‑Cl	> 10 mM
III‑5	> 10 mM
III‑6	> 10 mM
III‑7	> 10 mM
III‑8	> 80 mM
III‑9	> 80 mM
III‑10	> 80 mM
III‑11	> 80 mM
III‑12	> 80 mM

The anti-cancer properties of **III‑1‑III‑3**, **III‑4-Br**, **III‑4-Cl**, and **III‑5‑III‑12** against several NSCLC cell lines (NCI-H460, NCI-H1975, HCC827, and A549) were

153

evaluated by the MTT assay, as done previously by our group,[4,82] to create a SAR of C^2 substituted imidazolium salts with a highly lipophilic substituent (naphthylmethyl) or a more hydrophilic substituent (quinolylmethyl) at the N^1 and/or N^3 positions (Table III-2). Briefly, cells were grown to confluency and plated in 96-well plates at 5,000-7,000 cells per well depending on the cell line. Cells were allowed to adhere to the plate overnight. Following incubation, cells were exposed to **III‑1‑III‑3**, **III‑4‑Br**, **III‑4‑Cl**, and **III‑5‑III‑12** at four concentrations in growth medium, 1, 4, 16, and 32 μM. Cells were incubated for 72 hours and the optional MTT assay protocol was followed to determine the IC$_{50}$ value of each compound for the four cell lines tested (the concentration of compound that inhibits 50% of cell growth relative to control cells). Results were compared to cisplatin and **I-464** to establish a SAR of various alkyl groups at the C^2 position and naphthylmethyl and quinolylmethyl substituents at the N^1 and/or N^3 positions.

Table III-2. IC_{50} values of **III‑1‑III‑3**, **III‑4-Br**, **III‑4-Cl**, **III‑5‑III‑12**, **I-464**, and cisplatin determined by the MTT assay.

Compound	NCI-H460	NCI-H1975	HCC827	A549
III‑1	3	2	2	4
III‑2	14	7	12	> 30
III‑3	2	< 1	9	3
III‑4−Br	2	< 1	5	3
III‑4−Cl	2	< 1	2	3
III‑5	3	2	6	3
III‑6	3	2	6	3
III‑7	3	2	6	4
III‑8	8	2	13	15
III‑9	6	< 1	9	11
III‑10	5	1	7	10
III‑11	5	< 1	7	7
III‑12	8	2	8	14
I-464	4	6	9	n/a
cisplatin	2	6	3	7

Compound **III‑1** was synthesized to assess the anti-cancer activity of a C^2-phenyl substituted imidazolium salt with naphthylmethyl substituents at the N^1 and N^3 positions. This derivative gave insight suggesting how the steric bulk and lipophilicity at the C^2 position affects the anti-cancer activity. The IC_{50} values of **III‑1** for the four NSCLC cell lines tested were in the low micromolar range. This suggests that a large amount of steric bulk can be added to the C^2 position without negatively altering the anti-cancer properties of N^1 and N^3 naphthylmethyl substituted imidazolium salts. Unfortunately, this compound, like many other lipophilic imidazolium salts with high anti-cancer activity, was limited by poor aqueous solubility as described above.

Compound **III‑2** with naphthylmethyl substituents at both the N^1 and N^3 positions and a hydroxymethyl group at the C^2 position was synthesized to evaluate the anti-proliferative properties of a hydrophilic hydroxyl group at the C^2 position. Compound **III‑2** had moderate to poor activity against all four NSCLC cell lines. The hydroxyl group was added to the C^2 position to increase aqueous solubility, whereas naphthylmethyl substituents were at the N^1 and N^3 positions to maintain high anti-cancer activity. However, the hydroxyl group decreased the activity drastically in all but the H1975 cell line when compared to **I-464**, which has a hydrogen at the C^2 position. Unfortunately this chemical modification not only reduced the anti-proliferative effects when compared to related derivatives, but also did not significantly add aqueous solubility considering the aqueous solubility of **III‑2** was also quite poor. Results of the MTT assay for **III‑2** were similar to another previously published related compound with hydroxymethyl groups at the C^4 and C^5 positions suggesting that alcohols at any position of the imidazole ring reduce the anti-cancer activity of imidazolium salts against NSCLC.[82]

To increase solubility when compared to **I-464**, **III‑3**, **III‑4‑Br**, **4‑Cl**, and **III‑5‑III‑7** were synthesized with a naphthylmethyl at the N^1 position and a quinolylmethyl substituent at the N^3 position. The quinolylmethyl substituent is structurally and sterically similar to the naphthylmethyl substituent, but it has a nitrogen heteroatom in the planar, aromatic ring system to increase the hydrogen bonding capabilities of the imidazolium salt and consequently increase the aqueous solubility. Compounds **III‑3**, **III‑4‑Br**, **III‑4‑Cl**, and **III‑5‑III‑7** all had high anti-cancer activity against the four NSCLC lines tested with IC_{50} values in the nanomolar range for **III‑3**,

III‑4‑Br, and **III‑4‑Cl** against the H1975 cell line and the low micromolar range for all other compounds and cell lines. Although these compounds are more hydrophilic, these values are similar to the more lipophilic derivatives **III‑1** and **I-464**.

The IC_{50} values of **III‑4‑Br** and **III‑4‑Cl** were almost identical (2 μM (H460), < 1 μM (H1975), 5 μM (HCC827), and 3 μM (A549) for **III‑4‑Br** and 2 μM (H460), < 1 μM (H1975), 2 μM (HCC827), and 3 μM (A549) for **III‑4‑Cl**). This suggests that the anion has virtually no effect on the compounds anti-cancer properties. Considering **III‑4‑Cl** had over 2-fold higher aqueous solubility than **III‑4‑Br**, **III‑4‑Cl** not only has a clinically relevant solubility but it also has high-anti cancer activity. This suggests that it is desirable for imidazolium salts to be chloride salts versus bromide salts since chloride derivatives have higher solubility and equal anti-proliferative effects.

To maximize solubility from heteroatoms in the bicyclic ring systems, derivatives **III‑8‑III‑12** were synthesized, with quinolylmethyl substituents at both the N^1 and N^3 positions, and tested for their anti-proliferative properties. Compounds **III‑8‑III‑12** had high anti-cancer activity against the H1975 cell line with IC_{50} in the high nanomolar to low micromolar range. These highly water-soluble derivatives also had high to moderate activity against the other three NSCLC cell lines with values in the low micromolar range.

Two SARs can be established from the MTT assay results discussed. The first involves substituents at the C^2 position. A series of compounds were tested with various alkyl groups at the C^2 position with the substituents at the N^1 and N^3 positions remaining constant. The hydroxyl group at the C^2 positions clearly causes a reduction in anti-cancer

activity when comparing **III‑2** with **III‑1** and **IS29**. However, when comparing **III‑1** to **IS29**, there does not seem to be a substantial effect on the anti-cancer activity of a lipophilic phenyl substituent at the C^2 position, although **III‑1** does have slightly lower IC_{50} values. This trend, that the length of the alkyl chain does not have a significant effect on anti-cancer activity, remained constant when comparing **III‑3**, **III‑4‑Br**, **III‑4‑Cl**, and **III‑5‑III‑7** with **III‑8‑III‑12**. The second SAR considers the different aryl substituents at the N^1 and N^3 positions. Although the solubilities of **III‑3**, **III‑4‑Br**, **III‑4‑Cl**, and **III‑5‑III‑7** were increased when compared to **III‑1**, the IC_{50} values were comparable. However, a difference in activity was observed when comparing the highly hydrophilic derivatives **III‑8‑III‑12** to the more lipophilic compounds considering the more hydrophilic derivatives displayed less potent anti-cancer properties.

3.3.1.2. NCI-60 human tumor cell line screen

The National Cancer Institute's (NCI) Developmental Therapeutics Program (DTP) tested multiple compounds in the NCI-60 human tumor cell line screen. This allowed us to expand upon the SAR determined in our lab to include several more NSCLC cell lines than the ones we have available for use. The first stage of this program involves a one dose assay where all 60 cell lines are exposed to the compound at one dose (10 µM). Experimental procedures can be found on the DTP website (https://dtp.cancer.gov/discovery_development/nci-60/methodology.htm) to describe how the experiment was performed in greater detail. The growth percentage values are determined relative to growth with no drug added and the initial cell count. This allows

growth inhibition (growth percentage values between 0 and 100) and lethality values (growth percentage values between 0 and -100) to be determined.

The DTP tested **III‑1‑III‑3**, **III‑4‑Br**, **III‑5‑III‑12**, and **I-464** in their one-dose assay (Table III-3 and Table III-4). Compound **III‑1** had the lowest average growth percentage of all the compounds tested with an average lethality rate of -26.99% significantly lower than the other N,N'-bis(naphthylmethyl) derivative, **I-464**, at 38.08%. Compound **III‑2** with a hydroxyl group at the C^2 position had a high average growth rate at 60.67% while the more hydrophilic derivatives **III‑3**, **III-4-Br**, and **III-5-III-7** had average growth rates between 7.64 and 15.98%. The highly hydrophilic derivative **III‑8** had the highest average growth rate of 80.66% while **III‑9‑III‑11** had lower average growth rates ranging from 24.96% to 46.06%.

The results from the one-dose assay confirm the SAR established with the MTT assay described above. The most lipophilic derivative **III‑1** had the highest anti-cancer activity as expected. The hydroxyl group in **III‑2** caused a reduction in activity when compared to the other N,N'-bis-naphthylmethyl derivative **III‑1**. The slightly more hydrophilic derivatives **III‑3**, **III‑4‑Br**, and **III-5-III-7** had low average growth percentage values and were all comparable to each other. This also suggests that the difference in lipophilicity and steric bulk of a methyl, ethyl, propyl, butyl, and phenyl group do not have a significant influence on the anti-cancer activity. More drastic effects were seen with the highly hydrophilic derivatives **III‑8‑III‑12** whereas **III‑8** had very poor inhibitory effects with an average growth rate of 80.66%. The more lipophilic derivatives

III‑9‑III‑12 had lower growth percentage values compared to **III‑8** but higher than the related C^2 alkyl N^1/N^3 asymmetrically substituted derivatives. The overall trend observed with the MTT assay described above and results from the one-dose assay is that lipophilicity increases activity.

Table III-3. Growth percentage values for multiple NSCLC cell lines from the NCI-60 human tumor cell line one-dose assay against **III-1** - **III-5**.

Compound	Growth %									Average
	A549/ ATCC	EKVX	HOP-62	HOP-92	NCI-H226	NCI-H23	NCI-H322M	NCI-H460	NCI-H522	
III-1	12.48	3.50	-44.84	-69.65	-9.03	-38.74	8.84	-78.47	n/a	-26.99
III-2	68.58	83.29	75.01	-2.81	61.63	67.69	78.91	53.09	n/a	60.67
III-3	33.51	48.29	13.28	-6.10	12.73	2.01	26.02	10.17	3.95	15.98
III-4-Br	37.29	15.92	1.85	-20.13	19.65	-4.20	34.78	11.08	-27.43	7.64
III-5	39.11	41.63	8.38	-18.63	12.30	-11.55	25.72	7.73	-0.78	11.54
III-6	27.00	41.67	17.42	-33.86	14.22	-1.01	30.58	7.73	-8.22	10.61
III-7	45.30	38.36	16.53	-32.42	9.50	2.93	23.63	6.08	2.04	12.44

161

Table III-4. Growth percentage values for multiple NSCLC cell lines from the NCI-60 human tumor cell line one-dose assay against **III**‑**8**‑**III**‑**11** and **I-464**.

Compound	Growth %									Average
	A549/ATCC	EKVX	HOP-62	HOP-92	NCI-H226	NCI-H23	NCI-H322M	NCI-H460	NCI-H522	
III‑**8**	88.63	80.66	90.55	74.47	88.12	69.84	102.72	95.03	35.94	80.66
III‑**9**	57.44	31.88	40.89	-11.85	48.43	16.01	73.14	34.82	-3.51	31.84
III‑**10**	62.82	58.14	51.67	16.03	37.98	13.04	72.08	34.24	22.76	40.97
III‑**11**	44.83	50.89	25.25	4.31	26.68	4.77	41.44	16.51	10.02	24.96
III‑**12**	73.26	70.22	74.27	-6.03	36.19	22.87	85.86	41.63	16.24	46.06
I-464	67.63	51.65	42.12	-13.30	52.09	41.65	62.77	39.60	-11.71	38.06

The NCI's DTP also tested **III-1**, **III-3**, **III-4-Br**, **III-5-III-7**, **III-9-III-12**, and

I‑**464** in their five-dose assay (Table III-5, Table III-6, Table III-7, Table III-8, Figure

162

III-12, Figure III-13, Figure III-14, Figure III-15, Figure III-16, Figure III-17, Figure III-18, Figure III-19, Figure III-20, Figure III-21, and Figure III-22), whereas **III-2** and **III-8** were not considered active enough in the one-dose assay for the DTP to test them in the five-dose assay. The experimental details are the same for the five-dose assay as for the one-dose assay, except cells are exposed to each compound at five doses (10 nM, 100 nM, 1μ, 10 μM, and 100 μM) versus one dose. Results are also given in a different format and described as the GI50 (growth inhibition of 50% of cells relative to control cells), TGI (total growth inhibition), and LC50 (lethal concentration of 50% of cells relative to the initial cell count at the time of drug addition).

Compound **III‑1**, with a phenyl substituent at the C^2 position and naphthylmethyl substituents at the N^1 and N^3 positions had GI50 values from the mid nanomolar range (602 nM) to the low micromolar range (1.78 μM), all TGI values in the low micromolar range (2.28 μM – 3.52 μM), and LC50 values for only the NCI-H23 and NCI-H322M cell line in the low micromolar range (6.14 μM and 5.61 μM respectively). **IS29** with two naphthylmethyl groups and a proton at the C^2 position have GI50 values in the nanomolar to low micromolar range (172 nm – 8.40 μM), TGI values in micromolar range (1.39 μM – 22.9 μM) and LC50 values in the micromolar range (15.2 μM - 71.9 μM). Compounds **III‑3**, **III‑4‑Br**, and **III‑5-III‑7** with methyl, ethyl, propyl, butyl, and phenyl substituent at the C^2 position respectively, a naphthylmethyl at the N^1 position, and a quinolylmethyl substituent at the N^3 position had similar results with GI50 values in the low nanomolar range (184 nM) to low micromolar range (3.93 μM), TGI values in the mid nanomolar range (671 nM) to the low micromolar range (27.6 μM), and LC50 values all in the

163

micromolar range (3.67 µM - > 100 µM). Compounds **III‑9‑III‑12**, with an ethyl, propyl, butyl, or phenyl chain at the C^2 position respectively, and quinolylmethyl substituents at both the N^1 and N^3 positions, had GI50 values from the low nanomolar range (18 nM) to the low micromolar range (13.5 µM), TGI values from the mid nanomolar range (521 nM) to unmeasured valued in the micromolar range (> 100 µM), and LC50 values of (17.0 µM) to unmeasured values > 100 µM.

All compounds tested in the five-dose assay had good GI50 values comparable to the IC_{50} values determined in our lab. As the water solubility increases from **III‑1**, with the lowest solubility, to **III‑9‑III‑12**, with the highest solubilities, the TGI and LC50 values also increase, meaning the more water soluble derivatives have inferior anti-cancer activities. This follows the trend observed in both in vitro assays described above that lipophilicity is key to the anticancer activity observed with this class of imidazolium salts against NSCLC. When comparing **III‑3**, **III‑4‑Br**, and **III‑5-III-7** to each other, although they have similar results from the five-dose assay, on average, the most lipophilic derivatives have the lowest values or the best anti-cancer properties. This is consistent when comparing derivatives **III‑9-III‑12** to each other. Compound **III‑12** has the highest anti-cancer activity of this group and is the most lipophilic. Direct comparisons can also be made with **III‑4‑Br** to **III‑9** and with **III‑5** to **III‑10**. Derivatives **III‑4‑Br** and **III‑5** are more lipophilic than **III‑9** and **III‑10** and again have the higher anti-cancer activities further suggesting the need for lipophilicity when considering highly active compounds.

Table III-5. GI50, TGI, and LC50 values (µM) from the NCI-60 human tumor cell line five-dose assay for **III‑1**, **III‑3**, and **III‑4‑Br**. Results are shown for all the NSCLC cell lines tested by the DTP.

Cell line	GI50, TGI, and LC50 values (µM) from the five-dose assay								
	III‑1			**III‑3**			**III‑4‑Br**		
	GI50	TGI	LC50	GI50	TGI	LC50	GI50	TGI	LC50
A549/ATCC	1.78	3.52	n/a	1.31	13.1	43.5	0.997	14.1	46.1
EKVZ	1.58	3.43	n/a	3.93	27.6	> 100	0.442	7.34	38.7
HOP-62	1.46	3.23	n/a	1.53	6.66	34.5	1.40	7.02	32.1
HOP-92	0.602	2.28	n/a	0.518	3.81	27.0	0.184	0.671	7.04
NCI-H226	1.26	2.97	n/a	1.86	10.9	47.5	1.06	4.87	39.4
NCI-H23	0.775	2.35	6.14	1.83	13.4	62.0	0.311	3.23	37.0
NCI-H322M	1.42	2.82	5.61	3.27	14.7	40.4	2.86	13.8	38.1
NCI-H460	1.37	2.87	Na	0.959	14.4	47.0	0.456	10.8	49.5
NCI-H522	1.07	2.58	n/a	0.271	1.46	12.4	0.275	0.986	13.3

Table III-6. GI50, TGI, and LC50 values (μM) from the NCI-60 human tumor cell line five-dose assay for **III‑5**, **III‑9**, and **III‑11**. Results are shown for all the NSCLC cell lines tested by the DTP.

| Cell line | GI50, TGI, and LC50 values (μM) from the five-dose assay | | | | | | | | |
| | **III‑5** | | | **III‑6** | | | **III‑7** | | |
	GI50	TGI	LC50	GI50	TGI	LC50	GI50	TGI	LC50
A549/ATCC	1.88	11.8	37.3	1.18	10.8	38.4	2.59	10.6	42.5
EKVZ	2.16	14.9	52.7	0.702	11.1	40.2	1.56	11.3	38.7
HOP-62	1.63	5.38	26.1	1.45	4.71	21.7	1.18	5.63	30.4
HOP-92	0.188	1.12	9.13	0.206	0.910	3.67	0.203	1.74	8.74
NCI-H226	1.20	7.60	39.7	0.470	4.36	77.7	0.730	5.18	94.7
NCI-H23	0.479	10.6	52.0	0.309	2.30	30.7	0.532	3.99	30.0
NCI-H322M	3.46	15.0	39.6	1.79	8.32	30.0	2.19	6.97	25.7
NCI-H460	0.658	10.6	46.5	0.463	1.75	4.96	1.21	3.36	9.31
NCI-H522	0.249	1.13	45.9	0.331	1.21	4.32	0.404	1.90	6.82

Table III-7. GI50, TGI, and LC50 values (μM) from the NCI-60 human tumor cell line five-dose assay for **III-9-III-11**. Results are shown for all the NSCLC cell lines tested by the DTP.

| Cell line | GI50, TGI, and LC50 values (μM) from the five-dose assay | | | | | | | | |
| | **III‑9** | | | **III-10** | | | **III‑11** | | |
	GI50	TGI	LC50	GI50	TGI	LC50	GI50	TGI	LC50
A549/ATCC	5.27	> 100	> 100	6.78	> 100	> 100	4.76	18.5	47.6
EKVZ	0.343	41.5	> 100	12.5	> 100	> 100	4.00	22.0	72.4
HOP-62	4.66	31.5	> 100	4.28	19.4	62.6	2.80	12.0	39.8
HOP-92	0.018	0.521	19.7	0.399	3.23	23.2	0.339	3.36	20.1
NCI-H226	2.56	30.8	> 100	3.40	34.8	> 100	2.37	13.6	60.3
NCI-H23	0.257	8.66	> 100	0.865	10.5	> 100	0.480	7.27	43.6
NCI-H322M	6.33	41.9	> 100	4.68	41.9	> 100	3.57	16.3	42.0
NCI-H460	0.511	11.9	45.7	2.56	11.7	39.8	2.17	11.6	38.5
NCI-H522	0.084	1.49	37.9	0.601	4.30	27.1	0.435	4.19	32.0

Table III-8. GI50, TGI, and LC50 values (µM) from the NCI-60 human tumor cell line five-dose assay for **III‑11** and **I-464**. Results are shown for all the NSCLC cell lines tested by the DTP.

Cell line	GI50, TGI, and LC50 values (µM) from the five-dose assay					
	III‑12			**I-464**		
	GI50	TGI	LC50	GI50	TGI	LC50
A549/ATCC	13.5	51.1	> 100	7.97	22.9	55.3
EKVZ	2.91	31.4	> 100	2.51	15.5	4.75
HOP-62	5.66	20.8	55.1	3.26	17.0	45.9
HOP-92	0.269	2.47	17.0	0.160	1.39	15.2
NCI-H226	1.76	9.72	49.8	1.72	14.3	71.9
NCI-H23	1.23	9.58	94.4	0.901	10.1	39.4
NCI-H322M	4.74	19.3	61.1	8.40	21.3	47.3
NCI-H460	2.49	11.9	38.5	1.27	10.4	42.0
NCI-H522	1.92	8.72	40.0	0.393	3.11	26.8
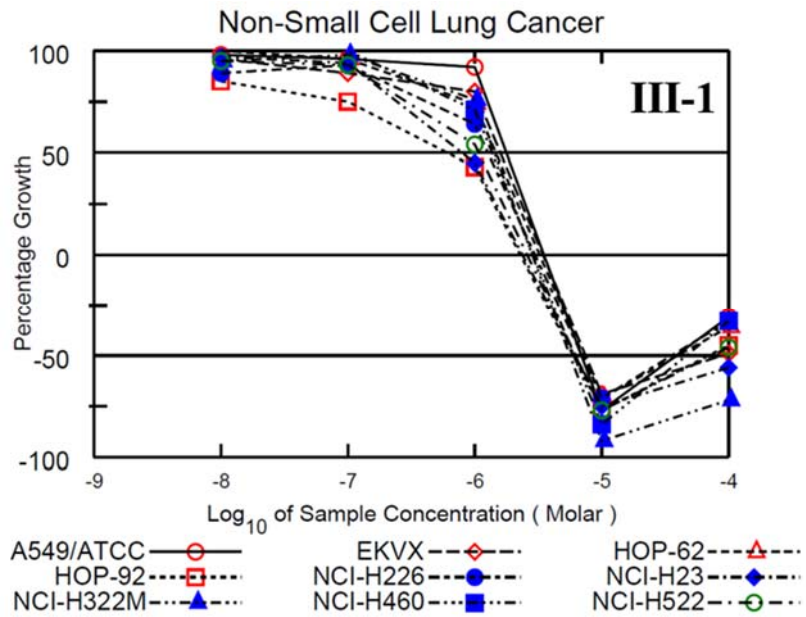
Figure III-12. Growth percentage charts from the NCI-60 human tumor cell line five-dose assay for **III-1**. Only results for the NSCLC cell line tested are shown.
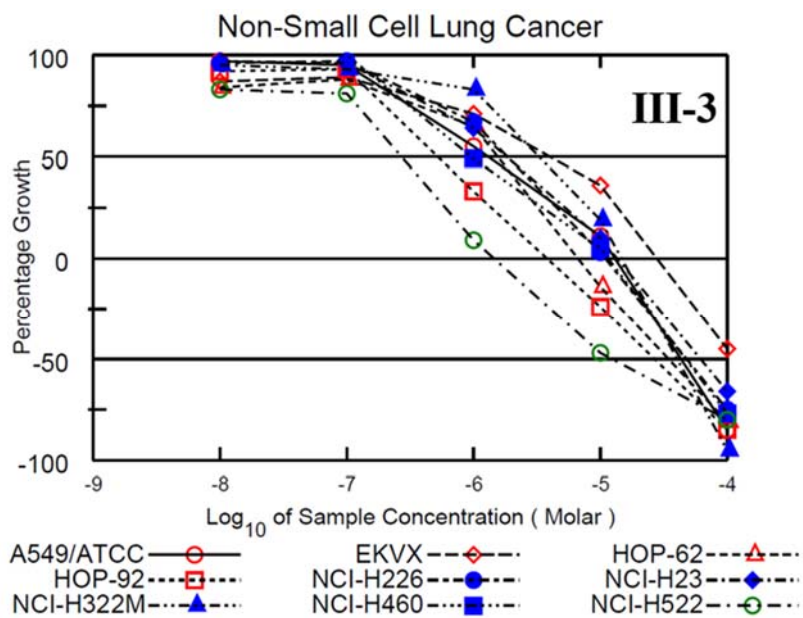
Figure III-13. Growth percentage charts from the NCI-60 human tumor cell line five-dose assay for **III-3**. Only results for the NSCLC cell line tested are shown.
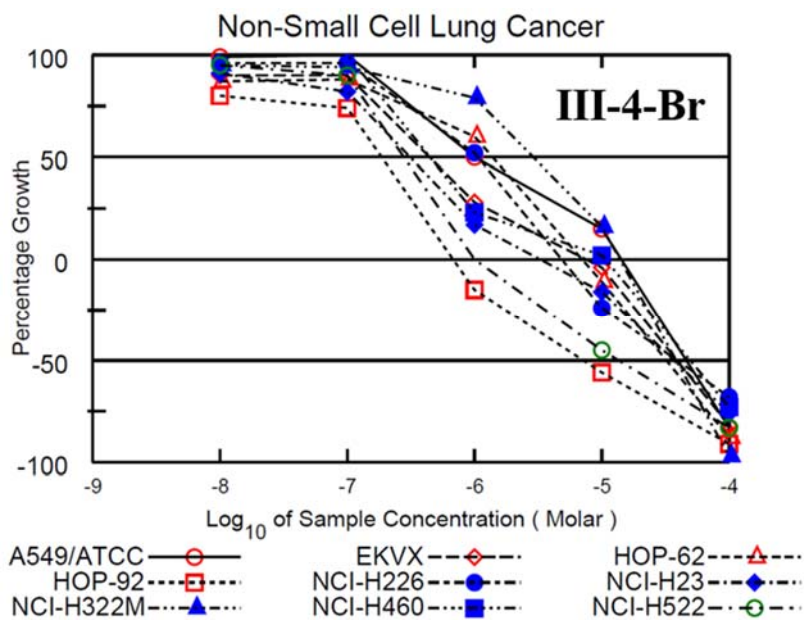
Figure III-14. Growth percentage charts from the NCI-60 human tumor cell line five-dose assay for **III-4-Br**. Only results for the NSCLC cell line tested are shown.
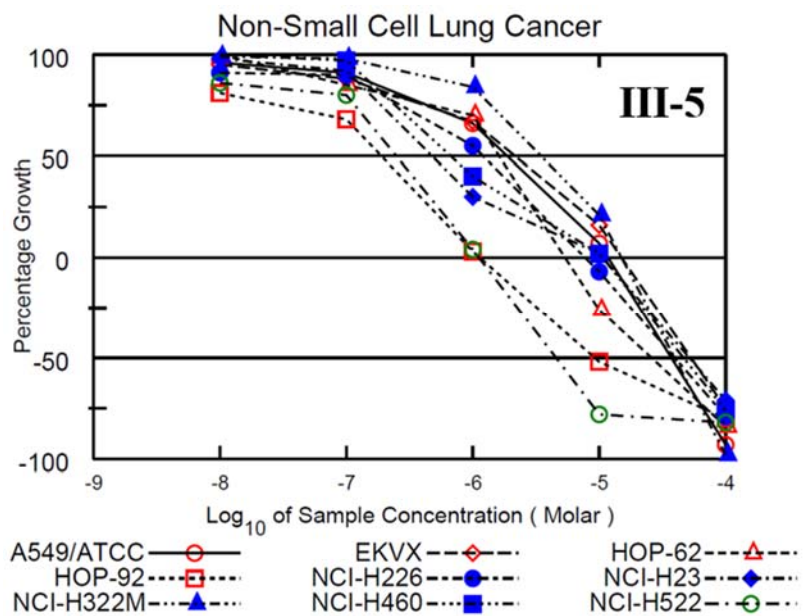
Figure III-15. Growth percentage charts from the NCI-60 human tumor cell line five-dose assay for **III-5**. Only results for the NSCLC cell line tested are shown.
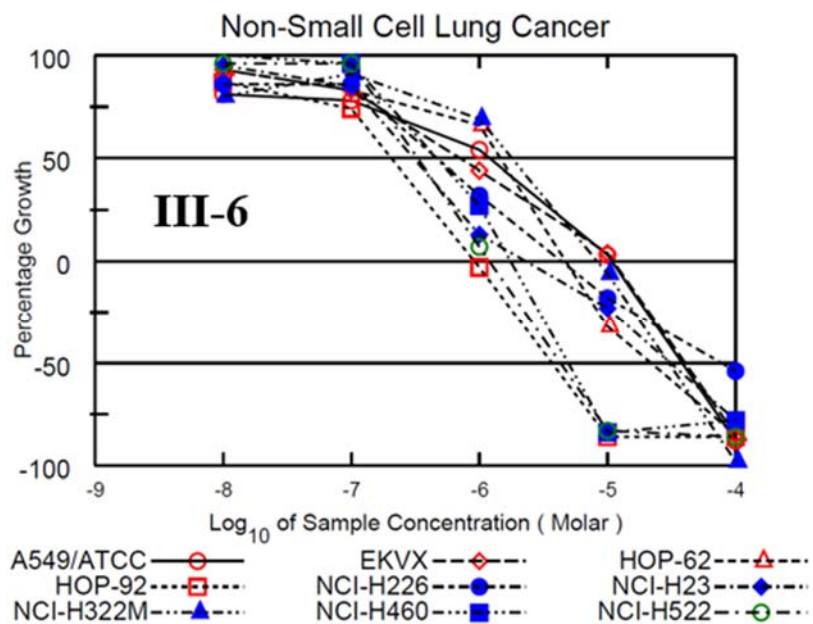
Figure III-16. Growth percentage charts from the NCI-60 human tumor cell line five-dose assay for **III-6**. Only results for the NSCLC cell line tested are shown.
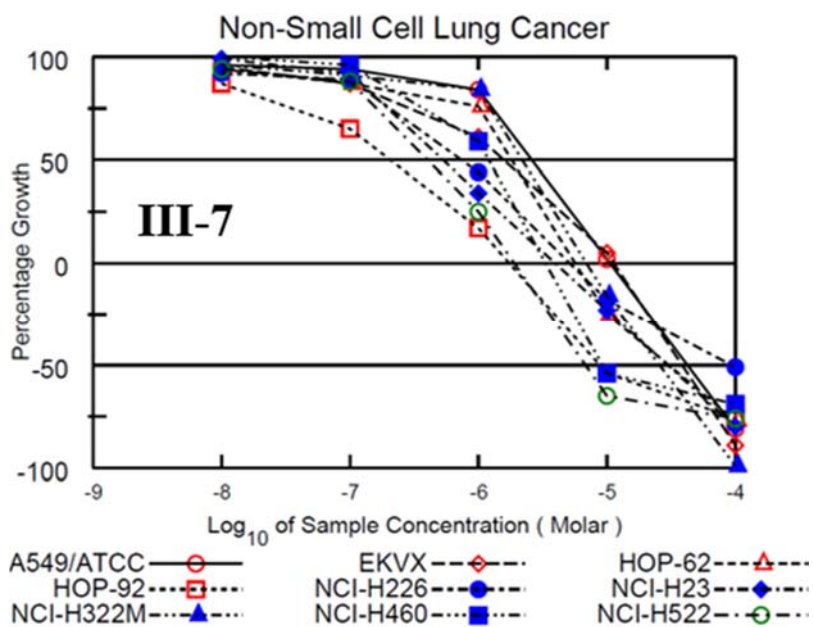
Figure III-17. Growth percentage charts from the NCI-60 human tumor cell line five-dose assay for **III-7**. Only results for the NSCLC cell line tested are shown.
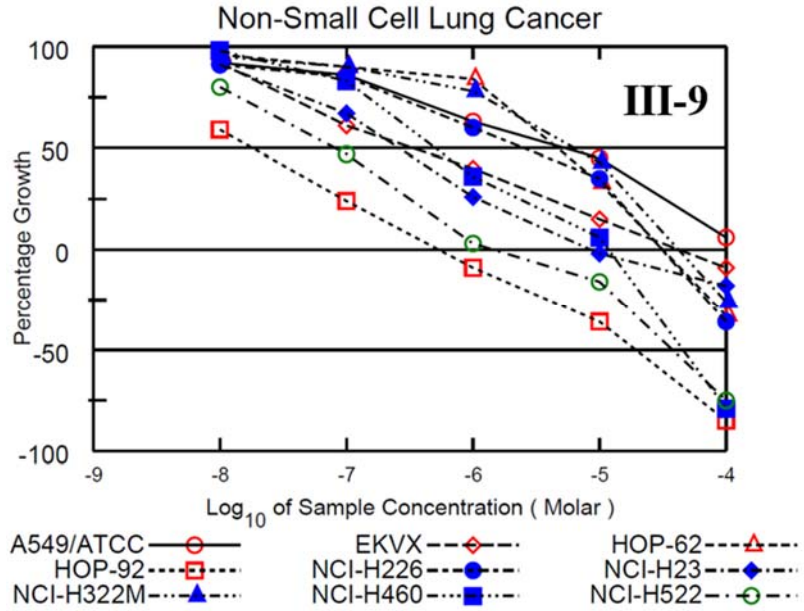
Figure III-18. Growth percentage charts from the NCI-60 human tumor cell line five-dose

assay for **III-9**. Only results for the NSCLC cell line tested are shown.
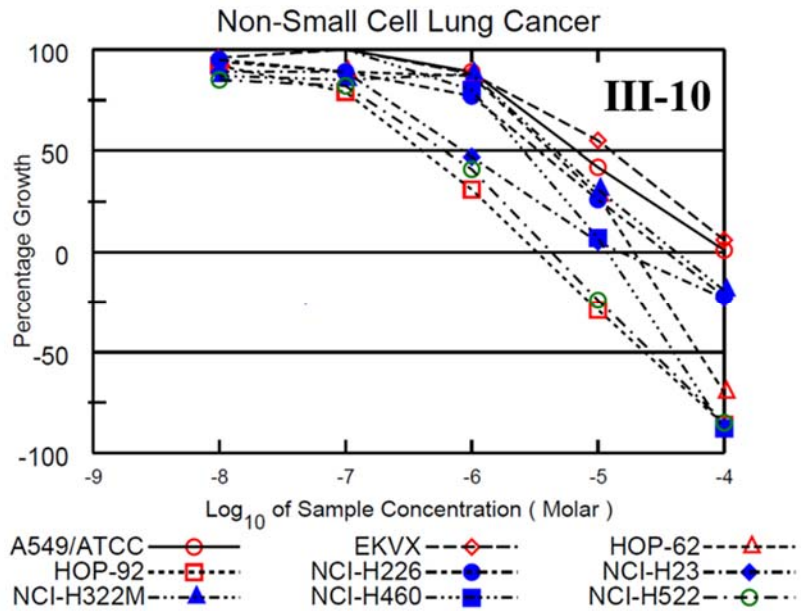
Figure III-19. Growth percentage charts from the NCI-60 human tumor cell line five-dose

assay for **III-10**. Only results for the NSCLC cell line tested are shown.

171
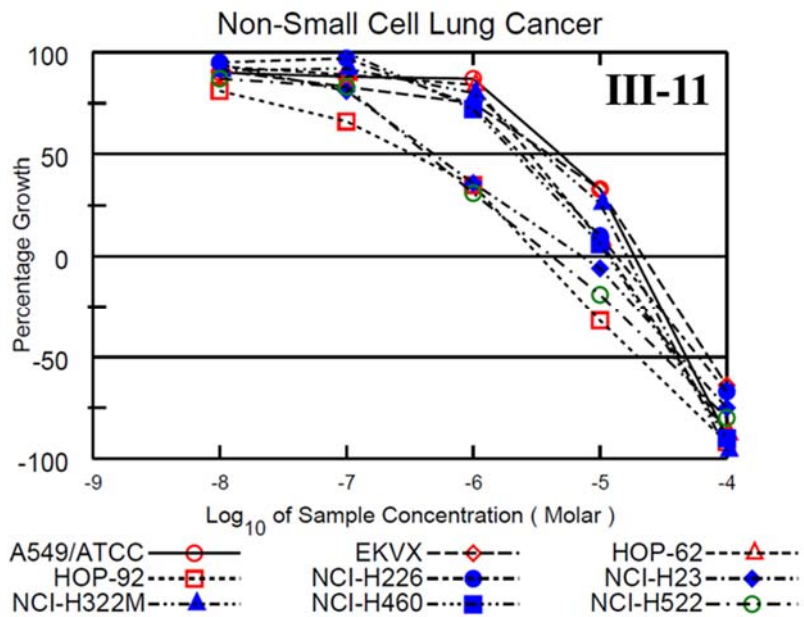
Figure III-20. Growth percentage charts from the NCI-60 human tumor cell line five-dose

assay for **III-11**. Only results for the NSCLC cell line tested are shown.
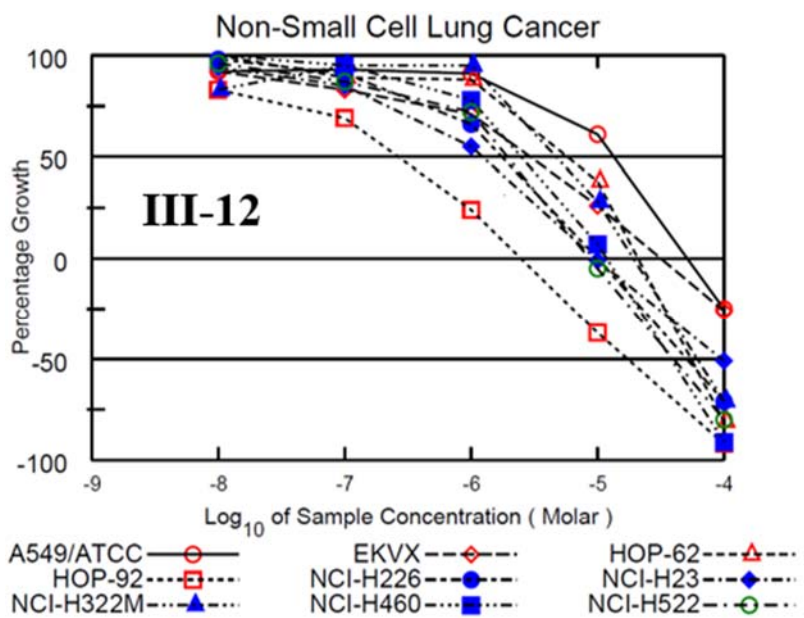
Figure III-21. Growth percentage charts from the NCI-60 human tumor cell line five-dose

assay for **III-12**. Only results for the NSCLC cell line tested are shown.

172
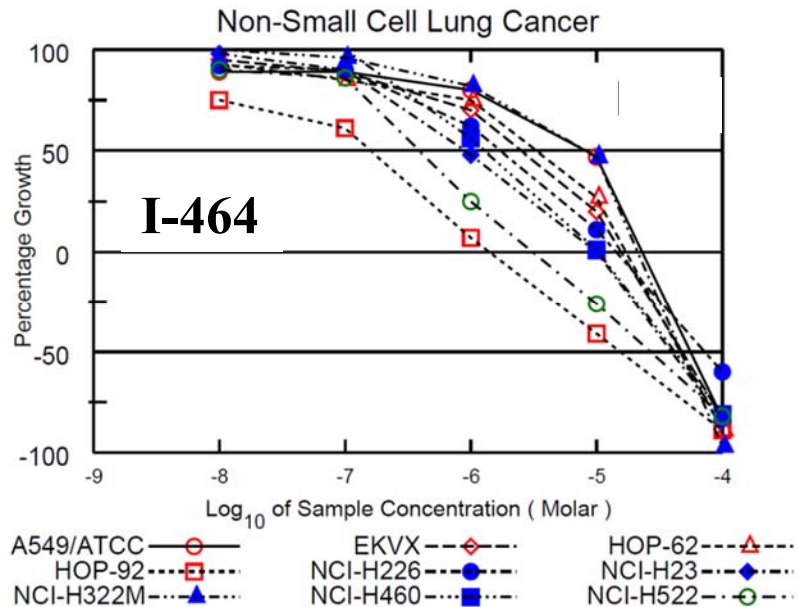
Figure III-22. Growth percentage charts from the NCI-60 human tumor cell line five-dose assay for **I-464**. Only results for the NSCLC cell line tested are shown.

3.4. Conclusions and future outlook

A series of C^2-alkyl substituted imidazolium salts with water solubilizing groups at the C^2 and N^1/N^3 positions were synthesized and evaluated for their anti-cancer properties against NSCLC to establish a SAR. The highly lipophilic derivative **III‑1** was extremely potent against a panel of NSCLC cell lines tested in our lab and by the NCI's DTP. However, this compound is limited by poor aqueous solubility without the use of a chemical excipient. The slightly more hydrophilic derivative **III‑2** had poor anti-cancer properties against the NSCLC cell lines despite the limited water solubility observed with a hydroxl functional group at the C^2 position. Although **III‑3** and **III‑4‑Br** had high anti-

173

cancer activity, these also had poor solubility, whereas **III‑4‑Cl** and **III‑5‑III‑7** had potent anti-proliferative effects and solubility sufficient for systemic administration. The solubility difference between the chloride and bromide derivative of **III‑4** was quite drastic with **III‑4‑Cl** having over a 2-fold increase in solubility compared to **III‑4‑Br** while both compounds had comparable anti-cancer activity suggesting use of the chloride anion is more effective in designing a chemoterapeutic imidazolium salt. Future studies will include more in vitro assays to determine the mechism of action and in vivo toxicity and lung xenograft models for these compounds due to properties they demonstrated. Compounds **III‑8‑III‑12** were highly soluble in aqueous solution but were less active than the more lipophilic derivatives. This concludes the SAR study suggesting lipophilicity will increase activity; however, asymmetrically substituted compounds with one naphthylmethyl and one quinolylmethyl substituent at the N^1 and N^3 positions with a chloride anion can produce highly active compounds with a clinically relevant solubilty. Although several compounds discussed herein merit further studies and show potential for clinical use, this will also help guide future derivatives to continue to optimize these highly active imidazolium salts as prospective chemotherapeutics.

3.5. Acknowledgements

174

guidance to help me solve several of the crystal structures. The DTP performed the NCI-60 cell line one-dose and five-dose assays.

3.6. Experimental

3.6.1. General Procedures

All reactions were carried out under aerobic conditions. 2-Methylimidazole was purchased from Alpha Aesar. 2-Ethyl imidazole was purchased from Acros Organics. 2-Propylimidazole was purchased from Ark Pharm, Inc. 2-Butylimidazole was purchased from TCI. 2-(Bromomethyl)naphthalene and 2-(chloromethyl)quinoline hydrochloride were purchased from Waterstone Technologies. All solvents were purchased from Fisher Scientific. All reagents were used as received without further purification. 2-(Chloromethyl)quinoline was obtained by neutralizing 2-(chloromethyl)quinoline hydrochloride and used without further purification. Melting points were obtained using a MelTemp apparatus with a calibrated thermometer. ^{1}H and ^{13}C NMR spectra were obtained on a Varian 500 MHz instrument with all spectra referenced to residual deuterated solvent (DMSO-d$_6$: ^{1}H NMR: 2.50 ppm, ^{13}C NMR: 39.5 ppm). Mass spectrometry was performed in the University of Akron mass spectrometry laboratory. Elemental analysis was performed by Atlantic Microlab in Norcross, Georgia.

The human NSCLC cell lines NCI-H1975 and HCC827 were generously provided by Dr. Lindner from the Cleveland Clinic. The human NSCLC cell lines NCI-H460 and A549 were purchased from ATCC (Manassas, VA, USA). All cell lines were grown at 37

°C with 5% CO_2 in RPMI 1640 medium supplemented with 10% fetal bovine serum and passed every 2-3 days.

3.6.2. X-ray analysis

Crystals of the compounds were coated in paratone oil, mounted on a CryoLoop and placed on a goniometer under a stream of nitrogen. Crystal structure data sets were collected on either a Bruker SMART APEX I CCD diffractometer with graphite-monochromated Mo Kα radiation (λ = 0.71073 Å) or a Bruker Kappa APEX II Duo CCD system equipped with a Mo ImuS source and a Cu ImuS micro-focus source equipped with QUAZAR optics (λ = 1.54178 Å). The unit cells were determined by using reflections from three different orientations. Data sets were collected using SMART or APEX II software packages. All data sets were processed using the APEX II software suite.[114,115] The data sets were integrated using SAINT.[116] An empirical absorption correction and other corrections were applied to the data sets using multi-scan SADABS.[117] Structure solution, refinement, and modelling were accomplished by using the Bruker SHELXTL package.[118] The structures were determined by full-matrix least-squares refinement of F^2 and the selection of the appropriate atoms from the generated difference map. Hydrogen atom positions were calculated and $U_{iso}(H)$ values were fixed according to a riding model.

3.6.3. MTT assay

Cells were grown to confluence and plated in 96-well plates at 5,000-7,000 cells per well, depending on the cell line. Cells were incubated for 24 h prior to adding the

compounds. Compounds were dissolved in either a DMSO/water solution or water and diluted in fresh medium to the desired concentrations of 32, 16, 4, and 1 µM. Cisplatin was dissolved in pure water by stirring for several hours at room temperature and then diluted to the appropriate concentrations. Compounds were added (6 replicates each) and cells were incubated for 72 h at which time the MTT assay protocol was followed. MTT reagent (10 µL) was added to each well and cells were incubated for 3-4 h, again depending on the cell line. Growth medium was removed by aspiration and DMSO (100 µL) was added to each well. Plates were incubated for 15 min. The optical density was read at 540 nm on a Fisher Scientific Multiskan FC plate reader. Each experiment was done in triplicate and reported results were averages from each independent experiment.

3.6.4. General Synthesis

3.6.4.1. Synthesis of 1,3-bis(naphthalen-2-ylmethyl)-2-phenylimidazolium bromide

(III‑1)

Sodium hydride (0.18 g, 7.5 mmol) was dissolved in organic dry dimethylformamide (15 mL) at 0°C. 2-Phenylimidazole (1.00 g, 6.9 mmol) was dissolved in organic dry dimethylformamide (10 mL) and slowly added to the solution of cooled sodium hydride. The reaction was slowly warmed to room temperature and stirred for 30 minutes. (2-Bromomethyl)naphthalene (1.53 g, 6.9 mmol) was added and stirred overnight. The volatiles were removed by rotary evaporation. Water (25 mL) was added to the yellow oil which was extracted with dichloromethane (3 x 25 mL). The combined organic layers

177

were washed with water (3 x 25 mL) and dried with sodium sulfate. The volatiles were removed by rotary evaporation and the residue was dissolved in acetonitrile (10 mL). (2-Bromomethyl)naphthalene (1.76 g, 7.96 mmol) was added and the mixture was refluxed overnight. A yellow solid precipitated from addition of diethyl ether, which was recrystallized from acetone to yield the white solid **III‑1** (2.03 g, 57.9 % yield). Mp: 194-197°C. Found C, 73.7; H, 5.2; N, 5.7 %. Calculated for $C_{31}H_{25}N_2Br_1$: C, 73.7; H, 5.0; N, 5.5 %. ^{1}H NMR (500MHz, DMSO- d_6) δ=8.16-8.18 (2H, m, Ar), 7.88-7.91 (4H, m, Ar), 7.81.7.84 (2H, m, Ar), 7.68-7.72 (3H, m, Ar), 7.57-7.60 (4H, m, Ar), 7.52-7.54 (4H, s, Ar), 7.26-7.28 (2H, m, Ar), 5.48 (4H, s, NCH_2). ^{13}C NMR (500MHz, DMSO-d_6) δ= 144.6 (NCN), 132.5 (Ar), 132.4 (Ar), 131.6 (Ar), 130.5 (Ar), 129.4 (Ar), 128.5 (Ar), 127.7 (Ar), 127.5 (Ar), 126.8 (Ar), 126.6 (Ar), 125.1 (Ar), 123.0 (Ar), 121.2 (Ar), 51.7 (CH_2). MS: m/z= 425.1 (theor for M^+ $C_{31}H_{25}N_2^+$ = 425.2).

Crystal data for **III‑1‑PF$_6$:** $C_{31}H_{25}N_2F_6P_1$, M = 570.50, *Monoclinic*, a = 12.0701(5) Å, b = 8.8644(4) Å, c = 24.9236(11) Å, β = 100.317(2)°, V = 2623.6(2) Å^3, T = 100(2) K, space group P2$_{1/c}$, Z = 4, 32975 reflections measured, 5308 [R(int) = 0.0410]. The final R_1 values were 0.0527 ($I > 2\sigma(I)$). The final $wR(F^2)$ values were 0.1269 ($I > 2\sigma(I)$). The final R_1 values were 0.0700 (all data). The final $wR(F^2)$ values were 0.1398 (all data). A single crystal of **III‑1‑PF$_6$** was obtained by slow evaporation of a concentrated solution of **III‑1‑PF$_6$** dissolved in acetonitrile. Crystallographic information file (CIF) can be found on the Cambridge Crystallographic Data Center website (CCDC # 1503023)

3.6.4.2. Synthesis of 2-(hydroxymethyl)-1,3-bis(naphthalen-2-ylmethyl)imidazolium

bromide (**III‑2**)

I-464 (0.50 g, 1.2 mmol), N,N-diisopropylethylamine (1.4 mL, 8.0 mmol), formalin

(0.3 mL, 3.0 mmol), and dimethylformamide (3 mL) were added to a pressure flask and

heated to 90°C for one hour. The flask was cooled to room temperature. Dichloromethane

(25 mL) was added to the flask and the solution was washed with a sodium bromide brine

solution (2 x 25 mL) and water (1 x 25 mL). The organic layer was dried with sodium

sulfate. The volatiles were removed by rotary evaporation and the resulting yellow solid

was washed with diethyl ether (3 x 30 mL), recrystallized from acetonitrile, and dried in

air to yield **III‑2** (0.37 g, 69% yield).   Mp = 208-209°C. HRMS (ESI$^+$) calcd for

$C_{26}H_{23}N_2O$ $^+$ [M-Br] of m/z = 379.1805, found m/z = 379.1825. ^{1}H NMR (500 MHz,

DMSO- d_6) δ = 7.95 (8H, m, Ar), 7.85 (2H, s, Ar), 7.55 (6H, m, Ar), 6.27 (1H, t, OH, J =

5.6 Hz), 5.71 (4H, s, CH_2), 5.03 (2H, d, CH_2, J = 5.4 Hz). ^{13}C NMR (125 MHz, DMSO-

d_6) δ = 145.3 (Ar), 132.7 (Ar), 132.6 (Ar), 131.9 (Ar), 128.6 (Ar), 127.8 (Ar), 127.6 (Ar),

127.2 (Ar), 126.6 (Ar), 125.5 (Ar), 122.7 (Ar), 51.3 (CH_2), 50.9 (CH_2). MS: m/z = 379.

(theor for M^+ $C_{26}H_{23}N_2O_1{}^+$ = 379.3).

Crystal data for **III‑2:** $C_{26}H_{23}N_2Br_1O_1,$ M = 459.37, *Orthorhombic*, a = 14.0733(7)

Å, b = 13.4541(7) Å, c = 11.0120(4) Å, V = 2085.05(17) Å^3, T = 100(2) K, space group

Pca2(1), Z = 4, 7619 reflections measured, 3578 [R(int) = 0.0342]. The final R_1 values were

0.0314 ($I > 2\sigma(I)$). The final $wR(F^2)$ values were 0.0633 ($I > 2\sigma(I)$). The final R_1 values

were 0.0397 (all data). The final $wR(F^2)$ values were 0.0666 (all data). A single crystal of

III‑2 was obtained by slow evaporation of a concentrated solution of **III‑2** dissolved in

acetonitrile. Crystallographic information file (CIF) can be found on the Cambridge Crystallographic Data Center website (CCDC # 1503024)

3.6.4.3. Synthesis of 2-methyl-3-(naphthalene-2-ylmethyl)-1-(quinoline-2-ylmethyl)imidazolium bromide (III‑3)

2-Methylimdazole (1.03 g, 12.5 mmol) dissolved in acetonitrile (15 mL) was combined with potassium hydroxide (0.73 g, 13.0 mmol) and stirred at 80°C for 30 minutes. 2-(Chloromethyl)quinoline hydrochloride (1.28 g, 5.98 mmol) and potassium hydroxide (0.428 g, 7.63 mmol) were added and the mixture was stirred at 80°C overnight. The mixture was filtered to remove a white solid (presumed to be potassium chloride) and the volatiles were removed from the filtrate to yield a yellow oil. The oil was suspended with dichloromethane (30 mL) and washed with a basic aqueous solution (30 mL) and water (2 x 25 mL). The organic layer was dried with magnesium sulfate and the volatiles were removed to yield a yellow oil. The oil was resuspended in acetonitrile (10 mL) and 2-(bromomethyl)naphthalene (1.407 g, 6.36 mmol) was added. The mixture was heated to 80°C overnight. A white solid precipitated from the hot acetonitrile, was filtered, washed with cold acetonitrile, and dried in air to yield III‑3 (1.20 g, 50% yield). Mp: 238-239°C. HRMS (ESI$^+$) calcd for C$_{25}$H$_{22}$N$_3^+$ [M-Cl] of m/z = 364.1808, found m/z = 364.1902. ^{1}H NMR (500 MHz, DMSO- d_6) δ = 8.46 (1H, d, Ar, J = 8.6 Hz), 8.04 (1H, d, Ar, J = 8.6 Hz), 7.99 (2H, m, Ar), 7.92 (3H, m, Ar), 7.85 (1H, m, Ar), 7.68 (1H, m, Ar), 7.61 (5H, m, Ar), 7.52 (1H, d, Ar, J = 8.1 Hz), 5.85 (2H, s, CH$_2$), 5.72 (2H, s, CH$_2$), 2.66 (3H, s, CH$_3$). ^{13}C NMR (125 MHz, DMSO- d_6) δ = 153.8 (Ar), 146.6 (Ar), 145.9 (Ar), 137.4 (Ar), 132.7

(Ar), 132.5 (Ar), 132.1 (Ar), 129.9 (Ar), 128.7 (Ar), 128.3 (Ar), 127.9 (Ar), 127.7 (Ar), 127.6 (Ar), 127.1 (Ar), 126.8 (Ar), 126.6 (Ar), 126.6 (Ar), 126.5 (Ar), 125.2 (Ar), 122.7 (Ar), 121.8 (Ar), 119.7 (Ar), 52.3 (CH_2), 50.9 (CH_2), 10.3 (CH_3).

3.6.4.4. Synthesis of 2-ethyl-3-(naphthalene-2-ylmethyl)-1-(quinoline-2-ylmethyl)imidazolium bromide (III‑4‑Br)

2-Ethylimidazole (0.756 g, 7.9 mmol) dissolved in acetonitrile (15 mL) was combined with potassium hydroxide (0.550 g, 9.8 mmol) and stirred at 80°C for 30 minutes. 2-(Chloromethyl)quinoline hydrochloride (1.45 g, 6.8 mmol) and potassium hydroxide (0.440 g, 7.8 mmol) were added and the mixture was stirred and heated at 80°C overnight. The reaction mixture was filtered to remove a white solid (presumed be potassium chloride) and the volatiles were removed from the filtrate to yield a yellow oil. The oil was suspended with dichloromethane (25 mL) and washed with a basic aqueous solution (4 x 25 mL) and water (2 x 25 mL). The organic layers were dried with magnesium sulfate and concentrated to a yellow oil. The oil was resuspended in acetonitrile and 2-(bromomethyl)naphthalene (1.50 g, 6.8 mmol) was added to the solution. The mixture was stirred and heated at 80°C overnight. A solid precipitated from the hot acetonitrile. The white solid was filtered, washed with acetonitrile, and dried in air to yield III‑4‑Br (.715 g, 23% yield). MP = 215-216°C. HRMS (ESI$^+$) calcd for $C_{26}H_{24}N_3^+$ [M-Br] of m/z = 378.1965, found m/z = 378.1942. ^{1}H NMR (500 MHz, DMSO- d_6) δ = 8.48 (1H, d, Ar, J = 8.3 Hz), 8.03 (2H, t, Ar, J = 8.8 Hz), 7.98 (1H, m, Ar), 7.93 (1H, m, Ar), 7.90 (3H, m, Ar), 7.76 (2H, m, Ar), 7.61 (4H, m, Ar), 7.50 (1H, m, Ar), 5.88 (2H, s, CH_2), 5.74 (2H, s,

CH$_2$), 3.17 (2H, q, CH$_2$, J = 7.6 Hz) 0.94 (3H, t, CH$_3$, J = 7.6 Hz). ^{13}C NMR (125 MHz, DMSO- d_6) δ = 154.2 (Ar), 149.1 (Ar), 146.7 (Ar), 137.4 (Ar), 132.7 (Ar), 132.5 (Ar), 132.4 (Ar), 130.1 (Ar), 128.7 (Ar), 128.3 (Ar), 128.0 (Ar), 127.7 (Ar), 127.7 (Ar), 127.1 (Ar), 126.9 (Ar), 126.7 (Ar), 126.6 (Ar), 126.4 (Ar), 125.0 (Ar), 123.1 (Ar), 122.1 (Ar), 119.8 (Ar), 52.3 (CH$_2$), 50.8 (CH$_2$), 16.6 (CH$_2$), 11.2 (CH$_3$).

3.6.4.5. Synthesis of 2-ethyl-1-(naphthalen-2-ylmethyl)-3-(quinolin-2-ylmethyl)imidazolium chloride (**III‑4‑Cl**)

2-Ethyl imidazole (1.01 g, 10.5 mmol) dissolved in acetonitrile (25 mL) was combined with potassium hydroxide (0.58 g, 10.3 mmol) and stirred for 30 minutes at 80°C. 2-(Bromomethyl)naphthalene (1.73 g, 7.8 mmol) was added and the mixture was stirred and heated at 80°C overnight. The reaction mixture was filtered to remove a white solid (presumed to be potassium bromide) and the volatiles were removed from the filtrate to yield a yellow oil. The oil was suspended with dichloromethane (40 mL) and washed with a basic aqueous solution (1 x 30 mL) and water (3 x 30 mL). The organic layers were dried with magnesium sulfate and concentrated to a yellow oil. The oil was resuspended in acetonitrile (7 mL) and 2-(chloromethyl)quinoline (1.59 g, 9.0 mmol) was added to the solution. The mixture was stirred and heated at 80°C overnight. A white solid precipitated from the hot acetonitrile and was filtered, washed with acetonitrile, and dried in air to yield **III‑4‑Cl** (0.850 g, 26% yield). MP = 204-207°C. HRMS (ESI$^+$) calcd for C$_{26}$H$_{24}$N$_3^+$ [M-Cl] of m/z = 378.1965, found m/z = 378.2000. ^{1}H NMR (500 MHz, DMSO- d_6) δ = 8.48 (1H, d, Ar, J = 8.8 Hz), 8.03 (2H, t, Ar, J = 8.3 Hz), 7.98 (1H, m, Ar), 7.93 (3H, m,

Ar), 7.90 (1H, m, Ar), 7.76 (2H, m, Ar), 7.64 (2H, m, Ar), 7.58 (2H, m, Ar), 7.50 (1H, m,

Ar), 5.90 (2H, s, CH_2), 5.76 (2H, s, CH_2), 3.17 (2H, q, CH_2, J = 7.6 Hz) 0.93 (3H, t, CH_3,

J = 7.6 Hz). ^{13}C NMR (125 MHz, DMSO- d_6) δ = 154.2 (Ar), 149.1 (Ar), 146.7 (Ar), 137.4

(Ar), 132.7 (Ar), 132.5 (Ar), 132.5 (Ar), 130.1 (Ar), 128.7 (Ar), 128.3 (Ar), 128.0 (Ar),

127.7 (Ar), 127.7 (Ar), 127.2 (Ar), 126.9 (Ar), 126.7 (Ar), 126.6 (Ar), 126.4 (Ar), 125.0

(Ar), 123.1 (Ar), 122.2 (Ar), 119.9 (Ar), 52.2 (CH_2), 50.8 (CH_2), 16.6 (CH_2), 11.2 (CH_3).

Crystal data for **III‑4‑Cl•H₂O:** $C_{26}H_{26}N_3O_1Cl_1$, M = 431.95, *Monoclinic*, a =

34.6333(13) Å, b = 9.5796(4) Å, c = 13.6475(5) Å, β = 92.286(2)°, V = 4524.8(3) Å^3, T =

100(2) K, space group C2/c, Z = 8, 16910 reflections measured, 4589 [R(int) = 0.0411].

The final R_1 values were 0.0475 ($I > 2\sigma(I)$). The final $wR(F^2)$ values were 0.1118 ($I > 2\sigma(I)$).

The final R_1 values were 0.0650 (all data). The final $wR(F^2)$ values were 0.1215 (all data).

A single crystal of **III‑4‑Cl•H₂O** was obtained by slow evaporation of a concentrated

solution of **III‑4‑Cl** dissolved in acetonitrile. Crystallographic information file (CIF) can

be found on the Cambridge Crystallographic Data Center website (CCDC # 1503025)

3.6.4.6. Synthesis of 2-propyl-3-(naphthalene-2-ylmethyl)-1-(quinoline-2-ylmethyl)imidazolium chloride (III‑5)

2-Propylimidazole (.500 g, 4.5 mmol) was dissolved in organic dry tetrahydrofuran

(10 mL) and slowly added to a stirred slurry of sodium hydride (0.165 g, 6.9 mmol) in

organic dry tetrahydrofuran (10 mL) cooled to 0°C in an ice bath. After 30 minutes,

tetrabutylammonium bromide (0.077 g, 0.24 mmol) was added to the reaction mixture.

2-(Bromomethyl)naphthalene (1.10 g, 5.0 mmol) was dissolved in organic dry

tetrahydrofuran (10 mL) and added to the reaction mixture dropwise. The reaction mixture was allowed to warm to room temperature and stirred overnight. The mixture was filtered through celite. The volatiles were removed from the filtrate by rotary evaporation to yield a yellow oil. The oil was resuspended in dichloromethane (25 mL), washed with deionized water (3 x 25 mL), and dried with magnesium sulfate. The volatiles were removed to yield a yellow oil which was resuspended in acetonitrile (10 mL). 2-(Chloromethyl)quinolone (0.900 g, 5.1 mmol) was added to the reaction mixture which was heated to 80°C and stirred overnight. A white precipitate formed, which was collected by filtration and air dried. Crystals also formed from the filtrate when cooled to -20°C which were collected, ground to a fine powder, air dried, and combined with the white precipitate to yield the white solid **III‑5** (0.904 g, 46% yield). Mp = 198-199 °C. HRMS (ESI$^+$) calcd for $C_{27}H_{26}N_3^+$ [M-Br] of m/z = 392.2121, found m/z = 392.2045. ^1H NMR (500 MHz, DMSO- d_6) δ = 8.47 (1H, d, Ar, J = 8.8 Hz), 8.02 (2H, m, Ar), 7.98 (3H, m, Ar), 7.93 (2H, m, Ar), 7.74 (2H, m, Ar), 7.68 (1H, d, Ar, J = 8.3 Hz), 7.61 (1H, m, Ar), 7.57 (2H, m, Ar), 7.53 (1H, m, Ar) 5.94 (2H, s, CH_2), 5.79 (2H, s, CH_2), 3.14 (2H, t, CH_2, J = 7.8 Hz), 1.33 (2H, m, CH_2), 0.77 (3H, t, CH_3, J = 7.3 Hz). ^{13}C NMR (125 MHz, DMSO- d_6) δ = 154.3 (Ar), 148.1 (Ar), 146.7 (Ar), 137.4 (Ar), 132.7 (Ar), 132.5 (Ar), 132.5 (Ar), 130.0 (Ar), 128.7 (Ar), 128.3 (Ar), 128.0 (Ar), 127.7 (Ar), 127.7 (Ar), 127.1 (Ar), 126.9 (Ar), 126.7 (Ar), 126.6 (Ar), 126.5 (Ar), 125.1 (Ar), 123.2 (Ar), 122.2 (Ar), 119.9 (Ar), 52.3 (CH_2), 50.9 (CH_2), 24.6 (CH_2), 20.2 (CH_2), 13.2 (CH_3).

Crystal data for **III‑5•CH₃CN:** $C_{29}H_{29}N_3Cl_1$, M = 469.01, *Monoclinic*, a = 7.0122(2) Å, b = 26.0462(6) Å, c = 13.1530(3) Å, β = 100.8312(15)°, V = 2396.56(10) Å^3,

T = 100(2) K, space group P2(1)/c, Z = 4, 4849 reflections measured, 4549 [R(int) =

0.0000]. The final R_I values were 0.0394 ($I > 2\sigma(I)$). The final $wR(F^2)$ values were 0.0860

($I > 2\sigma(I)$). The final R_I values were 0.0565 (all data). The final $wR(F^2)$ values were 0.0950

(all data). A single crystal of **III‑5•CH₃CN** was obtained by slow evaporation of a

concentrated solution of **III‑5** dissolved in acetonitrile. Crystallographic information file

(CIF) can be found on the Cambridge Crystallographic Data Center website (CCDC #

1503026)

3.6.4.7. Synthesis of 2-butyl-3-(naphthalene-2-ylmethyl)-1-(quinoline-2-ylmethyl)imidazolium chloride (III‑6)

2-Butylimidazole (0.500 g, 4.0 mmol) was dissolved in organic dry tetrahydrofuran

(10 mL) and added to a stirred slurry of sodium hydride (0.14 g, 5.8 mmol) in organic dry

tetrahydrofuran (10 mL) cooled to 0°C in an ice bath. After 30 minutes,

tetrabutylammonium bromide (0.070 g, 0.2 mmol) was added to the reaction mixture.

2-(Bromomethyl)naphthalene (1.00 g, 4.5 mmol) dissolved in organic dry tetrahydrofuran

(15 mL) was slowly added to the reaction mixture dropwise over 15 minutes. Reaction was

warmed to room temperature and stirred for 4 hours. The mixture was filtered through

celite and the volatiles were removed from the filtrate to form a light yellow oil. The oil

was suspended in water (30 mL) and extracted with dichloromethane (3 x 30 mL). The

organic layers were combined, washed with water (3 x 30 mL), and dried with magnesium

sulfate. The volatiles were removed to form a light yellow solid. The mono-alkylated

intermediate was dissolved in acetone leaving a white precipitate that was removed by

filtration. The volatiles were removed from the filtrate to form a light yellow residue. This residue was resuspended in acetonitrile (5 mL), combined with 2-(chloromethyl)quinoline (0.735 g, 4.2 mmol), and heated to 80°C overnight. A white solid precipitated from the reaction mixture which was washed with room temperature acetonitrile and diethyl ether. The white solid was dissolved in dichloromethane followed by removal of all volatiles by rotary evaporation and by vacuum with the compound under reduced pressure for 6 days to yield **III‑6** (0.256 g, 17% yield). Mp: 170-173°C. HRMS (ESI$^+$) calcd for $C_{28}H_{28}N_3{}^+$ [M-Cl] of m/z = 406.2278, found m/z = 406.2304. ^{1}H NMR (500 MHz, DMSO- d_6) δ = 8.48 (1H, d, Ar, J = 8.6 Hz), 8.01 (4H, m, Ar), 7.97 (1H, m, Ar), 7.92 (2H, m, Ar, 7.76 (2H, m, Ar), 7.67 (1H, d, Ar, J = 8.6 Hz), 7.61 (1H, m, Ar), 7.57 (2H, m, Ar), 7.51 (1H, d, Ar, J = 8.3 Hz), 5.93 (2H, s, CH$_2$), 5.78 (2H, s, CH$_2$), 3.12 (2H, m, CH$_2$), 1.15 (4H, m, CH$_2$, CH$_2$), 0.51 (3H, m, CH$_3$) . ^{13}C NMR (125 MHz, DMSO- d_6) δ = 154.2 (Ar), 148.1 (Ar), 146.2 (Ar), 137.4 (Ar), 132.6 (Ar), 132.5 (Ar), 132.4 (Ar), 130.1 (Ar), 128.7 (Ar), 128.3 (Ar), 127.9 (Ar), 127.7 (Ar), 127.6 (Ar), 127.1 (Ar), 126.9 (Ar), 126.7 (Ar), 126.6 (Ar), 126.6 (Ar), 125.1 (Ar), 123.2 (Ar), 122.2 (Ar), 119.9 (Ar), 52.4 (CH$_2$), 51.0 (CH$_2$), 28.3 (CH$_2$), 22.8 (CH$_2$), 21.5 (CH$_2$), 13.1 (CH$_3$).

3.6.4.8. Synthesis of 2-phenyl-3-(naphthalene-2-ylmethyl)-1-(quinoline-2-ylmethyl)imidazolium bromide (**III‑7**)

2-Phenylimidazole (6.88 g, 47.7 mmol) was added to stirred slurry of sodium hydride (1.26 g, 52.5 mmol) in organic dry dimethylformamide (80 mL) cooled in an ice bath at 0°C and stirred for one hour. 2-(Bromomethyl)naphthalene (10.20 g, 46.1 mmol)

was added to the reaction mixture and stirred overnight at room temperature. The volatiles were removed by rotary evaporation to form a yellow oil which was suspended in dichloromethane (50 mL), washed with water (3 x 50 mL), and dried with magnesium sulfate. The volatiles were removed by rotary evaporation to form a light yellow solid (1-(naphthalen-2-ylmethyl)-2-phenylimidazole) which was used without further purification. 1-(naphthalen-2-ylmethyl)-2-phenylimidazole (0.51 g, 1.8 mmol) was dissolved in acetonitrile (5 mL) and heated to 80°C. 2-(Chloromethyl)quinoline (0.370 g, 2.1 mmol) was added to the reaction mixture and stirred overnight. Acetonitrile (5 mL), diethyl ether (25 mL), and acetone (5 mL) was added to the reaction mixture and stirred overnight to produce a white precipitate. The white solid was collected by filtration and dried in air to yield **III‑7** (0.483 g, 58% yield). Mp: 128-134°C. HRMS (ESI$^+$) calcd for $C_{30}H_{24}N_3^+$ [M-Cl] of m/z = 426.1965, found m/z = 426.1938. ^{1}H NMR (500 MHz, DMSO-d_6) δ = 8.37 (1H, d, Ar, J = 11.7 Hz), 8.24 (1H, m, Ar), 8.18 (1H, m, Ar), 7.98 (1H, d, Ar, J = 8.3 Hz), 7.95 (2H, m, Ar), 7.84 (2H, m, Ar), 7.76 (1H, m, Ar), 7.61 (4H, m, Ar), 7.56 (2H, m, Ar), 7.47 (3H, m, Ar), 7.30 (1H, d, Ar, J = 8.3 Hz), 5.70 (2H, s, CH$_2$), 5.57 (2H, s, CH$_2$). ^{13}C NMR (125 MHz, DMSO-d_6) δ = 153.8 (Ar), 146.6 (Ar), 145.6 (Ar), 137.2 (Ar), 132.5 (Ar), 132.5 (Ar), 132.3 (Ar), 132.1 (Ar), 130.3 (Ar), 130.1 (Ar), 129.2 (Ar), 128.6 (Ar), 128.3 (Ar), 127.9 (Ar), 127.7 (Ar), 127.6 (Ar), 127.1 (Ar), 126.9 (Ar), 126.7 (Ar), 126.6 (Ar), 126.4 (Ar), 124.9 (Ar), 123.9 (Ar), 122.9 (Ar), 121.2 (Ar), 119.6 (Ar), 52.8 (CH$_2$), 51.7 (CH$_2$).

3.6.4.9. Synthesis of 2-methyl-1,3-bis(quinoline-2-ylmethyl)imidazolium chloride (**III‑8**)

2-Methylimidazole (0.752 g, 9.16 mmol) dissolved in acetonitrile (10 mL) was combined with potassium hydroxide (0.530 g, 9.45 mmol) and stirred at 80°C for 30 minutes. 2-(Chloromethyl)quinoline hydrochloride (1.307 g, 6.10 mmol) and potassium hydroxide (0.376 g, 6.70 mmol) were added to the reaction mixture which was heated at 80°C overnight. The reaction mixture was filtered to remove a white solid (presumed to be potassium chloride) and the volatiles were removed from the filtrate to form a yellow oil. The oil was diluted with dichloromethane (25 mL) and washed with a basic aqueous solution (2 x 25 mL) and water (25 mL). The organic layer was dried with magnesium sulfate. The volatiles were removed and the resulting yellow oil was resuspended in acetonitrile (25 mL). 2-(Chloromethyl)quinoline (1.24 g, 15.4 mmol) was added and the mixture was heated at 80°C overnight. Compound **III‑8** precipitated from hot acetonitrile to yield a white solid. The solid was washed with acetonitrile and dried in air (0.898 g, 37% yield).Mp: 265-268°C. Found C, 71.9; H, 5.1; N, 13.9%. Calculated for $C_{24}H_{21}N_4Cl_1$: C, 71.9; H, 5.3; N, 14.0%. HRMS (ESI$^+$) calcd for $C_{24}H_{21}N_4^+$ [M-Cl] of m/z = 365.1761, found m/z = 365.1667. ^{1}H NMR (500 MHz, DMSO- d_6) δ = 8.50 (2H, d, Ar, J = 8.8 Hz), 8.04 (2H, d, Ar, J = 7.8 Hz), 7.96 (2H, s, Ar), 7.75 (4H, m, Ar), 7.63 (4H, m, Ar), 5.94 (4H, s, CH$_2$), 2.69 (3H, s, CH$_3$). ^{13}C NMR (125 MHz, DMSO- d_6) δ = 154.2 (Ar), 146.8 (Ar), 146.7 (Ar), 137.5 (Ar), 130.0 (Ar), 128.4 (Ar), 127.9 (Ar), 127.1 (Ar), 126.9 (Ar), 122.4 (Ar), 119.7(Ar), 52.4 (CH$_2$), 10.3 (CH$_3$). MS: m/z = 354.9 (theor for M$^+$ $C_{24}H_{21}N_4^+$ = 365.2).

Crystal data for **III‑8**: $C_{24}H_{21}N_4Cl_1$, $M = 400.90$, *triclinic*, $a = 7.2134(12)$ Å, $b = 11.3725(19)$ Å, $c = 12.465(2)$ Å, $\alpha = 70.199(2)°$, $\beta = 79.785(2)°$, $\gamma = 81.710(2)°$, $V = 943.0(3)$ Å^3, $T = 100(2)$ K, space group p ‑1, $Z = 2$, 7537 reflections measured, 3788 [R(int) = 0.0382]. The final R_1 values were 0.0565 ($I > 2\sigma(I)$). The final $wR(F^2)$ values were 0.1210 ($I > 2\sigma(I)$). The final R_1 values were 0.0854 (all data). The final $wR(F^2)$ values were 0.1400 (all data). A single crystal of **III‑8** was obtained by slow evaporation of a concentrated solution of **III‑8** dissolved in d$_6$-DMSO. Crystallographic information file (CIF) can be found on the Cambridge Crystallographic Data Center website (CCDC # 1503027)

3.6.4.10. Synthesis of 2-ethyl-1,3-bis(quinoline-2-ylmethyl)imidazolium chloride (**III‑9**)

2-Ethylimidazole (0.802 g, 8.34 mmol) dissolved in acetonitrile (13 mL) was combined with potassium hydroxide (0.518 g, 9.23 mmol) and stirred at 80°C for 30 minutes. 2-(Chloromethyl)quinoline hydrochloride (1.84 g, 8.59 mmol) and potassium hydroxide (0.499 g, 8.89 mmol) were added to the reaction mixture which was heated at 80°C overnight. The reaction mixture was filtered to remove a white solid (presumed to be potassium chloride). 2-(Chloromethyl)quinoline (1.58 g, 8.89 mmol) was added to the filtrate and the reaction mixture was heated at 80°C overnight. Compound **III‑9** precipitated from acetonitrile and was washed with diethyl ether and hot acetonitrile and dried to yield an off white solid (0.928 g, 27% yield).Mp: 225-226°C. Found C, 71.0; H, 5.7; N, 13.1%. Calculated for $C_{25}H_{23}N_4Cl_1$: C, 72.4; H, 5.6; N, 13.5%. Calculated for $C_{25}H_{23}N_4Cl_1 \cdot H_2O$: C, 69.4; H, 5.8; N, 12.9%. HRMS (ESI$^+$) calcd for $C_{25}H_{23}N_4^+$ [M-Cl] of m/z = 379.1923, found m/z =379.1887. ^{1}H NMR (500 MHz, DMSO- d_6) δ = 8.51 (2H,

d, Ar, J = 8.6 Hz), 8.03 (4H, m, Ar), 7.83 (2H, d, Ar, J = 8.6 Hz), 7.75 (2H, m, Ar), 7.87

(2H, d, Ar, J = 8.6 Hz), 7.62 (2H, m, Ar) 5.99 (4H, s, CH_2), 3.20 (2H, q, CH_2, J = 7.5 Hz),

0.96 (3H, t, CH_3, J = 7.5 Hz). ^{13}C NMR (125 MHz, DMSO- d_6) δ = 154.4 (Ar), 149.6 (Ar),

146.8 (Ar), 137.5 (Ar), 130.1 (Ar), 128.4 (Ar), 128.0 (Ar), 127.1 (Ar), 126.9 (Ar), 122.8

(Ar), 119.8 (Ar), 52.3 (CH_2), 16.7 (CH_2), 11.2 (CH_3). MS: m/z = 378.9 (theor for M^+

$C_{25}H_{23}N_4^+$ = 379.2).

Crystal data for **III‑9‑PF₆:** $C_{25}H_{23}F_6N_4P$, M = 524.44, Orthorhombic, a = 14.929(2)

Å, b = 14.230(2) Å, c = 22.128(4) Å, V = 4700.8(12) Å^3, T = 100(2) K, space group Pbca,

Z = 8, 25560 reflections measured, 4769 [R(int) = 0.0660]. The final R_1 values were 0.0481

($I > 2\sigma(I)$). The final $wR(F^2)$ values were 0.1068 ($I > 2\sigma(I)$). The final R_1 values were 0.0928

(all data). The final $wR(F^2)$ values were 0.1282 (all data). A single crystal of **III‑9‑PF₆**

was obtained by slow evaporation of a concentrated solution of **III‑9‑PF₆** dissolved in

acetonitrile and ethanol. Crystallographic information file (CIF) can be found on the

Cambridge Crystallographic Data Center website (CCDC # 1503028)

3.6.4.11. Synthesis of 2-propyl-1,3-bis(quinoline-2-ylmethyl)imidazolium chloride

(III‑10)

2-Propylimidazole (0.967 g, 8.78 mmol) dissolved in acetonitrile (13 mL) was

combined with potassium hydroxide (0.496 g, 8.84 mmol) and stirred for 30 minutes at

80°C. 2-(Chloromethyl)quinoline hydrochloride (1.28 g, 5.98 mmol) and potassium

hydroxide (0.343 g, 6.11 mmol) were added to the reaction mixture and stirred overnight

at 80°C. The reaction mixture was filtered hot to remove a white precipitate (presumed to

be potassium chloride). The volatiles were removed from the filtrate to yield a yellow oil. The oil was suspended in dichloromethane (30 mL) and washed with a basic aqueous solution (25 mL) and with water (2 x 25 mL). The organic layer was dried with magnesium sulfate. The volatiles were removed and the resulting oil was resuspended in acetonitrile (10 mL). 2-(Chloromethyl)quinoline (1.11 g, 6.25 mmol) was added and the reaction mixture was heated at 80°C overnight. Compound **III‑10** precipitated from hot acetonitrile and was washed with cold acetonitrile to yield a white solid (0.495 g, 19% yield). Mp: 177-178°C. Found C, 69.6; H, 6.0; N, 12.3%. Calculated for $C_{26}H_{25}N_4Cl_1$: C, 72.8; H, 5.9; N, 13.1%. Calculated for $C_{26}H_{25}N_4Cl_1 \cdot H_2O$: C, 69.9; H, 6.1; N, 12.5%. HRMS (ESI$^+$) calcd for $C_{26}H_{25}N_4^+$ [M-Cl] of m/z = 393.2074, found m/z = 393.2049. ^{1}H NMR (500 MHz, DMSO- d_6) δ = 8.51 (2H, d, Ar, J = 8.6 Hz), 8.04 (2H, d, Ar, J = 8.1 Hz), 7.98 (2H, s, Ar), 7.82 (2H, d, Ar, J = 8.3 Hz), 7.76 (2H, m, Ar), 7.65 (4H, m, Ar) 5.95 (4H, s, CH$_2$), 3.14 (2H, t, CH$_2$, J = 8.1 Hz), 1.38 (2H, m, CH$_2$) 0.75 (3H, t, CH$_3$, J = 7.3 Hz). ^{13}C NMR (125 MHz, DMSO- d_6) δ = 154.5 (Ar), 148.6 (Ar), 146.8 (Ar), 137.5 (Ar), 130.2 (Ar), 128.4 (Ar), 128.0 (Ar), 127.2 (Ar), 127.0 (Ar), 122.9 (Ar), 119.8 (Ar), 52.4 (CH$_2$), 24.6 (CH$_2$), 20.3 (CH$_2$), 13.3 (CH$_3$). MS: m/z = 392.9 (theor for M$^+$ $C_{26}H_{25}N_4^+$ = 393.2).

Crystal data for **III‑10•1.5(H$_2$O):** $C_{52}H_{56}N_8Cl_2O_3$, M = 911.94, *Triclin*ic, a = 7.3455(3) Å, b =10.0987(4) Å, c = 16.9742(6) Å, α = 79.406(2)°, β = 78.845(2)°, γ = 69.336(2)°, V = 1146.69(8) Å^3, T = 100(2) K, space group P-1, Z = 1, 6761 reflections measured, 4268 [R(int) = 0.0239]. The final R_1 values were 0.0569 ($I > 2\sigma(I)$). The final $wR(F^2)$ values were 0.1528 ($I > 2\sigma(I)$). The final R_1 values were 0.0888 (all data). The final $wR(F^2)$ values were 0.1902 (all data). A single crystal of **III‑10•1.5(H$_2$O)** was obtained by

slow evaporation of a concentrated solution of **III‑10** dissolved in water. Crystallographic information file (CIF) can be found on the Cambridge Crystallographic Data Center website (CCDC # 1503029)

3.6.4.12. Synthesis of 2-butyl-1,3-bis(quinoline-2-ylmethyl)imidazolium chloride (**III‑11**)

2-Butylimidazole (0.927 g, 7.46 mmol) dissolved in acetonitrile (15 mL) was combined with potassium hydroxide (0.439 g, 9.23 mmol) and stirred at 80°C for 30 minutes. 2-(Chloromethyl)quinoline hydrochloride (1.27 g, 5.93 mmol), and potassium hydroxide (0.335 g, 5.97 mmol) were added to the reaction mixture which was heated at 80°C overnight. The mixture was filtered to remove a white solid (presumed to be potassium chloride) and the volatiles were removed from the filtrate to yield a yellow oil. The oil was diluted with dichloromethane (30 mL) and washed with a basic aqueous solution (2 x 25 mL) and water (25 mL). The organic layer was dried with magnesium sulfate and the volatiles were removed. The resulting yellow oil was resuspended in acetonitrile and 2-(chloromethyl)quinoline (1.14 g, 6.42 mmol) was added. The reaction mixture was heated overnight at 80°C. Compound **III‑11** precipitated from hot acetonitrile and was washed with cold acetonitrile (0.238 g, 9% yield).Mp: 196-198°C. Found C, 69.5; H, 6.3; N, 12.1%. Calculated for $C_{27}H_{27}N_4Cl_1$: C, 73.2; H, 6.1; N, 12.7%. Calculated for $C_{26}H_{25}N_4Cl_1 \cdot H_2O$: C, 70.4; H, 6.3; N, 12.2%. HRMS (ESI$^+$) calcd for $C_{27}H_{27}N_4^+$ [M-Cl] of m/z = 407.2230, found m/z = 407.2199. ^{1}H NMR (500 MHz, DMSO- *d6*) δ = 8.51 (2H, d, Ar, J = 8.6 Hz), 8.04 (2H, d, Ar, J = 8.1 Hz), 7.97 (2H, s, Ar), 7.83 (2H, d, Ar, J = 8.3

Hz), 7.77 (2H, m, Ar), 7.64 (4H, m, Ar) 5.93 (4H, s, CH$_2$), 3.12 (2H, q, CH$_2$, J = 7.9 Hz), 1.24 (2H, m, CH$_2$), 1.14 (2H, m, CH$_2$), 0.51 (3H, t, CH$_3$, J = 7.2 Hz). ^{13}C NMR (125 MHz, DMSO- d_6) δ = 154.4 (Ar), 148.7 (Ar), 146.8 (Ar), 137.5 (Ar), 130.1 (Ar), 128.4 (Ar), 128.0 (Ar), 127.2 (Ar), 127.0 (Ar), 122.9 (Ar), 119.8 (Ar), 52.5 (CH$_2$), 28.4 (CH$_2$), 22.8 (CH$_2$), 21.5 (CH$_2$), 13.1 (CH$_3$). MS: m/z = 406.9 (theor for M$^+$ C$_{27}$H$_{27}$N$_4$$^+$ = 407.2).

Crystal data for **III‑11-PF$_6$•1.5(H$_2$O):** C$_{54}$H$_{60}$F$_{12}$N$_8$O$_3$P$_2$, M = 1159.04, Monoclinic, a = 15.1142(7) Å, b = 48.741(2) Å, c = 7.3043(3) Å, V = 5345.1412) Å^3, T = 100(2) K, space group P2$_{1/c}$, Z = 4, 53996 reflections measured, 10736 [R(int) = 0.0592]. The final R_1 values were 0.0600 ($I > 2\sigma(I)$). The final $wR(F^2)$ values were 0.1274 ($I > 2\sigma(I)$). The final R_1 values were 0.0913 (all data). The final $wR(F^2)$ values were 0.1433 (all data). A single crystal of **III‑11-PF$_6$•1.5(H$_2$O)** was obtained by slow evaporation of a concentrated solution of **III‑11** dissolved in water. Crystallographic information file (CIF) can be found on the Cambridge Crystallographic Data Center website (CCDC # 1503030)

3.6.4.13. Synthesis of 2-phenyl-1,3-bis(quinoline-2-ylmethyl)imidazolium chloride

(III‑12)

2-Phenylimidazole (1.00 g, 6.94 mmol) dissolved in acetonitrile (15 mL) was combined with potassium hydroxide (0.430 g, 7.66 mmol) and was stirred at 80°C for 30 minutes. 2-(Chloromethyl)quinoline (1.23 g, 6.92 mmol) was added and the mixture was stirred overnight at 80°C. The reaction mixture was filtered to remove a white precipitate (presumed to be potassium chloride) and the volatiles of the filtrate were removed to form an oil. The oil was suspended in dichloromethane (25 mL) washed with a basic aqueous

solution (25 mL) and water (2 x 25 mL). The organic layer was dried with sodium sulfate

and the volatiles were removed to form an oil. The oil was diluted with acetonitrile (15

mL) and combined with 2-(chloromethyl)quinoline (1.32 g, 7.43 mmol) and stirred

overnight at 80°C. The reaction was cooled to room temperature and diethyl ether was

added to induce precipitation of **III‑12**. A white microcrystalline product was filtered and

dried to yield **III‑12** (1.03 g, 32% yield).Mp: 161-164°C. Found C, 72.5; H, 5.2; N, 11.6%.

Calculated for $C_{29}H_{23}N_4Cl_1$: C, 75.2; H, 5.0; N, 12.1%. Calculated for $C_{26}H_{25}N_4Cl_1 \bullet H_2O$:

C, 72.4; H, 5.2; N, 11.7%. HRMS (ESI$^+$) calcd for $C_{29}H_{23}N_4^+$ [M-Cl] of m/z = 427.1917,

found m/z = 427.1999. ^{1}H NMR (500 MHz, DMSO- d_6) δ = 8.40 (2H, d, Ar, J = 8.3 Hz),

8.24 (2H, s, Ar), 8.00 (2H, d, Ar, J = 7.6), 7.89 (2H, d, Ar, J = 8.6 Hz), 7.78 (2H, m, Ar),

7.63 (4H, m, Ar), 7.49 (1H, m, Ar), 7.46 (2H, d, Ar, J = 8.6), 7.39 (2H, m, Ar), 5.76 (4H,

s, CH$_2$). ^{13}C NMR (125 MHz, DMSO- d_6) δ = 154.0 (Ar), 146.7 (Ar), 146.3 (Ar), 137.3

(Ar), 132.1 (Ar), 130.3 (Ar), 130.1 (Ar), 128.9 (Ar), 128.4 (Ar), 127.9 (Ar), 127.1 (Ar),

126.9 (Ar), 123.6 (Ar), 121.3 (Ar), 119.5 (Ar), 52.9 (CH$_2$). MS: m/z = 426.9 (theor for M$^+$

$C_{29}H_{23}N_4^+$ = 427.2).

CHAPTER IV

SYNTHESIS, CHARACTERIZATION, IN VITRO SAR STUDY, AND

PRELIMINARY TOXICITY EVALUATION OF NAPHTHYLMETHYL

SUBSTITUTED BIS-IMIDAZOLIUM SALTS

4.1. Introduction

Cancer is expected to kill over one-half million Americans in the year 2016, accounting for one in every four deaths, with heart disease as the only more common cause of death.[120] Lung cancer is the leading cause of all cancer related deaths, accounting for one in every four deaths due to cancer. The treatment for lung cancer depends on the stage and type of cancer. The two major categories of lung cancer include small cell and non-small cell lung cancers (NSCLC), the latter of which makes up 83% of lung cancer cases. Treatment for NSCLC may include surgery, radiation, chemotherapy (first line treatments usually include a combination of platinum drugs i.e. cisplatin with a third-generation compound such as docetaxel or paclitaxel),[130] and/or a targeted therapy such as Cetuximab that competitively binds to the epidermal growth factor receptor (EGF-R) thereby preventing interaction with the epidermal growth factor (EGF) ligands.[131] Although therapies exist, the five-year survival rate for NSCLC is only

21%,[120] which means that these therapies are not highly effective and new forms of treatment are necessary to treat this devastating disease.

Imidazolium salts, such as **I-464** (Figure IV-1), are a class of compounds that have received significant attention in the literature for their anti-cancer properties against NSCLC.[4,20,31,42,43,46,49,50,52,82,127,132] Many of these compounds have IC_{50} values in the low micromolar and some in the nanomolar range against a variety of NSCLC (**I-464** had IC_{50} values of 4 µM (NCI-H460), 6 µM (NCI-H1975), and 9 µM (HCC827)).
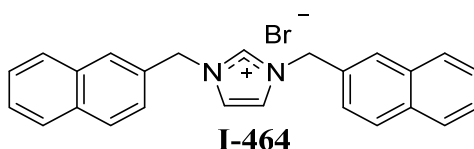
I-464

Figure IV-1. Structure of the naphthylmethyl-substituted imidazolium salt **I-464**.

The anti-cancer properties of these imidazolium salts are directly related to substituents at all positions of the imidazole ring. This applies to imidazolium salts with naphthylmethyl-substituents, such as **I-464**, and those with other substituents at the N^1 and N^3 positions such as a study done by Malhotra with a methyl group at the N^1 position and aliphatic substituents ranging from one to fourteen carbons at the N^3 position.[20] Those with one to seven carbons at the N^3 position were inactive; whereas, those with eight to fourteen carbons at the N^3 position were active as determined by the National Cancer Institute's (NCI) in vitro 60-human tumor cell line screen. Unfortunately, highly lipophilic derivatives have minimal solubility in aqueous solution and; therefore, are limited in their clinical potential.[82] Bis-imidazolium salts (Figure IV-2) have the advantage of two positively charged moieties to aid in increasing aqueous solubility.

196
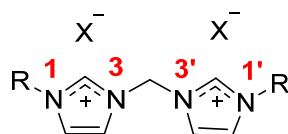
Figure IV-2. General depiction of bis-imidazolium salt.

Bis-imidazolium salts have been investigated for their ability to inhibit human galactosyltransferase and glycosyltransferase enzymes for their potential as anti-cancer drugs.[133] They are also precursors to metal-NHC complexes that have been investigated for a variety of applications including transmetallation agents and as catalysts.[134,135] Bis-imidazolium salts with naphthylmethyl substituents at the N^1 and $N^{1'}$ positions are structurally similar to the depsipeptide echinomycin (Figure IV-3), with planar, aromatic groups separated by a linking moiety. Echinomycin is a bis-intercalator considering it can intercalate between DNA base pairs with both quinoxaline units.[136] This depsipeptide has been investigated for its ability to bind to a sequence of DNA that codes for the hypoxia inducible factor-1.
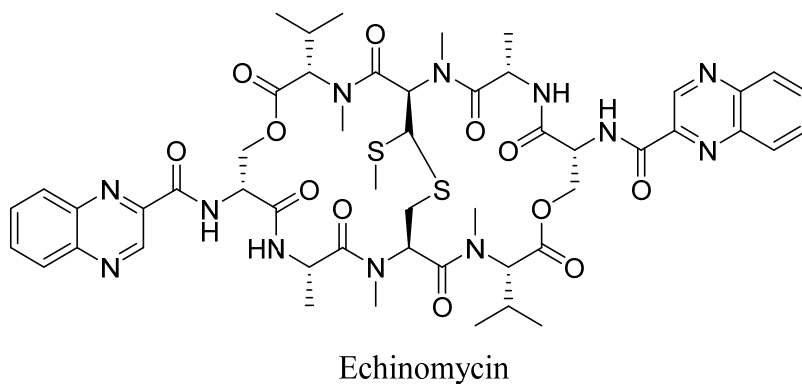
Echinomycin

Figure IV-3. Structure of the natural depsipeptide echinomycin.

Presented herein is a series of bis-imidazolium salts with naphthylmethyl-substituents at both the N^1 and $N^{1'}$ positions. The imidazole cores are bridged by alkyl chains ranging in length from a methyl to dodecyl group. This series of compounds was designed to: (1) create a SAR relating the length of the alkyl chain to the anti-cancer properties of each compound, (2) determine the solubility of doubly charged compounds and evaluate the effects of longer alkyl chains, and (3) to understand possible interactions with DNA and determine if these bis-imidazolium salts would behave similarly to echinomycin considering their structural similarities.

4.2. Results and discussion

4.2.1. Synthesis and characterization

Compound **IV‑1** was synthesized by reacting 2.2 molar equivalents of 2-(bromomethyl)naphthalene with di(imidazole-1-yl)methane dissolved in acetonitrile (Equation IV-1). The solution was refluxed overnight and produced a white precipitate, **IV‑1**. A mixture of water and ethanol (1:6) was used to recrystallize **IV‑1**.
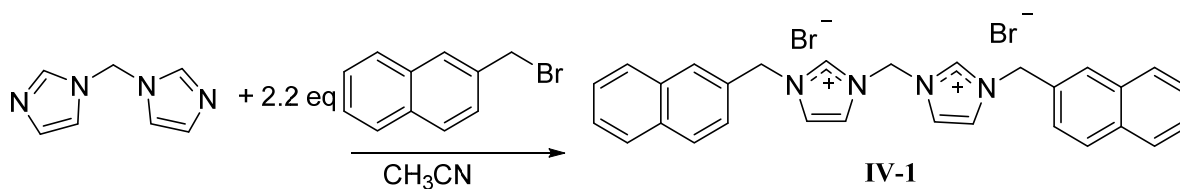
Equation IV-1. Synthesis of **IV‑1**.

198

1-(Naphthalen-2-ylmethyl)imidazole was synthesized by published procedures and used as starting material for the synthesis of **IV‑2**‑**IV‑12**. The appropriate di-bromoalkane was reacted with 2.2 molar equivalents of 1-(naphthalen-2-ylmethyl)imidazole to ensure no mono-cationic species would result. The di-bromoalkane was added to a solution of 1-(naphthalen-2-ylmethyl)imidazole in acetonitrile and refluxed overnight to synthesize **IV‑2**‑**IV‑12** (Equation IV-2). The workup varied slightly for each compound. Reactions to produce **IV‑2**‑**IV‑7** and **IV‑10** resulted in a precipitate from the refluxing acetonitrile that could be filtered and collected. Compounds **IV‑3**, **IV‑4**, **IV‑6**, and **IV‑7** were washed with cold acetonitrile to remove any unreacted starting materials. Compound **IV‑2** was washed with acetone, **IV‑5** was recrystallized from a solution of water and ethanol (1:6), whereas **IV‑10** was washed with acetone and diethyl ether. Compounds **IV‑8**, **IV‑9**, **IV‑11**, and **IV‑12** remained soluble in acetonitrile after cooling to room temperature. Compound **IV‑8** and **IV‑12** precipitated after removing the volatiles by rotary evaporation leaving white powders that were recrystallized from a water and ethanol mixture (1:5) in the case of **IV‑8** and dried to yield **IV‑12**. The crystals were washed with cold acetone to purify **IV‑8**. Compounds **IV‑9** and **IV‑11** were isolated after the volatiles were removed from the reaction mixture leaving an oil which was dissolved in water, washed with diethyl ether, and triturated with dichloromethane. Compounds **IV‑9** and **IV‑11** were difficult to isolate because they became oils under atmospheric conditions until they were isolated using a glove bag with a nitrogen atmosphere. Yields ranges from 16% to 87% with **IV‑1**, **IV‑3**, **IV‑4**, **IV‑6**, and **IV‑8** having high yields (87%, 84%, 76%, 77%, and 83%

respectively); **IV‑5**, **IV‑7**, **IV‑9**, **IV‑10**, and **IV‑12** having moderate yields (52%, 64%,

53%, and 49% respectively); and **IV‑2** and **IV‑11** having poor yields (16% and 18%

respectively).

n =	compound
2	**IV-2**
3	**IV-3**
4	**IV-4**
5	**IV-5**
6	**IV-6**
7	**IV-7**
8	**IV-8**
9	**IV-9**
10	**IV-10**
11	**IV-11**
12	**IV-12**
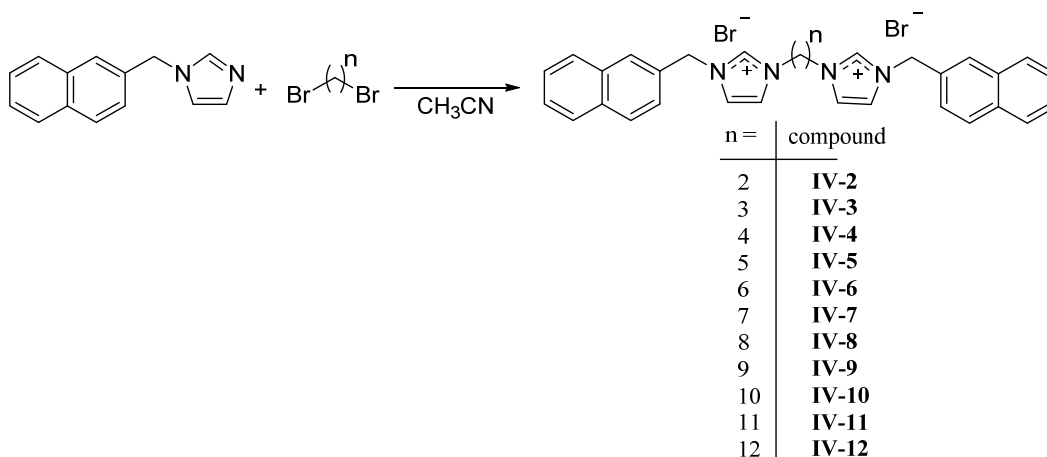
Equation IV-2. Synthesis of **IV‑2‑IV‑12**.

All compounds were characterized by ^{1}H NMR, ^{13}C NMR, and melting point

analysis while several were characterized by X-ray crystallography and HRMS. Two

singlet resonances in the ^{1}H NMR spectra most notably indicated the formation of the bis-

imidazolium salt (Figure IV-4). The first singlet resonance in each spectra ranged from

9.32 ppm to 9.70 ppm corresponding to the proton at the C^2 position of each imidazole ring

of the bis-imidazolium salt. Because the molecule is symmetric the proton on each

imidazole is chemically identical. This proton is shifted significantly downfield when

compared to the other protons in the spectra due to the positive charge of the imidazole

ring. The second most notable resonance suggesting the formation of the bis- imidazolium

salt had chemical shifts that ranged from 5.57 ppm to 5.68 ppm. The chemical shift of these

resonances were consistent with those of the methylene bridging the imidazole ring to the

naphthalene moiety.[4,82,96] Integrations of both distinctive resonances were consistent with the structure of the compound. A second resonance appeared in the ^{1}H NMR spectra for the crude products of **IV‑1**, **IV‑5**, and **IV‑8** in both regions discussed above. These impurities most likely corresponded to the mono-cationic species, indicating the reaction had not gone to completion. To remove the impurities, **IV‑1**, **IV‑5**, and **IV‑8** were recrystallized. The melting point analysis of **IV-1-IV-7**, **IV-10**, and **IV-12** revealed that these compounds went through a phase transition, possibly forming liquid crystals, instead of melting how other imidazolium salt derivatives did. However, experiments to confirm this were not yet performed. Also, the high-resolution mass spectrometry data suggested the parent ion was only singly charged, versus the doubly charged system we would expect to see. The C^2 proton could be easily removed to form a carbene at one imidazole leaving the second imidazole positively charged and the species that was observed.
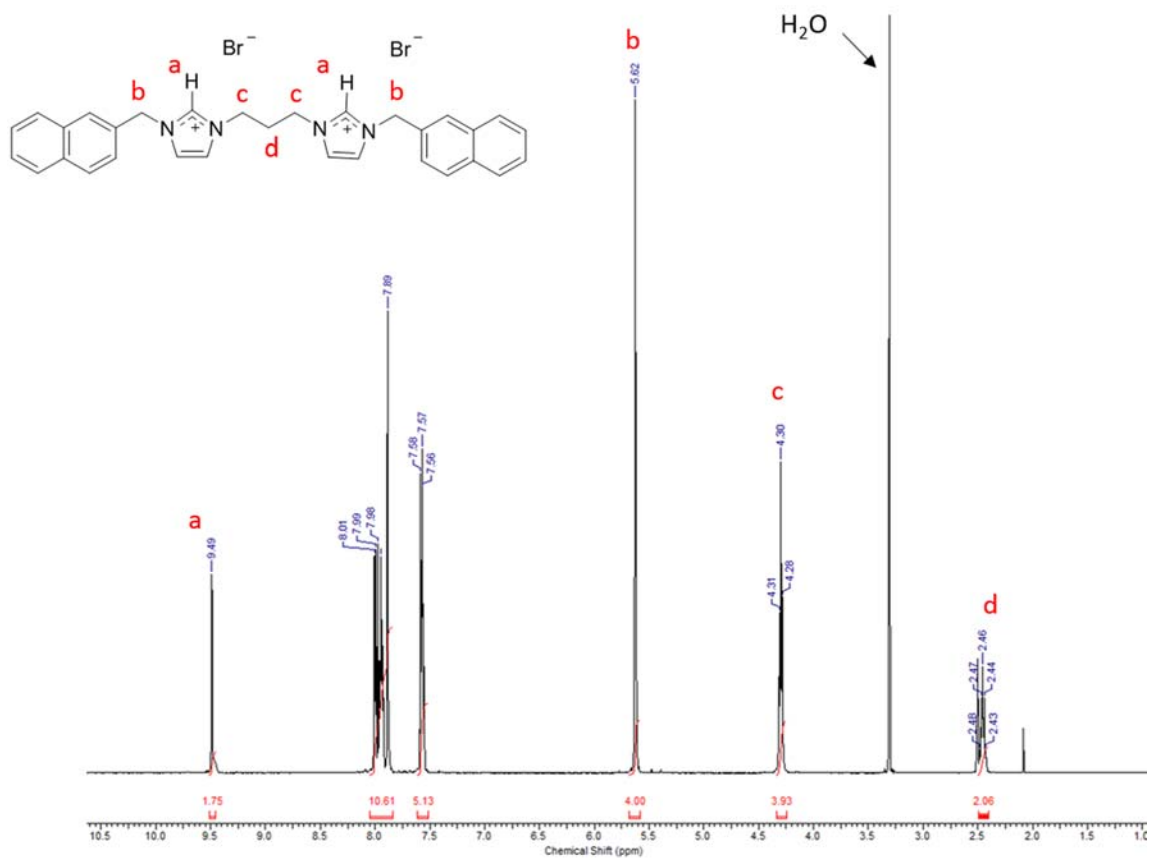
Figure IV-4. ^{1}H NMR spectrum of **IV-III**.

Compounds **IV‑2**, as the hexafluorophosphate salt (**IV‑2‑PF₆**), **IV‑3‑IV‑5**, **IV‑7**, as the hexafluorophosphate salt (**IV‑7‑PF₆**), and **IV‑8** were characterized by single crystal X-ray crystallography. Compound **IV‑2‑PF₆** was obtained by adding ammonium hexafluorophosphate to a solution of **IV‑2** dissolved in water. Once converted to the hexafluorophosphate salt, **IV‑2‑PF₆** is insoluble in water and precipitated from solution to form a white powder which was collected by filtration. A single crystal of **IV‑2‑PF₆** suitable for X-ray crystallography was obtained by slow evaporation of a solution of the white solid in a mixture of acetonitrile, chloroform, and 2-propanol (Figure IV-5). Single

crystals of **IV‑3•H₂O**, **IV‑4•2(H₂O)**, and **IV‑5•H₂O** suitable for X-ray crystallography were grown from concentrated solutions of the compound dissolved in ethyl acetate and tetrahydrofuran (**IV‑3**), methanol (**IV‑4**), and water (**IV‑5**) (Figure IV-6, Figure IV-7, and Figure IV-8 respectively). Compounds **IV‑3** and **IV‑5** co-crystallized with one water molecule and **IV‑4** co-crystallized with two water molecule. Compound **IV‑7** was converted to the hexafluorophosphate salt by the same route **IV‑2** was converted to the hexafluorophosphate salt. A single crystal of **IV‑7‑PF₆** suitable for X-ray analysis was obtained by slow evaporation of **IV‑7‑PF₆** in a concentrated solution of chloroform. A single crystal of **IV‑8** was obtained by slow evaporation of **IV‑8** dissolved in a mixture of acetonitrile, water, and diethylether.
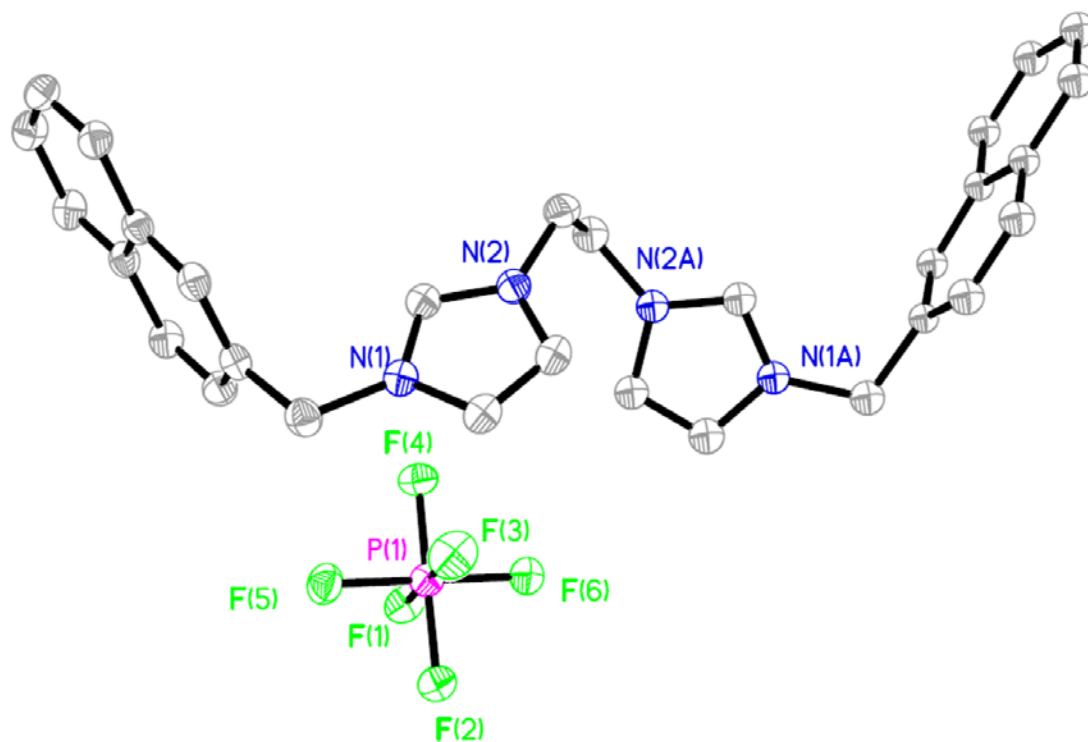
Figure IV‑5. Thermal ellipsoid plot of **IV‑2‑PF₆** with thermal ellipsoids drawn to the 50% probability level. Hydrogen atoms, carbon labels, and the second PF₆⁻ anion were removed for clarity.
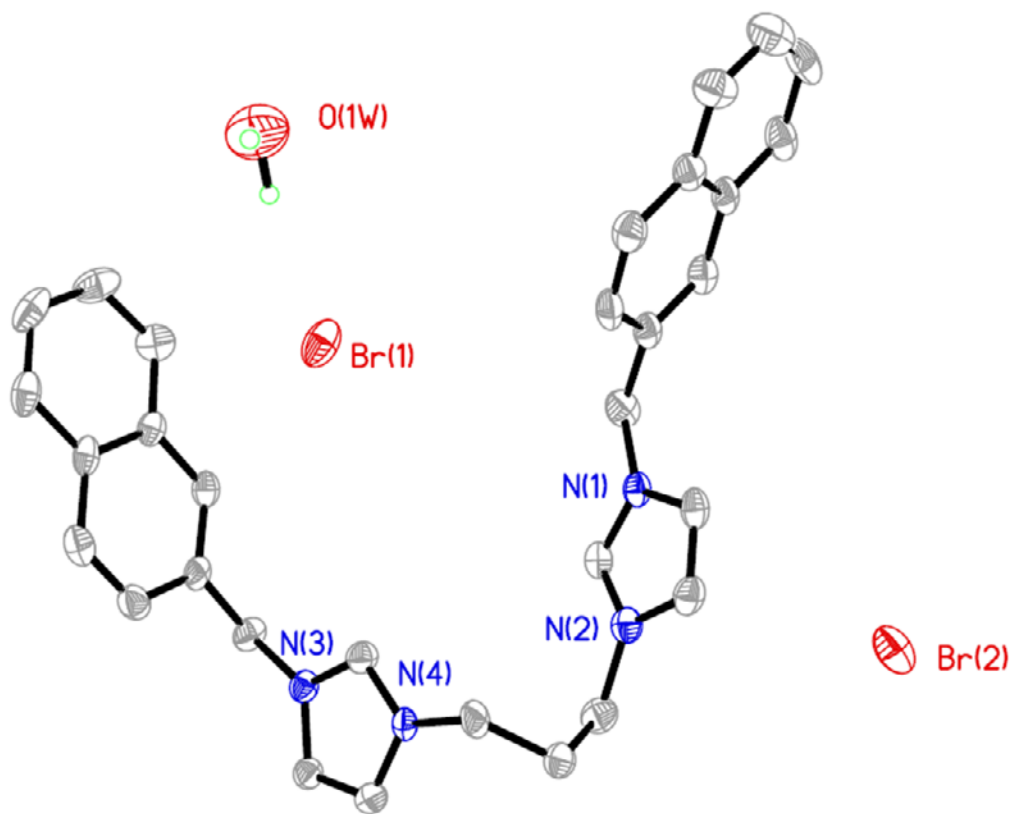
Figure IV-6. Thermal ellipsoid plot of **IV‑3•H₂O** with thermal ellipsoids drawn to the 50% probability level. Hydrogen atoms (except for those on the water) and carbon labels were removed for clarity.
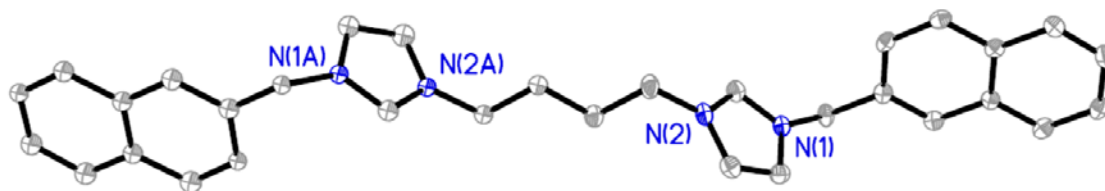
Figure IV-7. Thermal ellipsoid plot of **IV‑4•2(H₂O)** with thermal ellipsoids drawn to the 50% probability level. Hydrogen atoms, carbon labels, water solvent molecules, and bromide anions were removed for clarity.
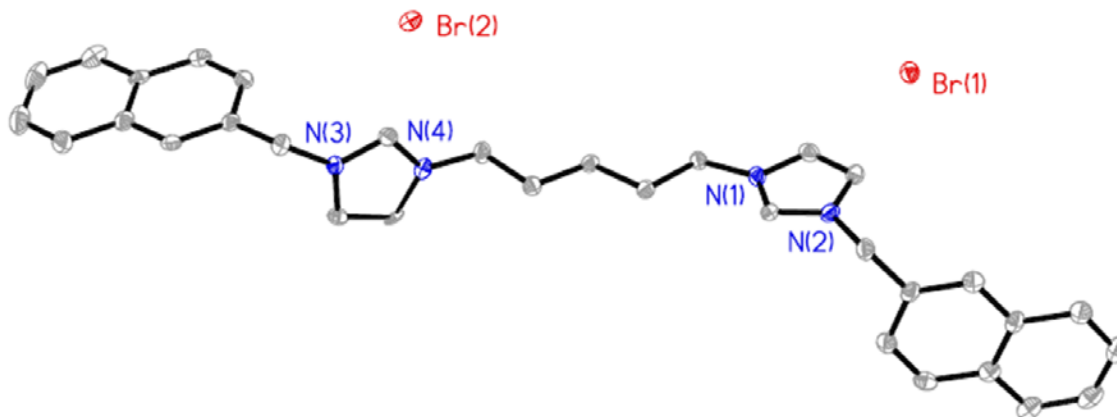
Figure IV-8. Thermal ellipsoid plot of **IV‑5•H₂O** with thermal ellipsoids drawn to the 50% probability level. Hydrogen atoms, carbon labels, and water solvent molecule were removed for clarity.
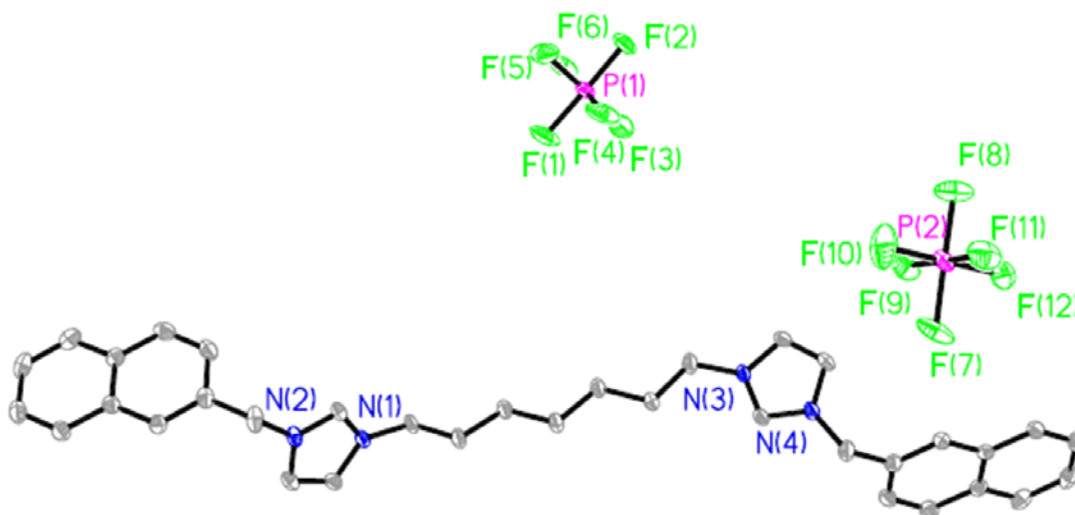
Figure IV-9. Thermal ellipsoid plot of **IV‑7‑PF₆** with thermal ellipsoids drawn to the 50% probability level. Hydrogen atoms and carbon labels were removed for clarity.
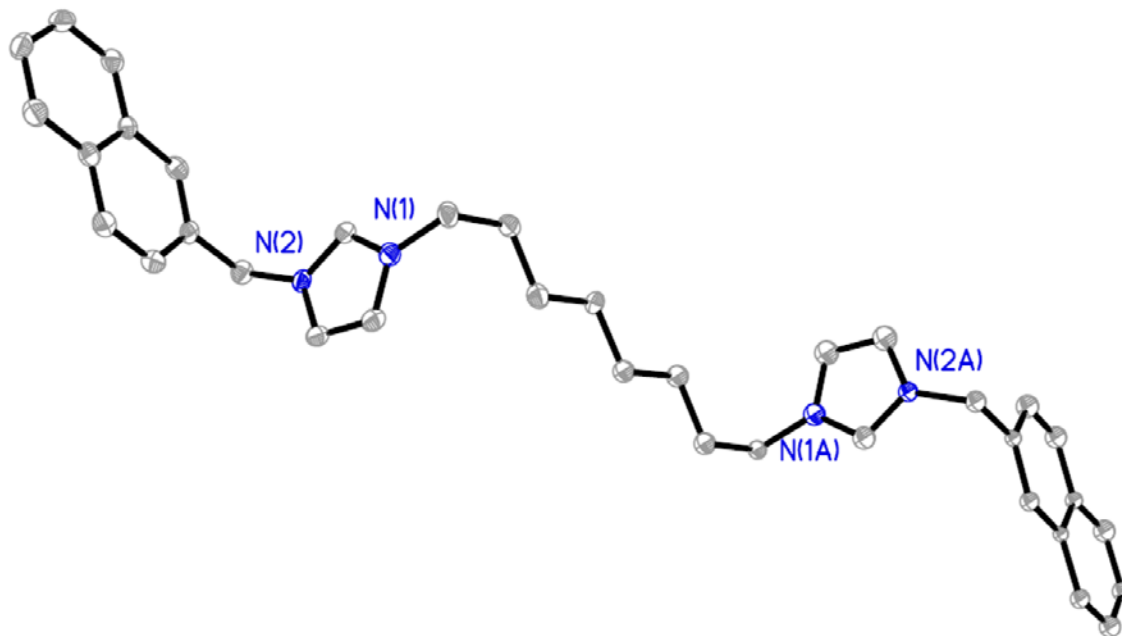
Figure IV‑10. Thermal ellipsoid plot of **IV‑8** with thermal ellipsoids drawn to the 50% probability level. Hydrogen atoms, carbon labels, and disordered water solvent molecules and bromide anions were removed for clarity.

4.2.2. In vitro evaluation

4.2.2.1. MTT assay

The solubility of each compound in aqueous solution was determined prior to evaluating their anti-cancer properties. The solubilities of compounds **IV-1-IV-7**, **IV-10**, and **IV-12** are described in Table IV-1. By observing the structure of each compound, one would predict that **IV-1** would have the highest aqueous solubility and **IV-12** would have the lowest solubility; however, a clear pattern was not established with this series of

compounds. Compound **IV-7** had the highest solubility at 5.2 mg/mL; whereas, the less

lipophilic derivatives **IV-1**, **IV-4**, and **IV-5** all had solubilities less than 2 mg/mL.

Table IV-1. Solubility information for compounds **IV-1-IV-7**, **IV-10**, and **IV-12**.

Compound	Aqueous solubility (mg/mL)
IV-1	< 2
IV-2	4.8
IV-3	4.8
IV-4	< 2
IV-5	< 2
IV-6	3.4
IV-7	5.2
IV-8	n/a
IV-9	n/a
IV-10	3.3
IV-11	n/a
IV-12	< 2

The anti-cancer properties of **IV‑1‑IV‑8**, **IV‑10**, and **IV‑12** were evaluated

against several NSCLC cell lines (NCI-H460, NCI-H1975, HCC827, and A549) to

determine their IC_{50} values (concentration that inhibits 50% growth of cells when

compared to control cells). This series of compounds was synthesized to establish a SAR

of naphthylmethyl-substituted bis-imidazolium salts with increasing alkyl chain lengths

bridging the two imidazole cores. Previously published anti-cancer studies of imidazolium

salts have suggested that lipophilicity increases anti-cancer activity;[4,82] herein, we have a

series of compounds with specific differences in lipophilicity between each derivative. The

original goal in synthesizing this series of compounds was to find the ideal chain length to

mimic the interaction of echinomycin with DNA as a bis-intercalator, and determine if the

alkyl chain length has more impact on anti-cancer properties than just the lipophilicity. However, the cellular target of bis-imidazolium salts has yet to be determined; therefore it is not certain that these compounds will have an interaction with DNA. To obtain IC_{50} values, cells were plated at 5,000-7,000 cells per well, depending on the cell line, and allowed to adhere to 96-well plates overnight. Cells were exposed to compounds **IV‑1‑IV‑8**, **IV‑10**, and **IV‑12** at concentrations of 1, 4, 16, and 32 μM for 72 hours at which time the optional MTT assay was utilized. Results were compared to the well-known chemotherapeutic agent cisplatin and the previously published imidazolium salt **I-464**.[4]

To prepare the aforementioned dilutions of each compound in growth medium, all compounds were dissolved in DMSO and diluted with water to prepare stock solutions at a concentration of 1 mM. All compounds except for **IV‑1** and **IV‑5** were completely soluble in the DMSO/water solution. Compounds **IV‑1** and **IV‑5** were mostly soluble and produced clear solutions with minor impurities. Each compound was further diluted into growth medium to the final testing concentrations. The maximum amount of DMSO in the testing solution was 0.032% (v/v); therefore, DMSO was not added to the growth medium of negative control cells. The stock solution of cisplatin was prepared by stirring cisplatin in water at room temperature for several hours to completely solubilize the compound.

The resulting IC_{50} values from the MTT assay performed on **IV‑1‑IV‑8**, **IV‑10**, **IV‑12**, cisplatin, and previously published results for **I-464** are summarized in Table IV-2. As seen previously the results follow the general trend of increased anti-proliferative effects being directly related to an increase in lipophilicity. Compound **IV‑1**, with the shortest alkyl chain linker, has the worst anti-cancer properties with IC_{50} values above the

testing concentration for three of the four cell lines (16 µM for H460 as the only measured value). Compound **IV‑12**, the derivative with the longest alkyl chain (dodecyl) and therefore the most lipophilic, had the best anti-cancer activity with IC$_{50}$ values < 1 µM for three of the four cell lines tested. These results are consistent with SAR studies performed previously that the lipophilicity of imidazolium salts is essential for anti-cancer activity against NSCLC.

Table IV-2. Table of IC50 values for **IV‑1‑IV‑8**, **IV‑10**, **IV‑12**, cisplatin, and **I-464**.

Compound	IC$_{50}$ Value (µM)			
	NCI-H460	NCI-H1975	HCC827	A549
IV‑1	16	> 30	> 30	> 30
IV‑2	14	> 30	> 30	> 30
IV‑3	20	> 30	> 30	22
IV‑4	4	11	13	4
IV‑5	2	12	> 30	4
IV‑6	2	6	12	< 1
IV‑7	3	3	10	2
IV‑8	2	3	15	2
IV‑10	< 1	2	7	< 1
IV‑12	< 1	< 1	4	< 1
Cisplatin	6	3	9	5
I-464	4	6	9	n/a

4.2.2.2. NCI-60 human tumor cell line screen

The national Cancer Institute's (NCI) Developmental Therapeutics Program (DTP) tested **IV‑1‑IV‑7**, **IV‑10**, and **IV‑12** in their NCI-60 human tumor cell line screen one-dose assay. There are nine NSCLC lung cancer cell lines included in the 60-human tumor

cell line screen and only results from these cell lines are discussed. Full experimental details can be found on the DTP's website (https://dtp.cancer.gov/discovery_development/ nci-60/methodology.htm). Briefly, cells are seeded at a concentration depending on their doubling rate and incubated for 24 hours. The experimental drug is then exposed to the cells at one dose (10 μM) for 48 hours at which time growth percentage values are determined. Results are given as a single value, growth percentage, relative to the initial cell population. A positive growth percentage value means there were more cells present at the end of the experiment than at the beginning. A negative growth percentage values means the compound was lethal at the concentration tested and less cell were present at the end of the experiment than at the beginning.

Results from the NCI-60 human tumor cell line screen one-dose assay against the nine NSCLC cell lines tested were consistent with IC_{50} values discussed above from the MTT assay performed in our lab (Table IV-3 and Table IV-4). The highest growth percentage values were from cells exposed to **IV‑1** and **IV‑2** with an average growth percentage of 79.55% and 80.88% respectively. As the alkyl chain lengthens from **IV‑2** to **IV‑12**, the average growth percentage values lower, meaning the compound was more effective at inhibiting the growth or was lethal against the NSCLC cell lines tested as in the case of **IV‑12**. Compound **IV‑12** was lethal against all NSCLC lung cancer lines tested and was the most effective compound tested with an average growth rate of negative 60.87%. The anti-cancer activity of this series of bis-imidazolium salts is directly related to the alkyl chain length when considering the trend the average growth rate follows. The SAR established from the NCI-60 human tumor cell line screen further enhances the

211

existing SARs described with imidazolium salts substituted at every position on the imidazole and benzimidazole ring with functional groups of varying hydrophilicities and lipophilicities.[4,82,83,98]

Table IV-3. Growth percentage values for **IV-1**-**IV-5** from the NCI-60 human tumor cell line screen one-dose assay.

Compound	A549/ATCC	EKVX	HOP-62	HOP-92	NCI-H226	NCI-H23	NCI-H322M	NCI-H460	NCI-H522	Average
		Growth %								
IV-1	70.78	89.40	84.22	66.99	92.61	88.32	87.60	85.07	50.99	79.55
IV-2	64.07	91.44	85.95	79.18	82.65	88.91	86.40	85.63	63.70	80.88
IV-3	62.32	82.70	67.18	67.47	81.89	77.85	84.40	75.28	56.58	72.85
IV-4	49.31	58.07	54.76	68.41	82.03	44.04	90.05	38.24	43.40	58.70
IV-5	41.68	47.15	57.01	66.04	72.59	45.32	86.17	30.48	38.74	53.91

212

Table IV-4. Growth percentage values for **IV‑6**, **IV‑7**, **IV‑10**, and **IV‑12** from the NCI-60 human tumor cell line screen one-dose assay.

Compound	Growth %									Average
	A549/ATCC	EKVX	HOP-62	HOP-92	NCI-H226	NCI-H23	NCI-H322M	NCI-H460	NCI-H522	
IV-6	38.64	37.30	55.83	59.93	69.59	30.46	76.24	24.59	33.07	47.29
IV-7	26.68	27.92	32.56	n/a	59.45	14.44	58.62	14.63	5.87	30.02
IV-10	18.55	13.71	-4.86	-23.56	39.46	5.67	34.54	11.00	-72.29	2.47
IV-12	-74.19	-62.61	-58.01	-68.19	-42.06	-80.31	-18.39	-69.88	-74.23	-60.87

The NCI's DTP also tested **IV‑10** and **IV‑12** in their five-dose assay considering they were lethal in a certain number of cell lines in the one-dose assay. These were the only

compounds that fulfilled the DTP's requirement and tested in the five-dose assay. The experimental procedures are the same for the five-dose assay as for the one-dose assay except the cells are exposed to the experimental drugs at five concentrations instead of one. Compound **IV‑10** was exposed to cells at 100 µM, 10 µM, 1 µM, 100 nM, and 10 nM; whereas, **IV‑12** was exposed to cells at 25 µM, 2.5 µM, 250 nM, 25 nM, and 2.5 nM. Results are given as three different values for the five-dose assay: (1) GI50 or growth inhibition of 50% of cells relative to control cells, (2) TGI or total growth inhibition, and (3) LC50 or lethal concentration of 50% of cells relative to control cells.

Results from the five-dose assay for **IV‑10** and **IV‑12** are summarized in Table IV-5 and growth percentage plots of the NSCLC cell lines exposed to **IV‑10** and **IV‑12** are shown in Figure IV-11 and Figure IV-12. Compound **IV‑10** had GI50 values in the range of 0.396 µM to 3.55 µM, TGI values ranging from 1.94 µM to 18.4 µM and LC50 values ranging from 15.2 µM to 58.4 µM. A value was not recorded with the NCI-H226 cell line because the LC50 concentration was higher than the testing conditions. A value was also not recorded for the A549/ATCC cell line because the growth percentage was below the GI50 mark at 10 nm then was above the GI50 mark at 100 nm and again came below the GI50 mark at 1 µM. From observing the graph, the growth percentage looks virtually the same for all three concentrations but the DTP did not assign a value based off the described pattern. Compound **IV‑12** had GI50 values ranging from 0.470 µM to 0.984 µM (all in the nanomolar range), TGI values from 1.25 µM to 5.52 µM, and LC50 values ranging from 7.29 µM to 14.6 µM. A LC50 value was not recorded for the NCI-H226 cell line because the LC50 concentration was above the testing threshold. On average, **IV‑12**

214

was again more active than **IV‑10** which was expected due to the differences in lipophilicity. All the GI50 values were in the nanomolar range for **IV‑12** again confirming the high anti-cancer activity of this derivative against NSCLC. The high anti-cancer activities of these compounds make them viable candidates for future studies including in vivo experiments to determine the cellular target.

Table IV-5. Results from the NCI-60 human tumor cell line screen five-dose assay for **IV‑10** and **IV‑12**. Results are given as GI50, TGI, and LC50 values.

Cell Line	Concentration (µM)					
	IV‑10			**IV‑12**		
	GI50	TGI	LC50	GI50	TGI	LC50
A549/ATCC	n/a	13.3	50.3	0.744	3.57	14.2
EKVX	0.442	9.07	58.4	0.893	4.20	20.8
HOP-62	1.09	7.24	44.5	0.815	2.65	12.2
HOP-92	0.396	2.96	15.2	0.500	1.40	7.29
NCI-H226	0.918	13.6	> 100	0.984	5.52	> 25
NCI-H23	0.445	3.35	39.9	0.722	2.40	11.2
NCI-H322M	3.55	18.4	48.1	0.859	3.90	10.4
NCI-H460	0.376	10.1	45.9	0.814	2.96	14.6
NCI-H522	0.436	1.94	5.95	0.470	1.25	9.89
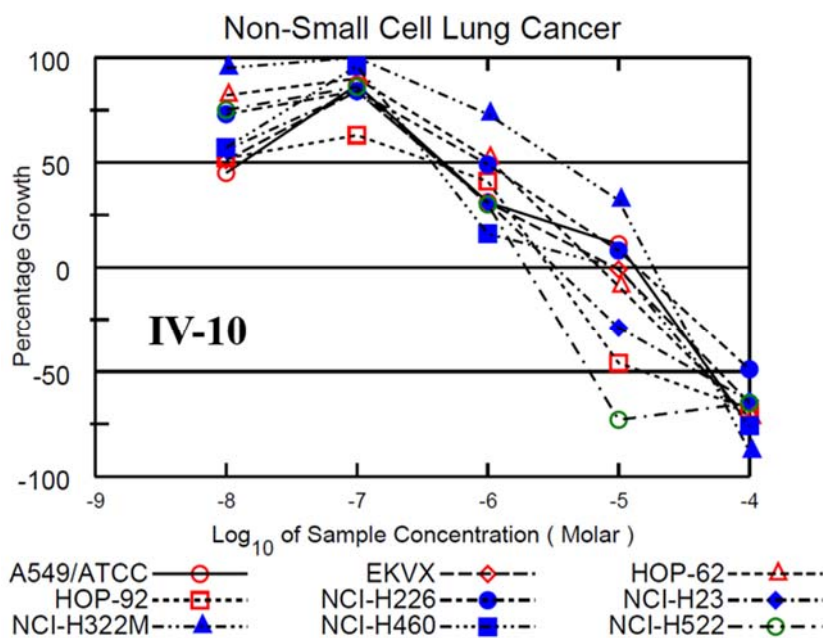
Figure IV-11. Growth percentage plots from the NCI-60 human tumor cell line screen five-dose assay of compound **IV‑10** against all NSCLC cell lines tested by the DTP.
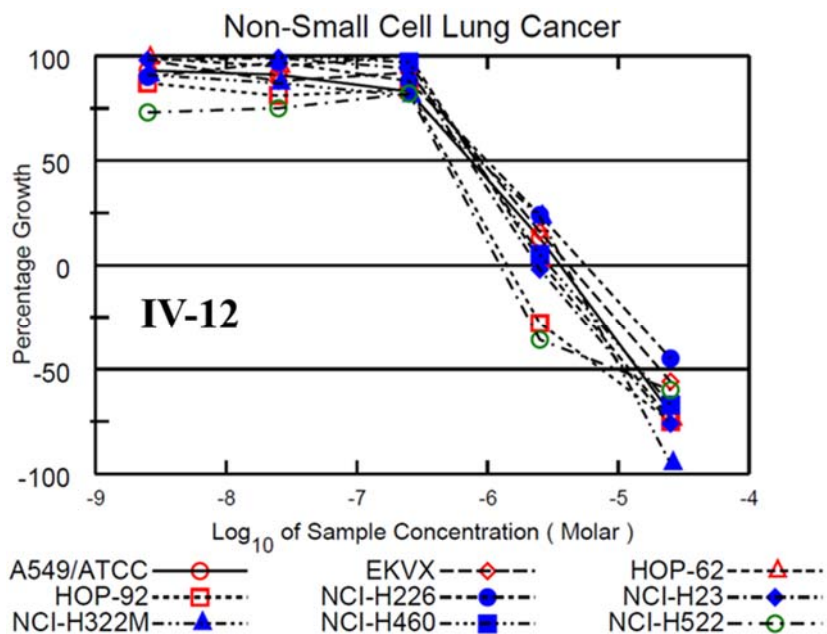
Figure IV-12. Growth percentage plots from the NCI-60 human tumor cell line screen five-dose assay of compound **IV‑12** against all NSCLC cell lines tested by the DTP.

4.2.3. Preliminary in vivo toxicity study

A preliminary in vivo toxicity study using C57BL/6 mice was performed using **IV‑10**. Compound **IV‑10** was chosen because of the high anti-cancer properties exhibited in the various in vitro studies described above and it could be solubilized by 2-hydroxypropyl-β-cyclodextrin (2-HPβCD), a chemical excipient that is FDA approved and used in several drug formulations.[93] Six week old C57BL/6 mice were allowed to acclimate in their cages for five-days prior to any injections. Animals were housed according to the experimental group (3 animals per cage). The behavior and weight of each animal was closely monitored for the duration of the experiment. Experimental animals were injected on days zero, seven, and fourteen with 100 µL of a 20 mg/kg dose (assuming an average

weight of 20 g per mouse) of **IV‑10** dissolved in a 20% (w/v) solution of 2-HPβCD by intraperitoneal (IP) injection. Vehicle control animals were injected with 100 μL of a 20% (w/v) solution of 2-HPβCD by IP injection on days zero, seven, fourteen, twenty-one, twenty-five, and twenty-nine. The weight and behavior of all animals were closely monitored each day for the duration of the experiment (Figure IV-13).

All mice in the vehicle control group survived and gained weight over the course of the entire experiment. Mice treated with **IV‑10** had an average weight loss of 10% after the initial injection but all animals survived for the entire duration of the experiment. There was not a drastic weight loss after the second and third injections and the mice continued to gain weight until the end of the experiment. The reason drastic weight loss did not occur after the second and third injections is unclear but overall the injections were well tolerated. However, a patch of fur was missing at the injection site of one animal on day 8. Antibiotics were used to treat this sore, but no further action was taken and the site improved over time. Overall, **IV‑10** was well tolerated at the treated dose regimen and provides a starting point for future toxicity studies and lung xenograft models considering **IV‑10** is an optimal candidate to move on to further studies.

Figure IV-13. Weight gain chart for compounds treated with 10 and vehicle control. Purple arrows signify the days experimental mice were injected with **IV‑10**.

4.3. Conclusions and future outlook

A series of bis-imidazolium salts was synthesized and assessed for anti-cancer properties against NSCLC by several methods to create a SAR study. Each structure differed by the length of the alkyl chain that connected the two imidazole cores resulting in differences in aqueous solubility and overall lipophilicity. The anti-cancer properties were determined by the MTT assay in our lab and through the one-dose and five-dose NCI-60 human tumor cell line screen assays. Results from all in vitro experiments were consistent and suggested that the lipophilicity is directly related to anti-cancer activity considering the least lipophilic derivative, **IV‑1**, had the worst anti-cancer activity, whereas **IV‑12**, the most lipophilic derivative, had the highest anti-proliferative effects.

219

This SAR will guide the synthesis of future derivatives to optimize the next generation of compounds. Compound **IV‑10**, with a decyl linker, also had extremely high activity and was used for a preliminary in vivo toxicity study with C57BL/6 mice. All animals survived the study and gained weight over the course of the experiment. This study gave valuable information about compound **IV‑10** and will be used to guide future experiments including a more intense toxicity study and lung xenograft models.

4.4. Acknowledgements

4.5. Experimental Section

4.5.1. General Procedures

All reactions were conducted under aerobic conditions except where indicated. 2-(Bromomethyl)naphthalene was purchased from Waterstone Technologies. 1,2-Dibromoethane was purchased from Baker. 1,3-Dibromopropane, 1,4-dibromobutane, 1,6-

dibromohexane, and 1,8-dibromooctane were purchased from Acros Organics. 1,5-Dibromopentane was purchased from Alfa Aesar. 1,7-Dibromoheptane and 1,10-dibromodecane were purchased from TCI. 1,11-Dibromoundecane was purchased from Aldrich. 1,12-Dibromododecane was purchased from Avocado. Imidazole was purchased from Acros Organics. Naphthylmethyl imidazole was synthesized according to literature procedures.[11] Di(imidazol-1-yl)methane was synthesized according to the literature and recrystallized from chloroform.[137] All solvents were purchased from Fisher Scientific. All reagents were used as received without further purification. ^{1}H and ^{13}C NMR spectra were obtained on a Varian 500 MHz instrument with all spectra referenced to residual deuterated solvent for compounds **IV‑1‑IV‑8**, **IV‑10**, and **IV‑12** (DMSO-d6: ^{1}H NMR: 2.50 ppm, ^{13}C NMR: 39.5 ppm). ^{1}H and ^{13}C NMR spectra were obtained on a Varian 300 MHz instrument with all spectra referenced to residual deuterated solvent for compounds **IV‑9** and **IV‑11** (DMSO-d6: 1H NMR: 2.50 ppm, 13C NMR: 39.5 ppm).

The human NSCLC cell lines NCI-H1975 and HCC827 were generously provided by Dr. Lindner from the Cleveland Clinic. The human NSCLC cell lines NCI-H460 and NCI-A549 were purchased from ATCC (Manassas, VA, USA). All cell lines were grown at 37 °C with 5% CO_2 in RPMI 1640 medium supplemented with 10% fetal bovine serum and passed every 2-3 days.

4.5.2. Single crystal X-ray crystallography procedures

Crystals of the compounds were coated in paratone oil, mounted on a CryoLoop and placed on a goniometer under a stream of nitrogen. Crystal structure data sets were

collected on either a Bruker SMART APEX I CCD diffractometer with graphite-monochromated Mo Kα radiation (λ = 0.71073 Å) or a Bruker Kappa APEX II Duo CCD system equipped with a Mo ImuS source and a Cu ImuS micro-focus source equipped with QUAZAR optics (λ = 1.54178 Å). The unit cells were determined by using reflections from three different orientations. Data sets were collected using SMART or APEX II software packages. All data sets were processed using the APEX II software suite.[114,115] The data sets were integrated using SAINT.[116] An empirical absorption correction and other corrections were applied to the data sets using multi-scan SADABS.[117] Structure solution, refinement, and modelling were accomplished by using the Bruker SHELXTL package.[118] The structures were determined by full-matrix least-squares refinement of F^2 and the selection of the appropriate atoms from the generated difference map. Hydrogen atom positions were calculated and $U_{iso}(H)$ values were fixed according to a riding model.

4.5.3. MTT assay

Cells were grown to confluence and plated in 96-well plates at 5,000-7,000 cells per well, depending on the cell line. Cells were incubated for 24 h prior to adding the compounds. All compounds were dissolved in a 1% DMSO solution and diluted in fresh medium to the desired concentrations of 1, 4, 16, and 32 μM. Compounds were added (6 replicates each) and cells were incubated for 72 h at which time the MTT assay protocol was followed. MTT reagent (10 μL) was added to each well and cells were incubated for 3-4 h, again depending on the cell line. Growth medium was removed by aspiration and

DMSO (100 μL) was added to each well. Plates were incubated for 15 min. The optical density was read at 540 nm on a Biotek Epoch plate reader.

4.5.4. Preliminary in vivo toxicity study

All animal procedures were reviewed and approved by the Institutional Animal Care and Use Committee at the University of Akron. Eight-week-old male C57BL/6 mice were obtained from Charles River laboratories. Animals were housed in a 12 h light/dark cycle, and food and water were provided ad libitum (n = 3 animals per cage). Prior to the toxicity testing, animals were allowed to acclimate for five days. Vehicle control mice received IP injections on days 0, 7, 14, 21, 25, and 29 of 100 μL of a 20% 2-HPβCD sterile PBS solution. Experimental mice received 100 μL of a 4 mg/mL 20% 2-HPβCD sterile PBS solution (0.4 mg/100 μL, or ~ 20 mg/kg assuming an average mouse weight of 20 g) of **10** by IP injection on days 0, 7, 14. Animals were closely monitored and weighed on a daily basis. All animals were sacrificed on day 29.

4.5.5. General Synthesis

4.5.5.1. Synthesis of 1-(naphthalen-2-ylmethyl)-3-((3-(naphthalen-2-ylmethyl)-imidazolium-1-yl)methyl)-imidazolium bromide (**IV‑1**)

Di(1H-imidazol-1-yl)methane (0.12 g, 0.8 mmol) was dissolved in acetonitrile (7 mL) and 2-(bromomethyl)naphthalene (0.40 g, 1.8 mmol) was added. The reaction was heated and stirred at 70 °C overnight. The volatile components were removed under

reduced pressure, and the white solid was washed with acetone (25 mL) and chloroform (15 mL), subsequently. The product was recrystallized in a solution of water and ethanol (1:6). After filtration, the crystals were ground to a fine powder by mortar and pestle and residual volatile components were removed under reduced pressure to purify the white solid, **IV‑1** (0.42 g, 87 % yield). Found C, 58.51; H, 4.28; N, 9.45%. Calculated for $C_{29}H_{26}N_4Br_2$: C, 59.0; H, 4.4; N, 9.5%. Phase Transition, 283 – 285°C. HRMS (ESI^{2+}) calcd for $C_{29}H_{26}N_4^{2+}$ [M-2(Br)] of m/z = 215.1073, calcd for $C_{26}H_{24}N_4^+$ [M-2(Br)H] of m/z = 429.2074, found m/z = 429.2140. ^{1}H NMR (500 MHz, DMSO-d_6) δ = 9.70 (2H, s, Ar), 8.13-7.93 (12H, m, Ar), 7.59-7.57 (6H, m, Ar), 6.72 (2H, s, CH$_2$), 5.68 (4H, s, CH$_2$). ^{13}C NMR (125 MHz, DMSO-d_6) δ = 137.8 (NCN), 132.8 (Ar), 132.6 (Ar), 131.5 (Ar), 128.7 (Ar), 128.0 (Ar), 127.8 (Ar), 127.6 (Ar), 126.8 (Ar), 126.7 (Ar), 125.9 (Ar), 123.3 (Ar), 122.5 (Ar), 58.3 (CH$_2$), 52.5 (CH$_2$).

4.5.5.2. Synthesis of 1-(naphthalen-2-ylmethyl)-3-(2-(3-(naphthalen-2-ylmethyl)-imidazolium-1-yl)ethyl)-imidazolium bromide (**IV‑2**)

1,2-Dibromoethane (56 μL, 0.7 mmol) and 1-(naphthalen-2-ylmethyl)-imidazole (0.30 g, 1.4 mmol) were heated in acetonitrile (5 mL) overnight. The volatile components were removed under reduced pressure, and the white solid was triturated with acetone and filtered. Residual volatile components were removed under reduced pressure to yield a white solid, **IV‑2** (0.06 g, 16 % yield). Found C, 60.67; H, 4.21; N, 9.37%. Calculated for $C_{30}H_{28}N_4Br_2$: C, 59.6; H, 4.7; N, 9.3%. Phase Transition, 285°C. HRMS (ESI^{2+}) calcd for $C_{30}H_{28}N_4^{2+}$ [M-2(Br)] of m/z = 222.1152, calcd for $C_{30}H_{27}N_4^+$ [M-2(Br)H] of m/z =

443.2230, found m/z = 443.2311.^{1}H NMR (500 MHz, DMSO-d_6) δ = 9.32 (2H, s, Ar), 7.98-7.91 (8H, m, Ar), 7.86 (2H, dd, Ar), 7.73 (2H, dd, Ar), 7.58-7.57 (4H, m, Ar), 7.48 (1H, d, Ar), 7.46 (1H, d, Ar), 5.57 (4H, s, CH$_2$), 4.75 (4H, t, CH$_2$). ^{13}C NMR (125 MHz, DMSO-d_6) δ = 136.8 (NCN), 132.7 (Ar), 132.6 (Ar), 131.8 (Ar), 128.7 (Ar), 127.8 (Ar), 127.63 (Ar), 127.60 (Ar), 126.8 (Ar), 126.7 (Ar), 125.6 (Ar), 122.94 (Ar), 122.86 (Ar), 52.2 (CH$_2$), 48.5 (CH$_2$).

Crystal data for **IV‑2‑PF$_6$**: C$_{30}$H$_{28}$F$_{12}$N$_4$P$_2$, M = 734.50, monoclinic, a = 35.130(2) Å, b = 6.9080(4) Å, c = 12.5665(8) Å, β = 101.406(3)°, V = 2989.4(3) Å^3, T = 100(2) K, space group C2/c, Z = 4, 11425 reflections measured, 3039 independent reflections (R$_{int}$ = 0.0413). The final R_1 values were 0.0477 ($I > 2σ(I)$). The final $wR(F^2)$ values were 0.1154 ($I > 2σ(I)$). The final R_1 values were 0.0713 (all data). The final $wR(F^2)$ values were 0.1308 (all data). A single crystal of **IV‑2‑PF$_6$** was obtained by slow evaporation of a concentrated solution of **IV‑2‑PF$_6$** dissolved in acetonitrile, chloroform, and 2-propanol.

4.5.5.3. Synthesis of 1-(naphthalen-2-ylmethyl)-3-(3-(3-(naphthalen-2-ylmethyl)-imidazolium-1-yl)propyl)-imidazolium bromide (**IV‑3**)

1,3-Dibromopropane (66 μL, 0.7 mmol) and 1-(naphthalen-2-ylmethyl)-imidazole (0.30 g, 1.4 mmol) were heated in acetonitrile (5 mL) overnight. The clear solution was cooled (-20 °C) to induce precipitation. The white power was filtered and washed with cold (-20 °C) acetonitrile (25 mL). A fine, white powder, **IV‑3** was collected (0.34 g, 84 % yield). Found C, 55.69; H, 4.94; N, 8.61%. Calculated for C$_{31}$H$_{30}$N$_4$Br$_2$: C, 60.2; H, 4.9; N, 9.1%. Phase Transition, 145 – 147°C. HRMS (ESI^{2+}) calcd for C$_{31}$H$_{30}$N$_4$$^{2+}$ [M-2(Br)] of

m/z = 229.1230, calcd for $C_{31}H_{29}N_4^+$ [M-2(Br)H] of m/z = 457.2387, found m/z = 457.2438. ^{1}H NMR (500 MHz, DMSO-d_6) δ = 9.49 (2H, s, Ar), 8.01-7.89 (12H, m, Ar), 7.59-7.55 (6H, m, Ar), 5.62 (4H, s, CH$_2$), 4.30 (4H, t, CH$_2$), 2.46 (2H, p, CH$_2$). ^{13}C NMR (125 MHz, DMSO-d_6) δ = 136.5 (NCN), 132.7 (Ar), 132.6 (Ar), 132.0 (Ar), 128.7 (Ar), 127.8 (Ar), 127.7 (Ar), 127.6 (Ar), 126.7 (Ar), 126.6 (Ar), 125.8 (Ar), 122.7 (Ar), 122.6 (Ar), 52.1 (CH$_2$), 46.0 (CH$_2$), 29.3 (CH$_2$).

Crystal data for **IV‑3•H$_2$O**: $C_{31}H_{30}N_4Br_2$, M = 636.42, monoclinic, a = 21.4487(8) Å, b = 12.5771(4) Å, c = 10.6265(4) Å, $β$ = 91.5181(17)°, V = 2865.62(18) Å^3, T = 100(2) K, space group P2$_1$/c, Z = 4, 51189 reflections measured, 5811 independent reflections (R_{int} = 0.0435). The final R_1 values were 0.0335 ($I > 2σ(I)$). The final $wR(F^2)$ values were 0.0784 ($I > 2σ(I)$). The final R_1 values were 0.0520 (all data). The final $wR(F^2)$ values were 0.0861 (all data). A single crystal of **IV‑3•H$_2$O** was obtained by slow evaporation of a concentrated solution of **IV‑3** dissolved in ethyl acetate and tetrahydrofuran.

4.5.5.4. Synthesis of 1-(naphthalen-2-ylmethyl)-3-(4-(3-(naphthalen-2-ylmethyl)-imidazolium-1-yl)butyl)-imidazolium bromide (**IV‑4**)

1,4-Dibromobutane (78 μL, 0.7 mmol) and 1-(naphthalen-2-ylmethyl)-imidazole (0.30 g, 1.4 mmol) were heated in acetonitrile (5 mL) overnight. A white precipitate formed, and the mixture was cooled (-20 °C) to induce further precipitation. The white power was filtered and washed with cold (-20 °C) acetonitrile (25 mL). A fine, white powder, **IV‑4** was collected (0.32 g, 76 % yield). Found C, 57.62; H, 5.13; N, 8.33%. Calculated for $C_{32}H_{32}N_4Br_2$: C, 60.8; H, 5.1; N, 8.9%. Phase Transition, 223 – 225°C.

HRMS (ESI^{2+}) calcd for C$_{32}$H$_{32}$N$_4^{2+}$ [M-2(Br)] of m/z = 236.1308, calcd for C$_{32}$H$_{31}$N$_4^+$ [M-2(Br)H] of m/z = 471.2543, found m/z = 471.2531. ^{1}H NMR (500 MHz, DMSO-d_6) δ = 9.37 (2H, s, Ar), 7.98-7.83 (12H, m, Ar), 7.58-7.52 (6H, m, Ar), 5.60 (4H, s, CH$_2$), 4.23 (4H, t, CH$_2$), 1.81 (4H, t, CH$_2$). ^{13}C NMR (125 MHz, DMSO-d_6) δ = 136.3 (NCN), 132.68 (Ar), 132.65 (Ar), 132.1 (Ar), 128.7 (Ar), 127.8 (Ar), 127.63 (Ar), 127.57 (Ar), 126.74 (Ar), 126.71 (Ar), 125.7 (Ar), 122.71 (Ar), 122.69 (Ar), 52.1 (CH$_2$), 48.2 (CH$_2$), 26.0 (CH$_2$).

Crystal data for **IV‑4•2(H$_2$O)**: C$_{32}$H$_{36}$N$_4$O$_2$Br$_2$, M = 668.47, monoclinic, a = 11.8237(4) Å, b = 11.7179(3) Å, c = 10.6439(3) Å, β = 99.8580(10)°, V = 1452.93(7) Å^3, T = 100(2) K, space group P2$_1$/c, Z = 2, 15219 reflections measured, 2950 independent reflections (R$_{int}$ = 0.0330). The final R_1 values were 0.0307 ($I > 2\sigma(I)$). The final $wR(F^2)$ values were 0.0801 ($I > 2\sigma(I)$). The final R_1 values were 0.0377 (all data). The final $wR(F^2)$ values were 0.0849 (all data). A single crystal of **IV‑4•2(H$_2$O)** was obtained by slow evaporation of a concentrated solution of **IV‑4** dissolved in methanol.

4.5.5.5. Synthesis of 1-(naphthalen-2-ylmethyl)-3-(5-(3-(naphthalen-2-ylmethyl)-imidazolium-1-yl)pentyl)-imidazolium bromide (**IV‑5**)

1,5-Dibromopentane (178 μL, 1.3 mmol) and 1-(naphthalen-2-ylmethyl)-imidazole (0.60 g, 2.9 mmol) were heated in acetonitrile (4 mL) overnight. The volatile components were removed under reduced pressure, and the white solid was triturated with cold (-20 °C) acetone (25 mL). The white powder was recrystallized in a solution of water and ethanol (1:6). The crystals were filtered and washed with acetone (15 mL). The volatile

components were removed under reduced pressure to yield a white powder, **IV‑5** (0.44 g, 52 % yield). Phase Transition, 226 – 228°C. HRMS (ESI^{2+}) calcd for $C_{33}H_{34}N_4^{2+}$ [M-2(Br)] of m/z = 243.1386, calcd for $C_{33}H_{33}N_4^+$ [M-2(Br)H] of m/z = 485.2700, found m/z = 485.2763.^{1}H NMR (500 MHz, DMSO-d_6) δ = 9.49 (2H, s, Ar), 8.00-7.87 (12H, m, Ar), 7.58-7.54 (6H, m, Ar), 5.63 (4H, s, CH$_2$), 4.21 (4H, t, CH$_2$), 1.85 (4H, tt, CH$_2$), 1.25 (2H, p, CH$_2$). ^{13}C NMR (125 MHz, DMSO-d_6) δ = 136.2 (NCN), 132.7 (Ar), 132.6 (Ar), 132.1 (Ar), 128.7 (Ar), 127.8 (Ar), 127.6 (Ar), 127.6 (Ar), 126.70 (Ar), 126.67 (Ar), 125.7 (Ar), 122.7 (Ar), 122.6 (Ar), 52.1 (CH$_2$), 48.5 (CH$_2$), 28.5 (CH$_2$), 22.0 (CH$_2$).

Crystal data for **IV‑5•H$_2$O**: $C_{33}H_{36}N_4Br_2O$, M = 664.48, monoclinic, a = 10.7412(9) Å, b = 23.605(3) Å, c = 11.5324(13) Å, β = 90.046(4)°, V = 2924.0(5) Å^3, T = 100(2) K, space group P2$_1$/n, Z = 4, 38687 reflections measured, 5562 independent reflections (R$_{int}$ = 0.0694). The final R_1 values were 0.0334 (I > 2σ(I)). The final $wR(F^2)$ values were 0.0735 (I > 2σ(I)). The final R_1 values were 0.0467 (all data). The final $wR(F^2)$ values were 0.0786 (all data). A single crystal of **IV‑5•H$_2$O** was obtained by slow evaporation of a concentrated solution of **IV‑5** dissolved in water.

4.5.5.6. Synthesis of 1-(naphthalen-2-ylmethyl)-3-(6-(3-(naphthalen-2-ylmethyl)-imidazolium-1-yl)hexyl)-imidazolium bromide (**IV‑6**)

1,6-Dibromohexane (135 µL, 0.9 mmol) and 1-(naphthalen-2-ylmethyl)-imidazole (0.40 g, 1.9 mmol) were heated in acetonitrile (7 mL) overnight. A white precipitate formed, and the reaction mixture was cooled (-20 °C) to induce further precipitation. The white precipitate was filtered and washed with cold (-20 °C) acetonitrile (30 mL) to afford

IV‑6 (0.44 g, 77 % yield). Found C, 61.62; H, 5.31; N, 8.42%. Calculated for

$C_{34}H_{36}N_4Br_2$:C, 61.8; H, 5.5; N, 8.5%. Phase Transition, 233 – 234°C. HRMS (ESI^{2+}) calcd

for $C_{34}H_{36}N_4^{2+}$ [M-2(Br)] of m/z = 250.1465, calcd for $C_{34}H_{35}N_4^+$ [M-2(Br)H] of m/z =

499.2856, found m/z = 499.2948. ^{1}H NMR (500 MHz, DMSO-d_6) δ = 9.57 (2H, s, Ar),

8.02-7.89 (12H, m, Ar), 7.59-7.54 (6H, m, Ar), 5.66 (4H, s, CH$_2$), 4.20 (4H, t, CH$_2$), 1.81

(4H, tt, CH$_2$), 1.27 (4H, t, CH$_2$). ^{13}C NMR (125 MHz, DMSO-d_6) δ = 136.2 (NCN), 132.7

(Ar), 132.6 (Ar), 132.2 (Ar), 128.7 (Ar), 127.8 (Ar), 127.58 (Ar), 127.56 (Ar), 126.7 (Ar),

126.6 (Ar), 125.7 (Ar), 122.7 (Ar), 122.5 (Ar), 52.0 (CH$_2$), 48.7 (CH$_2$), 28.9 (CH$_2$), 24.7

(CH$_2$).

4.5.5.7. Synthesis of 1-(naphthalen-2-ylmethyl)-3-(7-(3-(naphthalen-2-ylmethyl)-imidazolium-1-yl)heptyl)-imidazolium bromide (**IV‑7**)

1,7-Dibromoheptane (149 µL, 0.9 mmol) and 1-(naphthalen-2-ylmethyl)-imidazole

(0.40 g, 1.9 mmol) were heated in acetonitrile (7 mL) overnight. The clear solution was

cooled (-20 °C) and a white precipitate formed which was washed with cold (-20 °C)

acetonitrile (25 mL). The white powder was dried via aspirator filtration to afford **IV‑7**

(0.38 g, 64 % yield). Found C, 60.94; H, 5.67; N, 8.06%. Calculated for $C_{35}H_{38}N_4Br_2$: C,

62.3; H, 5.7; N, 8.3%. Phase Transition, 198 – 200°C. HRMS (ESI^{2+}) calcd for $C_{35}H_{38}N_4^{2+}$

[M-2(Br)] of m/z = 257.1543, calcd for $C_{35}H_{37}N_4^+$ [M-2(Br)H] of m/z = 513.3013, found

m/z = 513.3084. ^{1}H NMR (500 MHz, DMSO-d_6) δ = 9.53 (2H, s, Ar), 8.00-7.88 (12H, m,

Ar), 7.58-7.54 (6H, m, Ar), 5.64 (4H, s, CH$_2$), 4.19 (4H, t, CH$_2$), 1.79 (4H, tt, CH$_2$), 1.29

(2H, tt, CH$_2$), 1.22 (2H, p, CH$_2$). ^{13}C NMR (125 MHz, DMSO-d_6) δ = 136.2 (NCN), 132.7

(Ar), 132.6 (Ar), 132.2 (Ar), 128.7 (Ar), 127.8 (Ar), 127.60 (Ar), 127.55 (Ar), 126.7 (Ar), 126.6 (Ar), 125.6 (Ar), 122.7 (Ar), 122.6 (Ar), 52.0 (CH_2), 48.8 (CH_2), 29.0 (CH_2), 27.5 (CH_2), 25.2 (CH_2).

Crystal data for **IV-7-PF₆**: $C_{35}H_{38}N_4F_{12}P_2$, M = 804.63, monoclinic, a = 16.3885(12) Å, b = 10.9040(8) Å, c = 19.8011(13) Å, β = 93.425(4)°, V = 3532.1(4) Å³, T = 100(2) K, space group P2₁/c, Z = 4, 28400 reflections measured, 7158 independent reflections (R_{int} = 0.0547). The final R_1 values were 0.0540 ($I > 2\sigma(I)$). The final $wR(F^2)$ values were 0.1436 ($I > 2\sigma(I)$). The final R_1 values were 0.0699 (all data). The final $wR(F^2)$ values were 0.1571 (all data). A single crystal of **IV-7-PF₆** was obtained by slow evaporation of a concentrated solution of **IV-7** dissolved in acetonitrile.

4.5.5.8. Synthesis of 1-(naphthalen-2-ylmethyl)-3-(8-(3-(naphthalen-2-ylmethyl)-imidazolium-1-yl)octyl)-imidazolium bromide (**IV-8**)

1,8-Dibromooctane (161 μL, 0.9 mmol) and 1-(naphthalen-2-ylmethyl)-imidazole (0.40 g, 1.9 mmol) were heated in acetonitrile (3 mL) overnight. The volatile components were removed via rotary evaporation under reduced pressure. The off-white powder was washed and filtered with cold (-20 °C) acetone (25 mL). The powder was recrystallized in an ethanol and water solution (5:1). The crystals were washed and filtered with cold (-20 °C) acetone (15 mL). The crystals were crushed to an off-white powder which was dried under reduced pressure to afford **8** (0.50 g, 83 % yield). Found C, 59.58; H, 5.57; N, 7.65%. Calculated for $C_{36}H_{40}N_4Br_2$: C, 62.8; H, 5.9; N, 8.1%. ¹H NMR (500 MHz, DMSO-d_6) δ = 9.46 (2H, s, Ar), 7.99-7.86 (12H, m, Ar), 7.57-7.54 (6H, m, Ar), 5.63 (4H, s, CH_2), 4.18

(4H, t, CH$_2$), 1.78 (4H, tt, CH$_2$), 1.24-1.20 (8H, m, CH$_2$). ^{13}C NMR (125 MHz, DMSO-d_6)

δ = 136.2 (NCN), 132.7 (Ar), 132.6 (Ar), 132.2 (Ar), 128.7 (Ar), 127.8 (Ar), 127.6 (Ar),

127.5 (Ar), 126.70 (Ar), 126.68 (Ar), 125.6 (Ar), 122.7 (Ar), 122.6 (Ar), 52.1 (CH$_2$), 48.9

(CH$_2$), 29.1 (CH$_2$), 28.1 (CH$_2$), 25.3 (CH$_2$).

Crystal data for **IV‑8**: C$_{36}$H$_{40}$N$_4$Br$_2$, M = 688.54, monoclinic, a = 10.9871(9) Å, b

= 10.3592(8) Å, c = 15.1017(13) Å, β = 98.618(4)°, V = 1699.4(2) Å^3, T = 100(2) K, space

group P2$_1$/c, Z = 2, 14597 reflections measured, 3440 independent reflections (R$_{int}$ =

0.0465). The final R_1 values were 0.0697 ($I > 2\sigma(I)$). The final $wR(F^2)$ values were 0.2145

($I > 2\sigma(I)$). The final R_1 values were 0.0873 (all data). The final $wR(F^2)$ values were 0.2358

(all data). A single crystal of I**V-8** was obtained by slow evaporation of a concentrated

solution of **IV‑8** dissolved in acetonitrile, water, and diethylether.

4.5.5.9. Synthesis of 1-(naphthalen-2-ylmethyl)-3-(9-(3-(naphthalen-2-ylmethyl)-

imidazolium-1-yl)nonyl)-imidazolium bromide (**IV‑9**)

1,9-Dibromoundecane (293 μL, 1.4 mmol) and 1-(naphthalen-2-ylmethyl)-

imidazole (0.600 g, 2.9 mmol) were heated in acetonitrile (4 mL) overnight. The volatile

components from the reaction were removed under reduced pressure. The resulting

viscous, white oil was dissolved in deionized water (300 mL) and washed twice with

diethyl ether (100 mL). The water layer was collected and the water was removed under

reduced pressure. The viscous, transparent, and tan oil was triturated with methylene

chloride (100 mL) which induced precipitation of a tan solid. The mixture was filtered in

a glove bag with a nitrogen environment. The tan solid was collected and stored at ambient

conditions in open atmosphere to afford **IV‑9** (0.522 g, 53 % yield). Calculated for $C_{37}H_{42}N_4Br_2$: C, 63.7; H, 6.2; N, 7.8%. ^1H NMR (300 MHz, DMSO-d_6) δ = 9.43 (2H, s, Ar), 7.98-7.84 (12H, m, Ar), 7.59-7.53 (6H, m, Ar), 5.64 (4H, s, CH_2), 4.18 (4H, t, CH_2), 1.78 (4H, tt, CH_2), 1.23-1.20 (10H, m, CH_2).

4.5.5.10. Synthesis of 1-(naphthalen-2-ylmethyl)-3-(10-(3-(naphthalen-2-ylmethyl)-imidazolium-1-yl)decyl)-imidazolium bromide (**IV‑10**)

1,10-Dibromodecane (0.26 g, 0.9 mmol) and 1-(naphthalen-2-ylmethyl)-imidazole (0.40 g, 1.9 mmol) were heated in acetonitrile (3 mL) overnight. A white precipitate formed as the solution cooled to room temperature and was cooled (-20 °C) to induce further precipitation. The chilled mixture was filtered and the white solid was washed with acetone (25 mL). The white solid was subsequently washed with diethyl ether (25 mL) three times. The white solid was dried under reduced pressure to afford **IV‑10** (0.31 g, 49 % yield). Found C, 62.88; H, 6.26; N, 7.61%. Calculated for $C_{38}H_{44}N_4Br_2$: C, 63.7; H, 6.2; N, 7.8%. Phase Transition, 66°C. HRMS (ESI^{2+}) calcd for $C_{38}H_{44}N_4^{2+}$ [M-2(Br)] of m/z = 278.1778, calcd for $C_{38}H_{43}N_4^+$ [M-2(Br)H] of m/z = 555.3482, found m/z = 555.3456. ^1H NMR (500 MHz, DMSO-d_6) δ = 9.43 (2H, s, Ar), 7.99-7.85 (12H, m, Ar), 7.59-7.53 (6H, m, Ar), 5.62 (4H, s, CH_2), 4.18 (4H, t, CH_2), 1.78 (4H, tt, CH_2), 1.22-1.20 (12H, m, CH_2). ^{13}C NMR (125 MHz, DMSO-d_6) δ = 136.2 (NCN), 132.7 (Ar), 132.6 (Ar), 132.2 (Ar), 128.7 (Ar), 127.8 (Ar), 127.60 (Ar), 127.55 (Ar), 126.7 (Ar), 126.6 (Ar), 125.6 (Ar), 122.7 (Ar), 122.6 (Ar), 52.0 (CH_2), 48.8 (CH_2), 29.0 (CH_2), 27.5 (CH_2), 25.2 (CH_2).

4.5.5.11. Synthesis of 1-(naphthalen-2-ylmethyl)-3-(11-(3-(naphthalen-2-ylmethyl)-

imidazolium-1-yl)undecyl)-imidazolium bromide (**IV‑11**)

1,11-Dibromoundecane (340 μL, 1.4 mmol) and 1-(naphthalen-2-ylmethyl)-imidazole (0.601 g, 2.9 mmol) were heated in acetonitrile (4 mL) overnight. The volatile components from the reaction were removed under reduced pressure. The resulting viscous, white oil was dissolved in deionized water (300 mL) and extracted twice with diethyl ether (100 mL). The water layer was collected and the water was removed under reduced pressure. The viscous, clear oil was triturated with methylene chloride (100 mL) which induced precipitation of a white solid. The mixture was filtered in a glove bag with a nitrogen environment. The solid was taken out of the bag which caused it to phase transition to a clear oil again. The oil was dissolved in chloroform (40 mL) and evaporated at ambient conditions in open atmosphere. A white, crystalline solid, **IV‑11** was collected (0.182 g, 18 % yield). Calculated for $C_{39}H_{46}N_4Br_2$: C, 64.1; H, 6.4; N, 7.7%. ^{1}H NMR (300 MHz, DMSO-d_6) δ = 9.41 (2H, s, Ar), 7.99-7.87 (12H, m, Ar), 7.58-7.53 (6H, m, Ar), 5.63 (4H, s, CH_2), 4.18 (4H, t, CH_2), 1.78 (4H, tt, CH_2), 1.23-1.19 (14H, m, CH_2).

4.5.5.12. Synthesis of 1-(naphthalen-2-ylmethyl)-3-(12-(3-(naphthalen-2-ylmethyl)-

imidazolium-1-yl)dodecyl)-imidazolium bromide (**IV‑12**)

1,12-Dibromododdecane (0.29 g, 0.9 mmol) and 1-(naphthalen-2-ylmethyl)-imidazole (0.40 g, 1.9 mmol) were heated in acetonitrile (3 mL) overnight. The volatile components were removed under reduced pressure and the resultant off-white solid was washed with acetone (25 mL). The solid became a highly-viscous gel on the filter paper.

After a week of being undisturbed in a fume hood, the hardened, tan product was ground and collected to afford **IV‑12** (0.31 g, 48 % yield). Found C, 63.83; H, 6.45; N, 7.40%. Calculated for $C_{40}H_{48}N_4Br_2$: C, 64.5; H, 6.5; N, 7.5%. Phase Transition, $137 - 138°C$. HRMS (ESI^{2+}) calcd for $C_{40}H_{48}N_4{}^{2+}$ [M-2(Br)] of m/z = 292.1934, calcd for $C_{40}H_{47}N_4{}^+$ [M-2(Br)H] of m/z = 583.3795, found m/z = 583.3722. ^{1}H NMR (500 MHz, DMSO-d_6) δ = 9.46 (2H, s, Ar), 7.98-7.86 (12H, m, Ar), 7.58-7.54 (6H, m, Ar), 5.63 (4H, s, CH$_2$), 4.19 (4H, t, CH$_2$), 1.79 (4H, tt, CH$_2$), 1.23-1.19 (12H, m, CH$_2$). ^{13}C NMR (125 MHz, DMSO-d_6) δ = 136.2 (NCN), 132.7 (Ar), 132.6 (Ar), 132.2 (Ar), 128.7 (Ar), 127.8 (Ar), 127.6 (Ar), 127.5 (Ar), 126.68 (Ar), 126.65 (Ar), 125.6 (Ar), 122.7 (Ar), 122.6 (Ar), 52.0 (CH$_2$), 48.9 (CH$_2$), 29.2 (CH$_2$), 28.8 (CH$_2$), 28.3 (CH$_2$), 25.5 (CH$_2$).

CHAPTER V

CONCLUDING REMARKS

Imidazolium salts have been used for multiple applications over the past several decades, including the use as a precursors to N-heterocyclic carbenes and as 'green' solvents in the case of imidazolium salts that exist or can form ionic liquids at relatively low temperatures. Also, hundreds of imidazolium salts have been synthesized and evaluated for their anti-cancer properties for the potential treatment of a variety of different malignancies. Thus far, one imidazolium salts, **YM155** or **I-56**, has been in clinical trials but is not approved for the treatment of any cancers.

Numerous structure-activity relationship studies have been published for different classes of imidazolium salts. The overall theme observed throughout the literature is that higher lipophilicity increases activity. A study performed by the NCI's DTP comparing the anti-cancer properties of imidazolium salts with alkyl chains of different lengths was an early example of this observation. The compounds with longer chains were more active than the compounds with shorter chains. This trend was observed by several research groups. Unfortunately, the most active imidazolium salts were also the least soluble in aqueous media limiting the potential for clinical use.

Several strategies to improve aqueous solubility, without reducing the high anti-cancer activity observed with some derivatives, have been evaluated. One such strategy

was to chemically modify the imidazolium salts by replacing carbon atoms with heteroatoms as a minor alteration in structure to aid in solubility. This approach produced derivatives with high anti-cancer activity and increased solubility; however, the inclusion of too many heteroatoms or the addition of certain functional groups drastically decreased activity. The anti-cancer properties of most imidazolium salts was due to the cationic portion of the cation-anion pair. However, drastic effects on the solubility of the imidazolium salt was observed by changing the anion to different halogens. In one such case described above, the solubility was increased by 2-fold when assessing the bromide salt versus the chloride salt, the latter of which was more water soluble. Also, a chemical excipient, 2-hydroxypropyl-β-cyclodextrin, was used to increase the solubility of certain imidazolium salts 10-fold when compared to their solubility in water alone. The use of the chemical excipient has been accepted by the FDA and is used in several drug formulations. Unfortunately, not every imidazolium salt can be solubilized by the excipient making it useful for only certain imidazolium salts.

Another concern for the progression of imidazolium salts into the clinic is the limited data and knowledge discerning the mechanism of action by which these molecules cause death to human cells. It has been suggested that many of these imidazolium salts cause an apoptotic mode of cellular death with and without the use of cyclodextrin. Although these compounds are positively charged, which would attract them to the negatively charged backbone of DNA, and contain planar, aromatic moieties that could potential intercalate between base pairs of DNA, several in vitro assays suggest that particular imidazolium salts do not interact with DNA. However, a JC-1 assay suggested

236

that mitochondria could be the cellular target of imidazolium salts but further studies are underway to confirm this claim. Understanding the mechanism of action is essential to the progression of this class of compounds. By understanding the mechanism of action compounds can potentially be modified to obtain maximum effectiveness in killing cancerous tissue and minimizing death to healthy tissue.

Non-specificity of imidazolium salts is also a major concern for this class of compounds. Compounds that are highly active seem to kill various types of human cancerous tissue and are not specific to any one type of cancer, acting more as biocides than a potential treatment for a particular cancer. To combat this non-specificity, several strategies can be employed. One such strategy is to attach targeting moieties to the imidazolium ring. Considering the imidazole scaffold is easily manipulated, adding a targeting moiety could add the specificity needed to destroy only cancerous tissue and relieve potential side effects. Another strategy is to gain a better understanding of the mechanism of action and design a compound that will target one form of cancer. Although most of the research done in this dissertation was concerned with lung cancer, one of these imidazolium salts may be a perfect treatment for another form of cancer.

In conclusion, the class of imidazolium salts has largely been investigated by numerous researchers worldwide for their potential use as anti-cancer agents. Large SARs have been established to discover novel, active compounds. These studies involving a large number of compounds reveal the anti-cancer and solubility properties specific modifications lead to. However, more information is needed about the mechanism of action for these compounds to progress further and into the clinic.

REFERENCES

(1)   Kopple, J. D.; Swendseid, M. E. Evidence That Histidine Is an Essential Amino Acid in Normal and Chronically Uremic Man. *J. Clin. Invest.* **1975**, *55* (5), 881–891.

(2)   Philippu, A.; Prast, H. Importance of Histamine in Modulatory Processes, Locomotion and Memory. *Behav. Brain Res.* **2001**, *124* (2), 151–159.

(3)   Youngs, W. J.; Panzner, M. J.; Deblock, M. C.; Tessier, C. A.; Wright, B. D.; Wagers, P. O.; Robishaw, N. K. Azolium and Purinium Salt Anticancer and Antimicrobial Agents. US9278951B2, June 10, 2015.

(4)   Wright, B. D.; Deblock, M. C.; Wagers, P. O.; Duah, E.; Robishaw, N. K.; Shelton, K. L.; Southerland, M. R.; DeBord, M. A.; Kersten, K. M.; McDonald, L. J.; Stiel, J. A.; Panzner, M. J.; Tessier, C. A.; Paruchuri, S.; Youngs, W. J. Anti-Tumor Activity of Lipophilic Imidazolium Salts on Select NSCLC Cell Lines. *Med. Chem. Res.* **2015**, *24* (7), 2838–2861.

(5)   Glushkov, V.; Zhiguleva, M.; Maiorova, O.; Gorbunov, A. N-Heterocyclic Carbenes: V. Synthesis of Imidazolium Salts from Lupane Series. *Russ. J. Org. Chem.* **2012**, *48* (5), 699–704.

(6)   Zhou, B.; Liu, L.-X.; Deng, G.-G.; Chen, W.; Li, M.-Y.; Yang, L.-J.; Li, Y.; Yang, X.-D.; Zhang, H.-B. Synthesis and Antitumor Activity of Novel N-Substituted Tetrahydro-β- Carboline Imidazolium Salt Derivatives. *Org. Biomol. Chem.* **2016**, *14*, 9423–9430.

(7)   Arduengo, A. J.; Krafczyk, R.; Schmutzler, R.; Craig, H. a.; Goerlich, J. R.; Marshall, W. J.; Unverzagt, M. Imidazolylidenes, Imidazolinylidenes and Imidazolidines. *Tetrahedron* **1999**, *55* (51), 14523–14534.

(8)   Ding, J.; Armstrong, D. W. Chiral Ionic Liquids: Synthesis and Applications. *Chirality* **2005**, *17* (5), 281–292.

(9)   He, F.; Danopoulos, A. A.; Braunstein, P. Trifunctional pNHC, Imine, Pyridine Pincer-Type Iridium(III) Complexes: Synthetic, Structural, and Reactivity Studies. *Organometallics* **2016**, *35*, 198–206.

(10)   Furstner, A. Teaching Metathesis "Simple" stereochemistry. *Science (80-.).* **2013**, 1229713.

(11)   Arduengo III, A. J.; Harlow, R. L.; Kline, M. A Stable Crystalline Carbeme. *J. Am. Chem. Soc.* **1991**, *113*, 361–363.

(12)   Guncheva, M.; Paunova, K.; Ossowicz, P.; Rozwadowski, Z.; Janus, E.; Idakieva, K.; Todinova, S.; Raynova, Y.; Uzunova, V.; Apostolova, S.; Tzoneva, R.; Yancheva, D. Rapana Thomasiana Hemocyanin Modified with Ionic Liquids with Enhanced Anti Breast Cancer Activity. *Int. J. Biol. Macromol.* **2016**, *82*, 798–805.

(13)   Demberelnyamba, D.; Kim, K. S.; Choi, S.; Park, S. Y.; Lee, H.; Kim, C. J.; Yoo, I. D. Synthesis and Antimicrobial Properties of Imidazolium and Pyrrolidinonium Salts. *Bioorganic Med. Chem.* **2004**, *12* (5), 853–857.

(14)   Vik, A.; Hedner, E.; Charnock, C.; Tangen, L. W.; Samuelsen, Ø.; Larsson, R.; Bohlin, L.; Gundersen, L. L. Antimicrobial and Cytotoxic Activity of Agelasine and Agelasimine Analogs. *Bioorganic Med. Chem.* **2007**, *15* (12), 4016–4037.

(15)   Zhao, L.; Zhang, C.; Zhuo, L.; Zhang, Y.; Ying, J. Y. Imidazolium Salts: A Mild Reducing and Antioxidative Reagent. *J. Am. Chem. Soc.* **2008**, *130* (38), 12586–12587.

(16)   Ranke, J.; Stolte, S.; Störmann, R.; Arning, J.; Jastorff, B. Design of Sustainable Chemical Products--the Example of Ionic Liquids. *Chem. Rev.* **2007**, *107*, 2183–2206.

(17)   Frade, R. F. M.; Matias, A.; Branco, L. C.; Afonso, C. A. M.; Duarte, C. M. M. Effect of Ionic Liquids on Human Colon Carcinoma HT-29 and CaCo-2 Cell Lines. *Green Chem.* **2007**, *9*, 873–877.

(18)   Kumar, R. A.; Papaiconomou, N.; Lee, J.-M.; Salminen, J.; Clark, D. S.; Prausnitz, J. M. In Vitro Cytotoxicities of Ionic Liquids: Effect of Cation Rings, Functional Groups, and Anions R. *Envrionmental Toxicol.* **2008**, *24* (4), 388–395.

(19)   Frade, R. F. M.; Rosatella, A. A.; Marques, C. S.; Branco, L. C.; Kulkarni, P. S.; Mateus, N. M. M.; Afonso, A. M.; Duarte, C. M. M. Toxicological Evaluation on Human Colon Carcinoma Cell Line (CaCo-2) of Ionic Liquids Based on Imidazolium , Guanidinium , Ammonium , Phosphonium , Pyridinium and Pyrrolidinium Cations †. *Green Chem.* **2009**, *11*, 1660–1665.

(20)   Malhotra, S. V.; Kumar, V. A Profile of the in Vitro Anti-Tumor Activity of Imidazolium-Based Ionic Liquids. *Bioorganic Med. Chem. Lett.* **2010**, *20* (2), 581–585.

(21)   Zhang, Z. B.; Fu, S. B.; Duan, H. F.; Lin, Y. J.; Yang, Y. Brand-New Function of Well-Designed Ionic Liquid: Inhibitor of Tumor Cell Growth. *Chem. Res. Chinese Univ.* **2010**, *26* (5), 757–760.

(22)   Hossain, M. I.; Babaa, M.; El-harbawi, M.; Man, Z.; Hefter, G.; Yin, C. Synthesis , Characterization , Physical Properties , and Cytotoxicities of 1- (6-Hydroxyhexyl) -3-Alkylimidazolium Chloride Ionic Liquids. *J. Chem. Eng. Data* **2011**, *56*, 4188–4193.

(23) Kaushik, N. K.; Attri, P.; Kaushik, N.; Choi, E. H.; Bioscience, P. Synthesis and Antiproliferative Activity of Ammonium and Imidazolium Ionic Liquids against T98G Brain Cancer Cells. *Molecules* **2012**, *17*, 13727–13739.

(24) Wang, C.; Zhu, X.; Liu, S. Toxicity Studies of Ionic Liquids and Heavy Metal Compounds to MCF-7 and Photobacteria Q67. *Adv. Mater. Res.* **2012**, *610*, 721–724.

(25) Chen, H. L.; Kao, H. F.; Wang, J. Y.; Wei, G. T. Cytotoxicity of Imidazole Ionic Liquids in Human Lung Carcinoma A549 Cell Line. *J. Chinese Chem. Soc.* **2014**, *61*, 763–769.

(26) Paternò, A.; D'Anna, F.; Musumarra, G.; Noto, R.; Scirè, S. A Multivariate Insight into Ionic Liquids Toxicities. *RSC Adv.* **2014**, *4*, 23985–24000.

(27) Ferraz, R.; Costa-Rodrigues, J.; Fernandes, M. H.; Santos, M. M.; Marrucho, I. M.; Rebelo, L. P. N.; Prudêncio, C.; Noronha, J. P.; Petrovski, Ž.; Branco, L. C. Antitumor Activity of Ionic Liquids Based on Ampicillin. *ChemMedChem* **2015**, *10*, 1480–1483.

(28) Li, T. H.; Jing, C. Q.; Gao, K. L.; Yue, W. Y.; Li, S. F. Cytotoxicity of 1-Dodecyl-3-Methylimidazolium Bromide on HepG2 Cells. *Genet. Mol. Res.* **2015**, *14* (4), 13342–13348.

(29) Li, X.; Ma, J.; Wang, J. Cytotoxicity, Oxidative Stress, and Apoptosis in HepG2 Cells Induced by Ionic Liquid 1-Methyl-3-Octylimidazolium Bromide. *Ecotoxicol. Environ. Saf.* **2015**, *120*, 342–348.

(30) Messali, M.; Aouad, M. R.; Ali, A. A.-S.; Rezki, N.; Hadda, T. Ben; Hammouti, B. Synthesis, Characterization, and POM Analysis of Novel Bioactive Imidazolium-Based Ionic Liquids. *Med. Chem. Res.* **2015**, *24*, 1387–1395.

(31) Cui, B.; Zheng, B. L.; He, K.; Zheng, Q. Y. Imidazole Alkaloids from Lepidium Meyenii. *J. Nat. Prod.* **2003**, *66* (8), 1101–1103.

(32) Ballistreri, F. P.; Barresi, V.; Benedetti, P.; Caltabiano, G.; Fortuna, C. G.; Longo, L.; Musumarra, G. Design , Synthesis and in Vitro Antitumor Activity of New Trans 2- [2- (Heteroaryl) Vinyl] -1 , 3-Dimethylimidazolium Iodides. *Bioorg. Med. Chem.* **2004**, *12*, 1689–1695.

(33) Barresi, V.; Condorelli, D. F.; Fortuna, C. G.; Musumarra, G.; Scirè, S. In Vitro Antitumor Activities of 2,6-Di-[2-(Heteroaryl)vinyl]pyridines and Pyridiniums. *Bioorganic Med. Chem.* **2002**, *10*, 2899–2904.

(34) Fortuna, C. G.; Barresi, V.; Musumarra, G.; Chimiche, S. Design and Synthesis of Trans 2- (Furan-2-Yl) Vinyl Heteroaromatic Iodides with Antitumour Activity. *Bioorg. Med. Chem.* **2008**, *16*, 4150–4159.

(35) Fortuna, C. G.; Barresi, V.; Musumarra, G. Design, Synthesis and Biological Evaluation of Trans 2-(Thiophen-2-Yl)vinyl Heteroaromatic Iodides. *Bioorganic Med. Chem.* **2010**, *18* (12), 4516–4523.

(36) Barresi, V.; Bonaccorso, C.; Consiglio, G.; Goracci, L.; Musso, N.; Musumarra, G.; Satriano, C.; Fortuna, C. G. Modeling, Design and Synthesis of New Heteroaryl Ethylenes Active against the MCF-7 Breast Cancer Cell-Line. *Mol. Biosyst.* **2013**, *9*, 2426–2429.

(37) Nakahara, T.; Takeuchi, M.; Kinoyama, I.; Minematsu, T.; Shirasuna, K.; Matsuhisa, A.; Kita, A.; Tominaga, F.; Yamanaka, K.; Kudoh, M.; Sasamata, M. YM155, a Novel Small-Molecule Survivin Suppressant, Induces Regression of Established Human Hormone-Refractory Prostate Tumor Xenografts. *Cancer Res.* **2007**, *67* (17), 8014–8021.

(38) O'Connor, D. S.; Grossman, D.; Plescia, J.; Li, F.; Zhang, H.; Villa, a; Tognin, S.; Marchisio, P. C.; Altieri, D. C. Regulation of Apoptosis at Cell Division by p34cdc2 Phosphorylation of Survivin. *Proc. Natl. Acad. Sci. U. S. A.* **2000**, *97* (24), 13103–13107.

(39) Tolcher, A. W.; Mita, A.; Lewis, L. D.; Garrett, C. R.; Till, E.; Daud, A. I.; Patnaik, A.; Papadopoulos, K.; Takimoto, C.; Bartels, P.; Keating, A.; Antonia, S. Phase I and Pharmacokinetic Study of YM155, a Small-Molecule Inhibitor of Survivin. *J. Clin. Oncol.* **2008**, *26* (32), 5198–5203.

(40) Jong, Y. de; Oosterwijk, J. G. van; Kruisselbrink, A. B.; Bruijn, I. H. B.; Agrogiannis, G.; Baranski, Z.; Cleven, A. H. G.; Cleton-Jansen, A.-M.; Water, B. van de; Danen, E. H. J.; Bovée, J. V. M. G. Targeting Survivin as a Potential New Treatment for Chondrosarcoma of Bone. *Oncogenesis* **2016**, *5*, 1–9.

(41) Yang, X.; Zeng, X.; Zhang, Y.; Qing, C.; Song, W.; Li, L.; Zhang, H. Synthesis and Cytotoxic Activities of Novel Phenacylimidazolium Bromides. *Bioorg. Med. Chem. Lett.* **2009**, *19*, 1892–1895.

(42) Zeng, X.; Yang, X.; Zhang, Y.; Qing, C.; Zhang, H. Synthesis and Antitumor Activity of 1-Mesityl-3-(2-Naphthoylmethano)-1H-Imidazolium Bromide. *Bioorganic Med. Chem. Lett.* **2010**, *20* (6), 1844–1847.

(43) Chen, W.; Yang, X.-D.; Li, Y.; Yang, L.-J.; Wang, X.-Q.; Zhang, G.-L.; Zhang, H.-B. Design, Synthesis and Cytotoxic Activities of Novel Hybrid Compounds between Dihydrobenzofuran and Imidazole. *Org. Biomol. Chem.* **2011**, *9*, 4250–4255.

(44) Song, W.-J.; Yang, X.-D.; Zeng, X.-H.; Xu, X.-L.; Zhang, G.-L.; Zhang, H.-B. Synthesis and Cytotoxic Activities of Novel Hybrid Compounds of Imidazole Scaffold-Based 2-Substituted Benzofurans. *RSC Adv.* **2012**, *2* (11), 4612–4615.

(45) Yang, X.-D.; Wan, W.-C.; Deng, X.-Y.; Li, Y.; Yang, L.-J.; Li, L.; Zhang, H.-B. Design, Synthesis and Cytotoxic Activities of Novel Hybrid Compounds between 2-Phenylbenzofuran and Imidazole. *Bioorganic Med. Chem. Lett.* **2012**, *22*, 2726–2729.

(46) Liu, L.; Wang, X.; Yan, J.; Li, Y.; Sun, C.; Chen, W.; Zhou, B.; Zhang, H.; Yang, X. Synthesis and Antitumor Activities of Novel Dibenzo [B , D] Furan-Imidazole Hybrid Compounds. *Eur. J. Med. Chem.* **2013**, *66*, 423–437.

(47) Wang, X.-Q.; Liu, L.-X.; Li, Y.; Sun, C.-J.; Chen, W.; Li, L.; Zhang, H.-B.; Yang, X.-D. Design, Synthesis and Biological Evaluation of Novel Hybrid Compounds of Imidazole Scaffold-Based 2-Benzylbenzofuran as Potent Anticancer Agents. *Eur. J. Med. Chem.* **2013**, *62*, 111–121.

(48) Chen, W.; Deng, X.-Y.; Li, Y.; Yang, L.-J.; Wan, W.-C.; Wang, X.-Q.; Zhang, H.-B.; Yang, X.-D. Synthesis and Cytotoxic Activities of Novel Hybrid 2-Phenyl-3-Alkylbenzofuran and Imidazole/triazole Compounds. *Bioorg. Med. Chem. Lett.* **2013**, *23*, 4297–4302.

(49) Sun, C.-J.; Chen, W.; Li, Y.; Liu, L.-X.; Wang, X.-Q.; Li, L.-J.; Zhang, H.-B.; Yang, X.-D. Design, Synthesis and Antitumor Activity of Novel 8-Substituted 2,3,5,6-tetrahydrobenzo[1,2-b:4,5-B′]difuran Imidazolium Salt Derivatives. *RSC Adv.* **2014**, *4* (31), 16312–16319.

(50) Xu, X.; Wang, J.; Yu, C.; Chen, W.; Li, Y.; Li, Y.; Zhang, H.; Yang, X. Synthesis and Cytotoxic Activity of Novel 1- ((Indol-3-Yl) Methyl) – 1 H -Imidazolium Salts. *Bioorg. Med. Chem. Lett.* **2014**, *24*, 4926–4930.

(51) Wan, W.-C.; Chen, W.; Liu, L.-X.; Li, Y.; Yang, L.-J.; Deng, X.-Y.; Zhang, H.-B.; Yang, X.-D. Synthesis and Cytotoxic Activity of Novel Hybrid Compounds between 2-Alkylbenzofuran and Imidazole. *Med. Chem. Res.* **2014**, *23*, 1599–1611.

(52) Xu, X.; Yu, C.; Chen, W.; Li, Y.; Yang, L.-J.; Li, Y.; Zhang, H.-B.; Yang, X.-D. Synthesis and Antitumor Activity of Novel 2-Substituted Indoline Imidazolium Salt Derivatives. *Org. Biomol. Chem.* **2015**, *13*, 1550–1557.

(53) Liu, L.-X.; Wang, X.-Q.; Zhou, B.; Yang, L.-J.; Li, Y.; Zhang, H.-B.; Yang, X.-D. Synthesis and Antitumor Activity of Novel N-Substituted Carbazole Imidazolium Salt Derivatives. *Sci. Rep.* **2015**, *5*, 13101.

(54) Liu, J.-M.; Wang, M.; Zhou, Y.-J.; Yan, J.-M.; Yang, L.-J.; Li, Y.; Zhang, H.-B.; Yang, X.-D. Novel 3-Substituted Fluorine Imidazolium/triazolium Salt Derivatives: Synthesis and Antitumor Activity. *RSC Adv.* **2015**, *5*, 63936–63944.

(55) Dominianni, S. J.; Yen, T. T. Oral Hypoglycemic Agents. Discovery and Structure-Activity Relationships of Phenacylimidazolium Halides. *J. Med. Chem.* **1989**, *32*, 2301–2306.

(56) Chivikas, C. J.; Hodges, J. C. Phenacyl-Directed Alkylation of Imidazoles: A New Regiospecific Synthesis of 3-Substituted L-Histidines. *J. Org. Chem.* **1987**, *52* (16), 3591–3594.

(57) Bose, J. S.; Gangan, V.; Prakash, R.; Jain, S. K.; Manna, S. K. A Dihydrobenzofuran Lignan Induces Cell Death by Modulating Mitochondrial Pathway and G2/M Cell Cycle Arrest. *J. Med. Chem.* **2009**, *52*, 3184–3190.

(58) Miert, S. Van; Dyck, S. Van; Schmidt, T. J.; Brun, R.; Vlietinck, A.; Lemière, G.; Pieters, L. Antileishmanial Activity, Cytotoxicity and QSAR Analysis of Synthetic Dihydrobenzofuran Lignans and Related Benzofurans. *Bioorganic Med. Chem.* **2005**, *13*, 661–669.

(59) Komiyama, K.; Funayama, S.; Anraku, Y.; Ishibashi, M.; Takahashi, Y.; Omura, S. Novel antibiotics, furaquinocins A and B taxonomy, fermentation, isolation, and physico-chemical and biological characteristics. *J. Antibiot. (Tokyo).* **1990**, *XLIII* (3), 247–252.

(60) Nguyen, T. D.; Jin, X.; Lee, K.; Hong, Y. S.; Young, H. K.; Jung, J. L. Hypoxia-Inducible Factor-1 Inhibitory Benzofurans and Chalcone-Derived Diels-Alder Adducts from Morus Species. *J. Nat. Prod.* **2009**, *72*, 39–43.

(61) Katsanou, E. S.; Halabalaki, M.; Aligiannis, N.; Mitakou, S.; Skaltsounis, A. L.; Alexi, X.; Pratsinis, H.; Alexis, M. N. Cytotoxic Effects of 2-Arylbenzofuran Phytoestrogens on Human Cancer Cells: Modulation by Adrenal and Gonadal Steroids. *J. Steroid Biochem. Mol. Biol.* **2007**, *104*, 228–236.

(62) Halabalaki, M.; Alexi, X.; Aligiannis, N.; Alexis, M. N.; Skaltsounis, A. L. Ebenfurans IV-VIII from Onobrychis Ebenoides: Evidence That C-Prenylation Is the Key Determinant of the Cytotoxicity of 3-Formyl-2-Arylbenzofurans. *J. Nat. Prod.* **2008**, *71*, 1934–1937.

(63) Livingstone, M.; Larsson, O.; Sukarieh, R.; Pelletier, J.; Sonenberg, N. A Chemical Genetic Screen for mTOR Pathway Inhibitors Based on 4E-BP-Dependent Nuclear Accumulation of eIF4E. *Chem. Biol.* **2009**, *16*, 1240–1249.

(64) Hayakawa, I.; Shioya, R.; Agatsuma, T.; Furukawa, H.; Naruto, S.; Sugano, Y. A Library Synthesis of 4-Hydroxy-3-Methyl-6-Phenylbenzofuran-2-Carboxylic Acid Ethyl Ester Derivatives as Anti-Tumor Agents. *Bioorganic Med. Chem. Lett.* **2004**, *14*, 4383–4387.

(65) Zhang, G. N.; Zhong, L. Y.; Bligh, S. W. A.; Guo, Y. L.; Zhang, C. F.; Zhang, M.; Wang, Z. T.; Xu, L. S. Bi-Bicyclic and Bi-Tricyclic Compounds from Dendrobium Thyrsiflorum. *Phytochemistry* **2005**, *66*, 1113–1120.

(66) Cai, S.; Sun, S.; Zhou, H.; Kong, X.; Zhu, T.; Li, D.; Gu, Q. Prenylated Polyhydroxy- P -Terphenyls from Aspergillus Taichungensis ZHN-7-07. *J. Nat. Prod.* **2011**, *74*, 1106–1110.

(67) Ito, T.; Endo, H.; Shinohara, H.; Oyama, M.; Akao, Y.; Iinuma, M. Occurrence of Stilbene Oligomers in Cyperus Rhizomes. *Fitoterapia* **2012**, *83*, 1420–1429.

(68) Capon, R. J.; Peng, C.; Dooms, C. Trachycladindoles A-G: Cytotoxic Heterocycles from an Australian Marine Sponge, Trachycladus Laevispirulifer. *Org. Biomol. Chem.* **2008**, *6*, 2765–2771.

(69) Zhang, Y.; Au, Q.; Zhang, M.; Barber, J. R.; Ng, S. C.; Zhang, B. Identification of a Small Molecule SIRT2 Inhibitor with Selective Tumor Cytotoxicity. *Biochem. Biophys. Res. Commun.* **2009**, *386*, 729–733.

(70) Kwak, J. H.; Kim, Y.; Park, H.; Jang, J. Y.; Lee, K. K.; Yi, W.; Kwak, J. A.; Park, S. G.; Kim, H.; Lee, K.; Kang, J. S.; Han, S. B.; Hwang, B. Y.; Hong, J. T.; Jung, J. K.; Kim, Y.; Cho, J.; Lee, H. Structure-Activity Relationship of Indoline-2-Carboxylic Acid N-(Substituted)phenylamide Derivatives. *Bioorganic Med. Chem. Lett.* **2010**, *20*, 4620–4623.

(71) Lee, C. L.; Liao, Y. C.; Hwang, T. L.; Wu, C. C.; Chang, F. R.; Wu, Y. C. Ixorapeptide I and Ixorapeptide II, Bioactive Peptides Isolated from Ixora Coccinea. *Bioorganic Med. Chem. Lett.* **2010**, *20*, 7354–7357.

(72) Kemnitzer, W.; Sirisoma, N.; Jiang, S.; Kasibhatla, S.; Crogan-Grundy, C.; Tseng, B.; Drewe, J.; Cai, S. X. Discovery of N-Aryl-9-Oxo-9H-Fluorene-1-Carboxamides as a New Series of Apoptosis Inducers Using a Cell- and Caspase-Based High-Throughput Screening Assay. 2. Structure-Activity Relationships of the 9-Oxo-9H-Fluorene Ring. *Bioorganic Med. Chem. Lett.* **2010**, *20*, 1288–1292.

(73) Songsiang, U.; Thongthoom, T.; Boonyarat, C.; Yenjai, C. Claurailas A-D, Cytotoxic Carbazole Alkaloids from the Roots of Clausena Harmandiana. *J. Nat. Prod.* **2011**, *74*, 208–212.

(74) Laine, A. E.; Lood, C.; Koskinen, A. M. P. Pharmacological Importance of Optically Active Tetrahydro-β-Carbolines and Synthetic Approaches to Create the C1 Stereocenter. *Molecules* **2014**, *19*, 1544–1567.

(75) Gopalan, B.; Ke, Z.; Zhang, C.; Kng, Y.; Suhaimi, N. M.; Riduan, S. N. Metal-Free Imidazolium Salts Inhibit the Growth of Hepatocellular Carcinoma in a Mouse Model. *Lab. Investig.* **2011**, *91*, 744–751.

(76) Garrison, J. C.; Youngs, W. J. Ag (I) N-Heterocyclic Carbene Complexes : Synthesis , Structure , and Application. *Chem. Rev.* **2005**, *105*, 3978–4008.

(77) Hindi, K. M.; Siciliano, T. J.; Durmus, S.; Panzner, M. J.; Medvetz, D. A.; Reddy, D. V.; Hogue, L. A.; Hovis, C. E.; Hilliard, J. K.; Mallet, R. J.; Tessier, C. A.; Cannon, C. L.; Youngs, W. J. Synthesis , Stability , and Antimicrobial Studies of Electronically Tuned Silver Acetate N -Heterocyclic Carbenes. *J. Med. Chem.* **2008**, *51*, 1577–1583.

(78) Medvetz, D. A.; Hindi, K. M.; Panzner, M. J.; Ditto, A. J.; Yun, Y. H.; Youngs, W. J. Anticancer Activity of Ag(I) N-Heterocyclic Carbene Complexes Derived from 4,5-Dichloro-1H-Imidazole. *Met. Based. Drugs* **2008**, 1–7.

(79) Ornelas-Megiatto, C.; Shah, P. N.; Wich, P. R.; Cohen, J. L.; Tagaev, J. A.; Smolen, J. A.; Wright, B. D.; Panzner, M. J.; Youngs, W. J.; Fréchet, J. M. J.; Cannon, C. L. Aerosolized Antimicrobial Agents Based on Degradable Dextran Nanoparticles Loaded with Silver Carbene Complexes. *Mol. Pharm.* **2012**, *9* (11), 3012–3022.

(80) Wright, B. D.; Shah, P. N.; Mcdonald, L. J.; Shaeffer, M. L.; Wagers, P. O.; Panzner, M. J.; Smolen, J.; Tagaev, J.; Tessier, C. A.; Cannon, L.; Youngs, W. J. Synthesis, Characterization, and Antimicrobial Activity of Silver Carbene Complexes Derived from 4,5,6,7-Tetrachlorobenzimidazole against Antibiotic Resistant Bacteria. *Dalt. Trans.* **2012**, *41*, 6500–6506.

(81) Youngs, W. J.; Knapp, A. R.; Wagers, P. O.; Tessier, C. a. Nanoparticle Encapsulated Silver Carbene Complexes and Their Antimicrobial and Anticancer Properties: A Perspective. *Dalt. Trans.* **2012**, *41* (2), 327.

(82) Shelton, K. L.; Debord, M. A.; Wagers, P. O.; Southerland, M. R.; Taraboletti, A.; Robishaw, N. K.; Jackson, D. P.; Tosanovic, R.; Kofron, W. G.; Tessier, C. A.; Paruchuri, S.; Shriver, L. P.; Panzner, M. J.; Youngs, W. J. Synthesis , Anti-Proliferative Activity , and Toxicity of C4(C 5) Substituted N,N' -Bis (Arylmethyl) Imidazolium Salts. *Tetrahedron* **2016**, *72*, 5729–5743.

(83) Shelton, K. L.; Debord, M. A.; Wagers, P. O.; Southerland, M. R.; Williams, T. M.; Robishaw, N. K.; Shriver, L. P.; Tessier, C. A.; Panzner, M. J.; Youngs, W. J.; Williams, T. M.; Robishaw, N. K.; Shriver, L. P.; Tessier, C. A.; Panzner, M. J.; Youngs, W. J. Synthesis, Anti-Proliferative Activity, SAR Study, and Prelinimary in Vivo Toxicity Study of Substituted N,N'-bis(arylmethyl)benzimidazolium Salts against a Panel of Non-Small Cell Lung Cancer Cell Lines. *Bioorg. Med. Chem.* **2016**.

(84) American Cancer Society. *Cancer Facts & Figures*. **2017**. Atlanta: American Cancer Society; 2017.

(85) Hamilton, M.; Wolf, J. L.; Drolet, D. W.; Fettner, S. H.; Rakhit, A. K.; Witt, K.; Lum, B. L. The Effect of Rifampicin, a Prototypical CYP3A4 Inducer, on Erlotinib Pharmacokinetics in Healthy Subjects. *Cancer Chemother. Pharmacol.* **2014**, *73* (3), 613–621.

(86) Wangari-Talbot, J.; Hopper-Borge, E. Drug Resistance Mechanisms in Non-Small Cell Lung Carcinoma. *J Can Res Updat.* **2014**, *2* (4), 265–282.

(87) Yao, X.; Panichpisal, K.; Kurtzman, N.; Nugent, K. Cisplatin Nephrotoxicity: A Review. *Am. J. Med. Sci.* **2007**, *334* (2), 115–124.

(88)   Katano, K.; Kondo, A.; Safaei, R.; Holzer, A.; Samimi, G.; Mishima, M.; Kuo, Y. M.; Rochdi, M.; Howell, S. B. Acquisition of Resistance to Cisplatin Is Accompanied by Changes in the Cellular Pharmacology of Copper. *Cancer Res.* **2002**, *62* (22), 6559–6565.

(89)   American Cancer Society. Cancer Facts & Figures 2015. **2015**.

(90)   Mizusako, H.; Tagami, T.; Hattori, K.; Ozeki, T. Active Drug Targeting of a Folate-Based Cyclodextrin-Doxorubicin Conjugate and the Cytotoxic Effect on Drug-Resistant Mammary Tumor Cells *In Vitro*. *J. Pharm. Sci.* **2015**, *104* (9), 2934–2940.

(91)   Zarrabi, A.; Vossoughi, M. Paclitaxel/β-CD-G-PG Inclusion Complex: An Insight into Complexation Thermodynamics and Guest Solubility. *J. Mol. Liq.* **2015**, *208*, 145–150.

(92)   Jelić, R.; Tomović, M.; Stojanović, S.; Joksović, L.; Jakovljević, I.; Djurdjević, P. Study of Inclusion Complex of β-Cyclodextrin and Levofloxacin and Its Effect on the Solution Equilibria between gadolinium(III) Ion and Levofloxacin. *Monatshefte für Chemie - Chem. Mon.* **2015**, *146* (10), 1621–1630.

(93)   Brewster, M. E.; Loftsson, T. Cyclodextrins as Pharmaceutical Solubilizers. *Adv. Drug Deliv. Rev.* **2007**, *59*, 645–666.

(94)   Ng, H. S.; Ooi, C. W.; Show, P. L.; Tan, C. P.; Ariff, A.; Moktar, M. N.; Ng, E.-P.; Ling, T. C. Recovery of Bacillus Cereus Cyclodextrin Glycosyltransferase Using Ionic Liquid-Based Aqueous Two-Phase System. *Sep. Purif. Technol.* **2014**, *138*, 28–33.

(95)   Marangoci, N.; Ardeleanu, R.; Ursu, L.; Ibanescu, C.; Danu, M.; Pinteala, M.; Simionescu, B. C. Polysiloxane Ionic Liquids as Good Solvents for β-Cyclodextrin-Polydimethylsiloxane Polyrotaxane Structures. *Beilstein J. Org. Chem.* **2012**, *8* (1), 1610–1618.

(96)   Wagers, P. O.; Tiemann, K. M.; Shelton, K. L.; Kofron, W. G.; Panzner, M. J.; Wooley, K. L.; Youngs, W. J.; Hunstad, D. a. Imidazolium Salts as Small-Molecule Urinary Bladder Exfoliants in a Murine Model. *Antimicrob. Agents Chemother.* **2015**, *59* (9), AAC.00881-15.

(97)   Loftsson, T.; Duchêne, D. Cyclodextrins and Their Pharmaceutical Applications. *Int. J. Pharm.* **2007**, *329* (1–2), 1–11.

(98)   Debord, M. A.; Wagers, P. O.; Crabtree, S. R.; Tessier, C. A.; Panzner, M. J.; Youngs, W. J. Synthesis, Chracterization, and in Vitro SAR Evaluation of N,N'-Bis(arylmethyl)-C2-Alkyl Substituted Imidazolium Salts. *Bioorg. Med. Chem. Lett.* **2016**.

(99)   Ranke, J.; Stolte, S.; Störmann, R.; Aming, J.; Jastorff, B. Design of Sustainable Chemical Products - The Example of Ionic Liquids. *Chem. Rev.* **2007**, *107* (6), 2183–2206.

(100)   van Engeland, M.; Nieland, L. J. W.; Ramaekers, F. C. S.; Schutte, B.; Reutelingsperger, C. P. M. A Review on an Apoptosis Detection System Based on Phosphatidyserine Exposure. **1998**, *31*, 1–9.

(101)   Jensen, C. G.; Bleumink, A. R.; Wilson, W. R. Effects of Amsacrine and Other DNA-Intercalating Drugs on Nuclear and Nucleolar Structure in Cultured V79 Chinese Hamster Cells and PtK2 Rat Kangaroo Cells. *Cancer Res.* **1985**, *45*, 717–725.

(102)   Fu, X.-B.; Zhang, J.-J.; Liu, D.-D.; Gan, Q.; Gao, H.-W.; Mao, Z.-W.; Le, X.-Y. Cu(II)-Dipeptide Complexes of 2-(4'-thiazolyl)benzimidazole: Synthesis, DNA Oxidative Damage, Antioxidant and in Vitro Antitumor Activity. *J. Inorg. Biochem.* **2014**, *143C*, 77–87.

(103)   Boger, D. L.; Fink, B. E.; Brunette, S. R.; Tse, W. C.; Hedrick, M. P. A Simple, High-Resolution Method for Establishing DNA Binding Affinity and Sequence Selectivity. *J. Am. Chem. Soc.* **2001**, *123* (25), 5878–5891.

(104)   Kelley, S. O.; Stewart, K. M.; Mourtada, R. Development of Novel Peptides for Mitochondrial Drug Delivery: Amino Acids Featuring Delocalized Lipophilic Cations. *Pharm. Res.* **2011**, *28*, 2808–2819.

(105)   Kurtoglu, M.; Lampidis, T. J. From Delocalized Lipophilic Cations to Hypoxia : Blocking Tumor Cell Mitochondrial Function Leads to Therapeutic Gain with Glycolytic Inhibitors. *Mol. Nutr. Food Res.* **2009**, *53*, 68–75.

(106)   Wadia, J. S.; Chalmers-Redman, R. M.; Ju, W. J.; Carlile, G. W.; Phillips, J. L.; Fraser, a D.; Tatton, W. G. Mitochondrial Membrane Potential and Nuclear Changes in Apoptosis Caused by Serum and Nerve Growth Factor Withdrawal: Time Course and Modification by (-)-Deprenyl. *J. Neurosci.* **1998**, *18* (3), 932–947.

(107)   Smiley, S. T.; Reers, M.; Mottola-Hartshorn, C.; Lin, M.; Chen, A.; Smith, T. W.; Steele, G. D.; Chen, L. B. Intracellular Heterogeneity in Mitochondrial Membrane Potentials Revealed by a J-Aggregate-Forming Lipophilic Cation JC-1. *Proc. Natl. Acad. Sci. U. S. A.* **1991**, *88*, 3671–3675.

(108)   Castedo, M.; Hirsch, T.; Susin, S. A.; Zamzami, N.; Marchetti, P.; Macho, A.; Kroemer, G. Sequential Acquisition of Mitochondrial and Plasma Membrane Alterations during Early Lymphocyte Apoptosis. *J. Immunol.* **1996**, *157* (2), 512–521.

(109)   Sordella, R.; Bell, D. W.; Haber, D. A.; Settleman, J. Gefitinib-Sensitizing EGFR Mutations in Lung Cancer Activate Anti-Apoptotic Pathways. *Science (80-.).* **2004**, *305* (5687), 1163–1167.

(110) Koulermou, G.; Shammas, C.; Vassiliou, A.; Kyriakides, T. C.; Costi, C.; Neocleous, V.; Phylactou, L. A.; Pantelidou, M. CDKN2A and MC1R Variants Found in Cypriot Patients Diagnosed with Cutaneous Melanoma. *J. Genet.* **2017**, 1–6.

(111) Matsuda, N.; Lim, B.; Wang, Y.; Krishnamurthy, S.; Woodward, W.; Alvarez, R. H.; Lucci, A.; Valero, V.; Reuben, J. M.; Meric-Bernstam, F.; Ueno, N. T. Identification of Frequent Somatic Mutations in Inflammatory Breast Cancer. *Breast Cancer Res. Treat.* **2017**, 1–10.

(112) Haagensen, E. J.; Thomas, H. D.; Schmalix, W. A.; Payne, A. C.; Kevorkian, L.; Allen, R. A.; Bevan, P.; Maxwell, R. J.; Newell, D. R. Enhanced Anti-Tumour Activity of the Combination of the Novel MEK Inhibitor WX-554 and the Novel PI3K Inhibitor WX-037. *Cancer Chemother. Pharmacol.* **2016**, *78* (6), 1269–1281.

(113) Chen, C. Y.; Abell, A. M.; Moon, Y. S.; Kim, K. H. An Advanced Glycation End Product (AGE)-Receptor for AGEs (RAGE) Axis Restores Adipogenic Potential of Senescent Preadipocytes through Modulation of p53 Protein Function. *J. Biol. Chem.* **2012**, *287* (53), 44498–44507.

(114) Bruker. SMART (Version 5.625). Madison, Wisconsin, USA: Buker AXS Inc.; **2012**.

(115) Bruker. APEX II. Madison, Wisconsin, USA: Bruker ACS Inc.; **2012**.

(116) Bruker. SAINT. Madison, Wisconsin, USA. Bruker ACS Inc.; **2012**.

(117) Bruker. SADABS. Madison, Wisconsin, USA: Bruker AXS Inc.; **2012**.

(118) Sheldrick, G. M. Crystal Structure Refinement with SHELXL. *Acta Crystallogr. Sect. C Struct. Chem.* **2015**, *71* (Md), 3–8.

(119) Dhar, S.; Nethaji, M.; Chakravarty, A. R. DNA Cleavage on Photoexposure at the D − D Band in Ternary Copper (II) Complexes Using Red-Light Laser. *Inorg. Chem.* **2006**, *45*, 11043–11050.

(120) American Cancer Society. Cancer Facts & Figures. Atlanta 2016.

(121) Afzal, O.; Kumar, S.; Haider, M. R.; Ali, M. R.; Kumar, R.; Jaggi, M.; Bawa, S. A Review of Anticancer Potential of Bioactive Heterocycle Quinoline. *Eur. J. Med. Chem.* **2014**, 1–40.

(122) Wall, M. E.; Wani, M. C.; Cook, C. E.; Palmer, K. H. ~ 1.0,. *J. Am. Chem. Soc.* **1966**, *88*, 3888–3890.

(123) Hsiang, Y. H.; Hertzberg, R.; Hecht, S.; Liu, L. F. Camptothecin Induces Protein-Linked DNA Breaks via Mammalian DNA Topoisomerase I. *J. Biol. Chem.* **1985**, *260* (27), 14873–14878.

(124) Zhou, L.; Lichent, D.; Chen, X.; Li, X.; Li, Z.; Wen, Y.; Li, Z.; He, X.; Wei, Y.; Zhao, X.; Qian, Z. The Antitumor and Antimetastatic Effects of N-Trimethyl Chitosan-Encapsulated Camptothecin on Ovarian Cancer with Minimal Side Effects. *Oncol. Rep.* **2010**, *24*, 941–948.

(125) Huang, H. C.; Mallidi, S.; Liu, J.; Chiang, C. Te; Mai, Z.; Goldschmidt, R.; Ebrahim-Zadeh, N.; Rizvi, I.; Hasan, T. Photodynamic Therapy Synergizes with Irinotecan to Overcome Compensatory Mechanisms and Improve Treatment Outcomes in Pancreatic Cancer. *Cancer Res.* **2016**, *76* (5), 1066–1077.

(126) Hu, G.; Zekria, D.; Cai, X.; Ni, X. Current Status of CPT and Its Analogues in the Treatment of Malignancies. *Phytochem. Rev.* **2015**, *14*, 429–441.

(127) Riduan, S. N.; Zhang, Y. Imidazolium Salts and Their Polymeric Materials for Biological Applications. *Chem. Soc. Rev.* **2013**, *42* (23), 9055–9070.

(128) Shukla, V.; Scholar, R. Techniques for Solubility Enhancement of Poorly Soluble Drugs: An Overview. *J. Med. Pharm. Allied Sci.* **2016**, *1*, 18–38.

(129) Agelis, G.; Resvani, A.; Koukoulitsa, C.; Tumova, A.; Slaninova, J.; Kalavrizioti, D.; Spyridaki, K.; Afantitis, A.; Melagraki, G.; Siafaka, A.; Gkini, E.; Megariotis, G.; Grdadolnik, S. G.; Papadopoulos, M. G.; Vlahakos, D.; Maragoudakis, M.; Liapakis, G.; Mavromoustakos, T.; Matsoukas, J. Rational Design , Efficient Syntheses and Biological Evaluation of N ,N'-symmetrically Bis-Substituted Butylimidazole Analogs as a New Class of Potent Angiotensin II Receptor Blockers. *Eur. J. Med. Chem.* **2013**, *62*, 352–370.

(130) Ramalingam, S.; Sandler, A. B. Salvage Therapy for Advanced Non-Small Cell Lung Cancer: Factors Influencing Treatment Selection. *Oncol. Lung Cancer* **2006**, *11*, 655–665.

(131) Dempke, W. C. M.; Suto, T.; Reck, M. Targeted Therapies for Non-Small Cell Lung Cancer. *Lung Cancer* **2010**, *67*, 257–274.

(132) Chen, W.; Deng, X.-Y.; Li, Y.; Yang, L.-J.; Wan, W.-C.; Wang, X.-Q.; Zhang, H.-B.; Yang, X.-D. Synthesis and Cytotoxic Activities of Novel Hybrid 2-Phenyl-3-Alkylbenzofuran and Imidazole/triazole Compounds. *Bioorg. Med. Chem. Lett.* **20013**, *23*, 4297–4302.

(133) Gao, Y.; Vlahakis, J. Z.; Szarek, W. A.; Brockhausen, I. Selective Inhibition of Glycosyltransferases by Bivalent Imidazolium Salts. *Bioorg. Med. Chem.* **2013**, *21*, 1305–1311.

(134) Jurgens, E.; Buys, K. N.; Schmidt, A.-T.; Furfari, S. K.; Cole, M. L.; Moser, M.; Rominger, F.; Kunz, D. Optimized Synthesis of Monoanionic bis(NCH)-Pincer Ligand Precursors and Their Li-Complexes †. *New J. Chem.* **2016**.

(135) Pinto, M. F.; Cardoso, B. de P.; Barroso, S.; Martins, A. M.; Royo, B. Chelating Bis-N-Heterocyclis Carbene Complexes of iron(II) Containing Bipyridyl Ligands as Catalyst Precursors for Oxidation of Alcohols †. *Dalt. Trans.* **2016**, *45*, 13541–13546.

(136) Jarikote, D. V; Li, W.; Jiang, T.; Eriksson, L. A.; Murphy, P. V. Towards Echinomycin Mimetics by Grafting Quinoxaline Residues on Glycophane Scaffolds. *Bioorg. Med. Chem.* **2011**, *19*, 826–835.

(137) Haque, R. A.; Hasanudin, N.; Iqbal, M. A.; Ahmad, A.; Hashim, S.; Majid, A. A.; Ahamed, M. B. K. Synthesis, Crystal Structures , in Vitro Anticancer , and in Vivo Acute Oral Toxicity Studies of Bis-Imidazolium / Benzimidazolium Salts and Respective Dinuclear Ag (I) - N -Heterocyclic Carbene Complexes. *J. Coord. Chem.* **2013**, *66* (18), 3211–3228.

APPENDICES

APPENDIX A

APPROVAL FOR ANIMAL USE

May 15, 2015

Dr. Shriver
The University of Akron
Akron, OH 44325

Dear Dr. Shriver,

On May 15, 2015 the Institutional Animal Care and Use Committee approved your protocol titled: "Evaluation of Novel Chemotherapeutic Agents for Glioblastoma Multiforme" by Designated Member Review.

IACUC number 15-05-8-SME

Your project has received final approval on May 15, 2015.

You must notify the committee concerning modifications to the approved protocol. In addition, yearly updates regarding the status of this project are required. IACUC must also be notified of serious or adverse reactions that occur during the course of this project. Please use the IACUC number when submitting this information to the committee.

Please be aware that approval of your protocol does not guarantee space in the animal facility.

Sincerely,
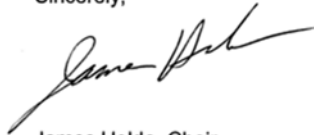
James Holda, Chair

APPENDIX B

ABBREVIATIONS AND ACRONYMS

Å	angstrom
α	crystallographic uni-cell angle between axes *b* and *c*
β	crystallographic uni-cell angle between axes *a* and *c*
^{0}C	degrees Celcius
μL	microliter
μM	micromolar
λ	crystallographic uni-cell angle between axes *a* and *b*
δ	scale (nmr) ppm
2-HPβCD	2-hydroxypropyl-β-cyclodextrin
a	crystallographic unit cell axis *a*
AA	amino acid
ACS	6-methyl-4-oxo-4H-1,2,3-oxathiazin-3-ide 2,2-dioxide
AMP	ampicillin
b	crystallographic unit cell axis *b*
BF_4	tetrafluoroborate
c	crystallographic unit cell axis *c*
Calcd.	calculated
CD	cyclodextrin
CT-DNA	calf thymus DNA
d	doublet
DCA	dicyanoamide
DLC	delocalized lipophilic cation
DMF	dimethylformamide
DMSO	dimethylsulfoxide
DNA	deoxyribonucleic acid
DTP	developmental Therapeutics Program
EB	ethidium bromide
EC_{50}	concentration to induce 50% response
EGF	epidermal growth factor
EGFR	epidermal growth factor receptor
F_c	calculated structure factor

F_o	observed Strucutre factor
FDA	Food and Drug Administration
$FeCl_4$	tetrachloroferrate(III)
FID	fluorescent intercalator displacement
F(000)	scaling coefficient for structure factors
GI_{50}	growth inhibition of 50% of cells relative to control cells
GRAS	generally regarded as safe
h	hour
IC_{50}	inhibitory concentration 50%
IP	intraperitoneal
IS23	4,5-dichloro-1,3-bis(naphthalen-2-ylmethyl)imidazolium bromide
IS29	1,3-bis(naphthalen-2-ylmethyl)imidazolium bromide
J	nuclear spin-spin coupling constant
K	kelvin
M	molecular weight
LD_{50}	lethal dose of 50% of a population
m	multiplet
mHz	megahertz
mL	milliliter
mmol	millimole
MNIB	1-mesityl-3-(2-naphthoylmethano)-1H-imidazolium bromide
Mp	melting point
mTOR	mammalian target of rapamycin
MTT	3-(4,5-dimethylthiazol-2-yl)-2,5-diphenyltetrazolium bromide
m/z	mass-to-charge ratio
NCI	national Cancer Institute
NHC	N-heterocyclic carbene
nm	nanometer
NMR	nuclear magnetic resonance
NSCLC	non-small cell lung cancer
NTF2	bistrifluoromethane-sulfonimidate
pEC50	negative logarithm of the EC_{50} value
PF_6	hexafluorophosphate
PI	propidium iodide
ppm	parts per million
PS	phosphatidylserine
R	residual factor or reliability factor
ROS	reactive oxygen species
RT	room temperature
s	singlet
SAC	3-oxo-3H-benzo[d]isothiazol-2-ide 1,1-dioxide
SAR	structure-activity relationship
T	temperature

t	triplet
THF	tetrahydrofuran
U	temperature factor
V	volume
wR$_2$	weighted residual based on
YM155	1-(2-methoxyethyl)-2-methyl-4,9-dioxo-3-(pyrazin-2-ylmethyl)-4,9-dihydro-1H-3l4-naphtho[2,3-d]imidazolium bromide
Z	the number of formula units related by symmetry